

The Total Spine of the Milnor Fibration of a Plane Curve Singularity

Pablo Portilla Cuadrado

Baldur Sigurðsson

Author address:

UNIVERSIDAD POLITÉCNICA MADRID, ESCUELA TÉCNICA SUPERIOR DE INGENIEROS INDUSTRIALES, JOSÉ GUTIÉRREZ ABASCAL 2, 28006 MADRID

Email address: p.portilla89@gmail.com

UNIVERSIDAD POLITÉCNICA MADRID, MATEMÁTICA E INFORMÁTICA APLICADAS A LAS INGENIERÍAS CIVIL Y NAVAL, C. DEL PROFESOR ARANGUREN 3, 28040 MADRID.

Email address: baldursigurds@gmail.com

Contents

Chapter 1. Introduction	1
1.1. Motivation	1
1.2. Future work	4
1.3. Organization of the paper	4
Chapter 2. General Setting	7
2.1. The complex gradient as a lift	7
2.2. The collapsing map	9
2.3. Isometric coordinates	12
2.4. Vector fields	12
Chapter 3. Embedded Resolutions	17
3.1. Embedded resolutions	17
3.2. Initial part and vanishing order	18
3.3. Invariants of the resolution: c_0, c_1 and the canonical divisor	19
3.4. Directions on the dual graph	22
3.5. The tangent associated with a divisor	24
Chapter 4. The Real Oriented Blow-up	27
4.1. An action on the normal bundle	28
4.2. Milnor fibration at radius zero	29
4.3. Scaling and extending the metric	30
Chapter 5. Resolving the Polar Locus	33
5.1. Generic polar curves	33
Chapter 6. The Invariant and Non-invariant Subgraphs	37
6.1. The polar weight	37
6.2. The invariant subgraph Υ of Γ_{\min}	38
6.3. The invariant subgraph of Γ_{pol}	42
6.4. The Jacobian ideal in Y_{\min} and polar curves in Y_{pol}	44
Chapter 7. The 1st Blow-up	51
7.1. Special coordinates	51
7.2. Scaling and extending the vector field	52
7.3. $\hat{\xi}_0$ in the normal direction	53
7.4. $\hat{\xi}_0$ in the tangent direction	54
7.5. The spine at radius zero over the 1st blow-up	57
7.6. Some homogeneous examples	58
Chapter 8. The Vector Field Near the Corners	65

8.1. Invariant intersection points	66
8.2. Non-invariant intersection points	69
8.3. The strict transform	71
8.4. Poincaré-Hopf indices	74
Chapter 9. Other Exceptional Divisors	77
9.1. Extension over the boundary	78
9.2. A potential for ξ_i on invariant vertices	80
Angle dependence	83
9.3. A potential for $\xi_{i,\theta}^{\text{ro}}$	84
Chapter 10. Singularities on the Boundary of $Y_{\text{pol}}^{\text{ro}}$	87
10.1. Spinal cells	87
10.2. The Hessian in U^{ro}	88
10.3. Center-stable manifolds	92
Chapter 11. The Total Spine of the Milnor Fibration	99
11.1. Broken trajectories	99
11.2. The total spine	101
Chapter 12. The Invariant Spine	103
12.1. Broken trajectories	103
12.2. The Petri dishes	107
12.3. The invariant Milnor fibration	116
Chapter 13. Example	121
Bibliography	131
Index	133

Abstract

For any plane curve singularity defined by an analytic function germ f , we construct a spine on each Milnor fiber simultaneously, that realizes the vanishing topology. In order to do so, we study the separatrices at the origin of the vector field $-\nabla \log |f|$. Under some genericity conditions on the metric, we produce a natural partition of the set of separatrices, S , into a finite collection smooth strata. As a byproduct of this theory, we construct a smooth fibration which is equivalent to the Milnor fibration, and lives on a quotient of the Milnor fibration at radius 0. The strict transform of S in this space induces the aforementioned spine for each fiber of this fibration. These fibers are naturally endowed with a vector field in such a way that the spine consists of trajectories which do not escape through the boundary.

Received by the editor 1st September 2023.

2020 *Mathematics Subject Classification.* Primary 32S05, 14H50, 37B35.

Key words and phrases. singularity theory, plane curve singularities, Milnor fibration, spine, gradient, low-dimensional topology.

The first author is supported by RYC2022-035158-I, funded by MCIN/AEI/10.13039/501100011033 and by the FSE+ and also was supported by the Labex CEMPI (ANR-11-LABX-0007-01).

The second author B.S. was partly supported by The Simons Foundation Targeted Grant (No. 558672) for the Institute of Mathematics, Vietnam Academy of Science and Technology, and Contratos María Zambrano para la atracción de talento internacional at Universidad Complutense de Madrid and Universidad Politécnica de Madrid.

CHAPTER 1

Introduction

1.1. Motivation

The motivation for this work comes from a question that Thom posed to Lê [Lê88]. More concretely, let $f : \mathbb{C}^n \rightarrow \mathbb{C}$ be a holomorphic map. Then there exists $\varepsilon, \eta > 0$ with ε small enough and η small with respect to ε such that the restriction of f yields a locally trivial fibration:

$$(1.1.1) \quad f|_{B_\varepsilon \cap f^{-1}(D_\eta)^*} : B_\varepsilon \cap f^{-1}(D_\eta^*) \rightarrow D_\eta^*$$

This is the Milnor fibration over the punctured disk. The following two results were proven by Milnor [Mil68]

- (1) The pair of spaces $(f^{-1}(0) \cap B_\varepsilon, B_\varepsilon)$ is homeomorphic to the pair of cones $(C(f^{-1}(0) \cap S_\varepsilon), C(S_\varepsilon))$.
- (2) When f has an isolated critical point at the origin, the Milnor fiber F has the homotopy type of a bouquet of spheres of real dimension $n - 1$.

In this context, according to [Lê88], Thom asked Lê if one could find a polyhedron P contained in this fiber F (the Milnor fiber), of real dimension $n - 1$, such that F would be a regular neighborhood of P . From this result one would obtain the construction of a continuous application which would send F to the special fiber F_0 , sending P to $\{0\}$ and $F \setminus P$ homeomorphically to $F_0 \setminus \{0\}$. This application would geometrically realize the collapsing of the homology $H(F)$ of F on the trivial homology of F_0 and this would give a geometric realization of the vanishing cycles of the function at the isolated critical point.

A solution to this problem in the more general context of germs of analytic maps with isolated singularity defined on analytic complex spaces $f : X \rightarrow \mathbb{C}$ was sketched by Lê in [Lê88] and later [LM17, Theorem 1], detailed by Lê and Menegon. More concretely, they proved the following: let F_t be the Milnor fiber of f and let F_0 be the central fiber. Then there exists a polyhedron $P_t \subset F_t$ of real dimension $\dim_{\mathbb{C}} F_t$ and a continuous simplicial map $\partial F_t \rightarrow P_t$ such that F_t is homeomorphic to the mapping cylinder of the map above. Furthermore, there exists a continuous map of pairs $\Psi_t : (F_t, P_t) \rightarrow (F_0, 0)$ such that its restriction $F_t \setminus P_t \rightarrow F_0 \setminus \{0\}$ is a homeomorphism. Their construction can be realized simultaneously only over a proper sector of the base space of the fibration, which is a punctured disk.

The starting point of this work is based on an original idea by A'Campo [A'C18] that can be summarized as follows:

- (1) Consider the inwards pointing radial vector field $\frac{-t}{|t|} \frac{\partial}{\partial t}$ on the disk D_η .
- (2) Lift the vector field to a vector field ξ^{lift} on $B_\varepsilon \setminus F_0$ using the connection given by the family of tangent planes which are the symplectic orthogonals to the vertical tangent bundle associated with the Milnor fibration.

- (3) Integrate the vector field and analyze the uniparametric family of diffeomorphisms that takes Milnor fibers along a ray all the way to the central fiber.
- (4) Analyze the maps $\rho_t : F_t \rightarrow F_0$ resulting from taking the limit of these diffeomorphisms and study the set $S_t = \rho_t^{-1}(0) \subset F_t$.

The set S_t is the expected *spine* for the Milnor fiber F_t but it is not clear, a priori, what kind of structure it has. At this moment a simple observation is due: Analyzing the set S_t amounts to analyzing the separatrices at 0 of ξ^{lift} , that is, the set of integral lines S of ξ^{lift} that converge to the origin. Intersecting this set with each Milnor fiber $S \cap F_t$ equally defines the set S_t . From now on, we consider the case of plane curves, that is, $n = 2$. We do not assume, however, that the plane curve is reduced.

Our program departs from A'Campo's idea but it quickly bifurcates. The lift of the vector field $\frac{-t}{|t|} \frac{\partial}{\partial t}$ is easily seen to be, up to multiplication by a positive real function, the vector field

$$\xi = -\nabla \log |f|.$$

In particular, ξ and ξ^{lift} have the same integral lines. So this problem turns out to be closely related to the study of integral lines of gradients of absolute values of complex analytic maps.

The set S is very complicated near the origin so a natural idea to study it, is to follow this strategy: with the notation $C = F_0$, and \tilde{C} the strict transform of C , blow up the origin

$$\pi_0 : (Y_0, \tilde{C} \cup D_0) \rightarrow (\mathbb{C}^2, C)$$

and see if the strict transform of the separatrices $\overline{\pi_0^{-1}(S)}$ intersects in a reasonable way the new exceptional divisor D_0 . It happens that, under some genericity conditions on the metric, some of the trajectories in S now meet D_0 transversely at a finite set of points Σ_0 . Moreover, one is able to suitably rescale $\pi_0^* \xi$ in such a way that the rescaled vector field extends over $D_0^\circ = D_0 \setminus \tilde{C}$ to a vector field $\hat{\xi}_0$ and its restriction $\xi_0 = \hat{\xi}_0|_{D_0^\circ}$ satisfies that

- (1) ξ_0 is the gradient with respect to the Fubini-Study metric on D_0 of a Morse function $D_0^\circ \rightarrow \mathbb{R}$.
- (2) The critical set of ξ_0 is precisely Σ_0 .
- (3) ξ_0 has fountain singularities and saddle points on interior points of D_0° but it does not have sink singularities.
- (4) The intersection points of D_0 with the strict transform \tilde{C} behave like sink singularities, that is, ξ_0 points towards the strict transform near these intersection points.

While we have *simplified* our set S , the problem is far from being solved: there are still many trajectories in $\pi_0^{-1}(S)$ that converge to intersection points in $\tilde{C} \cap D_0$. Some wishful thinking leads one to believe that further repeating of this technique will eventually *resolve* the set S and one shall be able to study these separatrices by studying some sort of nice Morse vector fields on the divisors D_i of, let's say, an embedded resolution $\pi : (Y, D = \bigcup_i D_i) \rightarrow (\mathbb{C}^2, C)$. This couldn't be further from the truth since a lot of things that behave nicely on the first blow up, go wrong. In particular, it is not *always* possible to re-scale and extend the (pullback of) the vector field ξ to the divisors D_i . This phenomenon occurs because the extension depends on the angle θ from which one approaches the origin. Once spotted the

problem and its origin, it becomes natural to perform a *real oriented blow up* of the resolution space Y along the exceptional set D . The real oriented blow up substitutes a manifold by the moduli of all the normal directions to this manifold. Note that the function $\arg(f)$ that gives the argument of f , is only well defined outside C . The real oriented blow up

$$\sigma : (Y^{\text{ro}}, D^{\text{ro}}) \rightarrow (Y, D)$$

resolves this indeterminacy: the function $\arg(f)$ lifts to a function $\arg^{\text{ro}}(f)$ that naturally extends over all Y^{ro} . With $\pi^{\text{ro}} = \pi \circ \sigma$, this same phenomenon allows us to rescale and extend the vector field $(\pi^{\text{ro}})^* \xi$ to vector fields ξ_i^{ro} that are defined on, and are tangent to, the exceptional divisors $D_i^{\text{ro}} = \sigma^{-1}(D_i)$.

The space Y^{ro} is a manifold with corners. As a topological manifold it has a boundary $\partial Y^{\text{ro}} = D^{\text{ro}}$ that fibers over the circle $\mathbb{R}/2\pi\mathbb{Z}$ via the map $\arg^{\text{ro}}(f)$. This topological fibration is equivalent to the Milnor fibration and it is usually known as *the Milnor fibration at radius 0* and its fiber F_θ^{ro} *the Milnor fiber at radius 0*. This fibration was described by A'Campo [A'C75] to describe a zeta function for the monodromy. See also [KN99] for a very similar construction.

When the metric used to define ξ satisfies other genericity conditions we show that the vector fields ξ_i^{ro} behave in a nice way:

- (1) $\xi_{i,\theta}^{\text{ro}} = \xi_i^{\text{ro}}|_{F_\theta^{\text{ro}} \cap D_i^{\text{ro}}}$ has a saddle-point singularity at a point $p \in D_{i,\theta}^{\text{ro},\circ}$ if and only if $\sigma(p) \in D_i$ is the intersection point of the strict transform of a particular relative polar curve and D_i .
- (2) $\xi_{i,\theta}^{\text{ro}}$ has no other singularities on $p \in D_{i,\theta}^{\text{ro},\circ}$.

At this point we have simplified enough the set of separatrices S and we conclude that it can be partitioned into manifolds of trajectories that converge either to some saddle point of some $\xi_{i,\theta}^{\text{ro}}$ or to a repeller on the first blow up. More concretely:

THEOREM A (Theorem 11.2.1). *Assuming that \mathbb{C}^2 is endowed with a generic metric, the punctured total spine $S \setminus \{0\}$ is the disjoint union of strata, each of which is a punctured disk, an open solid torus or an open solid Klein bottle. Each stratum corresponds to a point p on the exceptional divisor of an embedded resolution of $(C, 0)$, in that it is the union of trajectories of ξ whose lift to the resolution converges to p .*

In Chapter 12 we define the *invariant Milnor fibration at radius zero* which as a set, is a quotient of the Milnor fibration at radius zero.

THEOREM B (Theorem 12.3.12). *The invariant Milnor fibration naturally admits a smooth structure and a smooth vector field tangent to each Milnor fiber. The union of trajectories of this vector field, which do not escape through the boundary, is a spine for each Milnor fiber. As a set, this spine coincides with the intersection of strict transform of the total spine with the Milnor fibration at radius zero. Moreover, this spine has the structure of a piecewise smooth 1-dimensional CW complex and all the 1-cells meet transversely at the 0-cells*

Note that we are able to construct this spine for all $\theta \in \mathbb{R}/2\pi\mathbb{Z}$ at the same time and so, necessarily, the topological type of the spine changes with θ because, otherwise, we would get a finite order algebraic monodromy which is not always the case for plane curve singularities.

1.2. Future work

A large motivating factor for this project is to understand the integral monodromy and the variation map. A natural continuation of this work provides us with methods to explicitly describe both operators. This is the subject of a manuscript already in preparation.

A similar program in higher dimensions quickly becomes more complicated. For instance, the resolution complex in higher dimensions is not as well understood as the dual resolution graph of a plane curve singularity, whose structure is repeatedly used in this text. Another reason is that relative polar curves, which are heavily used in this work, have a simpler (but still very rich) nature than relative polar varieties which, for example, do not intersect the exceptional divisors in just isolated points.

1.3. Organization of the paper

In [Chapter 2](#) we recall the ideas of A’Campo [[A’C18](#)] and motivate our problem. Using results of Łojasiewicz [[Loj84](#)], we prove that the ideas of A’Campo yield a well defined collapsing map

$$\rho_t : F_t \rightarrow C$$

from each Milnor fiber over $t \in D_\eta^*$ to the central fiber C . We show that this map is a local diffeomorphism when restricted outside the preimage of the origin. One of the main goals of the rest of the paper is to understand the set

$$S_t = \rho_t^{-1}(0).$$

In [Chapter 3](#) we mainly recall the theory of embedded resolutions $\pi : (Y, D) \rightarrow (\mathbb{C}^2, C)$, this serves as well to introduce some important notation and invariants. We introduce a structure of directed graph to the dual graph of the resolution Γ and describe this structure in terms of defined invariants associated with the resolution.

[Chapter 4](#) is devoted to understand the real oriented blow up of the resolution along the exceptional set D . This procedure produces a manifold with corners Y^{ro} that is naturally foliated by manifolds Y_θ^{ro} where $\theta = \arg(f)$. A topological locally trivial fibration naturally appears on the boundary of the real oriented blow up: the Milnor fibration at radius 0.

In [Chapter 5](#), we recall some of the work by Tessier [[Tei77](#)] and we describe a particular kind of embedded resolutions $\pi_{\text{pol}} : Y_{\text{pol}} \rightarrow \mathbb{C}^2$: those that resolve also all the relative polar curves that live in a special dense and equisingular family. These are the resolutions used throughout the rest of the paper.

In [Chapter 6](#) we introduce an important invariant associated to each divisor of an embedded resolution, the *polar weight* $\varpi_i \in \mathbb{Z}_{\geq 0}$. The vertices where this invariant vanishes describe a special connected subgraph Υ of the resolution graph, the *invariant subgraph*. It is, furthermore, characterized as the subgraph consisting of all the geodesics in Γ that join the vertex 0 with vertices adjacent to some arrow head (which correspond to components of the strict transform of the curve). The complement of Υ is the (in general disconnected) non-invariant graph. This section ends with a detailed study of the generic relative polar curves of a plane curve singularity. In particular, using previous work of Michel [[Mic08](#)] we describe base points of the Jacobian ideal and some obstruction as to where the strict transforms

of generic relative polar curves intersect the exceptional divisors of the embedded resolution $\pi_{\text{pol}} : Y_{\text{pol}} \rightarrow \mathbb{C}^2$.

As we have said in the introduction, our program has a special treatment for the divisor D_0 and its corresponding counterpart D_0^{ro} in the real oriented blow up. Our program is carried away completely in this case in [Chapter 7](#). More concretely, we prove that, after appropriately rescaling the vector field $(\pi_{\text{pol}})^*\xi$ we can extend it over to a vector field ξ_0 defined on D_0° . Moreover, for a dense set of linear metrics which is made precise in that section, the restriction to D_0° is the gradient of a Morse function $D_0^{\circ} \rightarrow \mathbb{R}$. We finish the section by describing the spine a radius 0 over the 1st blow up. Note that this case is important since it completely finishes the program for homogeneous singularities, since they are resolved by one blow up. One can also think about this as the part that deals with the tangent cone of the singularity.

In [Chapters 8](#) and [9](#) we deal with the extension of the vector field $(\pi_{\text{pol}}^{\text{ro}})^*\xi$ over the boundary of the real oriented blow up D^{ro} . In order to do so, we introduce the numerical invariant called *the radial weight* that measures the order of the poles that $(\pi_{\text{pol}})^*\xi$ has over the divisors D_i^{ro} and, thus, indicates how to rescale $(\pi_{\text{pol}}^{\text{ro}})^*\xi$.

[Chapter 10](#) constitutes one of the main technical contributions of the paper. We prove that the vector fields extended in the previous sections have a manifold of trajectories converging to each saddle point in the interior of some divisor. The main ingredient for this part is the theory of center-stable manifolds as developed by A. Kelley in [[Kel67a](#), [Kel67b](#)].

In [Chapter 11](#) we prove the first main theorem ([Theorem A](#)) of this paper, showing that the total spine S naturally decomposes into smooth manifolds corresponding to the singularities of the extended vector fields. In particular, we prove that if a trajectory γ converges to the origin in \mathbb{C}^2 , its strict transform by the real oriented blow up converges to one of these singularities.

In [Chapter 12](#), we prove the second main result of the paper, [Theorem B](#), which also depends on the first one. First we describe the invariant Milnor fibration which is the natural fibration induced by the function \arg^{ro} on the boundary of the real oriented blow up of (Y, D) along a certain subset of divisors. We put a smooth structure on this space and show that our vector fields naturally extend and glue to give a smooth vector field. Then, the regularity of the extended vector field and the previous main theorem allows us to prove [Theorem B](#).

Finally, in [Chapter 13](#) we work out a detailed example where all the theory developed in the paper comes into play.

CHAPTER 2

General Setting

Let $f \in \mathcal{O}_{\mathbb{C}^2,0}$ be a germ of a holomorphic function on \mathbb{C}^2 which is not necessarily reduced. Let $C \subset \mathbb{C}^2$ be a representative of the germ $(Z(f), 0)$ defined by f . Thus, C is an analytic plane curve with possibly non-reduced components.

Let B_ε be a closed Milnor ball for C , that is, a ball such that all spheres $S_{\varepsilon'}$ with $0 < \varepsilon' \leq \varepsilon$ intersect C transversely. Let η be small enough with respect to ε . We define the set

$$\text{Tub} = \text{Tub}(\varepsilon, \eta) = B_\varepsilon \cap f^{-1}(D_\eta)$$

and call it a *Milnor tube*. In particular, if η is chosen small enough, Ehresmann's fibration theorem implies that

$$f|_{\text{Tub}^*} : \text{Tub}^* \rightarrow D_\eta^*$$

is a locally trivial fibration which is called *the Milnor fibration*. Here $\text{Tub}^* = \text{Tub} \setminus C$ and $D_\eta^* = D_\eta \setminus \{0\}$. For each $t \in D_\eta$, we denote by F_t the sets

$$F_t = f^{-1}(t) \cap B_\varepsilon \subset \text{Tub}.$$

When $t \neq 0$, the set F_t is *the Milnor fiber* at t . In this case, F_t is a, possibly disconnected, compact surface with non-empty boundary. The set $F_0 = C \cap B_\varepsilon$ is called the *central fiber* or the *special fiber*. For notational convenience we also denote F_0 by $C_\varepsilon = C \cap B_\varepsilon$.

2.1. The complex gradient as a lift

For the most of this section we essentially follow [A'C18].

Let ω be the standard real symplectic structure on \mathbb{C}^2 . We define a connection associated to the Milnor fibration on the tube as follows. For each $p \in \text{Tub} \setminus \{0\}$ we define the vector space

$$N_p^\omega := \{v \in T_p \text{Tub} : \omega(v, u) = 0 \text{ for all } u \in T_p F_{f^{-1}(f(p))}\}.$$

That is, N_p^ω is the symplectic orthogonal to the tangent space of the Milnor fiber that contains p . We consider the plane field

$$N^\omega := \bigcup_{p \in \mathbb{C}^2 \setminus \{0\}} N_p^\omega$$

which defines a connection on $\text{Tub} \setminus \{0\} \rightarrow D_\eta^*$. We call N^ω the *symplectic connection* associated with f .

Remark 2.1.1. In this remark we expose some properties of the symplectic connection.

- (1) By the non-degeneracy of ω we find that $\dim_{\mathbb{R}} N_p^\omega = 2$.

- (2) Since each fiber is a complex curve, the complex structure $J : T\mathbb{C}^2 \rightarrow T\mathbb{C}^2$ leaves invariant the tangent bundle to the fibers. So

$$\omega(u, v) = 0 \Leftrightarrow g_{\text{std}}(u, v) = \omega(u, Jv) = 0$$

where g_{std} is the standard Riemannian metric on \mathbb{C}^2 . Thus, the symplectic orthogonal to the tangent spaces of fibers coincides with the Riemannian orthogonal $N_p^{g_{\text{std}}}$ for each $p \in \text{Tub} \setminus \{0\}$.

- (3) Since f is a submersion on Tub^* we find that the map $df_p|_{N_p^\omega} : N_p^\omega \rightarrow T_{f(p)}\mathbb{C}$ is a \mathbb{C} -linear isomorphism (in particular conformal) for all $p \in \text{Tub}^*$, so N^ω is a connection for the Milnor fibration $\text{Tub}^* \rightarrow D_\eta^*$.

Let now $-t/|t|$ be the unit real radial vector field pointing inwards on D_η^* .

Definition 2.1.2. Let ξ^{lift} be the symplectic lift of $-t/|t|$ to Tub^* using the symplectic connection N^ω .

In the next lemma we recall an explicit formula the gradient of the logarithm of the absolute value of a holomorphic function and a characterization of it.

Lemma 2.1.3. Let $U \subset \mathbb{C}^n$ be an open subset and let $g : U \rightarrow \mathbb{C}$ be a holomorphic function. Then,

(1)

$$\nabla \log |g| = \left(\frac{\overline{\partial_1 g}}{\bar{g}}, \dots, \frac{\overline{\partial_n g}}{\bar{g}} \right)^\top$$

(2)

$$(Dg)(\nabla \log |g|) = \|\nabla \log |g|\|^2 g$$

where ∇ indicates the real gradient with respect to the standard Riemannian metric on \mathbb{C}^n and Dg is the differential of the function g .

PROOF. The first item 1 is a direct computation. For 2 again, the following direct computation

$$\begin{aligned} (Dg)(\nabla \log |g|) &= (\partial_1 g, \dots, \partial_n g) \cdot \left(\frac{\overline{\partial_1 g}}{\bar{g}}, \dots, \frac{\overline{\partial_n g}}{\bar{g}} \right)^\top \\ &= \frac{|\partial_1 g|^2}{\bar{g}} + \dots + \frac{|\partial_n g|^2}{\bar{g}} \\ &= \left(\frac{|\partial_1 g|^2}{|g|^2} + \dots + \frac{|\partial_n g|^2}{|g|^2} \right) g \\ &= \|\nabla \log |g|\|^2 g \end{aligned}$$

yields the result. \square

The following lemma relates the lift ξ^{lift} of the unit radial vector field and the gradient described before.

Lemma 2.1.4. The equality

$$\xi^{\text{lift}} = \frac{-1}{\|\nabla \log |f|\|^2 |f|} \cdot \nabla \log |f|$$

holds.

PROOF. Observe that the function $-\log|f| : \text{Tub}^* \rightarrow \mathbb{R}_{>0}$ takes constant values on $f^{-1}(\mathbb{S}_{\eta'}^1) \cap B_\varepsilon \subset \text{Tub}^*$, that is, on the preimage by f of circles of radius η' with $0 < \eta' < \eta$. By the definition of gradient, $-\nabla \log|f|$ is orthogonal with respect to the Riemannian metric g_{std} to the tangent spaces $T_p f^{-1}(\mathbb{S}_{\eta'}^1)$, so in particular it is g -orthogonal to the tangent spaces of the Milnor fibers and thus, by Remark 2.1.12, it is contained in N_p^ω . It follows from construction that $\xi^{\text{lift}}(p)$ is orthogonal to $T_p F_{f(p)}$. Since $dF_p|_{N_p^\omega} : N_p^\omega \rightarrow T_{f(p)}\mathbb{C}$ is conformal (Remark 2.1.1 3), the orthogonal complement to $\xi^{\text{lift}}(p)$ in N_p^ω is

$$T_p f^{-1}(\mathbb{S}_{\eta'}^1) \cap N_p^\omega.$$

This shows that there exists a positive (since both vector fields point in the same direction) real function k such that $\xi^{\text{lift}}(p) = k \cdot (-\nabla \log|f|)$ and we can compute it:

$$k^{-1} = \frac{\|Df(\nabla \log|f|)\|}{\|Df(\xi^{\text{lift}})\|} = \|Df(\nabla \log|f|)\|$$

because $\|Df(\xi^{\text{lift}})\| = 1$. So we conclude by applying Lemma 2.1.3, 2. \square

Once and for all, we put a name to this important vector field which is the central object studied in this work.

Definition 2.1.5. We define the vector field

$$\xi = -\nabla \log|f|.$$

Remark 2.1.6. (i) The vector fields ξ and ξ^{lift} have the same trajectories on Tub^* since they differ by a positive scalar function. For computational convenience, throughout this article we work with ξ instead of ξ^{lift} .

(ii) Furthermore, an analogous reasoning yields that these vector fields also have the same trajectories as $-\nabla|f|^2$.

(iii) Since $\arg(f)$ is constant along trajectories of ξ^{lift} (and ξ), these vector fields are tangent to $\arg(f)^{-1}(\theta) \subset \text{Tub}^*$ for all $\theta \in \mathbb{R}/2\pi\mathbb{Z}$.

2.2. The collapsing map

2.2.1. The collapsing map, $\rho : \text{Tub} \rightarrow C$, is defined as follows. Choose ε , and therefore also η , small enough. This means that $\text{Tub} = \text{Tub}(\varepsilon, \eta)$ is contained in an arbitrarily small neighborhood of 0 in \mathbb{C}^2 . In fact, given a small neighborhood U of $0 \in \mathbb{C}^2$, by a theorem of Łojasiewicz [Łoj84], we can choose ε small enough so that any trajectory of the vector field $-\nabla|f|^2$ starting at $p \in \text{Tub}$, does not escape U . Furthermore, each such trajectory γ_p satisfies:

- (a) it is defined on $\mathbb{R}_{\geq 0}$,
- (b) it has finite arc length, and
- (c) it converges to some point in U where $-\nabla|f|^2$ vanishes, i.e. a point of $C \cap U$.

In this construction, we can clearly replace the vector field $-\nabla|f|^2$ by $\xi = -\nabla \log|f|$, or the lifting ξ^{lift} , since these define the same trajectories in $U \setminus C$ (recall Remark 2.1.6 (i) and (ii) above). Note that if $p \in C$, then the trajectory of $-\nabla|f|^2$ is the constant path at p , and so the above results hold trivially.

Remark 2.2.2. For completeness, we recall how the result cited above follows from the existence of a Łojasiewicz exponent. Set $g = -|f|^2$. There exist $c > 0$ and $0 < \theta < 1$ so that in a neighborhood of the origin,

$$\|\nabla g\| \geq c|g|^\theta.$$

Let $x(t)$ be a trajectory of ∇g parametrized by arc length. This way, we have

$$\dot{x} = \frac{\nabla g}{\|\nabla g\|} = \frac{-\nabla \log |f|}{\|\nabla \log |f|\|} = \frac{\xi}{\|\xi\|}.$$

Here we assume that x is not a constant trajectory. This gives

$$\frac{dg(x(t))}{dt} = \langle \nabla g(x(t)), \dot{x} \rangle = \|\nabla g(x(t))\| \geq c|g(x(t))|^\theta,$$

and so (since $|g| = -g$)

$$\frac{d|g(x(t))|^{1-\theta}}{dt} = (1-\theta)|g(x(t))|^{-\theta} \frac{d|g(x(t))|}{dt} \leq -(1-\theta)c.$$

Therefore, a trajectory starting at p cannot be longer than

$$(1-\theta)c|g(p)|^{1-\theta} = (1-\theta)c|f(p)|^{2-2\theta}.$$

This shows that $x(t)$ has a limit, which must be a point where the vector field ∇g vanishes, i.e. a point on C .

Definition 2.2.3. With Tub as before, define the *collapsing map* $\rho : \text{Tub} \rightarrow C$ by setting

$$\rho(p) = \lim_{t \rightarrow \infty} \gamma_p(t), \quad p \in \text{Tub},$$

where γ_p is the trajectory of $-\nabla|f|^2$ starting at p (which by (a) is defined for all $t \in \mathbb{R}_{\geq 0}$). For $t \in D_\eta$, we set $\rho_t = \rho|_{F_t}$.

Definition 2.2.4. We say that a set K in a manifold with boundary M is a *spine* for M if $M \setminus K$ is a collar neighborhood of ∂M .

Lemma 2.2.6. Assume that $f = f_1^{r_1} \cdots f_s^{r_s}$, where f_1, \dots, f_s are irreducible, and set $C_i = f_i^{-1}(0)$. The collapsing map ρ has the following properties:

- (i) ρ is continuous and proper.
- (ii) The restriction of ρ_t to $F_t \setminus \rho_t^{-1}(0) \rightarrow C \setminus \{0\}$ is a local diffeomorphism.
- (iii) Let $q \in C_i \setminus \{0\}$, with $\|q\| < \varepsilon$. Then, for $|t|$ small enough, the fiber $\rho_t^{-1}(q)$ consists of r_i points.

PROOF. For (i), it suffices to show that ρ is continuous since Tub is compact. Let $p \in \text{Tub}$, set $q = \rho(p)$ and let V be a neighborhood of q in \mathbb{C}^2 . By 2.2.1, there exists a smaller neighborhood of q , $V' \subset V$ so that trajectories starting in V' do not escape V . The trajectory of ξ starting at p ends up in $q \in V'$, which means that the flow of ξ at some time sends a neighborhood U' of p to V' . As a result, trajectories starting in U' ultimately do not escape V , and so $\rho(U') \subset \overline{V}$, which proves continuity.

Next we prove (ii) and (iii). First, consider the case when $f = f_1^{r_1}$ has one branch with some multiplicity $r_1 \geq 1$, and f_1 is smooth. In this case, the vector fields $-\nabla|f|^2$ and $-\nabla|f_1|^2$ have the same trajectories, and the function $-|f_1|^2$ is Morse-Bott. In this case, the Milnor fiber F_t is the disjoint union of r_1 disks, and

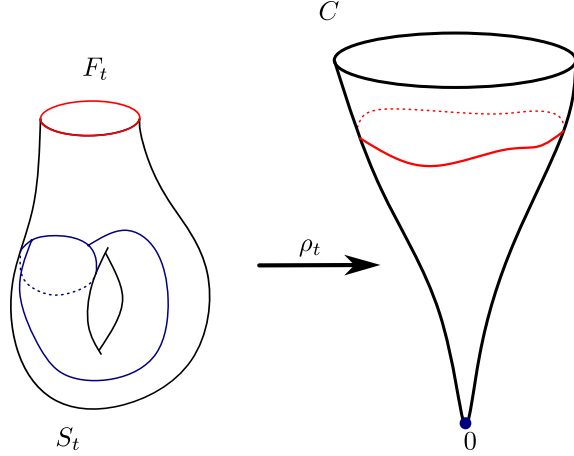


FIGURE 2.2.5. On the left, the Milnor fiber of the singularity $y^2 + x^3$. In blue we see the part of the Milnor fiber that maps to the origin by the collapsing map. In the central fiber we see the image of the boundary component of the Milnor fiber (red).

ρ_t embeds each of them in the smooth curve $\{f_1 = 0\}$. Thus, (ii) and (iii) hold in this case.

In general, assume that $p \in F_t \setminus \rho_t^{-1}(0)$ with $t \in D_\eta^*$, and set $q = \rho(p)$. Then there exist small neighborhoods $V \supset V' \ni q$ so that $C \cap V$ is a smooth curve with some multiplicity, and trajectories starting in V' do not escape V . The flow of ξ^{lift} at some time sends a neighborhood of p in F_t diffeomorphically to a neighborhood in $V' \cap F_{t'}$ for some t' . By the above case, for $|t'|$ small enough, $\rho_{t'}|_{V'} : V' \rightarrow C$ is a local diffeomorphism. This proves (ii).

For (iii), we can choose small neighborhoods V' and V in \mathbb{C}^2 with $q \in V' \subset V$ so that if $|t|$ is small, then $\rho_t^{-1}(q) \cap V'$ consists of r_i points. This follows from the case above, where $f = f_1^{r_i}$ and f_1 is smooth. If $V'' \subset V'$ is a closed neighborhood of q , then the complement $(C \cap B_\varepsilon) \setminus V'$ can be covered with finitely many neighborhoods with the property that if p is in any of them, then the trajectory starting at p does not escape $\text{Tub} \setminus V''$. As a result, $\rho_t^{-1}(q) \subset V''$ for $|t|$ small enough. \square

Corollary 2.2.7. *For $t \in D_t^*$, the complement of the spine in the Milnor fiber F_t is a collar neighborhood of the boundary,*

$$F_t \setminus \rho_t^{-1}(0) \cong \partial F_t \times (0, 1].$$

PROOF. The punctured central fiber is the union of trajectories of the vector field

$$\nabla((|x|^2 + |y|^2)|_{C \setminus \{0\}})$$

That is, the gradient (with respect to $g|_{C \setminus \{0\}}$) of the restriction of the square distance function to the central fiber. Each of these trajectories is transverse to all spheres $S_{\varepsilon'}^3$, for $0 \leq \varepsilon' \leq \varepsilon$. This gives a product structure

$$C \cap B_{\varepsilon'} \setminus \{0\} \cong (C \cap S_{\varepsilon'}^3) \times (0, 1]$$

for ε' small. This pulls back to a product structure on $F_t \setminus \rho_t^{-1}(0)$. \square

As we said in the introduction, this work is devoted to study the set of trajectories of ξ that converge to the origin. The closure of this set, by definition, contains the origin. After [Definition 2.2.4](#) and [Corollary 2.2.7](#), the following definition is justified.

Definition 2.2.8. The *total spine* $S \subset \text{Tub}$ and the *spine* $S_t \subset F_t$ of each Milnor fiber are defined as

$$S = \rho^{-1}(0), \quad S_t = \rho_t^{-1}(0), \quad t \in D_\eta.$$

2.3. Isometric coordinates

In this subsection we define the notion of *isometric coordinates* that we use throughout the text. This captures the idea that changing the metric by a linear transformation and taking a linear change of coordinates are equivalent operations and thus, one can always work with the standard metric if one is willing to change the equation of f .

Definition 2.3.1. For $A \in \text{GL}(\mathbb{C}, 2)$ define a Hermitian metric on \mathbb{C}^2 by setting

$$h_A(v, w) = w^* A^* A v.$$

In particular h_{id} is the standard metric. Equivalently, h_A is the metric obtained by pulling back the standard metric on \mathbb{C}^2 via the linear change of coordinates $A : \mathbb{C}^2 \rightarrow \mathbb{C}^2$. Associated with h_A we have its real part g_A which is a Riemannian metric and its imaginary part ω_A which is a symplectic form.

Two linear functions $x, y : \mathbb{C}^2 \rightarrow \mathbb{C}$ form *isometric coordinates* with respect to A if the induced linear map $(x, y) : (\mathbb{C}^2, g_A) \rightarrow (\mathbb{C}^2, g_{\text{id}})$ is an isometry.

2.4. Vector fields

In this subsection we recall some notions about vector fields and fix some notation.

Let ζ be a vector field defined on an open neighborhood U of an n -dimensional manifold M around a point $p \in M$. In local coordinates, ζ is given by

$$\zeta = (\zeta^1, \dots, \zeta^n) : U \rightarrow \mathbb{R} \times \mathbb{R}^n.$$

The following definition is inspired by the usual notion of Hessian when the vector field admits a potential.

Definition 2.4.1. Assume that $\zeta(p) = 0$. We define the *Hessian matrix* of ζ at $p \in M$ as the matrix of partial derivatives

$$\text{Hess}_p \zeta = \begin{pmatrix} \partial_1 \zeta^1(p) & \partial_2 \zeta^1(p) & \cdots & \partial_n \zeta^1(p) \\ \partial_1 \zeta^2(p) & \partial_2 \zeta^2(p) & \cdots & \partial_n \zeta^2(p) \\ \vdots & \vdots & \ddots & \vdots \\ \partial_1 \zeta^n(p) & \partial_2 \zeta^n(p) & \cdots & \partial_n \zeta^n(p) \end{pmatrix}.$$

The *Hessian* of ζ at p is the linear operator $T_p M \rightarrow T_p M$ represented by the above matrix.

Definition 2.4.2. A *singularity of a vector field* is a point p where the vector field is not defined (for example a puncture of M) or where the vector field takes the value 0.

We follow the nomenclature of the book [AR67], in particular Corollary 22.5 and text after.

Definition 2.4.3. A linear operator is *elementary* if its eigenvalues all have non-zero real part.

A singularity p of a vector field ζ where $\zeta(p) = 0$ is an *elementary singularity* if the Hessian of the vector field is elementary as an operator.

We say that a vector field ξ is *elementary* if it only has elementary singularities.

Elementary singularities allow us to apply the theorem of Grobman-Hartman and *linearize* the vector field near the singularity.

Example 2.4.4. A consequence of Grobman-Hartman is that there are only three types of elementary singularities (see Figure 2.4.5) that can appear in a vector field defined on a topological surface:

- (1) a *fountain* or *repeller*, which happens when the Hessian has two eigenvalues with positive real part,
- (2) a *sink* or *attractor*, when the two eigenvalues of the Hessian have negative real part, and
- (3) a *saddle point*, when one eigenvalue has positive real part and the other has negative real part.

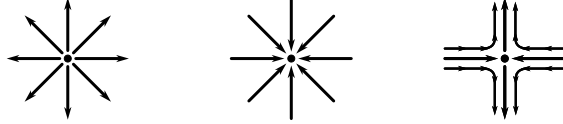


FIGURE 2.4.5. From left to right: a fountain, a sink and a saddle point.

Next, we recall the notions of winding number function of a curve relative to a vector field and Poincaré-Hopf index of a vector field. For more on winding number functions see [HJ89] or [Chi72].

Definition 2.4.6. Let ζ be a vector field on an oriented surface M with punctures and boundary components. Let $\gamma : S^1 \rightarrow M$ be a simple closed oriented curve in M . Assume that ζ does not vanish at any point of γ . We define the *winding number of ζ around γ* by

$$w_\zeta(\gamma) = \frac{1}{2\pi} \int_{S^1} d\text{ang}((\gamma'(t), \zeta(\gamma(t))))$$

where $\text{ang}(\cdot, \cdot)$ is the angle function with respect to some metric on M . It can be shown that it does not depend on the chosen metric and that it is also invariant under isotopies of γ that do not cross any singularities of ζ .

Assume that the curve γ is the boundary of a small disk centered at an isolated singularity p (puncture or zero) of ζ , and that γ is oriented as the boundary of such disk. Then $w_\zeta(\gamma)$ relates to the classical Poincaré-Hopf index of ζ at p denoted by $\text{Ind}_\zeta(p)$ as follows

$$(2.4.7) \quad w_\zeta(\gamma) = 1 - \text{Ind}_\zeta(p).$$

Let L be a boundary component of M and let $N(L)$ be a small collar neighborhood of L . Assume that ζ does not vanish at any point of $N(L) \setminus L$. We define the

winding number of ζ around L , denoted by $w_\zeta(L)$, as $w_\zeta(L')$ where L' is a closed curve in $N(L) \setminus L$ parallel to L and oriented with the orientation induced by M on L .

Example 2.4.8. Consider the vector field $\zeta = \bar{z}^k$ on \mathbb{C} with $k \geq 0$. This vector field has, outside the origin and up to scaling, the same integral lines as the vector field z^{-k} . Therefore we can compute its index at the origin by the Cauchy integral formula and get

$$(2.4.9) \quad \text{Ind}_\zeta(0) = -k.$$

Note that in this case the vector field \bar{z}^k defines a $k + 1$ -pronged singularity at the origin (see the left part of [fig. 2.4.10](#)). If the surface M has a boundary component

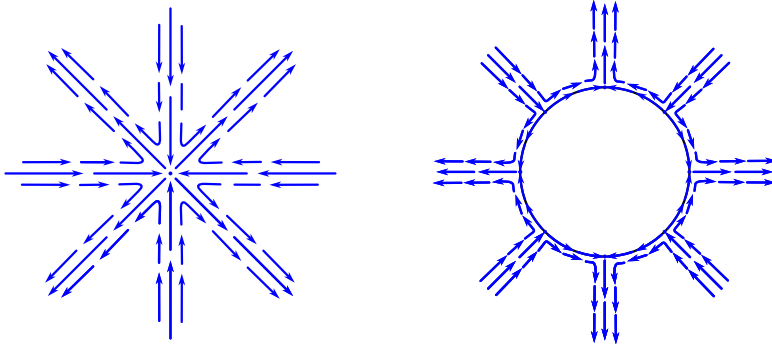


FIGURE 2.4.10. A 4-pronged singularity on the left corresponding to the vector field \bar{z}^3 . And a 4-pronged boundary on the right.

L such that after being contracted to a point, looks like a $k + 1$ -pronged singularity (see the right part of [fig. 2.4.10](#)), then

$$w_\zeta(L) = 1 + k$$

Similarly, for the vector field $\zeta = z^k$ on \mathbb{C} with $k \geq 0$, we get a $k + 1$ -petal singularity (see [fig. 2.4.12](#)). By a similar computation the index in this case is

$$(2.4.11) \quad \text{Ind}_\zeta(0) = k.$$

And, if M has a boundary component L such that after being contracted to a point, looks like a $k + 1$ -petal singularity, then

$$w_\zeta(L) = 1 - k$$

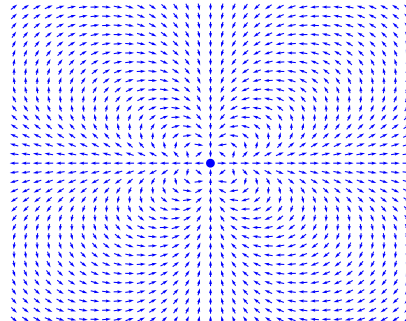


FIGURE 2.4.12. The vector field near the singularity of the vector field given by z^3 : a 4-petal singularity.

CHAPTER 3

Embedded Resolutions

In this section we explain several notions related to the resolutions of plane curve singularities, we also introduce notation and fix our conventions. We start by talking about different embedded resolutions and their dual graphs. We introduce the *group of cycles* associated with a modification and the notion of *initial part* and *vanishing order* of a function with respect to a variable or hypersurface. The latter two concepts play a central role in many of the subsequent proofs of this work.

After this, we introduce the *maximal* and *canonical* cycles which lead to the definition of two numerical invariants, c_0 and c_1 , which allow us later to describe precisely the spine. We also include easy algorithms to compute them from the resolution process. For more details on the invariants and classical objects defined in these subsections, see [Ném99] or [Wal04].

In the last two subsections we introduce the structure of directed graph on the dual resolution graph Γ and we introduce the notion of tangent associated with a divisor.

3.1. Embedded resolutions

Notation 3.1.1. Let $(C, 0) \subset (\mathbb{C}^2, 0)$ be an isolated plane curve singularity defined by a germ $f : (\mathbb{C}^2, 0) \rightarrow (\mathbb{C}, 0)$. Let $\pi : Y \rightarrow \mathbb{C}^2$ be an embedded resolution, that is, π is a modification of \mathbb{C}^2 with $\pi^{-1}(0)$ a strict normal crossings divisor. Factorize π as

$$(3.1.2) \quad \pi = \pi_0 \circ \pi_1 \circ \cdots \circ \pi_s$$

where $\pi_i : (Y_i, D_i) \rightarrow (Y_{i-1}, p_i)$ are blow-ups. Set also $\bar{\pi}_i = \pi_i \circ \cdots \circ \pi_0 : Y_i \rightarrow \mathbb{C}^2$. In particular, π_0 is the usual blow-up of \mathbb{C}^2 at the origin. We identify the divisors $D_i \in Y_i$ with their strict transforms in Y_j for $j > i$. Set

$$D = \bigcup_{i=0}^s D_i \subset Y = Y_s.$$

Let \tilde{C} be the strict transform of C in Y .

Examples of embedded resolutions that appear in this work are

$$\pi_{\min} : (Y_{\min}, D_{\min}) \rightarrow (\mathbb{C}^2, 0)$$

which is the minimal embedded resolution. Similarly, we have

$$\pi_{\text{pol}} : (Y_{\text{pol}}, D_{\text{pol}}) \rightarrow (\mathbb{C}^2, 0)$$

which is the minimal embedded resolution that also resolves the generic polar locus (cf. [Section 5.1](#)).

Notation 3.1.3. Let Γ be the dual graph associated with the resolution $Y \rightarrow \mathbb{C}^2$ and the function f . This graph has set of vertices $\mathcal{W} = \mathcal{V} \cup \mathcal{A}$ where $\mathcal{V} = \{0, 1, \dots, s\}$, and \mathcal{A} is in bijection with the branches of $(C, 0)$, where $(C, 0) = \bigcup_{a \in \mathcal{A}} (C_a, 0)$. Then $i, j \in \mathcal{W}$ are joined by an edge ij in Γ if and only if $D_i \cap D_j \neq \emptyset$. Here, if $a \in \mathcal{A}$, we are denoting by D_a the strict transform of C_a in Y . In this case, we denote by p_{ij} the intersection point $D_i \cap D_j$.

Set $D_{\mathcal{V}} = D$, as well as $D_{\mathcal{A}} = \bigcup_{a \in \mathcal{A}} D_a$ and $D_{\mathcal{W}} = \bigcup_{w \in \mathcal{W}} D_w$. For $i \in \mathcal{W}$, set

$$D_i^\circ = D_i \setminus \bigcup_{j \in \mathcal{W} \setminus \{i\}} D_j.$$

Similarly we can define the graphs Γ_i associated with the modifications $\bar{\pi}_i : Y_i \rightarrow \mathbb{C}^2$ for $i = 0, 1, \dots, s$. These have a set of vertices $\mathcal{W}_i = \mathcal{V}_i \cup \mathcal{A}_i$. Furthermore, for each j, k with $j < k$ there is a canonical injective map $\mathcal{V}_j \rightarrow \mathcal{V}_k$ and a bijective map $\mathcal{A}_j \rightarrow \mathcal{A}_k$.

The graphs Γ and Γ_i (for all i) are trees (see [Wal04, Section 3.6]). In particular, given two vertices $j, k \in \mathcal{W}$ or \mathcal{W}_i , there is a unique *geodesic* (path with the smallest number of edges possible) joining j and k .

Next we recall the notion of *group of cycles* associated with a modification of \mathbb{C}^2 .

Definition 3.1.4. The *group of cycles* L associated with the modification $Y \rightarrow \mathbb{C}^2$ is the free Abelian group generated by the exceptional divisors D_i for $i \in \mathcal{V}$.

Remark 3.1.5. Set $V = \pi^{-1}(B_\varepsilon)$, where B_ε is a Milnor ball. By, [Wal04, Lemma 8.1.1], the group of cycles is isomorphic to $H_2(V; \mathbb{Z}) \cong H^2(V, \partial V; \mathbb{Z})$, that is, this homology group is freely generated by the homology classes of exceptional components D_i , $i \in \mathcal{V}$. Furthermore, since $\partial V \cong S^3$, the long exact sequence of the pair $(V, \partial V)$ induces an isomorphism

$$H_2(V; \mathbb{Z}) \rightarrow H_2(V, \partial V; \mathbb{Z}) \cong H^2(V; \mathbb{Z}).$$

As a result, with the identification $L = H_2(V, \mathbb{Z})$, Poincaré duality induces a unimodular pairing

$$(\cdot, \cdot) : L \times L \rightarrow \mathbb{Z}.$$

Definition 3.1.6. We define the *antidual basis* D_j^* , $j \in \mathcal{V}$ as the unique elements $D_j^* \in L$ satisfying $(D_i, D_j^*) = -\delta_{ij}$.

3.2. Initial part and vanishing order

Here we define several notions related to the order of vanishing of a real analytic function taking values in \mathbb{C} .

Definition 3.2.1. Let $g : (\mathbb{C}^2, 0) \rightarrow (\mathbb{C}, 0)$ be a Laurent series in coordinates u, v given by

$$g(u, v) = \sum_{i, j, k, l \in \mathbb{Z}} a_{ijkl} u^i v^j \bar{u}^k \bar{v}^l.$$

Let $\text{ord } g = \min \{i + j + k + l \mid a_{ijkl} \neq 0\}$. Then, we define the *initial part* of g as

$$\text{in } g(u, v) = \sum_{i+j+k+l=\text{ord } g} a_{ijkl} u^i v^j \bar{u}^k \bar{v}^l.$$

Definition 3.2.2. Let $g : (\mathbb{C}^2, 0) \rightarrow (\mathbb{C}, 0)$ be a Laurent series in coordinates u, v given by

$$g(u, v) = \sum_{i,j,k,l \in \mathbb{Z}} a_{ijkl} u^i v^j \bar{u}^k \bar{v}^l.$$

We define the *vanishing order* of g with respect to u as

$$\text{ord}_u g = \min \{i + k \mid a_{ijkl} \neq 0\}.$$

Then, we define the *initial part* of g with respect to u as the Laurent series given by

$$(\text{in}_u g)(u, v) = \sum_{i+k=\text{ord}_u g} a_{ijkl} u^i v^j \bar{u}^k \bar{v}^l$$

Definition 3.2.3. Let $h : (\mathbb{C}^2, 0) \rightarrow (\mathbb{C}, 0)$ be the germ of a real analytic function, and let $\pi : Y \rightarrow \mathbb{C}^2$ be as in [Notation 3.1.1](#) and let $p \in D_i \subset Y$ with $i \in \mathcal{V}$. And let $U \subset Y$ a coordinate neighborhood around p with coordinates u, v so that $D_i \cap U$ is defined by $u = 0$. We define the *vanishing order of h along D_i* by

$$\text{ord}_{D_i}(h) = \text{ord}_u(\pi^* h).$$

Remark 3.2.4. Given a function $h : (\mathbb{C}^2, 0) \rightarrow (\mathbb{C}, 0)$ and a modification $\pi : Y \rightarrow \mathbb{C}^2$ with dual graph Γ , there is a cycle associated to $\pi^* h$ defined by

$$(\pi^* h) = \sum_{i \in \mathcal{V}} \text{ord}_{D_i}(h) D_i.$$

In the antidual basis D_j^* , the cycle takes the form

$$(\pi^* h) = \sum_{i \in \mathcal{V}} a_i D_i^*,$$

where a_i is the multiplicity intersection of D_i and the strict transform of $\{h = 0\}$, that is, the number of intersection points of D_i with a small perturbation of the strict transform of $\{h = 0\}$. (See [[Ném99](#)]).

Definition 3.2.5. For $i \in \mathcal{W}$, we set

$$m_i = \text{ord}_{D_i}(f).$$

Note that, if $a \in \mathcal{A}$, then m_a is the vanishing order of f along one of the branches of C (which might be bigger than 1 if f has non isolated critical points).

3.3. Invariants of the resolution: c_0, c_1 and the canonical divisor

In this subsection, we introduce numerical invariants of the modification $Y \rightarrow \mathbb{C}^2$. In particular, these do not depend on f or the metric g . All of this subsection is either part of the classical theory of plane curve singularities, or it may be deduced from [[BdSFP22](#)], (for example [Lemma 3.3.7](#) is implied by [[BdSFP22](#), Lemma 3.6]). However, since our setting is different and we need to fix notation, we briefly rework this theory.

Definition 3.3.1. Denote by Z_{\max} the *maximal cycle* in Y , and denote by $c_{0,i}$ its coefficients. Thus,

$$Z_{\max} = \sum_{i \in \mathcal{V}} c_{0,i} D_i.$$

and we have $c_{0,i} = \text{ord}_{D_i}(\ell)$, where $\ell : \mathbb{C}^2 \rightarrow \mathbb{C}$ is a generic linear function. Here *generic* means that the strict transform of $\{\ell = 0\}$ intersects D_0° , or equivalently, that $\{\ell = 0\}$ is not a tangent of C at the origin.

Since $c_{0,i} = \text{ord}_{D_i}(\ell)$ we can similarly define these numbers for arrowheads, that is for $i \in \mathcal{A}$. In this case $c_{0,i} = \text{ord}_{D_i}(\ell) = 0$.

Remark 3.3.2. We recall a basic fact about vanishing orders of linear functions (see for example [Ném99]). If ℓ is a generic linear function and ℓ' is any other linear function then,

$$\text{ord}_{D_i}(\ell') \geq \text{ord}_{D_i}(\ell)$$

for all $i \in \mathcal{V}$. We also have

$$c_{0,i} = \min\{\text{ord}_{D_i}(x), \text{ord}_{D_i}(y)\}$$

for x, y any coordinate system in \mathbb{C}^2 .

Definition 3.3.3. Denote by K the *canonical cycle* on Y and by $\nu_i - 1$ its coefficients. Thus,

$$K = \sum_{i \in \mathcal{V}} (\nu_i - 1) D_i.$$

A *canonical divisor* on a smooth variety X of dimension d is defined as the divisor defined by any section of the canonical sheaf Ω_X^d . The canonical cycle defined above is the unique canonical divisor supported on the exceptional set of π . In fact, for $d = 2$ take the standard holomorphic two-form $dx \wedge dy \in \Omega_{\mathbb{C}^2}^2$ on \mathbb{C}^2 . Then K is the divisor defined by the section $\pi^*(dx \wedge dy)$ of Ω_Y^2 .

K can be seen as a Cartier divisor as follows. If $U \subset Y$ is a coordinate chart, with coordinates u, v , we have a Jacobian matrix

$$\text{Jac } \pi(u, v) = \begin{pmatrix} \partial_u \pi^* x & \partial_v \pi^* x \\ \partial_u \pi^* y & \partial_v \pi^* y \end{pmatrix}.$$

The pairs $(U, \det \text{Jac } \pi)$ constitute a Cartier divisor, whose associated Weil divisor is K .

Yet another characterization goes as follows. K is the unique exceptional divisor satisfying the *adjunction formulas*:

$$(K, D_i) = -D_i^2 - 2, \quad i \in \mathcal{V}.$$

3.3.4. Let $p \in D_i^\circ$ for some $i \in \mathcal{V}$, and choose a (small) coordinate neighborhood U of p . Assume that x, y are coordinates in \mathbb{C}^2 , with x a generic linear function. Then the function π^*x vanishes with order $c_0 = c_{0,i}$ along D_i , and does not vanish on $U \setminus D_i$. As a result, coordinates u, v can be chosen for U so that $\pi^*x = u^{c_0}$. Expand the second coordinate around $p \in U$ as

$$\pi^*y = \sum_{k \geq c_0} u^k g_k(v),$$

where g_k are holomorphic functions defined in a neighborhood of p in D_i° (possibly smaller than $U \cap D_i^\circ$). We are interested in the smallest number k so that g_k really depends on v , i.e. is not constant. Denote this number by c_1 . The Jacobian of π in these coordinates has a triangular form

$$(3.3.5) \quad \begin{pmatrix} \partial_u \pi^* x & \partial_v \pi^* x \\ \partial_u \pi^* y & \partial_v \pi^* y \end{pmatrix} = \begin{pmatrix} c_0 u^{c_0-1} & 0 \\ \sum_k k u^{k-1} g_k(v) & \sum_k u^k g'_k(v) \end{pmatrix}$$

and so c_1 is the order of vanishing of $\partial_v \pi^* y$ along D_i° . That is

$$\text{ord}_u(\partial_v \pi^* y) = c_1.$$

Furthermore, we see that

$$\text{ord}_u(\det \text{Jac } \pi) = c_0 + c_1 - 1.$$

But this order of vanishing is $\nu_i - 1$ (recall [Definition 3.3.3](#)), which is independent of the choices we made so far. This motivates the following definition of the numbers $c_{1,i}$:

Definition 3.3.6. For each vertex $i \in \mathcal{V}$, set

$$c_{1,i} = \nu_i - c_{0,i}.$$

As we did in [Definition 3.3.1](#), just set $c_{1,i} = 0$ for $i \in \mathcal{A}$.

Lemma 3.3.7. Let $\pi_i : (Y_i, D_i) \rightarrow (Y_{i-1}, p_i)$ be the i -th blow up as in [Notation 3.1.1](#). Then,

- If $i = 0$, then

$$c_{0,0} = c_{1,0} = 1.$$

- If there is $j < i$, such that p_i lies on a smooth point of the exceptional divisor D_j , that is $p_i \in D_j^\circ$, then

$$c_{0,i} = c_{0,j}, \quad c_{1,i} = c_{1,j} + 1.$$

- If there are $j, k < i$, such that p_i lies at the intersection, $p_i \in D_j \cap D_k$, then

$$c_{0,i} = c_{0,j} + c_{0,k}, \quad c_{1,i} = c_{1,j} + c_{1,k}.$$

PROOF. The first equality is a direct computation using the usual coordinates $\pi_0^* x = u, \pi_0^* y = uv$. The two formulas for $c_{0,i}$ follow immediately, since this is the vanishing of a generic linear function along the divisor D_i (see the more general, [[Wal04](#), Lemma 8.1.2]). The formula for $c_{1,i}$ follows, using the [Definition 3.3.6](#), and the well known fact (see the proof of [[Wal04](#), Proposition 8.1.8]) that $\nu_i = \nu_j + 1$ if p_i is a smooth point, and $\nu_i = \nu_j + \nu_k$ if p_i is an intersection point of two divisors. \square

As a direct consequence of the recursive formulas, we have the following corollary.

Corollary 3.3.8. For any $i \in \mathcal{V}$, we have $c_{1,i} \geq c_{0,i}$, with equality if and only if $i = 0$.

The next important corollary yields a hierarchy on the set of vertices \mathcal{V} . We make explicit use of this hierarchy in the next subsection and throughout the rest of the paper.

Corollary 3.3.9. If i, j are neighbors in the resolution graph Γ , then we have a nonzero determinant

$$(3.3.10) \quad \begin{vmatrix} c_{0,i} & c_{1,i} \\ c_{0,j} & c_{1,j} \end{vmatrix} \neq 0.$$

Furthermore, the above determinant is negative if and only if the geodesic (in Γ) from 0 to i passes through j .

PROOF. We use induction on $i = 0, 1, \dots, s$. Assume the statement holds for Γ_{i-1} . We recall from [Notation 3.1.3](#) that the set of vertices \mathcal{V}_{i-1} of Γ_{i-1} naturally embeds in the set of vertices \mathcal{V}_i of Γ_i . Actually, there is a unique extra vertex $i \in \mathcal{V}_i$ that is not in \mathcal{V}_{i-1} . We treat two different cases depending on whether p_i is a smooth point or an intersection point between two divisors (see also [fig. 3.4.2](#)).

Case 1. If p_i lies on a smooth point of D_j , then there is a unique edge ij in Γ_i that is not in Γ_{i-1} . In this case i is further from 0 than j , and [Lemma 3.3.7](#) gives

$$\begin{vmatrix} c_{0,i} & c_{1,i} \\ c_{0,j} & c_{1,j} \end{vmatrix} = c_{0,i}c_{1,j} - c_{1,i}c_{0,j} = c_{0,i}c_{1,j} - (c_{1,j} + 1)c_{0,i} = -c_{0,i} < 0.$$

Case 2. If p_i is the intersection point $D_j \cap D_k$, then there are two edges ik and ij in Γ_i that are not in Γ_{i-1} . In this case, [Lemma 3.3.7](#) gives

$$\begin{vmatrix} c_{0,i} & c_{1,i} \\ c_{0,j} & c_{1,j} \end{vmatrix} = \begin{vmatrix} c_{0,k} & c_{1,k} \\ c_{0,i} & c_{1,i} \end{vmatrix} = \begin{vmatrix} c_{0,k} & c_{1,k} \\ c_{0,j} & c_{1,j} \end{vmatrix}$$

because

$$c_{0,i} = c_{0,j} + c_{0,k}, \quad c_{1,i} = c_{1,j} + c_{1,k}$$

and row operations preserve determinants. \square

Corollary 3.3.11. *If $i \in \mathcal{V}$ is a neighbor of the vertex 0, which corresponds to the first blow-up, then $c_{i,1} = c_{0,i} + 1$.*

3.4. Directions on the dual graph

We endow Γ with the structure of a directed graph and deduce some combinatorial properties of this structure in terms of c_0 and c_1 .

Definition 3.4.1. The graph Γ is seen as a directed graph as follows. Let i, j be neighbors in Γ . The edge ij is directed from j to i if and only if the determinant [eq. \(3.3.10\)](#) is negative. In order to express that the edge ij is oriented from j to i we write $j \rightarrow i$.

Similarly, the graphs Γ_i corresponding to the modifications $\bar{\pi}_i : Y_i \rightarrow \mathbb{C}^2$ are directed for each $i = 0, 1, \dots, s$ following the same criterion.

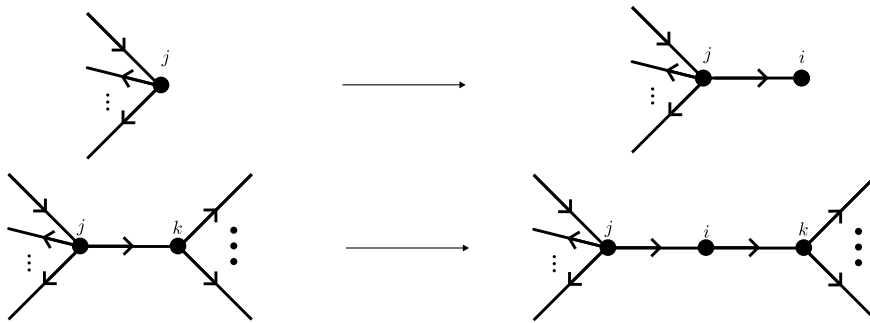


FIGURE 3.4.2. Effect of a blow-up on directed graphs. On top the effect of blowing up a smooth point at D_j . On bottom, the effect of blowing up the intersection point $D_j \cap D_k$.

Remark 3.4.3. The orientations of the edges defined in [Definition 3.4.1](#) are the same as the ones induced by the criterion:

“orient an edge ij from j to i if i is further from 0 than j .”

Observe that each vertex $i \in \mathcal{V}$ with $i \neq 0$ has exactly one neighbor j such that $j \rightarrow i$. This allows the following definition.

Definition 3.4.4. Let i be a vertex in the directed graph Γ , as above. If $i \neq 0$, let j be the unique neighbor of i such that $j \rightarrow i$. The *branch* ([fig. 3.4.6](#)) of Γ at i is

- (1) Γ , if $i = 0$ and,
- (2) otherwise, the connected component of Γ with the edge ji removed, containing i .

Remark 3.4.5. The branch of Γ at i is a tree rooted at i (note that i is the vertex which is the closest to 0 among all vertices of the branch). Moreover, if Ξ is a branch of Γ at i then, it satisfies that if $j \in \mathcal{W}_\Xi$ and $j \rightarrow k$, then $k \in \mathcal{W}_\Xi$.

Arrowheads in Γ are included in the above definition. Thus, the branch at i contains a subset of the arrowheads of Γ .

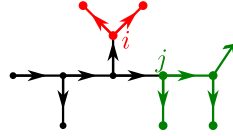


FIGURE 3.4.6. In red the branch at the vertex i and in green the branch at the vertex j .

Lemma 3.4.7. Let $i, j \in \mathcal{V}$, and assume that Γ has an edge $j \rightarrow i$. If $g \in \mathcal{O}_{\mathbb{C}^2,0}$, then

$$\det \begin{pmatrix} c_{0,i} & \text{ord}_{D_i}(g) \\ c_{0,j} & \text{ord}_{D_j}(g) \end{pmatrix} \leq 0.$$

If $\bar{\mathcal{V}} \subset \mathcal{V}$ is the set of vertices on the branch of Γ at i , then equality holds if and only if the strict transform of the curve defined by $g = 0$ does not intersect any D_k for $k \in \bar{\mathcal{V}}$.

PROOF. In this proof, cycles are considered in the group $L \otimes \mathbb{Q} \simeq H_2(V; \mathbb{Q})$. Set $n_k = \text{ord}_{D_k}(g)$ for $k \in \mathcal{V}$, and $Z = \sum_k n_k D_k \in L$. Thus, Z is the cycle associated with $\pi^* g$. This cycle can be written in terms of the antidual basis as $Z = \sum_{k \in \mathcal{V}} a_k D_k^*$, with $a_k \geq 0$ (recall [Remark 3.2.4](#)).

Let Γ be the branch of Γ at i , with vertex set $\bar{\mathcal{V}} \subset \mathcal{V}$. Since the intersection form is negative definite, there exist unique rational cycles \bar{D}_k^* for $k \in \bar{\mathcal{V}}$ supported on $\bar{\Gamma}$ satisfying $(\bar{D}_k^*, D_l) = -\delta_{k,l}$ for $l \in \bar{\mathcal{V}}$, and furthermore, \bar{D}_k^* has positive coefficients in the standard basis $\{D_i\}_{i \in \bar{\mathcal{V}}}$.

Define $\bar{Z} = \sum_{k \in \bar{\mathcal{V}}} a_k \bar{D}_k^*$. Then $\bar{Z} = \sum_{k \in \bar{\mathcal{V}}} \bar{n}_k D_k$, with nonnegative coefficients $\bar{n}_k \in \mathbb{Q}$. For $k \in \bar{\mathcal{V}}$, set $n'_k = n_k - \bar{n}_k$ and $Z' = \sum_{k \in \bar{\mathcal{V}}} n'_k D_k$. Thus, Z' is supported on $\bar{\Gamma}$, and we have

$$(Z', D_k) = -n_j \delta_{ik}, \quad k \in \bar{\mathcal{V}}.$$

Indeed, if $k \in \bar{\mathcal{V}}$, with $k \neq i$, then D_k only intersects exceptional divisors D_l with $l \in \bar{\mathcal{V}}$, and so

$$(Z', D_k) = (Z, D_k) - (\bar{Z}, D_k) = (-a_k) - (-a_k) = 0.$$

If, however, $k = i$, then $D_k = D_i$ intersects D_j once, but no other D_l with $l \in \mathcal{V} \setminus \bar{\mathcal{V}}$, and so in this case

$$(Z', D_k) = (Z - n_j D_j, D_k) - (\bar{Z}, D_k) = (-a_k) - n_j - (-a_k) = -n_j.$$

As a result, $Z' = n_j \bar{D}_i^*$.

In a similar way, if we set $\bar{Z}_{\max} = \sum_{k \in \bar{\mathcal{V}}} c_{0,k} D_k$, we have $(\bar{Z}_{\max}, D_k) = -c_{0,j} \delta_{ik}$, i.e. $\bar{Z}_{\max} = c_{0,j} \bar{D}_i^* = c_{0,j}/n_j Z'$. As a result,

$$n_i = n'_i + \bar{n}_i \geq n'_i = \frac{n_j c_{0,i}}{c_{0,j}},$$

and so the determinant from the statement of this lemma equals $c_{0,i} n_j - c_{0,j} n_i \leq 0$. Furthermore, we have equality if and only if all the a_k vanish for $k \in \bar{\mathcal{V}}$. But these coefficients are nothing but the intersection between the strict transform of the vanishing set of g and D_k . \square

Example 3.4.8. We consider the case of a toric modification of \mathbb{C}^2 , see [Ful93] for definitions used here. Let Δ be a regular subdivision of the positive quadrant. This gives a modification $\pi_\Delta : Y \rightarrow \mathbb{C}^2$, where Y is smooth. An irreducible component of the exceptional divisor corresponds to a ray $\rho \in \Delta$ generated by a unique primitive vector $(a, b) \in \mathbb{Z}^2$ with $a, b > 0$ and $\gcd(a, b) = 1$. Call the component D_ρ . We can choose an adjacent ray θ generated similarly by (c, d) , so that $\eta = \rho + \theta$ is a two-dimensional cone in Δ and $ad - bc = 1$. The affine toric variety $U_\eta \cong \mathbb{C}^2$ provides a coordinate neighborhood containing all but one point of D_ρ . Denoting by u, v the coordinates in D_η , we have

$$\pi_\Delta(u, v) = (u^a v^c, u^b v^d), \quad U_\eta \cap D_\rho = \{u = 0\}.$$

We therefore have $\text{ord}_{D_\rho} x = a$, $\text{ord}_{D_\rho} y = b$ and so $c_{0,\rho} = \min\{a, b\}$. Assuming that $a \leq b$, take a local coordinate change $\tilde{u} = uv^{a/c}, \tilde{v} = v$. Then we have $x = \tilde{u}^{c_{0,\rho}}$, and $y = \tilde{u}^b \tilde{v}^{d-bc/a}$. It follows that $c_{1,\rho} = b = \max\{a, b\}$.

3.5. The tangent associated with a divisor

We associate a tangent to each connected component of $\Gamma \setminus \{0\}$ and prove an easy, but useful, inequality of vanishing orders of linear functions.

Definition 3.5.1. Setting $\pi' = \pi_1 \circ \dots \circ \pi_s$, we have a factorization $\pi = \pi_0 \circ \pi'$. For $p \in D \subset Y$, we define the *tangent associated with p* as the line in \mathbb{C}^2 corresponding to the point $\pi'(p) \in D_0 \subset Y_0$. If $i \neq 0$, then the tangent associated with $p \in D_i$ is independent of p . So whenever $i \neq 0$, we also speak of the *tangent associated with D_i* .

The following lemma expresses the idea that tangents are precisely the *non-generic* complex lines relative to a given plane curve.

Lemma 3.5.2. *Let $i \in \mathcal{V} \setminus \{0\}$, and let x, y be linear coordinates in \mathbb{C}^2 such that $\{y = 0\}$ is the tangent associated with D_i . Then*

$$\text{ord}_{D_i}(y) > \text{ord}_{D_i}(x) = c_{0,i}.$$

PROOF. Since $\{x = 0\}$ is not the tangent associated with D_i , the vanishing order of π^*x along D_i is that of a generic linear function which is, by definition

(recall [Definition 3.3.1](#)) $c_{0,i}$. In particular, since y is another linear function, by [Remark 3.3.2](#) we have the inequality

$$\text{ord}_{D_i}(y) \geq \text{ord}_{D_i}(x).$$

The fact that $\{y = 0\}$ is the tangent associated to D_i implies that its strict transform by the first blow up π_0 does not pass through D_0° (it has to pass through one of the intersection, let's say p points of the strict transform of C by π_0). Since we are assuming that $i \neq 0$, we know that the resolution $\pi = \pi_0 \circ \pi_1 \circ \dots \circ \pi_s$ includes the blow up at $p \in D_0$. Let $\pi_k : Y_k \rightarrow Y_{k-1}$ be the blow up at p . Then $\text{ord}_{D_k}(x) = 1$ and $\text{ord}_{D_k}(y) = 2$. Necessarily $i \geq k$ and after each new blow up, the order of vanishing of y increases at least as that of x . This settles the strict inequality. \square

CHAPTER 4

The Real Oriented Blow-up

In this section, we recall the definition of the real oriented blow-up of an embedded resolution along the exceptional set. This construction has been used before by other authors, see for example [A'C75] or, in a more general setting, [KN99].

Let $(Y, D) \rightarrow (\mathbb{C}^2, 0)$ be a modification of the origin as above ([Notation 3.1.1](#)). Denote by $\sigma_i : Y_i^{\text{ro}} \rightarrow Y$ the *real oriented blow-up* of Y along the submanifold $D_i \subset Y$ for $i \in \mathcal{W}$ constructed as follows. If $U \subset Y$ is a chart with coordinates u, v such that $u = 0$ is an equation for $D_i \cap U$, then we take a coordinate chart $U^{\text{ro}} \subset Y_i^{\text{ro}}$ with coordinates $r, \alpha, v \in \mathbb{R}_{\geq 0} \times \mathbb{R}/2\pi\mathbb{Z} \times \mathbb{C}$, where r and α are polar coordinates for u , that is:

$$(4.0.1) \quad r = |u| : U^{\text{ro}} \rightarrow \mathbb{R}, \quad \alpha = \arg(u) : U^{\text{ro}} \rightarrow \mathbb{R}/2\pi\mathbb{Z}.$$

We can cover D_i by such charts in order to define an atlas for Y_i^{ro} . In each of these charts, the map σ_i is given by $\sigma_i(r, \theta, v) = (re^{i\theta}, v)$. Denote the fiber product of these maps by

$$(4.0.2) \quad \sigma = \bigtimes_{i \in \mathcal{W}} \sigma_i : (Y^{\text{ro}}, D_{\mathcal{W}}^{\text{ro}}) \rightarrow (Y, D_{\mathcal{W}}).$$

The spaces Y_i^{ro} are manifolds with boundary, and the space Y^{ro} is a manifold with corners and, as a topological manifold, its boundary ∂Y^{ro} coincides with $D_{\mathcal{W}}^{\text{ro}}$. Denote by π^{ro} the composition

$$\pi^{\text{ro}} = \pi \circ \sigma : Y^{\text{ro}} \rightarrow \text{Tub.}$$

Similarly, we can consider the real oriented blow up of \mathbb{C} at the origin

$$\sigma' : \mathbb{C}^{\text{ro}} \rightarrow \mathbb{C}.$$

In this case, $\mathbb{C}^{\text{ro}} \simeq \mathbb{R}_{\geq 0} \times \mathbb{R}/2\pi\mathbb{Z}$ and $\sigma'(r, \theta) = re^{2\pi i\theta}$. The real-oriented blow up construction is functorial, that is, there exists a well defined map $f^{\text{ro}} : Y^{\text{ro}} \rightarrow \mathbb{C}^{\text{ro}}$ that makes the diagram in [eq. \(4.0.3\)](#) commutative. We also say that the map σ resolves the indeterminacy locus of the function $\arg(f)$ which results in a well defined function

$$\arg(f^{\text{ro}}) = \arg \circ f^{\text{ro}} : Y^{\text{ro}} \rightarrow \mathbb{R}/2\pi\mathbb{Z}.$$

We fit all this information in the following commutative diagram:

(4.0.3)

$$\begin{array}{ccccccc}
& & \pi^{\text{ro}} & & & & \\
& \partial Y^{\text{ro}} & \xrightarrow{\quad} & Y^{\text{ro}} & \xrightarrow{\sigma} & Y & \xrightarrow{\pi} \text{Tub} \xleftarrow{\quad} \text{Tub}^* \\
& \arg(f^{\text{ro}})|_{\partial Y^{\text{ro}}} & \searrow & f^{\text{ro}} \downarrow & \swarrow (\pi^{\text{ro}})^* f & \downarrow \pi^* f & \downarrow f \\
& & \mathbb{C}^{\text{ro}} & \xrightarrow{\arg} & \mathbb{C} & \xrightarrow{\sigma'} & \mathbb{R}/2\pi\mathbb{Z} \\
& & \arg & & & & \\
& & \nearrow \arg(f^{\text{ro}}) & & \nearrow \arg(f) & & \\
& & \mathbb{R}/2\pi\mathbb{Z} & & & &
\end{array}$$

Notation 4.0.4. The corners of Y^{ro} induce a stratification indexed by the graph Γ as follows. Set $D_{\emptyset}^{\text{ro}} = Y^{\text{ro}} \setminus D_{\mathcal{W}}^{\text{ro}}$. For $i, j \in \mathcal{W}$, we define the following subspaces of ∂Y^{ro} :

$$D_i^{\text{ro}, \circ} = \sigma^{-1}(D_i^\circ), \quad D_i^{\text{ro}} = \sigma^{-1}(D_i), \quad D_{i,j}^{\text{ro}} = \sigma^{-1}(D_i \cap D_j).$$

Note that $\sigma^{-1}(D_i) = \overline{D_i^{\text{ro}, \circ}}$.

4.1. An action on the normal bundle

For an $i \in \mathcal{W}$, the elements of $\sigma_i^{-1}(D_i) = \partial Y_i^{\text{ro}}$ correspond to oriented real lines in the normal bundle of $D_i \subset Y$, which has a complex structure. This induces a \mathbb{C}^* -action on ∂Y_i^{ro} , with stabilizer $\mathbb{R}_{>0} \subset \mathbb{C}^*$, which reduces to a principal action of $\mathbb{R}/2\pi\mathbb{Z} \cong \mathbb{C}^*/\mathbb{R}_{>0}$. In particular, $D_i^{\text{ro}, \circ}$ is naturally a principal S^1 -bundle over D_i° , and $D_{i,j}^{\text{ro}} \cong S^1 \times S^1$. Denote this action by \cdot_i . In the coordinates r, α, v on U^{ro} introduced before in Chapter 4, this action is given by

$$\eta \cdot_i (0, \alpha, v) = (0, \alpha + \eta, v), \quad \eta \in \mathbb{R}/2\pi\mathbb{Z}.$$

for a point $(0, \alpha, v) \in \partial U^{\text{ro}}$.

Let $p \in D_i \cap D_j$ be an intersection point, and $U \ni p$ a coordinate chart with $U \cap D_i = \{u = 0\}$ and $U \cap D_j = \{v = 0\}$. We have polar coordinates (r, s, α, β) on $\sigma^{-1}(U) = U^{\text{ro}}$ so that $\sigma(r, s, \alpha, \beta) = (re^{i\alpha}, se^{i\beta})$. The corner

$$\sigma^{-1}(p) = \{(r, s, \alpha, \beta) \in U^{\text{ro}} \mid r = s = 0\}$$

has two $\mathbb{R}/2\pi\mathbb{Z}$ -actions. For $\eta, \nu \in \mathbb{R}/2\pi\mathbb{Z}$

$$\eta \cdot_i \nu \cdot_j (0, 0, \alpha, \beta) = (0, 0, \alpha + \eta, \beta + \nu).$$

Thus, the torus $\sigma^{-1}(p)$ is an $\mathbb{R}/2\pi\mathbb{Z} \times \mathbb{R}/2\pi\mathbb{Z}$ -torsor.

Definition 4.1.1. Let $U \subset Y$ and $U^{\text{ro}} = \sigma^{-1}(U)$. A function $f : U^{\text{ro}} \rightarrow \mathbb{C}$ is \cdot_i -equivariant of weight $k \in \mathbb{Z}$ if for all $p \in D_i^{\text{ro}} \cap U^{\text{ro}}$ and $\eta \in \mathbb{R}/2\pi\mathbb{Z}$, we have $f(\eta \cdot_i p) = e^{ik\eta} f(p)$. A function which is equivariant of weight 0, is said to be invariant.

Lemma 4.1.2. If $U \subset Y$ is open, and $h : U \rightarrow \mathbb{C}$ is a meromorphic function which is holomorphic on $U \setminus D_i$ and has vanishing order $k \in \mathbb{Z}$ along $D_i \cap U$. Then the pull-back $r^{-k}\sigma^*h$ of $|u|^{-k}h$ by σ , extends over the boundary to a real analytic equivariant function of weight k .

Similarly, the pull-back of $|u|^{-k}\bar{h}$ extends over the boundary to a real analytic equivariant function of weight $-k$.

PROOF. Since the statement of the lemma is local, we can assume that U is a small coordinate chart around some $p \in D_i$, with coordinates u, v so that the set $U \cap D_i$ is defined by $u = 0$. Expand $h = \sum_{j=k}^{\infty} a_j(v)u^j$, where a_i are holomorphic functions in the variable v . Then, using polar coordinates as in eq. (4.0.1),

$$r^{-k}\sigma^*h(r, \alpha, v) = \sum_{j=k}^{\infty} r^{-k+j}a_k(v)e^{ij\alpha}$$

which shows that $r^{-k}\sigma^*h$ is real analytic function which is well defined on all U^{ro} . Restricting to the boundary, that is $r = 0$, we get:

$$(r^{-k}\sigma^*h)|_{r=0} = a_k(v)e^{ki\alpha}$$

and the first statement follows. The second statement is completely analogous. \square

4.2. Milnor fibration at radius zero

In this subsection we introduce the *Milnor fibration at radius zero*, which is the fibration given by the map

$$\arg(f^{\text{ro}})|_{\partial Y^{\text{ro}}} : \partial Y^{\text{ro}} \rightarrow \mathbb{R}/2\pi\mathbb{Z}.$$

Definition 4.2.1. For $\theta \in \mathbb{R}/2\pi\mathbb{Z}$, we define the *Milnor ray* at angle θ , as

$$\text{Tub}_\theta^* = \arg(f)^{-1}(\theta) \subset \text{Tub}^*,$$

as well as the subsets of Y^{ro} :

$$(4.2.2) \quad \begin{aligned} Y_\theta^{\text{ro}} &= \arg(f^{\text{ro}})^{-1}(\theta), & D_{i,\theta}^{\text{ro}} &= Y_\theta^{\text{ro}} \cap D_i^{\text{ro}}, \\ D_{i,\theta}^{\text{ro},\circ} &= Y_\theta^{\text{ro}} \cap D_i^{\text{ro},\circ}, & D_{i,j,\theta}^{\text{ro}} &= Y_\theta^{\text{ro}} \cap D_{i,j}^{\text{ro}}. \end{aligned}$$

Lemma 4.2.3. For any $\theta \in \mathbb{R}/2\pi\mathbb{Z}$, the set Y_θ^{ro} is a submanifold of Y which intersects the boundary strata transversely.

PROOF. It suffices to show that for every stratum $S \subset Y^{\text{ro}}$, the restriction

$$\arg(f^{\text{ro}})|_S : S \rightarrow \mathbb{R}/2\pi\mathbb{Z}$$

is a submersion. For $S = D_{\emptyset}^{\text{ro}}$, this follows from the chain rule, and the fact that if $p \in Y^{\text{ro}} \setminus D_{\mathcal{W}}^{\text{ro}} \cong \text{Tub} \setminus C$, then

$$D((\pi^{\text{ro}})^*f)_p : TY_p \rightarrow T\mathbb{C}_{f(p)}$$

is a non-zero complex linear map, in particular, it is surjective.

Now take $p \in S = D_i^{\text{ro},\circ}$ and let U^{ro} be a chart around p with coordinates r, α, v and such that $D_i^{\text{ro},\circ} \cap U^{\text{ro}}$ is defined by $r = 0$. The function f in the chart U^{ro} takes the form

$$f = r^{m_i} e^{im_i\alpha} \tilde{f}$$

with \tilde{f} a unit on U^{ro} . Now, the function f^{ro} (recall eq. (4.0.3)), in these coordinates, looks like

$$f^{\text{ro}}(r, \alpha, v) = (r^{m_i}|\tilde{f}|, m_i\alpha + \arg(\tilde{f})) \in \mathbb{R}_{\geq 0} \times \mathbb{R}/2\pi\mathbb{Z}.$$

Now, we can compute

$$\arg(f^{\text{ro}})(r, \alpha, v) = m_i\alpha + \arg(\tilde{f})$$

which, restricted to S , takes the form

$$\arg(f^{\text{ro}})|_S(\alpha, v) = m_i \alpha + \arg(\tilde{f}).$$

Since $\partial_\alpha(\arg(f^{\text{ro}})|_S) = m_i \neq 0$, because $\arg(\tilde{f})$ does not depend on α , we get again that $\arg(f^{\text{ro}})|_S$ is a submersion.

A similar argument applies to $D_{i,j}^{\text{ro}}$. \square

As a consequence of [Lemma 4.2.3](#) the map

$$\arg(f^{\text{ro}})|_{\partial Y^{\text{ro}}} : \partial Y^{\text{ro}} \rightarrow \mathbb{R}/2\pi\mathbb{Z}$$

is a locally trivial topological fibration which is smooth when restricted to each of the strata ([Notation 4.0.4](#)) of ∂Y^{ro} . Moreover, it is equivalent as a C^0 -fibration to the Milnor fibration.

Definition 4.2.4. The locally trivial fibration induced by $\arg(f^{\text{ro}})|_{\partial Y^{\text{ro}}}$ is called *the Milnor fibration at radius 0*. We call its fiber $F_\theta^{\text{ro}} = \arg(f^{\text{ro}})|_{\partial Y^{\text{ro}}}^{-1}(\theta)$ *the Milnor fiber at radius 0 over the angle θ* .

Remark 4.2.5. Note that F_θ^{ro} is a topological, piecewise smooth manifold and that, for each $\theta \in \mathbb{R}/2\pi\mathbb{Z}$ it has a natural partition induced by the stratification of the exceptional set D :

$$F_\theta^{\text{ro}} = \bigsqcup_{i \in \mathcal{V}} D_{i,\theta}^{\text{ro},\circ} \bigsqcup_{\substack{i,j \in \mathcal{V} \\ D_i \cap D_j \neq \emptyset}} D_{i,j,\theta}^{\text{ro}}.$$

4.3. Scaling and extending the metric

In this subsection we explain how the pullback metric on Y^{ro} induces a metric on $D_{i,\theta}^{\text{ro},\circ}$ for each $i \in \mathcal{V} \setminus \{0\}$ and each $\theta \in \mathbb{R}/2\pi\mathbb{Z}$.

Fix a vertex $i \in \mathcal{V} \setminus \{0\}$ and a value $\theta \in \mathbb{R}/2\pi\mathbb{Z}$. The set $D_{i,\theta}^{\text{ro},\circ}$ covers the Riemann surface D_i° , and so is a Riemann surface. Choose isometric coordinates ([Definition 2.3.1](#)), x, y so that $\{y = 0\}$ is the tangent associated with D_i . Let U be a small coordinate chart of some point as in [3.3.4](#), with coordinates u, v chosen so that the pullback $\pi^*x = u^{c_{0,i}}$, and in particular $u = 0$ defines $D_i \cap U$. Recall that by [Lemma 3.5.2](#), π^*y vanishes with strictly higher order along D_i than π^*x . By abuse of notation, we write x rather than π^*x , and denote its partials with respect to u and v by x_u and x_v , and so forth. With these assumptions, we have $x_v = 0$. Denote by $\text{Jac } \pi$ the Jacobian matrix [eq. \(3.3.5\)](#). Then, outside of the exceptional divisor, the pullback of the standard Hermitian metric in \mathbb{C}^2 is given by the Hermitian matrix

$$\text{Jac } \pi^* \cdot \text{Jac } \pi = \begin{pmatrix} \bar{x}_u & \bar{y}_u \\ 0 & \bar{y}_v \end{pmatrix} \begin{pmatrix} x_u & 0 \\ y_u & y_v \end{pmatrix} = \begin{pmatrix} |x_u|^2 + |y_u|^2 & \bar{y}_u y_v \\ \bar{y}_v y_u & |y_v|^2 \end{pmatrix} \in \text{Mat}(2 \times 2, \mathbb{C})$$

which does not extend to give a Hermitian metric on all of U . Here $\text{Jac } \pi^*$ denotes the hermitian adjoint of the complex matrix $\text{Jac } \pi$. However, the lower diagonal $|y_v|^2$ entry vanishes with order precisely $2c_{1,i}$. Thus, if we scale the metric by the function $|u|^{-2c_{1,i}} = |x|^{-2c_{1,i}/c_{0,i}}$, this lower diagonal entry gives a real 2×2 matrix which is diagonal, and whose diagonal entries are the restriction to $U \cap D_i$ of the extension of $|y_v|^2/|u|^{2c_{1,i}}$ over $U \cap D_i$. Denote this function by h_U . Thus, if $(0, v) \in D_i \cap U$, then

$$h_U(v) = \lim_{u \rightarrow 0} \frac{|y_v|^2}{|u|^{2c_{1,i}}}.$$

Since this construction was made by scaling the pullback of the standard metric by the function $|x|^{-2c_{1,i}/c_{0,i}} = |u|^{-2c_{1,i}}$, this gives a metric of the whole set D_i° , which in the coordinate neighborhood $U \cap D_i^\circ$ is given by the real 2×2 matrix

$$\begin{pmatrix} h_U & 0 \\ 0 & h_U \end{pmatrix} \in \text{Mat}(2 \times 2, \mathbb{R})$$

In fact, one may verify that if U' is another coordinate neighborhood, then the above matrices define the same metric on the intersection. Since $D_{i,\theta}^{\text{ro},\circ}$ covers D_i° , the Riemann surface $D_{i,\theta}^{\text{ro},\circ}$ inherits a Riemannian metric.

Definition 4.3.1. Denote by g_i and $g_{i,\theta}^{\text{ro}}$ the Riemannian metrics on D_i° and $D_{i,\theta}^{\text{ro},\circ}$ constructed above.

Remark 4.3.2. A holomorphic coordinate v in a chart $U \cap D_i^\circ$, as above, induces a trivialization of the tangent and cotangent bundles of $U \cap D_i^\circ$, which identifies a vector field or a one form with a complex function. Write $v = s + it$, so that s, t are real coordinates. A vector field $\zeta = a\partial_s + b\partial_t$ on $U \cap D_i^\circ$ corresponds to the complex function $a + ib$, and a differential form $\eta = \alpha ds + \beta dt$ corresponds to the function $\alpha + i\beta$.

The form η is dual to the vector field ζ with respect to the metric g_i , that is, $\eta = g_i(\zeta, \cdot)$ if and only if

$$\alpha + i\beta = h_U \cdot (a + ib).$$

If ϕ is a real function on $D_i^\circ \cap U$, then the gradient of ϕ with respect to the metric g_i is given by

$$\nabla\phi = h_U^{-1} \cdot (\phi_s \partial_s + \phi_t \partial_t).$$

CHAPTER 5

Resolving the Polar Locus

In this section we specify a genericity condition for the metric that involves the relative polar curves of the plane curve singularity. Before doing so, we review part of the needed theory.

5.1. Generic polar curves

In this subsection, we fix notation regarding relative polar curves and recall a result from Tessier that says that there is an equisingular family of relative polar curves which is dense among all polar curves.

Let $w = (w_1, w_2) \in \mathbb{C}^2 \setminus \{0\}$ be a vector. By the canonical isomorphism $T_p \mathbb{C}^2 \cong \mathbb{C}^2$ for any $p \in \mathbb{C}^2$, we identify w with a vector field ∂_w on \mathbb{C}^2 . We denote the corresponding partial $\partial_w f$ of f by f_w .

Definition 5.1.1. The function $f_w : \mathbb{C}^2 \rightarrow \mathbb{C}$ defines a plane curve. We denote this plane curve by

$$P_w = \{f_w = 0\}.$$

That is, P_w is the vanishing set of f_w . We call P_w the *relative polar curve* of f associated with w .

Observe that $P_w = P_{\lambda w}$ for any $\lambda \in \mathbb{C}^*$, and so P_w only depends on the equivalence class $[w] \in \mathbb{CP}^1$. Denote the strict transform of P_w in a modification Y of \mathbb{C}^2 by \tilde{P}_w .

5.1.2. By [Tei77, pg. 269-270, Théorème 2.], the family P_w for $[w] \in \mathbb{CP}^1$ is equisingular on a Zariski open dense subset Ω of \mathbb{CP}^1 . More concretely, there exists a modification

$$\pi : Y \rightarrow \mathbb{C}^2$$

as in [eq. \(3.1.2\)](#) and a set $\Omega \subset \mathbb{CP}^1$ satisfying the properties

- (1) if $[w] \in \Omega$, then $D \cup \tilde{X} \cup \tilde{P}_w$ is a normal crossing divisor. That is, π is an embedded resolution for each P_w with $w \in \Omega$,
- (2) if $[w], [w'] \in \Omega$ and $i \in \mathcal{V}$, then the strict transforms of both associated polar curves \tilde{P}_w and $\tilde{P}_{w'}$ intersect each divisor in the same number of points, that is $|D_i \cap \tilde{P}_w| = |D_i \cap \tilde{P}_{w'}|$. Equivalently,

$$\mathrm{ord}_{D_i} \pi^* f_w = \mathrm{ord}_{D_i} \pi^* f_{w'}.$$

Or, equivalently, the cycles associated with $\pi^* f_w$ and $\pi^* f_{w'}$ coincide (recall [Remark 3.2.4](#)). We put a name to this cycle in [Definition 5.1.5](#).

- (3) Ω does not contain any of the tangents to $(C, 0)$.

Definition 5.1.3. We denote by $\pi_{\mathrm{pol}} : (Y_{\mathrm{pol}}, D_{\mathrm{pol}}) \rightarrow (\mathbb{C}^2, 0)$ the minimal embedded resolution of $(C, 0)$ satisfying the above properties, and by $\Omega \in \mathbb{CP}^1$ the corresponding open set. Denote by Γ_{pol} its resolution graph, with $\mathcal{V}_{\mathrm{pol}}$ the set of

vertices corresponding to exceptional components. Denote by C_{pol} and P_{pol} the strict transform of the curve C and a polar curve P_w for a $w \in \Omega$, respectively.

- Remark 5.1.4.**
- (1) Observe that π_{pol} can be obtained from π_{\min} by iteratively blowing map at intersection points of P_{\min} with the exceptional set.
 - (2) Any embedded resolution $\pi : Y \rightarrow \mathbb{C}^2$ that resolves the Jacobian ideal $J = (f_x, f_y)$, i.e. such that π^*J is principal, satisfies properties 5.1.2 1, 2 and 3 above.

Property 5.1.2 2 above leads to the following definition:

Definition 5.1.5. For $[w] \in \Omega$ and $i \in \mathcal{V}_{\text{pol}}$, define a cycle $Z_P \in L$ (in the group of cycles associated with the modification π_{pol}) and integers p_i for $i \in \mathcal{V}$ by

$$Z_P = \sum_{i \in \mathcal{V}} |P_{\text{pol}} \cap D_i| D_i^* = \sum_{i \in \mathcal{V}} p_i D_i.$$

For $a \in \mathcal{A}$ we define $p_a = \text{ord}_{D_a} f_w = m_a - 1$.

Remark 5.1.6. Recall that by Remark 3.2.4, $\text{ord}_{D_i}(f_w) = p_i$. An equivalent definition of the numbers p_i (for any resolution), which does not depend on any choice, is

$$(5.1.7) \quad p_i = \min\{\text{ord}_{D_i}(f_x), \text{ord}_{D_i}(f_y)\}.$$

This is because a relative polar curve is defined by taking a linear combination of the partials f_x and f_y .

The next lemma shows that the number of intersection points of a generic polar curve with the first exceptional divisor is controlled by the number of tangents of the plane curve.

Lemma 5.1.8. *For $w \in \Omega$, the number of intersection points of the divisor D_0 corresponding to the first blow-up and P_{pol} is $|D_0 \cap P_{\text{pol}}| = t - 1$, where t is the number of different tangents of $(C, 0)$.*

PROOF. Let e be the multiplicity of $(C, 0)$ so that $f = \text{in}(f) + \dots$ where $\text{in}(f)$ is a homogeneous polynomial of degree e , and \dots stands for higher order terms. Distinct linear factors of $\text{in}(f)$ correspond to tangents of $(C, 0)$. Therefore, we have distinct points $[a_i, b_i] \in \mathbb{CP}^1$, and positive integers e_i so that $e_1 + \dots + e_t = e$ and

$$\text{in}(f)(x, y) = \prod_{i=1}^t (a_i x - b_i y)^{e_i}$$

We can assume $w = (0, 1)$ up to a change of coordinates. In this case $f_w = f_y$. Then the intersection points $D_0 \cap P_{\text{pol}}$ correspond to the roots of the homogeneous polynomial $\text{in}(f)_y$, which are not roots of $\text{in}(f)$. Note that $\text{in}(f_y) = \text{in}(f)_y$, because, since y is not a tangent, $\text{in}(f)$ has the monomial y^e with nonzero coefficient. As a result, $\text{in}(f_y)$ is a homogeneous polynomial of degree $e - 1$, and has a root of multiplicity $(e_i - 1)$ at $[a_i, b_i]$.

To finish the proof, it is enough to show that the Jacobian ideal has no base point on D_0 outside the strict transform of C in Y_0 . In other words, it suffices to show that $\text{in } f_x$ and $\text{in } f_y$ have no common factors other than the roots of $\text{in}(f)$. But a common root of $\text{in}(f_x), \text{in}(f_y)$ is a root of $\text{in}(f)$ by Euler's identity $x \text{in}(f_x) + y \text{in}(f_y) = e \text{in}(f)$. \square

Remark 5.1.9. In the above proof, we have seen that the Jacobian ideal $(f_x, f_y) \subset \mathcal{O}_{C,0}$ does not have base points on the exceptional divisor of the blow-up $\pi_0 : Y_0 \rightarrow \mathbb{C}^2$, outside the strict transform of C . As a result, the vertex 0 of Γ_{pol} has precisely t neighbors in \mathcal{W} .

Definition 5.1.10. With Ω as above, let $G_{\text{pol}} \subset \text{GL}(\mathbb{C}, 2)$ be the set of matrices $A \in \text{GL}(\mathbb{C}, 2)$ satisfying the following property: If $v, w \in \mathbb{C}^2 \setminus \{0\}$ are such that v is a tangent of $(C, 0)$ and $h_A(v, w) = 0$, then $[w] \in \Omega$. We call such a metric h_A , a *P-generic metric*.

CHAPTER 6

The Invariant and Non-invariant Subgraphs

In [Section 6.1](#), we define the numerical invariant ϖ_i associated to each divisor of an embedded resolution of C . This invariant distinguishes between two types of divisors: those where ϖ_i vanishes (*invariant*) and those where it does not (*non invariant*). In [Chapter 9](#), we see that invariance is precisely the condition which allows for a scaling of the pullback of ξ to the minimal resolution to be extended over a component of the exceptional divisor.

In [Section 6.2](#), we give a combinatorial description of the induced subgraph of Γ_{\min} on the invariant vertices, only in terms of Γ_{\min} .

6.1. The polar weight

In this subsection we define an integral invariant associated to an embedded resolution and we prove a formula for it. We work with the embedded resolution $\pi_{\text{pol}} : Y_{\text{pol}} \rightarrow \mathbb{C}$ ([Definition 5.1.3](#)) of the curve $(C, 0)$. Recall the properties of p_i in [Remark 5.1.6](#) and that $m_i = \text{ord}_{D_i}(f)$. Also, as we already did in [Chapter 4](#), by abuse of notation, we sometimes write x rather than π^*x , and denote its partials with respect to u and v by x_u and x_v , and so forth. Similarly f_v denotes the partial derivative ∂_v of π^*f .

Definition 6.1.1. The *polar weight* of the vertex $i \in \mathcal{V}$ is the integer

$$\varpi_i = c_{1,i} - m_i + p_i.$$

The vertex $i \in \mathcal{V}$, or the divisor D_i , is *invariant* if $\varpi_i = 0$. An edge ij joining $i, j \in \mathcal{V}$, or the intersection point in $D_i \cap D_j$, is *invariant* if both i and j are invariant. An edge ij is said to be *non-invariant* if $\varpi_i \neq 0$ or $\varpi_j \neq 0$.

Example 6.1.2. If $i = 0$, then $c_{1,i} = 1$, and $p_i = m_i - 1$, and so $\varpi_0 = 0$. In other words, the divisor D_0 appearing in the first blow-up is invariant.

Lemma 6.1.3. Let $i \in \mathcal{V}$ and $p \in D_i^\circ$, and let $U \subset Y$ be a coordinate neighborhood around p with coordinates u, v satisfying $\pi^*x = u^{c_{0,i}}$. Assume also that the standard metric in the coordinates x, y is P -generic. Then

$$(6.1.4) \quad \varpi_i = \text{ord}_u f_v - \text{ord}_u f.$$

In particular, $\varpi_i \geq 0$ with a strict inequality if and only the initial part $\text{in}_u f$ does not depend on v , and so $\text{in}_u f$ is a nonzero constant multiple of u^{m_i} .

PROOF. As in [3.3.4](#), we have $x_v = 0$ and $\text{ord}_u y_v = c_{1,i}$. Furthermore, by the chain rule,

$$f_v = x_v f_x + y_v f_y = y_v f_y.$$

Therefore,

$$c_{1,i} - m_i + p_i = \text{ord}_u f_v - \text{ord}_u f,$$

proving [eq. \(6.1.4\)](#). The other statements follow from the last equation and the definition of ϖ_i . \square

6.2. The invariant subgraph Υ of Γ_{\min}

In this subsection, we use arbitrary coordinates x, y for \mathbb{C}^2 , with the only condition that $\{y = 0\}$ is a tangent of C . In particular, we make no use of a generic metric. We work with the minimal resolution $Y_{\min} \rightarrow \mathbb{C}^2$. We recall that the characterization of the numbers p_i given in [eq. \(5.1.7\)](#), for $i \in \mathcal{V}_{\min}$ (or for $i \in \mathcal{V}$ for \mathcal{V} the vertex set of any embedded resolution), is independent of any genericity conditions. The main result of this subsection is [Lemma 6.2.3](#), which characterizes invariant vertices in Γ_{\min} .

Notation 6.2.1. Since Γ_{\min} is a tree, any pair of vertices in Γ_{\min} is joined by a *geodesic*, i.e. a shortest path, which is unique. The *degree* $\deg_{\min}(i)$ of a vertex $i \in \mathcal{V}_{\min}$ in Γ_{\min} is the number of adjacent vertices, including arrowheads.

Definition 6.2.2. Let $\Upsilon \subset \Gamma_{\min}$ be the smallest connected subgraph of Γ_{\min} containing the vertex corresponding to the first blow-up $0 \in \mathcal{V}_{\min}$, as well as any vertex in \mathcal{V}_{\min} adjacent to an arrow-head $a \in \mathcal{A}$. Let $\mathcal{V}_{\Upsilon} \subset \mathcal{V}_{\min}$ be the vertex set of Υ .

The next lemma characterizes the vertex set of Υ . We postpone its proof to the end of this subsection (until we have developed the necessary tools for it). The rest of the subsection is a collection of technical results, most of them of a combinatorial nature, that are of interest on their own.

Lemma 6.2.3. *The vertex $i \in \mathcal{V}_{\min}$ is invariant, i.e. $\varpi_i = 0$, if and only if $i \in \mathcal{V}_{\Upsilon}$.*

6.2.4. Let $\mathcal{V}_y \subset \mathcal{V}_{\min}$ be the set of vertices of Γ_{\min} whose associated tangent is the line $\{y = 0\}$. The induced subgraph $\Gamma_y \subset \Gamma$ is one of the connected components of the graph Γ_{\min} , with the vertex 0 removed. We have a coordinate chart in Y_0 with coordinates s, t so that π_0 is given by $(s, t) \mapsto (s, st)$. Denote by $p_0 \in Y_0$ the intersection point of D_0 and the strict transform of $\{y = 0\}$, given in s, t -coordinates as $(0, 0)$, and let $g \in \mathcal{O}_{Y_0, p}$ be the pullback of f , given by

$$g(s, t) = f(s, st).$$

The morphism $Y_{\min} \rightarrow Y_0$ (restricted to a preimage of a small neighborhood of p_0) is the minimal resolution of the plane curve germ defined by g . For $i \in \mathcal{V}_y$, we denote by $c_{0,i,y}, c_{1,i,y}, p_{i,y}, m_{i,y}$ and $\varpi_{i,y}$ the invariants so far introduced corresponding to this resolution. Note that we have $m_{i,y} = m_i$, since g is the pullback of f . Since s, t are coordinates around $p_0 \in Y_0$, we have

$$c_{0,i,y} = \min\{\text{ord}_{D_i}(s), \text{ord}_{D_i}(t)\}, \quad p_{i,y} = \min\{\text{ord}_{D_i}(g_s), \text{ord}_{D_i}(g_t)\}.$$

Using [Lemma 3.3.7](#), one also verifies that

$$(6.2.5) \quad c_{1,i,y} = c_{1,i} - c_{0,i}.$$

We can repeat the construction of the graph Υ as in [Definition 6.2.2](#) for the function g . We denote the result of this subgraph of Γ_y by Υ_y . Denote by $D_y = \{y = 0\} \subset \mathbb{C}^2$. By abuse of notation, we also denote by D_y the strict transform of D_y in any modification of \mathbb{C}^2 . Then D_y intersects a unique exceptional component in Y_{\min} . By renaming of vertices, we assume that this component is D_1 , and that the

geodesic from 1 to 0 in Γ_{\min} is $1, 2, \dots, k, 0$. Set $\mathcal{V}' = \{1, \dots, k\} \subset \mathcal{V}_{\min}$. We refer the reader to [fig. 6.2.14](#) for an example showing the use of this notation.

Example 6.2.6. Let $f(x, y) = y^7 + x^3y^4 + x^6y^2 + x^{11}$. This is a Newton nondegenerate germ, which can be resolved using a toric modification with 5 exceptional components, as seen in [fig. 6.2.14](#). Using the notation in [6.2.4](#), we find

$$g(s, t) = f(s, st) = (st)^7 + s^3(st)^4 + s^6(st)^2 + s^{11} = s^7(t^7 + t^4 + st^2 + s^4).$$

This curve has three branches at the origin $(s, t) = (0, 0)$, one of which is not reduced. The graph Γ_y contains the four vertices to the right in [fig. 6.2.14](#).

Lemma 6.2.7. *With the above notation, there exists a morphism $\pi' : Y' \rightarrow Y_0$ which is a sequence of blow-ups, so that the minimal resolution factorizes as*

$$\begin{array}{ccc} & Y' & \\ Y_{\min} & \swarrow \quad \searrow & \downarrow \pi' \\ & & Y_0 \end{array}$$

and the exceptional divisor of π' is $D_1 \cup \dots \cup D_k$.

PROOF. The minimal resolution is obtained by repeatedly blowing up any point of the total transform of C which is not normal crossing. If we add the rule that we only blow up intersection points on the total transform of D_y , we get a shorter sequence of blow-ups $\pi' : Y' \rightarrow Y_0$. The dual graph to the exceptional divisor of Y' is a string, and the strict transform of C in Y' only intersects smooth points on the total transform of D_y . Finishing the resolution process gives a map $Y_{\min} \rightarrow Y'$, and an identification of the exceptional divisor of Y' with $D_1 \cup \dots \cup D_k \subset Y_{\min}$. \square

6.2.8. The composed morphism $Y' \rightarrow Y_0 \rightarrow \mathbb{C}^2$ is a toric morphism with respect to the standard toric structure on \mathbb{C}^2 , as in [Example 3.4.8](#). Let Δ_y be the corresponding fan. Along with the natural basis vectors $(1, 0)$ and $(0, 1)$, the vectors

$$w_l = (\text{ord}_{D_l}(x), \text{ord}_{D_l}(y)) = (c_{0,l}, c_{1,l}), \quad l = 0, 1, \dots, k$$

generate the rays in Δ_y . In particular, $w_0 = (1, 1)$. Denote throughout [Section 6.2](#) by $\text{wt}_l(f)$ and $\text{in}_l f$ the weight and initial part of a function $f \in \mathcal{O}_{\mathbb{C}^2, 0}$ with respect to the weight vector w_l . Thus, if

$$f(x, y) = \sum_{i,j} a_{i,j} x^i y^j, \quad \text{supp}(f) = \{(i, j) \in \mathbb{Z}_{\geq 0}^2 \mid a_{i,j} \neq 0\},$$

then

$$\text{wt}_l(f) = \min \{\langle w_l, (i, j) \rangle \mid (i, j) \in \text{supp}(f)\},$$

$$\text{in}_l(f) = \sum \{a_{i,j} x^i y^j \mid \langle w_l, (i, j) \rangle = \text{wt}_l(f)\}.$$

Furthermore,

$$\text{ord}_{D_l}(f) = \text{wt}_l(f).$$

In the rest of the results of the present subsection we use the notation introduced in [6.2.4](#) and [6.2.8](#).

Lemma 6.2.9. *Assume $i \in \mathcal{V}_y$. The following holds*

- (1) *if $i \in \mathcal{V}'$, then $\text{ord}_{D_i}(y) = c_{1,i}$ and*
- (2) *if $i \notin \mathcal{V}'$, then $\text{ord}_{D_i}(y) < c_{1,i}$.*

PROOF. The first statement follows from the computations made in [Example 3.4.8](#). By construction, the strict transform of any branch of C with tangent $\{y = 0\}$ in Y' intersects the exceptional divisor in a smooth point. If D_l has such a point, and we blow it up to get a new vertex j , then by [Lemma 3.3.7](#), we have $c_{1,j} = c_{1,l} + 1$, whereas $\text{ord}_{D_j}(y) = \text{ord}_{D_l}(y)$. By continuing the resolution process, the difference $c_{1,j} - \text{ord}_{D_j}(y)$ can only increase. This proves the second statement. \square

Corollary 6.2.10. *If $i \in \mathcal{V}_y \setminus \mathcal{V}'$, then the (pullback of the) function*

$$(6.2.11) \quad \frac{y^{\text{ord}_{D_i}(x)}}{x^{\text{ord}_{D_i}(y)}}$$

is a nonzero constant along D_i° .

PROOF. Set $k = \text{ord}_{D_i}(y)$, and note that $\text{ord}_{D_i}(x) = c_{0,i}$. Let U be a coordinate chart around some point in D_i° as in [3.3.4](#), with coordinates u, v so that $x = u^{c_{0,i}}$. Then, the fraction [eq. \(6.2.11\)](#), restricted to D_i° equals $g_k(v)^{c_{0,i}}$. Since $k < c_{1,i}$ by the previous lemma, the function $g_k(v)$ is constant, by construction in [3.3.4](#). Since the fraction [eq. \(6.2.11\)](#) has vanishing order zero, this constant is not zero. \square

Lemma 6.2.12. *Let $i \in \mathcal{V}_y$. The following are equivalent*

- (1) *i is invariant, i.e. $\varpi_i = 0$,*
- (2) *the fraction*

$$\frac{f^{c_{0,i}}}{x^{m_i}}$$

restricts to a nonzero constant function along D_i° ,

- (3) *If $h \in \mathcal{O}_{\mathbb{C}^2,0}$ is any function satisfying $\text{ord}_{D_i}(h) = c_{0,i}$, then the fraction*

$$\frac{f^{c_{0,i}}}{h^{m_i}}$$

restricts to a nonzero constant function along D_i° ,

PROOF. The equivalence of 1 and 2 follows from [Lemma 6.1.3](#). If $\text{ord}_{D_i}(h) = c_{0,i}$, then h vanishes at 0, and has a linear term $ax + by$, with $a \neq 0$, since all monomials other than 1 and x vanish with strictly higher order than $c_{0,i}$. Then

$$\frac{f^{c_{0,i}}}{h^{m_i}} = \frac{f^{c_{0,i}}}{(ax + by + \text{h.o.t.})^{m_i}} = a^{-m_i} \frac{f^{c_{0,i}}}{x^{m_i}}.$$

along D_i° , which proves that 2 and 3 are equivalent. \square

Lemma 6.2.13. *If $l \in \mathcal{V}'$, then the following are equivalent*

- (1) *l is in Υ ,*
- (2) *$\text{in}_l f$ does depend on y , i.e. $\text{in}_l f$ is not a monomial of the form ax^n ,*
- (3) *l is invariant.*

PROOF. We first show [2 \$\Leftrightarrow\$ 3](#). If 2 does not hold, then, since $\partial_y x^n = 0$, we have

$$c_{1,l} + p_i = \text{wt}_l(yf_y) > \text{wt}_l(f) = m_i,$$

where we use [Lemma 6.2.9](#). This gives $\varpi_i > 0$, i.e. 3 does not hold. Conversely, if 2 holds, then the partial operator ∂_y does not kill the initial part of f with respect to the weight vector w_l , and we have an equality above, i.e. $\varpi_i = 0$.

To prove 1 \Leftrightarrow 2, consider first the case when the x -axis D_y is a component of C . In this case, all vertices in \mathcal{V}' are in \mathcal{V}_Υ by construction, since \mathcal{V}' is the set of vertices along the geodesic connecting the strict transform of D_y with the first blow-up. That is, all elements $l \in \mathcal{V}'$ satisfy 1. In this case, f is divisible by y , and so all elements of \mathcal{V}' also satisfy 2.

In the case when the strict transform of C passes through the intersection point of D_y and D_1 , we also find that all elements of \mathcal{V}' are in \mathcal{V}_Υ , and also satisfy 2.

Otherwise, the strict transform of C intersects only the smooth part of the total transform of D_y in Y' . For $l \in \mathcal{V}'$, the strict transform intersects D_l if and only if $\text{in}_l(f)$ is not a monomial, in which case the convex hull of $\text{supp}(\text{in}_l(f))$ is a face of the Newton polyhedron of f . If l and j are two such vectors corresponding to adjacent faces, then $\text{in}_s(f)$ is the monomial at the intersection of the two faces, if s is a vertex in between l and j . These are precisely the vertices in Υ , and for the rest of the vertices, the initial part of f is a monomial whose exponent is a vertex on the Newton diagram which also lies on the x -axis. \square

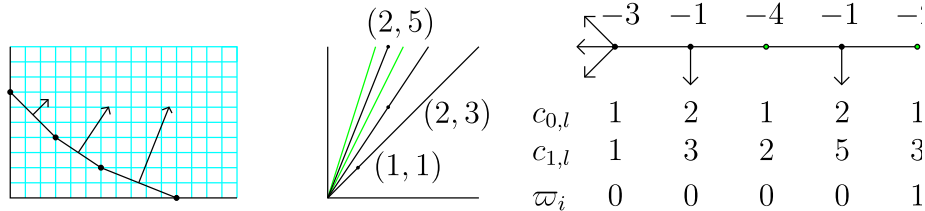


FIGURE 6.2.14. A Newton diagram for the function $f(x, y) = y^7 + x^3y^4 + x^6y^2 + x^{11}$, along with the corresponding regular subdivision of $\mathbb{R}_{\geq 0}^2$. The vertex to the left on the resolution graph corresponds to the first blow-up, the other vertices are in \mathcal{V}' . The vertex to the right is not invariant. Correspondingly, the initial part of f with respect to the weight vector $(1, 3)$ is x^{11} .

Lemma 6.2.15. *If $i \in \mathcal{V}_y \setminus \mathcal{V}'$, then $i \in \Upsilon_y$ if and only if $i \in \Upsilon$.*

PROOF. The first blow-up in the resolution of g creates a vertex in \mathcal{V}' . Therefore, the geodesic in Γ_y from an arrowhead to the first blow-up in Γ_y , and the geodesic from the same arrowhead in Γ_{\min} to $0 \in \mathcal{V}_{\min}$ both start as the geodesic starting from this arrowhead, going towards \mathcal{V}' . It follows that

$$\mathcal{V}_\Upsilon \cap (\mathcal{V}_y \setminus \mathcal{V}') = \mathcal{V}_{\Upsilon_y} \setminus \mathcal{V}'.$$

Finally, we are ready to prove the lemma stated at the beginning of this subsection.

PROOF OF [LEMMA 6.2.3](#). We prove the statement by induction on the cardinality of \mathcal{V}_{\min} . The base case is when \mathcal{V}_{\min} consists of 1 single vertex, which means that the singularity consists of smooth branches (not necessarily reduced) with different tangents. In this case the result follows by [Example 6.1.2](#). Assume now that \mathcal{V}_{\min} has more than one element. If $i \in \mathcal{V}'$, then the statement follows

from [Lemma 6.2.13](#). Assume, therefore, that $i \notin \mathcal{V}'$. By induction, we have $i \in \Upsilon_y$ if and only if $\varpi_{i,y} = 0$. Thus, by [Lemma 6.2.15](#), it suffices to show that

$$(6.2.16) \quad \varpi_i = 0, \quad \text{if and only if} \quad \varpi_{i,y} = 0.$$

Recall the coordinates s, t in [6.2.4](#), with $(x, y) = (s, st)$. Since $c_{0,i,y} = \min\{\text{ord}_{D_i}(s), \text{ord}_{D_i}(t)\}$ (recall [Remark 3.3.2](#)), we consider two cases.

First, assume that $\text{ord}_{D_i}(s) \leq \text{ord}_{D_i}(t)$. Then $c_{0,i,y} = \text{ord}_{D_i}(s) = \text{ord}_{D_i}(x) = c_{0,i}$, and

$$\frac{g^{c_{0,i,y}}}{s^{m_{i,y}}} = \frac{f^{c_{0,i}}}{x^{m_i}}.$$

Using the characterization of [Lemma 6.2.12](#), the equivalence [eq. \(6.2.16\)](#) follows.

Assume next that $\text{ord}_{D_i}(t) < \text{ord}_{D_i}(s)$. Then $c_{0,i,y} = \text{ord}_{D_i}(t) = \text{ord}_{D_i}(y/x)$, and $c_{0,i} = \text{ord}_{D_i}(x)$. We find

$$\left(\frac{g^{c_{0,i,y}}}{t^{m_{i,y}}}\right)^{c_{i,0}} = \left(\frac{f^{\text{ord}_{D_i}(y/x)}}{x^{-m_i} y^{m_i}}\right)^{\text{ord}_{D_i}(x)} = \left(\frac{f^{c_{0,i}}}{x^{m_i}}\right)^{c_{0,i,y}} \cdot \left(\frac{y^{\text{ord}_{D_i}(x)}}{x^{\text{ord}_{D_i}(y)}}\right)^{-m_i}$$

By [Corollary 6.2.10](#), the factor to the right is constant along D_i° . Since $c_{0,i}$ and $c_{0,i,y}$ are positive integers, [eq. \(6.2.16\)](#) again follows from [Lemma 6.2.12](#). \square

6.3. The invariant subgraph of Γ_{pol}

In this subsection we show that the invariant subgraph Υ of Γ_{min} does not get modified by the extra blow-ups $Y_{\text{pol}} \rightarrow Y_{\text{min}}$ needed to get to the polar resolution (other than the Euler numbers may be lowered). That is, no invariant edges are split up. We conclude with [Corollary 6.3.7](#), which is used in the proofs of [Lemmas 8.2.4](#) and [9.3.3](#). Our [Corollary 6.3.3](#) has been proved in the case of an isolated plane curve in [\[LMW89\]](#).

For this subsection we choose some $[w] \in \Omega$ that defines a generic relative polar curve P_w . We recall that we denote its strict transform in Y_{min} by P_{min} .

Lemma 6.3.1. *If ij is an invariant edge in Γ_{min} , then P_{min} does not pass through the intersection point $D_i \cap D_j$.*

PROOF. We consider coordinates x, y in \mathbb{C}^2 so that $\{y = 0\}$ is the tangent associated with D_i and such that $\{f_w = 0\} = \{f_y = 0\}$. Take coordinates u, v in a small chart $U \subset Y_{\text{min}}$ near $D_i \cap D_j$ so that $x = u^{c_{0,i}} v^{c_{0,j}}$. We can write $\pi^* f(u, v) = u^{m_i} v^{m_j} (a + \text{h.o.t.})$ for some $a \in \mathbb{C}^*$ in these coordinates. A chain rule computation gives

$$(6.3.2) \quad f_y = \frac{-x_v f_u + x_u f_v}{\det \text{Jac } \pi} = \frac{u^{c_{0,i}-1} v^{c_{0,j}-1}}{\det \text{Jac } \pi} \cdot (-c_{0,j} u f_u + c_{0,i} v f_v).$$

The first factor on the right hand side does not vanish on $U \setminus (D_i \cup D_j)$. But since

$$u f_u = u^{m_i} v^{m_j} (m_i a + \text{h.o.t.}), \quad v f_v = u^{m_i} v^{m_j} (m_j a + \text{h.o.t.}),$$

we get

$$-c_{0,j} u f_u + c_{0,i} v f_v = u^{m_i} v^{m_j} \left(a \begin{vmatrix} m_i & c_{0,i} \\ m_j & c_{0,j} \end{vmatrix} + \text{h.o.t.} \right)$$

The determinant in this formula does not vanish, by [Lemma 3.4.7](#). Indeed, [Lemma 3.4.7](#) guarantees that this determinant vanishes if and only if the branch of Γ at i does not meet an arrowhead. Now because the edge ij is invariant, by [Lemma 6.2.3](#) it is an

edge of Υ , so it lies on a geodesic between i and an arrowhead. Therefore, the second factor on the right hand side of [eq. \(6.3.2\)](#) does not vanish outside $U \cap (D_i \cup D_j)$ either, and so the strict transform of the polar curve does not intersect U . \square

Corollary 6.3.3. *If P' is a component of P_{\min} , then either $P' \cap C_{\min} = \emptyset$, or $P' \subset C_{\min}$. The inclusion only happens when C is not reduced.*

PROOF. As in the previous lemma, we consider coordinates x, y in \mathbb{C}^2 so that $\{y = 0\}$ is the tangent associated with D_i and such that $\{f_w = 0\} = \{f_y = 0\}$. Let $i \in \mathcal{V}$ and $p \in D_i$, and assume that there is a component C' of C_{\min} passing through p . Choose a small chart U containing $p = (0, 0)$ with coordinates u, v so that $\pi_{\min}^* x = u^{c_{0,i}}$. Since π_{\min} is an embedded resolution, we can write $\pi^* f(u, v) = u^{m_i}(au + bv + \text{h.o.t.})^{m'}$, where $a \in \mathbb{C}$, $b \in \mathbb{C}^*$, and m' is a positive integer. A computation like in the previous proof gives

$$f_y = \frac{x_u f_v}{\det \text{Jac } \pi} = \frac{c_{0,i} u^{c_{0,i}-1+m_i m'} (b + \text{h.o.t.})}{\det \text{Jac } \pi} (au + bv + \text{h.o.t.})^{m'-1}.$$

The fraction on the right hand side does not vanish in $U \setminus D_i$. The second factor is 1 if $m' = 1$, in which case P_{\min} does not pass through U , and vanishes precisely along C' if $m' > 1$, in which case $P_{\text{pol}} \cap U = C_{\text{pol}} \cap U$ as reduced sets. \square

Lemma 6.3.4. *The subgraph $\Upsilon \subset \Gamma_{\min}$ naturally embeds in Γ_{pol} as the smallest connected subgraph containing the vertex 0 and all $i \in \mathcal{V}_{\text{pol}}$ satisfying $C_{\text{pol}} \cap D_i \neq \emptyset$.*

PROOF. By [Lemma 6.3.1](#) and [Corollary 6.3.3](#), invariant edges or intersection points with C_{\min} are not modified by the resolution process used to obtain Υ . \square

Lemma 6.3.5. *If $i \in \mathcal{V}_{\text{pol}}$, then $i \in \mathcal{V}_{\Upsilon}$ if and only if $\varpi_i = 0$.*

PROOF. If $i \in \mathcal{V}_{\min} \subset \mathcal{V}_{\text{pol}}$, then the statement is clear from [Lemma 6.2.3](#). To prove the lemma, it suffices to show that if $i \in \mathcal{V}_{\text{pol}} \setminus \mathcal{V}_{\min}$, then $\varpi_i \neq 0$. If i is such a vertex, then D_i is the exceptional divisor of a blow-up $(Y_i, D_i) \rightarrow (Y_{i-1}, q_i)$, where q_i is a point on the exceptional divisor in Y_{i-1} . Let us assume that q_i is an intersection point of D_j and D_k . The case when q_i lies on a smooth point of the exceptional divisor is similar.

By [Remark 5.1.4 1](#), q_i is an intersection point of P_{\min} and D . Therefore, we have

$$p_i > p_j + p_k.$$

By [Corollary 6.3.3](#), the strict transform of C does not pass through q_i , and so we have

$$m_i = p_j + p_k.$$

Using [Lemma 3.3.7](#), we find

$$\varpi_i = c_{1,i} - m_i + p_i > c_{1,j} - m_j + p_j + c_{1,k} - m_k + p_k = \varpi_j + \varpi_k \geq 0. \quad \square$$

Corollary 6.3.6. *Let i, j be neighbors in Γ_{pol} , with an edge going from j to i . The following are equivalent:*

- (1) *The vertex i is invariant.*
- (2) *The edge ji is invariant.*
- (3) *The branch at i contains arrowheads (see [Definition 3.4.4](#) and [Remark 3.4.5](#)).*
- (4) *We have*

$$\begin{vmatrix} c_{0,i} & m_i \\ c_{0,j} & m_j \end{vmatrix} \neq 0.$$

(5) *The vector (m_i, m_j) is not a positive rational multiple of $(c_{0,i}, c_{0,j})$.*

PROOF. By construction of Υ , and [Lemma 6.3.4](#), the branch of Γ_{pol} at i contains arrowheads if and only if $i \in \Upsilon$, which, by the previous lemma, is equivalent to $\varpi_i = 0$, which is equivalent to $\varpi_i = \varpi_j = 0$, proving [1 \$\Leftrightarrow\$ 2 \$\Leftrightarrow\$ 3](#). [Lemma 3.4.7](#) gives [3 \$\Leftrightarrow\$ 4](#). Finally, [4](#) is equivalent to [5](#), since both $c_{0,i}$ and m_i are positive. \square

Corollary 6.3.7. *Let i, j be vertices in Γ_{pol} , with a directed edge $j \rightarrow i$. Then*

$$\begin{vmatrix} c_{0,i} & \varpi_i \\ c_{0,j} & \varpi_j \end{vmatrix} \leq 0,$$

with equality if and only if $\varpi_i = \varpi_j = 0$.

PROOF. If $\varpi_i = \varpi_j = 0$, then the statement is clear. It follows from the construction of Υ and [Lemma 6.3.5](#), that if $\varpi_j \neq 0$, then $\varpi_i \neq 0$ as well, so let us assume that $\varpi_i \neq 0$. We have

$$\begin{vmatrix} c_{0,i} & \varpi_i \\ c_{0,j} & \varpi_j \end{vmatrix} = \begin{vmatrix} c_{0,i} & c_{1,i} \\ c_{0,j} & c_{1,j} \end{vmatrix} - \begin{vmatrix} c_{0,i} & m_i \\ c_{0,j} & m_j \end{vmatrix} + \begin{vmatrix} c_{0,i} & p_i \\ c_{0,j} & p_j \end{vmatrix}.$$

The first term on the right hand side is negative by [Definition 3.4.1](#), and the last term is nonpositive by [Lemma 3.4.7](#). Since $\varpi_i \neq 0$, the middle term vanishes by [Corollary 6.3.6 4](#). \square

Remark 6.3.8. One can change Y_{pol} for any other resolution that arises from blowing up Y_{\min} either at non-invariant vertices or base points of the polar locus. In this case, all the results in this section are still true.

6.4. The Jacobian ideal in Y_{\min} and polar curves in Y_{pol}

The main result of this subsection is [Lemma 6.4.11](#), which gives a description of the strict transform of the polar curve in Y_{\min} and Y_{pol} . The lemma follows from some of the properties of these modifications we have seen so far, and a strong result of François Michel [[Mic08](#)].

Recall ([Notation 6.2.1](#)) that if, $i \in \mathcal{V}_{\min}$, we denote by $\deg_{\min}(i)$ the *degree* of i in Γ_{\min} , i.e. the number of adjacent edges (this includes edges adjacent to arrowheads). Since Υ is naturally embedded both in Γ_{\min} and Γ_{pol} , a vertex $i \in \mathcal{V}_{\Upsilon}$ has a well-defined $\deg_{\min}(i)$.

Definition 6.4.1. Let $\mathcal{N}_{\min} \subset \mathcal{V}_{\min}$ be the set of *nodes*, i.e. vertices with degree ≥ 3 . Let $\mathcal{E} \subset \mathcal{V}_{\min}$ be the set of *ends*, i.e. vertices of degree 1.

This notion of node is used in some classical references as in [[NW05](#)]. Sometimes the corresponding divisors are referred to as *branching* or *rupture*.

Lemma 6.4.2. *An invariant vertex has at most one non-invariant neighbor in Γ_{\min} . Furthermore, a connected component of the complement of Υ in Γ_{\min} is a bamboo, that is, a string of vertices, as shown in red on the left part of [fig. 6.4.8](#).*

PROOF. This statement can be seen to follow from the explicit process of resolving a plane curve. Alternatively, we can use induction, see [6.2.4](#) for notation. If Ξ is a connected component of $\Gamma_{\min} \setminus \Upsilon$, then Ξ is either the induced subgraph on the vertices in $\mathcal{V}' \setminus \mathcal{V}_{\Upsilon}$, or we have $\mathcal{V}_{\Xi} \subset \mathcal{V}_{\min} \setminus \mathcal{V}'$. In the first case, the connected component Ξ has precisely one neighbor, which does not have other non-invariant neighbors. In the second case, use induction. \square

6.4.3. Let $n \in \mathcal{N}_{\min}$ be a node, and assume that n has a non-invariant neighbor i_1 . Denote by i_1, i_2, \dots, i_h the vertices on the connected component of $\Gamma_{\min} \setminus \Upsilon$ containing the i_1 , such that i_j and i_{j+1} are adjacent for $j = 1, \dots, h-1$, and i_h is an end. Let $-b_j = D_{i_j}^2$ be the Euler numbers of these vertices. We use the notation

$$[b_1, \dots, b_h] = b_1 - \frac{1}{b_2 - \frac{1}{\dots - \frac{1}{b_h}}}$$

for the *negative continued fraction* associated with the sequence b_h, \dots, b_1 . Recursively define

$$\alpha_j = \begin{cases} 1 & j = h, \\ b_h & j = h-1, \\ b_{j+1}\alpha_{j+1} - \alpha_{j+2}, & j = 0, \dots, h-2. \end{cases}$$

Definition 6.4.4. Let $n \in \mathcal{N}_{\min} \setminus \{0\}$. If n has a non-invariant neighbor in Γ_{\min} , set $\alpha_n = \alpha_0$, as defined above. Otherwise, set $\alpha_n = \infty$.

Remark 6.4.5. If $\alpha_n = \infty$, then it is understood that $1/\alpha_n = 0$.

Definition 6.4.6. Let $n \in \mathcal{N}_{\min}$ be a node in Γ_{\min} . With the above notation, set $\mathcal{V}_{\min}(n) = \{i_0, i_1, \dots, i_h\}$ with $i_0 = n$. Let $\mathcal{V}_{\text{pol}}(n)$ be the set of vertices in $\mathcal{V}_{\min}(n)$, as well as any vertex appearing when blowing up a point in the preimage of the union of the D_i for $i \in \mathcal{V}_{\min}(n)$. See [fig. 6.4.8](#).

Remark 6.4.7. The set $\mathcal{V}_{\min}(n) \subset \mathcal{V}_{\min}$ is the set of vertices in the connected component containing n in the graph obtained from Γ_{\min} by removing all invariant edges. A similar description holds for $\mathcal{V}_{\text{pol}}(n) \subset \mathcal{V}_{\text{pol}}$.

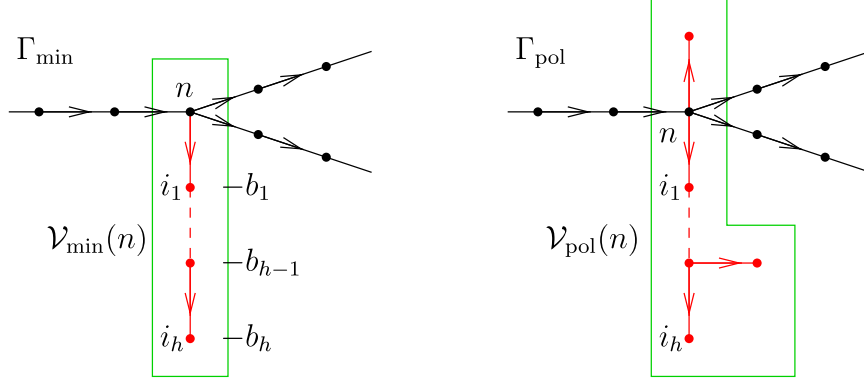


FIGURE 6.4.8. On the right hand side, we see two new vertices appear in $\mathcal{V}_{\text{pol}}(n)$.

By recursion, we find that $\alpha_{j-1} > \alpha_j$, and $\gcd(\alpha_{j+1}, \alpha_j) = 1$, as well as the formula

$$(6.4.9) \quad [b_j, b_{j+1}, \dots, b_h] = \frac{\alpha_{j-1}}{\alpha_j}.$$

Indeed, by induction

$$[b_j, b_{j+1}, \dots, b_h] = b_j - \frac{1}{[b_{j+1}, \dots, b_h]} = b_j - \frac{\alpha_{j+1}}{\alpha_j} = \frac{b_j \alpha_j - \alpha_{j+1}}{\alpha_j} = \frac{\alpha_{j-1}}{\alpha_j}.$$

With this in mind, we have the following lemma.

Lemma 6.4.10. *For $j = 0, \dots, h$, we have*

$$\alpha_j = \frac{m_{i_j}}{m_{i_h}} = \frac{c_{0,i_j}}{c_{0,i_h}}.$$

PROOF. Since the edges $i_j i_{j+1}$ are non-invariant, it suffices, by [Corollary 6.3.6](#), to prove the first equality.

Since the strict transform C_{\min} of the curve defined by f does not intersect D_{i_j} for $j > 0$, and the divisor $\sum_i m_i D_i + C_{\min} = (\pi_{\min}^* f)$ is principal, we find

$$0 = (D_{i_j}, \pi_{\min}^* f) = \begin{cases} m_{i_{h-1}} - b_h m_{i_h}, & j = h, \\ m_{i_{j+1}} - b_j m_{i_j} + m_{i_{j-1}}, & 1 \leq j < h. \end{cases}$$

Clearly, $\alpha_h = 1 = m_{i_h}/m_{i_h}$. The case $j = h$ above gives $\alpha_{h-1} = b_h = m_{i_{h-1}}/m_{i_h}$. For $j < h - 1$, induction gives

$$\frac{m_{i_j}}{m_{i_h}} = b_{j+1} \frac{m_{i_{j+1}}}{m_{i_h}} - \frac{m_{i_{j+2}}}{m_{i_h}} = \alpha_{j+1} \left(b_{j+1} - \frac{1}{[b_{j+2}, \dots, b_h]} \right) = \alpha_j. \quad \square$$

We are ready to state the main result of this section whose proof is postponed to the end.

Lemma 6.4.11. *With the notation introduced above, the following hold.*

- (1) *The Jacobian ideal has no base points on D_0 . If t is the number of tangents of C , then*

$$(P_{\text{pol}}, D_0) = (P_{\min}, D_0) = \deg_{\min}(0) - 1 = t - 1.$$

- (2) *If $i \in \mathcal{V}_{\text{T}} \setminus \mathcal{N}_{\min}$, then*

$$D_i \cap P_{\text{pol}} = D_i \cap P_{\min} = \emptyset.$$

- (3) *If $n \in \mathcal{N}_{\min}$, then, with the notation as in [6.4.3](#),*

$$(6.4.12) \quad \sum_{i \in \mathcal{V}_{\text{pol}}(n)} (P_{\text{pol}}, m_i D_i) = \sum_{j=0}^h (P_{\min}, m_{i_j} D_{i_j}) = m_n \left(\deg_{\min}(n) - 2 - \frac{1}{\alpha_n} \right).$$

Furthermore, every intersection point in $P_{\min} \cap D_n^\circ$ is a base point of the Jacobian ideal.

Example 6.4.13. The curve singularities defined by the polynomials

$$f(x, y) = y^4 + x^6 + x^5 y, \quad g(x, y) = y^4 + x^3 y^2 + x^6 + x^5 y.$$

at the origin have the same topological type. In fact, they are both Newton non-degenerate, and have the same Newton polyhedron. Thus, f and g are resolved by a toric morphism π_Δ , as described in [Example 3.4.8](#). The Newton polyhedron has one compact face, with normal vector $(2, 3)$.

The Newton polyhedron of a generic partial $af_x + bf_y$ has two compact faces, one with normal vector $(2, 3)$, and one with normal vector $(1, 2)$.

The Newton polyhedron of a generic partial $ag_x + bg_y$ has one compact face with normal vector $(3, 5)$.

To the left of [fig. 6.4.14](#), we see the minimal resolution of f , with two red arrows representing the strict transform of the polar curve, as well as, we see the same resolution, with one additional blow-up, giving an embedded resolution of a generic polar curve of g .

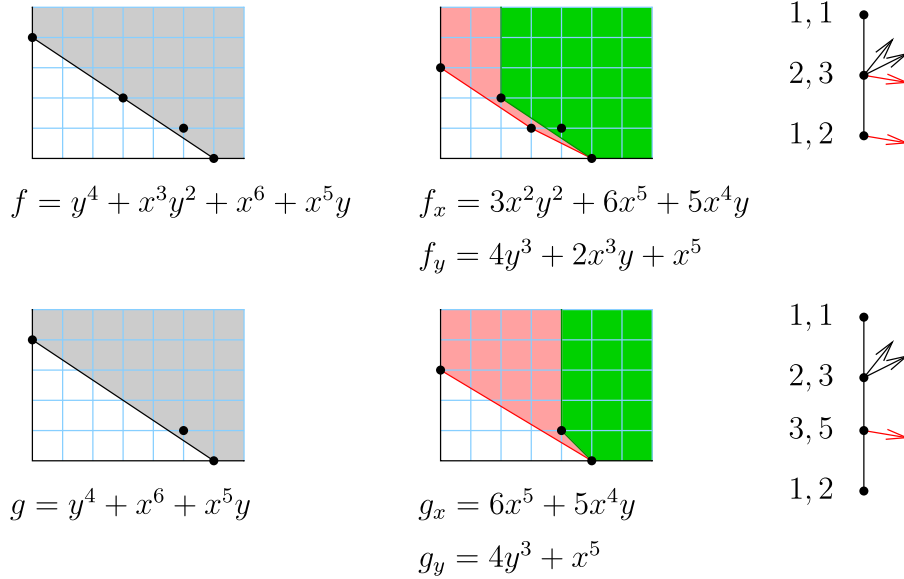


FIGURE 6.4.14. Left and center: Newton polyhedrons of f and g and their partials. To the right: resolution graphs showing the generic polar curve in red.

Lemma 6.4.15. *Use the notation introduced in 6.2.4. If $i \in \mathcal{V}_y \cap \mathcal{V}_\Upsilon$, then*

$$\text{ord}_{D_i}(xf_x) \geq \text{ord}_{D_i}(yf_y).$$

Equality holds, unless $i \in \mathcal{V}'$ and $\text{in}_i(f)$ does not depend on x , i.e. $\text{in}_i(f) = by^m$ for some $b \in \mathbb{C}^$ and $m \in \mathbb{Z}_{>0}$.*

PROOF. **Case 1.** Assume first that $i \in \mathcal{V}'$. Since we assumed that $i \in \mathcal{V}_\Upsilon$, that means by Lemma 6.2.13 that $\text{in}_i(f)$ does depend on y , so

$$\text{ord}_{D_i}(yf_y) = \text{ord}_{D_i}(f) \leq \text{ord}_{D_i}(xf_x).$$

If $\text{in}_i(f)$ does depend on x , then the above inequality is actually an equality.

Case 2. Assume next that $i \in \mathcal{V}_y \setminus \mathcal{V}'$. Since $i \in \mathcal{V}_\Upsilon$, i is an invariant vertex, i.e. we have $\varpi_i = 0$, by Lemma 6.2.3. If we take coordinates u, v in a neighborhood of some point $p \in D_i^\circ$, such that $\pi_{\min}^* x = u^{c_{0,i}}$, then the chain rule gives, since $x_v = 0$,

$$(6.4.16) \quad \begin{aligned} f_u &= x_u f_x + y_u f_y, & f_x &= \frac{f_u}{x_u} - \frac{y_u f_v}{x_u y_v}, \\ f_v &= y_v f_y, & f_y &= \frac{f_v}{y_v}. \end{aligned}$$

Since f and x vanish along D_i , we find

$$\text{ord}_{D_i}(f_u) = m_i - 1, \quad \text{ord}_{D_i}(x_u) = \text{ord}_{D_i}(x) - 1, \quad \text{ord}_{D_i}\left(x \frac{f_u}{x_u}\right) = m_i.$$

By Lemma 6.2.9, we have $\text{ord}_{D_i}(y) < c_{1,i}$, and so $\text{ord}_{D_i}(y_u) < c_{1,i} - 1$. By 3.3.4 we have $\text{ord}_{D_i}(y_v) = c_{1,i}$. By Lemmas 6.1.3 and 6.2.3, we have $\text{ord}_{D_i}(f_v) = m_i$. Put

together,

$$\text{ord}_{D_i} \left(x \frac{y_u f_v}{x_u y_v} \right) < c_{0,i} + (c_{1,i} - 1) + m_i - (c_{0,i} - 1) - c_{1,i} = m_i.$$

These two lines, along with [eq. \(6.4.16\)](#), give

$$\text{ord}_{D_i}(xf_x) = \text{ord}_{D_i} \left(x \frac{y_u f_v}{x_u y_v} \right) = m_i - c_{1,i} + \text{ord}_{D_i}(y).$$

Similarly,

$$\text{ord}_{D_i}(yf_y) = \text{ord}_{D_i} \left(\frac{y f_v}{y_v} \right) = m_i - c_{1,i} + \text{ord}_{D_i}(y). \quad \square$$

Corollary 6.4.17. *Use the notation introduced in [6.2.4](#). If $i \in \mathcal{V}_y$ is an invariant vertex, and $i \neq 0$, then $\text{ord}_{D_i}(f_y) < \text{ord}_{D_i}(f_x)$.*

PROOF. If $i \in \mathcal{V}'$ and $\text{in}_i(f) = by^m$, with $b \in \mathbb{C}^*$, then

$$\text{ord}_{D_i}(f_y) = \text{wt}_i(y^{m-1}) < \text{wt}_i(x^{-1}y^m) < \text{ord}_{D_i}(f_x).$$

We are using that by [6.2.8](#), *orders* can be computed as *weights*. Also, the last strict inequality follows since the operator ∂_x kills the initial part $\text{in}_i(f) = by^m$.

Otherwise, by [Lemma 6.4.15](#), we find

$$\text{ord}_{D_i}(f_y) = \text{ord}_{D_i}(f_x) + \text{ord}_{D_i}(x) - \text{ord}_{D_i}y < \text{ord}_{D_i}(f_x). \quad \square$$

Corollary 6.4.18. *If $i \in \mathcal{V}_Y \setminus \{0\}$ and $p \in D_i^\circ \cap P_{\min}$, then p is a base point of the Jacobian ideal (f_x, f_y) .*

PROOF. We can assume that $i \in \mathcal{V}_y \cap \mathcal{V}_Y$. Let p be an intersection point of P_{\min} and D_i . Since $\text{ord}_{D_i}(f_y) < \text{ord}_{D_i}(f_x)$ by [Corollary 6.4.17](#), the strict transform of the curve $af_x + f_y = 0$ passes through p for any $a \in \mathbb{C}$. \square

PROOF OF [LEMMA 6.4.11](#). 1 was proved in [Lemma 5.1.8](#) and the fact that, by [Remark 5.1.9](#), the Jacobian ideal has no base points on D_0 .

The statements 2 and 3 follow from the work of Michel [\[Mic08\]](#), as follows. Assume that x is any generic linear function $\mathbb{C}^2 \rightarrow \mathbb{C}$, and consider the finite morphism $(f, x) : (\mathbb{C}^2, 0) \rightarrow (\mathbb{C}^2, 0)$. The polar curve P is called the *Jacobian curve* in [\[Mic08\]](#), and the *Hironaka number* of $i \in \mathcal{V}_{\min}$ is defined as

$$q_i = \frac{\text{ord}_{D_i}(f)}{\text{ord}_{D_i}(x)} = \frac{m_i}{c_{0,i}}.$$

By [Lemma 3.4.7](#) and [Corollary 6.3.6](#), the Hironaka number is strictly increasing along invariant edges, and constant along non-invariant edges, in either Γ_{\min} or Γ_{pol} . Thus, if $i \in \Upsilon$ and $\deg_{\min}(i) = 2$, then the vertex i has no neighbor with the same Hironaka number, and thus by [\[Mic08, Theorem 4.9\]](#), the polar curve P_{\min} does not pass through D_i , proving the second equality in 2. The first equality follows immediately, since the modification $Y_{\text{pol}} \rightarrow Y_{\min}$ therefore does not modify D_i .

If $n \in \mathcal{N}_{\min}$, then, using the notation in [6.4.3](#), the set $\{n, i_1, \dots, i_h\}$ is a *rupture zone*, as defined in [\[Mic08, Definitions 1.4\]](#), i.e. a connected component in Γ_{\min}

of the induced subgraph of Γ_{\min} on the vertices with Hironaka number q_n . Using $i_0 = n$ as before, then [Mic08, Theorem 4.9] states that

$$(6.4.19) \quad \sum_{\gamma} V_f(\gamma) = - \sum_{j=0}^h m_{i_j} \chi(D_{i_j}^{\circ}).$$

Here, γ runs through the connected components of P_{\min} which pass through a point $p \in D_i$ for some $i \in \mathcal{V}_{\min}(n)$, and if $\nu : (\mathbb{C}, 0) \rightarrow (\gamma, p)$ is the normalization of such a branch, then $V_f(\gamma) = \text{ord}_t(\nu^* \pi_{\min}^* f(t))$ where t is a coordinate in \mathbb{C} . As a result, we have

$$V_f(\gamma) = (\gamma, (\pi_{\min}^* f)) = \sum_{i \in \mathcal{V}_{\min}} (\gamma, D_i),$$

since γ does not intersect the strict transform C_{\min} , by Corollary 6.3.3. A similar statement holds for π_{pol} . The terms on the right hand side of eq. (6.4.19) all vanish, except for $j = 0$ and $j = h$, and we have

$$-\chi(D_{i_0}^{\circ}) = -\chi(D_n^{\circ}) = \deg_{\min}(n) - 2, \quad -\chi(D_{i_h}^{\circ}) = \deg_{\min}(i_h) - 2 = -1.$$

Furthermore, $m_{i_h} = m_n/\alpha_n$ by Lemma 6.4.10. Now eq. (6.4.12) follows, since

$$\left(P_{\min}, \sum_{j=0}^h m_{i_j} D_{i_j} \right) = \sum_{\gamma} V_f(\gamma) = \sum_{i \in \mathcal{V}_{\text{pol}}(n)} (P_{\text{pol}}, m_i D_i). \quad \square$$

CHAPTER 7

The 1st Blow-up

In this section we extend the pullback of the vector field ξ to the exceptional divisor of the 1st blow up $\pi_0 : Y_0 \rightarrow \text{Tub}$. As we will notice, this construction cannot be further continued to divisors of subsequent blow-ups since, in general, the vector field is not invariant in the sense of [Definition 4.1.1](#).

After that, we also extend the vector field to the boundary of the real oriented blow up of Y_0 along D_0 . We introduce some genericity conditions on the metric (but not on the defining function f) in order for these extensions to admit potentials that are Morse functions.

7.1. Special coordinates

For this subsection fix the standard metric on \mathbb{C}^2 . Let x, y be isometric linear coordinates ([Definition 2.3.1](#)) on \mathbb{C}^2 with respect to some $A \in U(2)$ such that $\{x = 0\}$ is not a tangent of $(C, 0)$. In the x, y coordinates the vector field ξ , by [Lemma 2.1.3](#) is represented by the column vector

$$(7.1.1) \quad -\nabla^{g_{\text{std}}} \log |f| = -\left(\frac{\bar{f}_x}{\bar{f}}, \frac{\bar{f}_y}{\bar{f}}\right)^{\top}.$$

Let $\pi_0 : Y_0 \rightarrow \mathbb{C}^2$ be the first blow up. The vector field $\pi_0^* \xi$ is a vector field well defined on $Y_0 \setminus \pi_0^{-1}(C)$. In this section we re-scale the vector field by a positive real function so that it can be extended over the exceptional divisor D_0° . Let $U \subset Y_0$ be the standard chart with coordinates u, v such that $\pi_0(u, v) = (u, uv)$ on U . Then the Jacobian of π_0 in those coordinates is given by:

$$\text{Jac } \pi_0 = \begin{pmatrix} x_u & x_v \\ y_u & y_v \end{pmatrix} = \begin{pmatrix} 1 & 0 \\ v & u \end{pmatrix}.$$

Here we are using the notation $x_u = \partial_u \pi_0^* x(u, v)$ and similar for the other variables.

In particular, $\det \text{Jac } \pi_0 = u$ and the expression for $\pi_0^* \xi$ leaves us with

$$(7.1.2) \quad \pi_0^* \xi = (\text{Jac } \pi_0)^{-1} \cdot \xi = \frac{-1}{u\bar{f}} \begin{pmatrix} u\bar{f}_x \\ -v\bar{f}_x + \bar{f}_y \end{pmatrix} = \begin{pmatrix} \xi^u \\ \xi^v \end{pmatrix}.$$

The last equality defines the real analytic functions ξ^u and ξ^v on $U \setminus D_0$ as the coordinates of the vector field $\pi_0^* \xi$.

In this chart the divisor D_0 is given by $\{u = 0\}$ and $\pi_0^* \xi$ has a pole along it. Next we compute the order of this pole.

Lemma 7.1.3. $\text{ord}_u \xi^u \geq -1$ and $\text{ord}_u \xi^v = -2$.

PROOF. The first inequality is true regardless of the chosen coordinates.

$$\text{ord}_u \xi^u = \text{ord}_u \frac{u\bar{f}_x}{u\bar{f}} = \text{ord}_u \frac{\bar{f}_x}{\bar{f}} \geq -1.$$

For the second equality, we use that we have chosen special coordinates as in the beginning of this subsection such that $\{x = 0\}$ is not a tangent of $(C, 0)$. This implies that $\text{in}(\bar{f})$ contains the monomial \bar{y}^e with a non-zero coefficient, where e is the multiplicity of $(C, 0)$. So \bar{f}_y contains the monomial \bar{y}^{e-1} . This gives us that $\text{ord}_u \bar{f}_y = e - 1$. We observe that $\text{ord}_u(-v\bar{f}_x) = \text{ord}_u \bar{f}_x \geq e - 1$ as the first inequality of the lemma shows. Also, $\text{in}(v\bar{f}_x)$ does not contain antiholomorphic monomials, so the initial parts of $-v\bar{f}_x$ and \bar{f}_y do not cancel. We conclude that $\text{ord}_u(-v\bar{f}_x + \bar{f}_y) = \text{ord}_u \bar{f}_y = e - 1$. Finally, since $\text{ord}_u(u\bar{f}) = e + 1$ and $e - 1 - (e + 1) = -2$ we get:

$$\text{ord}_u \xi^v = \text{ord}_u \frac{-v\bar{f}_x + \bar{f}_y}{u\bar{f}} = -2. \quad \square$$

7.2. Scaling and extending the vector field

Recall that we denote by $\tilde{C} \subset Y_0$ the strict transform of $C \subset \text{Tub}$.

Lemma 7.2.1. *There exists a unique vector field on $Y_0 \setminus \tilde{C}$ which is equal to*

$$\pi_0^*(\delta \cdot \xi)$$

outside D_0° , where $\delta(x, y) = |x|^2 + |y|^2$. Furthermore, it is tangent to D_0 and does not vanish identically along D_0° .

PROOF. With the previous notation, $\pi_0^*\delta = |u|^2(1 + |v|^2)$ has vanishing order 2 along D_0 . Since $(1 + |v|^2)$ is a unit, it suffices to show that the functions $|u|^2\xi^u$ and $|u|^2\xi^v$ extend analytically across D_0° .

We can express each of these two functions explicitly. First we have

$$|u|^2\xi^u = |u|^2 \frac{\bar{f}_x}{\bar{f}} = u \frac{\bar{u}\bar{f}_x}{\bar{f}}.$$

We observe that $\frac{\bar{u}\bar{f}_x}{\bar{f}}$ is an anti-holomorphic function because, by Lemma 7.1.3, $\text{ord}_u \xi^u \geq -1$ and so $\text{ord}_u \frac{\bar{u}\bar{f}_x}{\bar{f}} \geq 0$. We conclude that $u \frac{\bar{u}\bar{f}_x}{\bar{f}}$ is real analytic and that $\text{ord}_u u \frac{\bar{u}\bar{f}_x}{\bar{f}} \geq 1$ which means that the extension of ξ^u vanishes along D_0 .

Secondly, we have

$$|u|^2\xi^v = |u|^2 \frac{-v\bar{f}_x + \bar{f}_y}{u\bar{f}} = \bar{u} \frac{-v\bar{f}_x + \bar{f}_y}{\bar{f}} = -v \frac{\bar{u}\bar{f}_x}{\bar{f}} + \frac{\bar{u}\bar{f}_y}{\bar{f}}.$$

Similarly as in the previous case, the function $|u|^2\xi^v$ extends as a real analytic function over D_0° . Furthermore, by Lemma 7.1.3 $\text{ord}_u |u|^2\xi^v = 2 - 2 = 0$. This means that the extension of $|u|^2\xi^v$ over D_0° is not identically 0. \square

Definition 7.2.2. Let $\hat{\xi}_0$ be the vector field on $Y_0 \setminus \tilde{C}$ described by Lemma 7.2.1 and let $\xi_0 = \hat{\xi}_0|_{D_0^\circ}$ be its restriction.

One of the goals of this section is to prove (Theorem 7.4.9) that, except for a measure 0 set in the set of Hermitian metrics, $\hat{\xi}_0$ is an elementary vector field (recall Definition 2.4.3).

Remark 7.2.3. Let π_0^{ro} be the composition

$$\pi_0^{\text{ro}} = \pi_0 \circ \sigma_0 : Y_0^{\text{ro}} \rightarrow \text{Tub}$$

of the blow-up at the origin and the real oriented blow up of Y_0 along D_0 .

Then, we can also extend $(\pi_0^{\text{ro}})^*(\delta \cdot \xi)$ to a vector field on all $Y_0^{\text{ro}} \setminus \sigma_0^{-1}(\tilde{C})$ (recall Lemma 4.1.2). Equivalently, we can simply take the pullback of $\hat{\xi}_0$ by σ_0 .

Definition 7.2.4. Let $\hat{\xi}_0^{\text{ro}} = \sigma_0^* \hat{\xi}_0$ be the pullback of the previously constructed vector field to the real oriented blow up outside the strict transform $Y_0^{\text{ro}} \setminus \sigma_0^{-1}(\tilde{C})$. Let $\xi_{0,\theta}^{\text{ro}} = \hat{\xi}_0^{\text{ro}}|_{D_{0,\theta}^{\text{ro},\circ}}$ for $\theta \in \mathbb{R}/2\pi\mathbb{Z}$.

7.3. $\hat{\xi}_0$ in the normal direction

Let $p \in D_0^\circ$ be a zero of ξ_0 . In this subsection, we change conventions with respect to the previous subsection and consider a chart $V \subset Y_0$ with coordinates u, v in such a way that $p = (0, 0)$ and $\{u = 0\}$ defines $D_0 \cap V$. In other words, p corresponds to the line $\{x = 0\} \subset \mathbb{C}^2$. In these coordinates the blow up is expressed as $\pi(u, v) = (uv, u)$.

In these coordinates we have

$$\text{Jac } \pi_0 = \begin{pmatrix} v & u \\ 1 & 0 \end{pmatrix}$$

and so

$$\text{Jac } \pi_0^{-1} = \frac{1}{-u} \begin{pmatrix} 0 & -u \\ -1 & v \end{pmatrix}.$$

In particular, we find that $\xi^u = -\bar{f}_y/\bar{f}$.

Since $\hat{\xi}_0$ is tangent to D_0° , the Hessian of $\hat{\xi}_0$ at p has $T_p D_0$ as invariant subspace. Therefore, the spectrum of $\text{Hess}_p(\hat{\xi}_0)$ is the union of the spectrum of its restriction of to $T_p D_0$ and the spectrum of the induced operator on the quotient $T_p Y_0 / T_p D_0$.

Observe that $\hat{\xi}_0$ only has zeroes on D_0 . Therefore, by the starting paragraph of this subsection, it is enough to show that the parts of the Hessian corresponding to $T_p Y_0 / T_p D_0$ and to $T_p D_0$ are elementary for each zero $p \in D_0^\circ$.

Lemma 7.3.1. *Let $p \in D_0^\circ$ be a singularity of $\hat{\xi}_0$. Then $\text{Hess}_p(\hat{\xi}_0)$ has two negative eigenvalues in the part corresponding to $T_p Y_0 / T_p D_0$.*

PROOF. Using the coordinates described at the beginning of this section, we have that $p = (0, 0)$. We also have

$$\pi_0^* f = au^e + \text{h.o.t.}$$

with $a \neq 0$ some complex number. Therefore,

$$\pi_0^* f_y = ae u^{e-1} + \text{h.o.t.},$$

and,

$$\frac{\bar{u} \bar{f}_y}{\bar{f}} = e + \text{h.o.t.}$$

Finally,

$$|u|^2 \xi^u = -u \frac{\bar{u} \bar{f}_y}{\bar{f}} = -eu + \text{h.o.t.}$$

Since $\hat{\xi}_0$ is tangent to D_0° , we find that its linearization matrix, is of the form

$$\begin{pmatrix} -e & 0 & 0 \\ 0 & -e & * \\ * & * & * \end{pmatrix}. \quad \square$$

7.4. $\hat{\xi}_0$ in the tangent direction

Consider the space of constant Hermitian metrics $GL(2, \mathbb{C})/U(2)$ of \mathbb{C}^2 . This space is a real manifold of dimension 4. We identify a small neighborhood of the identity matrix $\text{id} \in GL(2, \mathbb{C})/U(2)$ with a small neighborhood $\mathcal{H} \subset \mathbb{R}^4$ of $(1, 0, 0, 1) \in \mathbb{R}^4$ such that for all points $(a, b, c, d) \in \mathcal{H}$, the matrix

$$H = \begin{pmatrix} a & b + ci \\ b - ci & d \end{pmatrix}$$

is a Hermitian inner product. Finally, let δ_H be the squared norm with respect to the metric H , that is $\delta_H(x, y) = (\bar{x} \ \bar{y}) H \begin{pmatrix} x \\ y \end{pmatrix}$. In this setting, we define the family of real valued functions:

$$\begin{aligned} \Phi : \mathcal{H} \times \mathbb{C}^2 \setminus \{C\} &\rightarrow \mathbb{R} \\ (a, b, c, d, x, y) &\mapsto -\log \frac{|f(x, y)|}{(\delta_H(x, y))^{e/2}}. \end{aligned}$$

Assume that one of the tangents of $(C, 0)$ is $\{y = 0\}$. We can always do so up to a linear change of coordinates that preserves the Hermitian metric (simply a complex rotation). We take a standard chart of Y_0 with coordinates u, v such that $D_0^\circ \subset Y \setminus \tilde{C}$ is defined by $u = 0$ and v is a coordinate for it. As usual, in these coordinates π_0 is given by $\pi_0(u, v) = (u, uv)$. Now we pullback the family Φ to $\mathcal{H} \times Y_0 \setminus \pi_0^{-1}(C)$ and prove that it actually extends over $Y_0 \setminus \tilde{C}$. First we observe that

$$\pi_0^* \delta_H(u, v) = |u|^2 ((b + ic)v + (dv + b - ic)\bar{v} + a).$$

Then, writing $\pi_0^* f(u, v) = u^e (\tilde{f}(u, v))$, a direct computation yields:

$$\begin{aligned} -\log \frac{|\pi_0^* f(u, v)|}{(\pi_0^* \delta_H(u, v))^{\frac{e}{2}}} &= -\log |\pi_0^* f(u, v)| + \log (\pi_0^* \delta(u, v))^{\frac{e}{2}} \\ (7.4.1) \quad &= -\log |\tilde{f}(u, v)| - \log |u|^e + \log \pi_0^* \delta(u, v)^{\frac{e}{2}} \\ &= -\log |\tilde{f}(u, v)| - e \log |u| + e \log |u| \\ &\quad + \frac{e}{2} \log ((b + ic)v + (dv + b - ic)\bar{v} + a) \\ &= -\log |\tilde{f}(u, v)| + \frac{e}{2} \log ((b + ic)v + (dv + b - ic)\bar{v} + a). \end{aligned}$$

Let $g(v) = \tilde{f}(0, v)$ be the restriction of \tilde{f} to D_0° . Let s, t be real coordinates for D_0° , that is, $v = s + ti$. Thus, we have constructed a well defined family of functions

$$\begin{aligned} \Phi_0 : \mathcal{H} \times D_0^\circ &\rightarrow \mathbb{R} \\ (a, b, c, d, s, t) &\mapsto -\log |g(v)| + \frac{e}{2} \log (ds^2 + dt^2 + 2bs - 2ct + a). \end{aligned}$$

For each $(a, b, c, d) = H \in \mathcal{H}$, we define

$$\begin{aligned} \phi_{H,0} : D_0^\circ &\rightarrow \mathbb{R} \\ (s, t) &\mapsto \Phi_0(a, b, c, d, s, t). \end{aligned}$$

Lemma 7.4.2. *There exists a Lebesgue measure 0 set \mathcal{H}_0 in the space \mathcal{H} , such that for all $H \in \mathcal{H} \setminus \mathcal{H}_0$ the function*

$$\phi_{H,0} : D_0^\circ \rightarrow \mathbb{R}$$

is Morse.

PROOF. The theorem follows after checking that the hypotheses of [Nic11, Theorem 1.2.1] are satisfied by our family Φ_0 . More concretely, we only need to check that

$$\text{rk} \begin{pmatrix} (\Phi_0)_{as} & (\Phi_0)_{bs} & (\Phi_0)_{cs} & (\Phi_0)_{ds} \\ (\Phi_0)_{at} & (\Phi_0)_{bt} & (\Phi_0)_{ct} & (\Phi_0)_{dt} \end{pmatrix} = 2$$

for all $(a, b, c, d, s, t) \in \mathcal{H} \times D_0^\circ$. For convenience of notation, let

$$h(a, b, c, d, s, t) = ds^2 + dt^2 + 2bs - 2ct + a.$$

We observe that $g(v)$ does not depend on a, b, c or d , so we find that

$$\begin{aligned} & \begin{pmatrix} (\Phi_0)_{as} & (\Phi_0)_{bs} & (\Phi_0)_{cs} & (\Phi_0)_{ds} \\ (\Phi_0)_{at} & (\Phi_0)_{bt} & (\Phi_0)_{ct} & (\Phi_0)_{dt} \end{pmatrix} \\ &= \frac{e}{2} \begin{pmatrix} \frac{h_{ash}-h_a h_s}{h^2} & \frac{h_{bs}h-h_b h_s}{h^2} & \frac{h_{cs}h-h_c h_s}{h^2} & \frac{h_{ds}h-h_d h_s}{h^2} \\ \frac{h_{at}h-h_a h_t}{h^2} & \frac{h_{bt}h-h_b h_t}{h^2} & \frac{h_{ct}h-h_c h_t}{h^2} & \frac{h_{ct}h-h_c h_t}{h^2} \end{pmatrix} \\ &= \frac{e}{2} \begin{pmatrix} \frac{-h_s}{h^2} & \frac{h_{bs}h-h_b h_s}{h^2} & \frac{h_{cs}h-h_c h_s}{h^2} & \frac{h_{ds}h-h_d h_s}{h^2} \\ \frac{-h_t}{h^2} & \frac{h_{bt}h-h_b h_t}{h^2} & \frac{h_{ct}h-h_c h_t}{h^2} & \frac{h_{ct}h-h_c h_t}{h^2} \end{pmatrix} \end{aligned}$$

Where the last equality follows from the fact that $h_a = 1$. We are also using that h is never 0 in order to divide by h^2 .

We perform elementary column operations on the last matrix of the above equation and get:

$$\begin{aligned} & \text{rk} \begin{pmatrix} \frac{-h_s}{h^2} & \frac{h_{bs}h-h_b h_s}{h^2} & \frac{h_{cs}h-h_c h_s}{h^2} & \frac{h_{ds}h-h_d h_s}{h^2} \\ \frac{-h_t}{h^2} & \frac{h_{bt}h-h_b h_t}{h^2} & \frac{h_{ct}h-h_c h_t}{h^2} & \frac{h_{ct}h-h_c h_t}{h^2} \end{pmatrix} \\ &= \text{rk} \begin{pmatrix} -h_s & h_{bs}h - h_b h_s & h_{cs}h - h_c h_s & h_{ds}h - h_d h_s \\ -h_t & h_{bt}h - h_b h_t & h_{ct}h - h_c h_t & h_{ct}h - h_c h_t \end{pmatrix} \\ &= \text{rk} \begin{pmatrix} -h_s & h_{bs}h & h_{cs}h & h_{ds}h \\ -h_t & h_{bt}h & h_{ct}h & h_{ct}h \end{pmatrix} \\ &= \text{rk} \begin{pmatrix} -h_s & h_{bs} & h_{cs} & h_{ds} \\ -h_t & h_{bt} & h_{ct} & h_{ct} \end{pmatrix} \\ &= \text{rk} \begin{pmatrix} -h_s & 2 & 0 & h_{ds} \\ -h_t & 0 & -2 & h_{ct} \end{pmatrix} = 2 \end{aligned}$$

The cited criterion, [Nic11, Theorem 1.2.1] gives exactly the statement of this lemma. \square

Definition 7.4.3. For $(a, b, c, d) = (1, 0, 0, 1)$, that is, for the standard Hermitian metric, we denote

$$\phi_0 = \phi_{\text{id}, 0}.$$

Lemma 7.4.4. *The vector field ξ_0 is the gradient of $\phi_0(v)$ with respect to the Fubini-Study metric on $D_0^\circ \subset \mathbb{CP}^1$.*

PROOF. We make a few observations on the second coordinate ξ^v of $\pi_0^* \xi$. First we compute it from the formula $\pi_0^* \xi = -(\text{Jac } \pi_0)^{-1} \left(\frac{\bar{f_x}(u, uv)/\bar{f}(u, uv)}{\bar{f_y}(u, uv)/\bar{f}(u, uv)} \right)$ and we find that

$$(7.4.5) \quad \xi^v(u, v) = \frac{-1}{u \bar{f}(u, uv)} \left(-v \bar{f_x}(u, uv) + \bar{f_y}(u, uv) \right)$$

Let $\text{in}(f)$ be the initial part (recall [Definition 3.2.2](#)) of f , that is,

$$f = \text{in}(f) + \text{h.o.t.}$$

and $\text{in}(f)$ is a homogeneous polynomial of degree e . Thus, $\pi_0^* f$ is divisible by u^e . Then

$$\frac{\pi_0^* f}{u^e} \Big|_{D_0^\circ} = \frac{\pi^* \text{in}(f)}{u^e} \Big|_{D_0^\circ} = \text{in}(f)(1, v) = g(v)$$

with $g(t) \in \mathbb{C}[t]$. Similarly, $\pi_0^* f_x$ and $\pi_0^* f_y$ are divisible by u^{e-1} , and

$$\frac{\pi_0^* f_x}{u^{e-1}} \Big|_{D_0^\circ} = \frac{\pi_0^* (\text{in}(f))_x}{u^{e-1}} \Big|_{D_0^\circ} = (\text{in}(f))_x(1, v) = eg(v) - vg'(v)$$

and

$$\frac{\pi_0^* f_y}{u^{e-1}} \Big|_{D_0^\circ} = \frac{\pi^* (\text{in}(f))_y}{u^{e-1}} \Big|_{D_0^\circ} = (\text{in}(f))_y(1, v) = g'(v).$$

Using the above two equations in [eq. \(7.4.5\)](#) and, after scaling the vector field with δ , we find

$$\begin{aligned} \pi_0^*(\delta) \cdot \xi^v \Big|_{D_0^\circ} &= \frac{|u|^2(1+|v|^2)}{uf(u, uv)} (ve\bar{u}^{e-1}g(\bar{v}) - |v|^2\bar{u}^{e-1}g'(\bar{v}) - e\bar{u}^{e-1}g'(\bar{v})) \Big|_{D_0^\circ} \\ (7.4.6) \quad &= \frac{(1+|v|^2)}{g(\bar{v})} (veg(\bar{v}) - |v|^2g'(\bar{v}) - g'(\bar{v})) \\ &= (1+|v|^2) \left(ve - (1+|v|^2) \frac{g'(\bar{v})}{g(\bar{v})} \right) \end{aligned}$$

On another hand we compute the differential of ϕ_0 :

$$\begin{aligned} D\phi_0 &= -\frac{g'(\bar{v})}{g(\bar{v})} + \frac{ve}{1+|v|^2} \\ (7.4.7) \quad &= \frac{1}{1+|v|^2} \left(ve - (1+|v|^2) \frac{g'(\bar{v})}{g(\bar{v})} \right) \end{aligned}$$

Finally, if we denote by $\nabla^{\text{FS}} \phi_0$ the gradient of ϕ_0 with respect to the Fubini-Study metric, then

$$\nabla^{\text{FS}} \phi_0 = (1+|v|^2)^2 \cdot D\phi_0.$$

So the lemma follows from [eq. \(7.4.6\)](#) and [eq. \(7.4.7\)](#). \square

Let $\hat{\xi}_{H,0}$ be the vector field analogous to $\hat{\xi}_0$ but computed with the metric H .

Corollary 7.4.8. *The vector field $\hat{\xi}_{H,0}|_{D_0^\circ}$ is the gradient of $\phi_{H,0}(v)$.*

PROOF. Find $A \in \text{GL}(\mathbb{C}, 2)$ such that $A^* A = H$, then take the isometric coordinates induced by A and apply the previous lemma. \square

Theorem 7.4.9. *There exists a measure 0 set \mathcal{H}_0 in \mathcal{H} , such that for all Hermitian metrics $H \in \mathcal{H} \setminus \mathcal{H}_0$, the restriction of the vector field $\hat{\xi}_{H,0}|_{D_0^\circ}$ is elementary.*

PROOF. The proof is a direct application of [Lemma 7.4.2](#) and [Corollary 7.4.8](#) plus the observation that gradients of Morse functions are elementary vector fields. \square

Definition 7.4.10. Let $G_0 \subset \mathrm{GL}(2, \mathbb{C})$ be the set of matrices A such that

$$A^* A \in \mathcal{H} \setminus \mathcal{H}_0$$

Definition 7.4.11. We denote by $\Sigma_0 \subset D_0^\circ$ the set of singularities of ξ_0 on D_0° .

The following lemma shows that ξ_0 may only have fountains or saddle points (fig. 2.4.5).

Lemma 7.4.12. *If $H \in \mathcal{H} \setminus \mathcal{H}_0$, then $\xi_{H,0}$ does not have sink singularities.*

PROOF. If $p \in D_0^\circ$ is a sink singularity of $\xi_{H,0}$, that is, if the vector field $\xi_{H,0}$ has a sink in the direction tangent to D_0 , then the vector field $\hat{\xi}_{H,0}$ has an sink at p by Lemma 7.3.1. In particular, for each Milnor fiber, there is a whole disk in it that forms part of the spine, which contradicts the fact that the spine contains no disks with positive volume which is proved in [A'C18, Theorem 2.2]. \square

Lemma 7.4.13. *Let p be a point in $D_0 \cap \tilde{C}$. Then, the vector field ξ_0 points towards p in a small neighborhood around p . As a consequence, the Poincaré-Hopf index of ξ_0 at the puncture p is 1.*

PROOF. By the expression of ϕ_0 given in eq. (7.4.1) we get that $\phi_0 \rightarrow +\infty$ for points approaching p . By Lemma 7.4.4, the vector field ξ_0 is the gradient of ϕ_0 and so it points in the direction where ϕ_0 grows.

The statement about the index is a direct consequence of the dynamics of ξ_0 near p which behaves effectively as a sink (recall Definition 2.4.6). \square

7.5. The spine at radius zero over the 1st blow-up

We are now ready to construct the spine at radius zero for homogeneous singularities. Consider the real oriented blow up

$$\sigma_0 : Y_0^{\mathrm{ro}} \rightarrow Y_0$$

of Y_0 along $D_0 \cup C$.

First we construct a 1-dimensional CW-complex which is a spine for D_0° . Let $I_0 \subset \Sigma_0$ be the set of saddle points of ξ_0 . For each saddle point $p \in I_0$ we consider its stable manifold \tilde{B}_p which consists of the union of two trajectories B_p^+ and B_p^- together with p , that is,

$$\tilde{B}_p = B_p^+ \sqcup B_p^- \sqcup \{p\}.$$

Let $I_{0,\theta}^{\mathrm{ro}} \subset \Sigma_{0,\theta}^{\mathrm{ro}}$ be the set of saddle points of $\xi_0^{\mathrm{ro}}|_{D_{0,\theta}^{\mathrm{ro},\circ}}$. For each saddle point $q \in I_{0,\theta}^{\mathrm{ro}}$ we consider the corresponding stable manifold,

$$\tilde{B}_q^{\mathrm{ro}} = B_q^+ \sqcup B_q^- \sqcup \{q\}.$$

We recall that by Definition 7.2.4, the vector field $\xi_0^{\mathrm{ro}}|_{D_{0,\theta}^{\mathrm{ro},\circ}}$ is just the pullback of ξ_0 by the map $\sigma_0|_{D_{0,\theta}^{\mathrm{ro},\circ}} : D_{0,\theta}^{\mathrm{ro},\circ} \rightarrow D_0^\circ$, which is a m_0 -fold regular covering. In particular,

$$\left(\sigma_0|_{D_{0,\theta}^{\mathrm{ro},\circ}}\right)^{-1}(\tilde{B}_p) = \bigcup_{q \in \left(\sigma_0|_{D_{0,\theta}^{\mathrm{ro},\circ}}\right)^{-1}(p)} \tilde{B}_q^{\mathrm{ro}}.$$

By Lemma 7.4.12 all the singularities in $R_0 = \Sigma_0 \setminus I_0$ are repellers and thus, have empty stable manifolds. Analogously, all singularities in $R_{0,\theta}^{\text{ro}} = \Sigma_{0,\theta}^{\text{ro}} \setminus I_{0,\theta}^{\text{ro}}$ are also repellers. We define the set

$$S_0 = \bigsqcup_{p \in I_0} \tilde{B}_p \bigsqcup_{p \in R_0} \{p\}.$$

Definition 7.5.1. We define the set

$$S_{0,\theta}^{\text{ro}} = \bigsqcup_{q \in I_{0,\theta}^{\text{ro}}} \tilde{B}_q^{\text{ro}} \bigsqcup_{q \in R_{0,\theta}^{\text{ro}}} \{q\}$$

and call it the *spine at radius 0 and angle θ over D_0* .

Lemma 7.5.2. *The set S_0 is a spine for D_0° and the set $S_{0,\theta}^{\text{ro}}$ is a spine for $D_{0,\theta}^{\text{ro},\circ}$ for each $\theta \in \mathbb{R}/2\pi\mathbb{Z}$.*

PROOF. We know that near the punctures of D_0 the vector field points towards the punctures (Lemma 7.4.13). By definition, the complement of S_0 consists of trajectories that necessarily converge to one of these punctures because there are no sinks in D_0° (Lemma 7.4.12). Pick a small simple closed curve around each of these punctures and let it flow by ξ_0 forward and backwards. The union of all these curves and their translates by ξ_0 equals an union of disjoint cylinders, as many as punctures in D_0° . This shows that S_0 is a spine of D_0° .

The second statement follows directly after the observation that $\sigma|_{D_{0,\theta}^{\text{ro},\circ}} : D_{0,\theta}^{\text{ro},\circ} \rightarrow D_0^\circ$ is a regular covering for each θ . \square

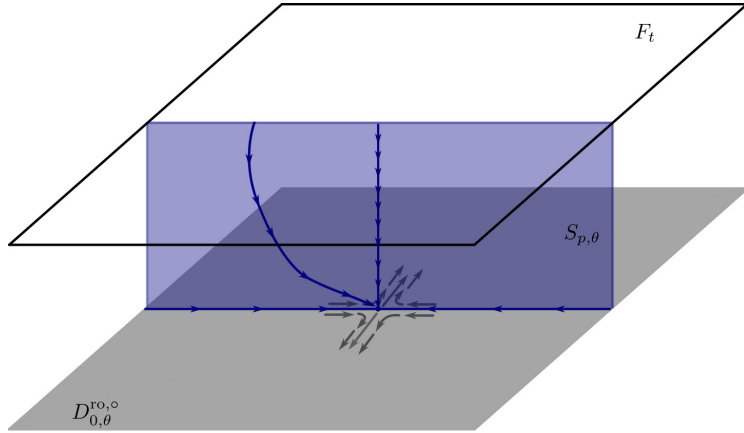


FIGURE 7.5.3. In blue, the stable-manifold associated with a saddle point of $\xi_{0,\theta}^{\text{ro}}$. In darker blue we can see two trajectories contained in $S_{p,\theta}$. On top, the Milnor fiber over $t \in D_\eta$ with $\arg(t) = \theta$. Below, in gray, a part of $D_{0,\theta}^{\text{ro},\circ}$.

7.6. Some homogeneous examples

In this subsection we apply the theory developed on this section to some base case examples.

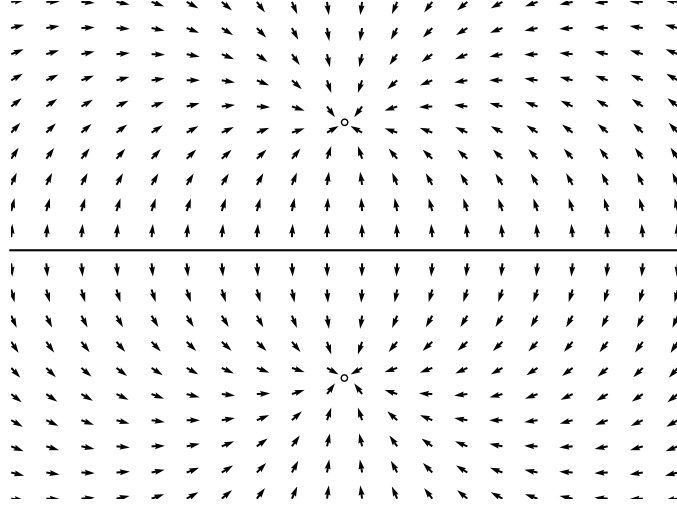


FIGURE 7.6.2. In black the vector field on the chart U . The horizontal line on the center is part of a whole S^1 of zeroes of ξ_0

Example 7.6.1. We start by considering the Morse singularity $f(x, y) = y^2 + x^2$. Let $\pi_0 : Y_0 \rightarrow \text{Tub}$ be the blow up at the origin $0 \in \text{Tub}$. Take the local chart $U \subset Y_0$ with coordinates u, v such that

$$\pi_0(u, v) = (u, uv).$$

In these local coordinates we have:

$$\pi_0^* f = (v^2 + 1)u^2, \quad \text{Jac } \pi_0 = \begin{pmatrix} 1 & 0 \\ v & u \end{pmatrix}, \quad \det \text{Jac } \pi_0 = u.$$

We use eq. (7.1.2) and we compute

$$\begin{pmatrix} \xi^u \\ \xi^v \end{pmatrix} = \frac{-1}{u(\bar{v}^2 + 1)\bar{u}^2} \begin{pmatrix} 2u\bar{u} \\ 2\bar{u}\bar{v} - 2v\bar{u} \end{pmatrix} = \begin{pmatrix} -\frac{2}{\bar{u}\bar{v}^2 + \bar{u}} \\ \frac{2(v - \bar{v})}{\bar{u}\bar{v}^2 + \bar{u}} \end{pmatrix}.$$

We compute

$$\lim_{u \rightarrow 0} |u|^2 \begin{pmatrix} -\frac{2}{\bar{u}\bar{v}^2 + \bar{u}} \\ \frac{2(v - \bar{v})}{\bar{u}\bar{v}^2 + \bar{u}} \end{pmatrix} = \begin{pmatrix} 0 \\ \frac{2(v - \bar{v})}{\bar{v}^2 + 1} \end{pmatrix}.$$

That is, for the chart $U \cap D_0^\circ$ with coordinate v ,

$$\xi_0 = \frac{2(v - \bar{v})}{\bar{v}^2 + 1}.$$

We can see from the expression above that the vector field has non-isolated zeroes (see fig. 7.6.2). More concretely, the whole line $\text{Re}(v) = 0$ is a line of zeros in $U \cap D_0^\circ$. Actually, this line forms part of a S^1 of zeroes in D_0° . In particular, this shows that the standard metric here does not come from a matrix A in G_0 (Definition 7.4.10) since the vector field cannot be the gradient of any Morse function.

In the next example we consider the Morse singularity obtained from $y^2 + x^2$ after the linear change of coordinates $y \mapsto y$ and $x \mapsto x + y$.

Example 7.6.3. Consider the polynomial $f(x, y) = y^2 + (y + x)^2$. Let $\pi_0 : Y_0 \rightarrow$ Tub and $U \subset Y_0$ as before. We find:

$$\pi_0^* f = (2v^2 + 2v + 1) u^2, \quad \text{Jac } \pi_0 = \begin{pmatrix} 1 & 0 \\ v & u \end{pmatrix}, \quad \det \text{Jac } \pi_0 = u.$$

And so, following [eq. \(7.1.2\)](#), we find

$$\begin{pmatrix} \xi^u \\ \xi^v \end{pmatrix} = \frac{-1}{u(2\bar{v}^2 + 2\bar{v} + 1)\bar{u}^2} \begin{pmatrix} 2\bar{u}(\bar{u} + \bar{v}) \\ -2v\bar{u}(1 + \bar{v}) + 2\bar{u}(1 + 2\bar{v}) \end{pmatrix} = \begin{pmatrix} \frac{2(\bar{v}+1)}{2\bar{u}\bar{v}^2+2\bar{u}\bar{v}+\bar{u}} \\ \frac{2((v-2)\bar{v}+v-1)}{2u\bar{u}\bar{v}^2+2u\bar{u}\bar{v}+u\bar{u}} \end{pmatrix}.$$

As before, we now compute the scaling and extension of

$$\lim_{u \rightarrow 0} |u|^2 \begin{pmatrix} \frac{2(\bar{v}+1)}{2\bar{u}\bar{v}^2+2\bar{u}\bar{v}+\bar{u}} \\ \frac{2((v-2)\bar{v}+v-1)}{2u\bar{u}\bar{v}^2+2u\bar{u}\bar{v}+u\bar{u}} \end{pmatrix} = \begin{pmatrix} 0 \\ \frac{2((v-2)\bar{v}+v-1)}{2\bar{v}^2+2\bar{v}+1} \end{pmatrix}.$$

So on $U \cap D_0^\circ$ we have the expression,

$$\xi_0 = \frac{2((v-2)\bar{v}+v-1)}{2\bar{v}^2+2\bar{v}+1}.$$

This vector field has isolated singularities on D_0° at the points

$$v_0 = (1 - \sqrt{5})/2, \quad v_1 = (1 + \sqrt{5})/2.$$

We compute the Hessian of ξ_0 at those singularities. For that we write $v = s + it$ and compute the partials of the vector field evaluated at those points. For v_0 we get:

$$\begin{aligned} \partial_s \xi_0|_{((1-\sqrt{5})/2, 0)} &= -\frac{4((s+it-2)(s-it)+s+it-1)(2s-2it+1)}{\left(2(s-it)^2+2s-2it+1\right)^2} \\ &\quad + \frac{2(2s-1)}{2(s-it)^2+2s-2it+1} \Big|_{((1-\sqrt{5})/2, 0)} \\ &= \frac{-2\sqrt{5}}{5-2\sqrt{5}} \end{aligned}$$

and

$$\begin{aligned} \partial_t \xi_0|_{((1-\sqrt{5})/2, 0)} &= -\frac{4((s+it-2)(s-it)+s+it-1)(-2is-2t-i)}{\left(2(s-it)^2+2s-2it+1\right)^2} \\ &\quad + \frac{2(2t+3i)}{2(s-it)^2+2s-2it+1} \Big|_{((1-\sqrt{5})/2, 0)} \\ &= \frac{6i}{5-2\sqrt{5}} \end{aligned}$$

So the Hessian is, up to a positive real constant,

$$\text{Hess}_{((1-\sqrt{5})/2, 0)} \xi_0 = \begin{pmatrix} \frac{-2\sqrt{5}}{5-2\sqrt{5}} & 0 \\ 0 & \frac{6}{5-2\sqrt{5}} \end{pmatrix},$$

which indicates that v_0 is a saddle point. A similar computation for v_1 leads to the Hessian

$$\text{Hess}_{((1+\sqrt{5})/2, 0)} \xi_0 = \begin{pmatrix} \frac{2\sqrt{5}}{2\sqrt{5}+5} & 0 \\ 0 & \frac{6}{2\sqrt{5}+5} \end{pmatrix}.$$

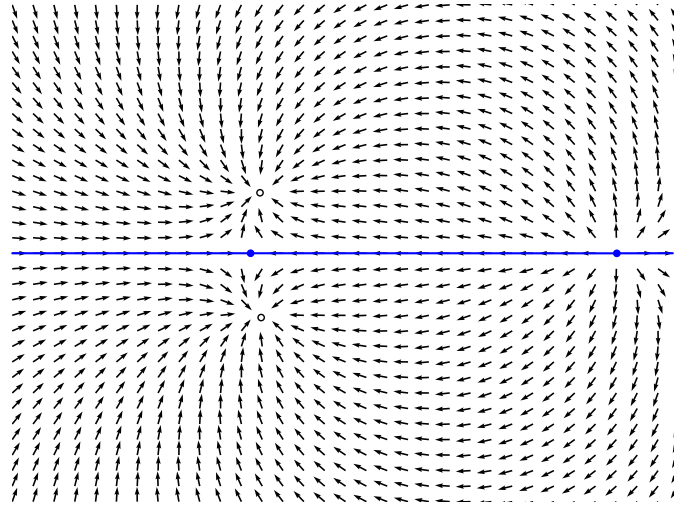


FIGURE 7.6.4. In black the vector field on the chart U . In this case the vector field has a potential which is a Morse function so all the zeroes are isolated. We see a saddle point and a fountain. In blue the spine S_0

That is, v_1 is a fountain (see Figure 7.6.4).

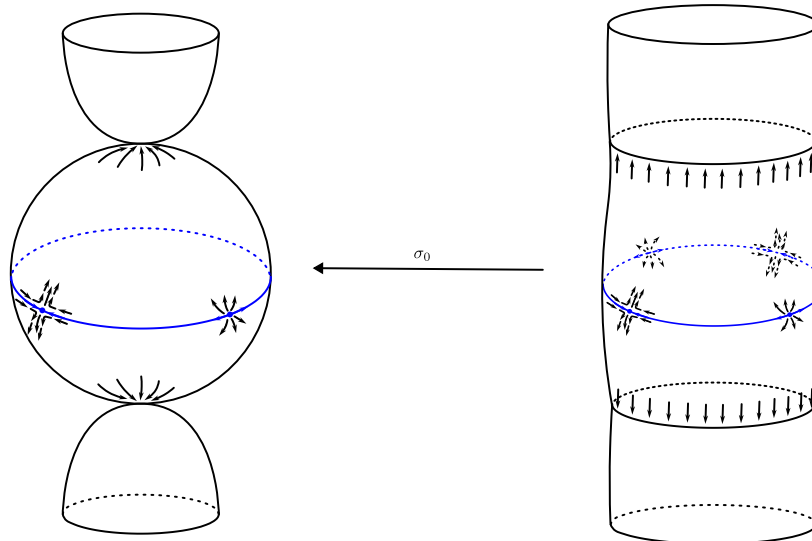


FIGURE 7.6.5. On the left we see the exceptional set of Y_0 , the vector field in black and the spine S_0 in blue. On the right we see the corresponding picture for a fixed angled on the Milnor fiber at radius zero.

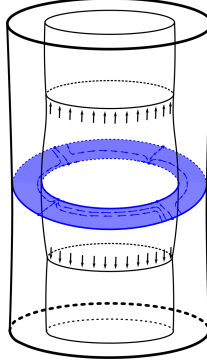


FIGURE 7.6.6. The inner cylinder represents the Milnor fiber at radius 0 and angle θ . The outer cylinder represents a Milnor fiber over a point t with $\arg(t) = \theta$. In light blue we see the closure of the union of all trajectories starting at the Milnor fiber F_t that converge to some point in the Milnor fiber at radius 0. In darker blue we see some of the trajectories together with the spine S_t on the Milnor fiber F_t and the spine $S_{0,\theta}^{\text{ro}}$ at radius 0 and angle θ .

Example 7.6.7. Let $f(x, y) = y^3 + x^3$ and let $\pi_0 : Y_0 \rightarrow \text{Tub}$ be the blow up at the origin $0 \in \text{Tub}$. Take the local chart $U \subset Y_0$ with coordinates u, v such that

$$\pi_0(u, v) = (u, uv).$$

In these local coordinates we have:

$$\pi_0^* f = u^3(v^2 - v + 1)(v + 1), \quad \text{Jac } \pi_0 = \begin{pmatrix} 1 & 0 \\ v & u \end{pmatrix}, \quad \det \text{Jac } \pi_0 = u.$$

And so, following [eq. \(7.1.2\)](#), we find

$$\begin{pmatrix} \xi^u \\ \xi^v \end{pmatrix} = \frac{1}{u(\bar{v}^2 - \bar{v} + 1)(\bar{v} + 1)\bar{u}^3} \begin{pmatrix} 3u\bar{u}^2 \\ -3v\bar{u}^2 + 3\bar{u}^2\bar{v}^2 \end{pmatrix} = \begin{pmatrix} -\frac{3}{\bar{u}\bar{v}^3 + \bar{u}} \\ -\frac{3(\bar{v}^2 - v)}{\bar{u}\bar{v}^3 + \bar{u}} \end{pmatrix}.$$

We can compute

$$\lim_{u \rightarrow 0} |u|^2 \begin{pmatrix} -\frac{3}{\bar{u}\bar{v}^3 + \bar{u}} \\ -\frac{3(\bar{v}^2 - v)}{\bar{u}\bar{v}^3 + \bar{u}} \end{pmatrix} = \begin{pmatrix} 0 \\ -\frac{3(\bar{v}^2 - v)}{\bar{v}^3 + 1} \end{pmatrix}.$$

That is, for the chart $U \cap D_0^\circ$ with coordinate v ,

$$\xi_0 = -\frac{3(\bar{v}^2 - v)}{\bar{v}^3 + 1}.$$

A direct computation, shows that this vector field vanishes at the origin and at the 3rd roots of unity, that is, at the points

$$v = 0, \quad v = 1, \quad v = -1/2(1 + i\sqrt{3}), \quad v = 1/2(-1 + i\sqrt{3}).$$

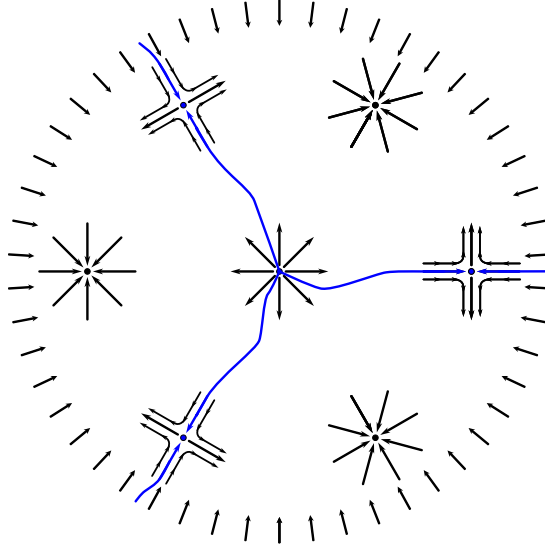


FIGURE 7.6.8. In black the vector field on the chart U . The inwards pointing outer arrows indicate that there is a fountain at infinity (or rather at the only point of D_0 that U does not see). In blue the stable manifolds of the three saddle points.

Next we compute the Hessian of ξ_0 at those points. Take real coordinates s, t such that $v = s + it$. We compute the partials and evaluate at $(s, t) = (0, 0)$

$$\partial_s \xi_0|_{(0,0)} = \left. \frac{9((s-it)^2 - s - it)(s-it)^2}{((s-it)^3 + 1)^2} - \frac{3(2s - 2it - 1)}{(s-it)^3 + 1} \right|_{(0,0)} = 3$$

and

$$\partial_t \xi_0|_{(0,0)} = \left. -\frac{9i((s-it)^2 - s - it)(s-it)^2}{((s-it)^3 + 1)^2} - \frac{3(-2is - 2t - i)}{(s-it)^3 + 1} \right|_{(0,0)} = 3i$$

which yields the Hessian

$$\text{Hess}_{(0,0)} \xi_0 = \begin{pmatrix} 3 & 0 \\ 0 & 3 \end{pmatrix},$$

that shows that ξ_0 has a fountain at the origin.

When $v = 1$, that is $(s, t) = (1, 0)$, we have

$$\text{Hess}_{(1,0)} \xi_0 = \begin{pmatrix} -3/2 & 0 \\ 0 & 9/2 \end{pmatrix},$$

which shows that ξ_0 has a saddle point at $(1, 0)$. A similar computation shows that ξ_0 has also saddle points at $(-1/2, -\sqrt{3}/2)$ and $(-1/2, \sqrt{3}/2)$. So, in the chart U , the vector field looks as in Figure 7.6.8.

By taking another chart, an analogous computation yields that ξ_0 has a fountain at the only point in D_0° not seen by the chart U .

The Milnor fiber at radius 0 minus a tubular neighborhood of its boundary is a 3-fold regular cover of D_0° . Therefore, each of the two fountains give rise to 3 vertices of the spine at radius 0.

CHAPTER 8

The Vector Field Near the Corners

Near an intersection point $D_i \cap D_j$ of two exceptional components in Y , the pull-back of ξ has poles along $D_i \cap D_j$. Assuming that the edge ij is invariant, [Definition 6.1.1](#) after rescaling $\pi^*(\xi)$ by a positive factor, the vector field extends to an analytic vector field near $D_i \cap D_j$, which does not vanish identically along D_i or D_j . If the edge is not invariant, a similar scaling of the further pullback $(\pi^{\text{ro}})^*(\xi)$ to the real oriented blow-up extends over the boundary. The vanishing order of this positive factor is given by the *radial weights* τ_i defined below.

In this section we work with the resolution $\pi_{\text{pol}} : Y_{\text{pol}} \rightarrow \mathbb{C}^2$ which, in particular, resolves generic polar curves (see [Definition 5.1.3](#)). We use the notation $\pi = \pi_{\text{pol}}$.

We sometimes write simply f and f_x instead of $\pi_{\text{pol}}^* f$ and $\pi_{\text{pol}}^* f_x$ to avoid cumbersome formulas. It is clear from the context and the coordinates use therein. Furthermore, the partials of $x = \pi_{\text{pol}}^* x$ and $\pi_{\text{pol}}^* f$ with respect to u, v are denoted x_u, x_v, f_u, f_v , and so on.

Definition 8.0.1. The *radial weight* of the vertex $i \in \mathcal{V}$ is the integer

$$\tau_i = c_{1,i} + m_i - p_i.$$

Remark 8.0.2. It follows from definition that $\tau_i + \varpi_i = 2c_{1,i}$. By [Lemma 6.1.3](#), we therefore have $\tau_i \leq 2c_{1,i}$ for all $i \in \mathcal{V}$. Equality holds precisely for the invariant vertices, i.e. when $i \in \mathcal{V}_Y$, by [Lemma 6.3.5](#). In particular, τ_i is even in this case.

8.0.3. Let $i, j \in \mathcal{V}$, and assume that there is a directed edge $j \rightarrow i$ in Γ (see [Definition 3.4.1](#)). Note that this implies that $i \neq 0$, since all edges adjacent to 0 point away from 0. Corresponding to the edge ij , we have an intersection point $p \in D_i \cap D_j$. Choose isometric coordinates x, y in \mathbb{C}^2 so that $y = 0$ defines the tangent associated with p (see [Definition 3.5.1](#)). Let $U \subset Y$ be a small chart containing p with coordinates u, v . We choose u, v in such a way that

$$(8.0.4) \quad \begin{aligned} \pi^* x &= u^{c_{0,i}} v^{c_{0,j}} \\ \pi^* y &= u^k v^\ell \eta(u, v) \end{aligned}$$

where $\eta(0, 0) \neq 0$. Since $i \neq 0$, we have $k > c_{0,i}$ ([Lemma 3.5.2](#)). Similarly, $\ell \geq c_{0,j}$ with equality if and only if $j = 0$.

On $U \setminus D$, we have an explicit description of the pullback of ξ

$$(8.0.5) \quad \pi|_{U \setminus D}^* \xi = \begin{pmatrix} \xi^u \\ \xi^v \end{pmatrix} = \frac{-1}{\det \text{Jac } \pi \cdot \bar{f}} \begin{pmatrix} y_v \bar{f}_x - x_v \bar{f}_y \\ -y_u \bar{f}_x + x_u \bar{f}_y \end{pmatrix}$$

Since f_y defines a generic polar curve (by the definition of π_{pol} and the assumption on the coordinate y), it vanishes along D_i, D_j with multiplicities p_i, p_j , we can write $\pi^* f_y(u, v) = u^{p_i} v^{p_j} (b + \text{h.o.t.})$ where $b \in \mathbb{C}^*$. We can therefore explicitly write

$$x_v \bar{f}_y = u^{c_{0,i}} \bar{u}^{p_i} v^{c_{0,j}-1} \bar{v}^{p_j} (c_{0,j} \bar{b} + \text{h.o.t.})$$

with $b \in \mathbb{C}^*$. Here, once again, we are identifying f_y with its pullback. We can now write $\pi^* f_x(u, v) = u^{p'_i} v^{p'_j} (b' + \text{h.o.t.})$ with the inequalities $p'_i \geq p_i$ and $p'_j \geq p_j$ because the x -axis is a tangent by hypothesis. Again using the observation after eq. (8.0.4), we can write

$$y_v \bar{f}_x = u^k \bar{u}^{p'_i} v^{\ell-1} \bar{v}^{p'_j} (\ell b' + \text{h.o.t.}) = u^{c_{0,i}} \bar{u}^{p_i} v^{c_{0,j}-1} \bar{v}^{p_j} (0 + \text{h.o.t.})$$

with $b' \in \mathbb{C}$. Together this yields

$$y_v \bar{f}_x - x_v \bar{f}_y = u^{c_{0,i}} \bar{u}^{p_i} v^{c_{0,j}-1} \bar{v}^{p_j} (-c_{0,j} \bar{b} + \text{h.o.t.}).$$

By an analogous reasoning we find,

$$-y_u \bar{f}_x + x_u \bar{f}_y = u^{c_{0,i}-1} \bar{u}^{p_i} v^{c_{0,j}} \bar{v}^{p_j} (c_{0,i} \bar{b} + \text{h.o.t.}).$$

Similarly, we can also write

$$(8.0.6) \quad \begin{aligned} \pi^* f(u, v) &= u^{m_i} v^{m_j} (a + \text{h.o.t.}) \quad a \in \mathbb{C}^* \\ \det \text{Jac } \pi(u, v) &= u^{\nu_i-1} v^{\nu_j-1} (c + \text{h.o.t.}) \quad c \in \mathbb{C}^*. \end{aligned}$$

Setting $d = \bar{b}/(c\bar{a}) \in \mathbb{C}^*$, we get (recall Definition 3.3.6)

$$(8.0.7) \quad |u|^{\tau_i} |v|^{\tau_j} \pi|_{U \setminus D}^* \xi = \left(\frac{\bar{u}}{|u|} \right)^{\varpi_i} \left(\frac{\bar{v}}{|v|} \right)^{\varpi_j} d \left(\frac{u(c_{0,j} + \text{h.o.t.})}{v(-c_{0,i} + \text{h.o.t.})} \right).$$

We recall the notation $r = |u|$ from Chapter 4 and introduce the notation $s = |v|$. Do not confuse with the notation s, t used in Example 7.6.7.

The previous discussion, in particular the above equation, yields the following result.

Lemma 8.0.8. (i) If $p \in D_i \cap D_j$, with ij an invariant edge, then the vector field

$$(8.0.9) \quad |u|^{\tau_i} |v|^{\tau_j} \pi|_{U \setminus D}^* \xi$$

extends to an analytic vector field on U that is tangent to $D_i \cap U$ and $D_j \cap U$. And it does not vanish identically there.

(ii) The scaled pull-back

$$(8.0.10) \quad r^{\tau_i} s^{\tau_j} \pi^{\text{ro}}|_{U^{\text{ro}} \setminus \partial U^{\text{ro}}}^* \xi$$

extends to an analytic vector field on U^{ro} , which is tangent to both $D_i^{\text{ro}} \cap U^{\text{ro}}$ and $D_j^{\text{ro}} \cap U^{\text{ro}}$. Furthermore, if ij is a non-invariant edge, it does not vanish identically along $D_{i,j}^{\text{ro}}$.

Definition 8.0.11. Denote by ξ_U^{ro} the analytic vector field on U^{ro} whose restriction to $U^{\text{ro}} \setminus \partial U^{\text{ro}}$ coincides with eq. (8.0.10). We denote by $\xi_{i,j,\theta}^{\text{ro}}$ the restriction of ξ_U^{ro} to a neighborhood of $D_{i,j,\theta}^{\text{ro}}$ in the Milnor fiber F_θ^{ro} at radius 0 and angle θ .

Similarly, for p an invariant intersection point, denote by ξ_U the analytic vector field on U whose restriction to $U \setminus D$ coincides with eq. (8.0.9).

8.1. Invariant intersection points

In this subsection we consider an invariant edge ij in the graph Γ . We use the notation from 8.0.3, and assume $\varpi_i = \varpi_j = 0$ and that $j \rightarrow i$.

Lemma 8.1.1. The number d from eq. (8.0.7) is a positive real number if the edge ij is invariant.

PROOF. Denote by l the coefficient of $u^{c_{1,i}}v^{c_{1,j}}$ in the expansion of π^*y in u, v . We have

$$\det \text{Jac } \pi(u, v) = x_u y_v - x_v y_u = c_{0,i} u^{c_{0,i}-1} v^{c_{0,j}} y_v - c_{0,j} u^{c_{0,i}} v^{c_{0,j}-1} y_u,$$

and so we can compute the number c from eq. (8.0.6):

$$c = (c_{0,i} c_{1,j} - c_{0,j} c_{1,i})l.$$

A chain rule computation gives

$$\begin{aligned} f_y &= \frac{-x_v f_u + x_u f_v}{x_u y_v - y_u x_v} \\ &= \frac{u^{c_{0,i}+m_i-1} v^{c_{0,j}+m_j-1} (a(c_{0,j} m_i - c_{0,i} m_j) + \text{h.o.t.})}{u^{\nu_i-1} v^{\nu_j-1} (c + \text{h.o.t.})} \\ &= -\frac{a}{c} \cdot \begin{vmatrix} c_{0,i} & m_i \\ c_{0,j} & m_j \end{vmatrix} (u^{p_i} v^{p_j} + \text{h.o.t.}) \end{aligned}$$

and so $b = a(m_i c_{0,j} - m_j c_{0,i})/c$, i.e. $d = \bar{b}/(c\bar{a}) = (m_i c_{0,j} - m_j c_{0,i})/|c|^2 > 0$ where the last inequality follows from the fact that $(c_{0,i} m_j - c_{0,j} m_i) < 0$ by Lemma 3.4.7. \square

Lemma 8.1.2. *If $p \in D_i \cap D_j$ is an invariant intersection point, then the vector field ξ_U has an elementary singularity at p , whose unstable manifold is D_i and whose stable manifold is D_j .*

PROOF. Since d is positive by Lemma 8.1.1, the result follows from the Grobman-Hartman theorem and eq. (8.0.7). \square

The previous lemma talks about the Hessian of the vector field ξ_U in Y_{pol} , it is also useful later on the text to be able to speak about the Hessian of the vector field ξ_U^{ro} in $Y_{\text{pol}}^{\text{ro}}$.

8.1.3. Here we briefly explain how to obtain useful formulas for the pullback of our vector field to Y^{ro} . We use polar coordinates r, s, α and β (in this order), where $u = r e^{i\alpha}, v = s e^{i\beta}$ for the chart $U^{\text{ro}} = \sigma^{-1}(U) \subset Y^{\text{ro}}$. We can write

$$\xi_U^{\text{ro}} = (\xi^{\text{ro},r}, \xi^{\text{ro},s}, \xi^{\text{ro},\alpha}, \xi^{\text{ro},\beta})^\top.$$

The formulas

$$(8.1.4) \quad \begin{aligned} \xi^{\text{ro},r} &= \text{Re}(e^{-i\alpha} \sigma^* \xi^u), & \xi^{\text{ro},s} &= \text{Re}(e^{-i\beta} \sigma^* \xi^v), \\ \xi^{\text{ro},\alpha} &= \text{Im}(r^{-1} e^{-i\alpha} \sigma^* \xi^u), & \xi^{\text{ro},\beta} &= \text{Im}(s^{-1} e^{-i\beta} \sigma^* \xi^v), \end{aligned}$$

follow from a direct computation in polar coordinates. We carry on this direct computation of the formulas for $\xi^{\text{ro},r}$. We observe that in U^{ro} , the real oriented blow up σ is expressed as

$$(r, s, \alpha, \beta) \mapsto (r e^{i\alpha}, s e^{i\beta})$$

and so its Jacobian is

$$\text{Jac } \sigma = \begin{pmatrix} \cos \alpha & 0 & -r \sin \alpha & 0 \\ \sin \alpha & 0 & r \cos \alpha & 0 \\ 0 & \cos \beta & 0 & -s \sin \beta \\ 0 & \sin \beta & 0 & s \cos \beta \end{pmatrix}.$$

This matrix is, up to permutation of the second and third columns, a block diagonal matrix. So we can compute its inverse by blocks and find that

$$(8.1.5) \quad (\text{Jac } \sigma)^{-1} = \begin{pmatrix} \cos \alpha & \sin \alpha & 0 & 0 \\ 0 & 0 & \cos \beta & \sin \beta \\ -\frac{\sin \alpha}{r} & \frac{\cos \alpha}{r} & 0 & 0 \\ 0 & 0 & -\frac{\sin \beta}{s} & \frac{\cos \beta}{s} \end{pmatrix}.$$

By definition of the pullback of a vector field we know that

$$\xi_U^{\text{ro}} = (\text{Jac } \sigma)^{-1}(\text{Re}(\sigma^* \xi^u), \text{Im}(\sigma^* \xi^u), \text{Re}(\sigma^* \xi^v), \text{Im}(\sigma^* \xi^v))^\top.$$

So using eq. (8.1.5), we compute, on one hand:

$$(8.1.6) \quad \xi^{\text{ro},r} = (\cos \alpha) \cdot \text{Re}(\sigma^* \xi^u) + (\sin \alpha) \cdot \text{Im}(\sigma^* \xi^u).$$

And on the other hand:

$$(8.1.7) \quad \begin{aligned} \text{Re}(e^{-i\alpha} \sigma^*(\xi^u)) &= \text{Re}((\cos \alpha - i \sin \alpha) \cdot (\text{Re}(\sigma^* \xi^u) + i \text{Im}(\sigma^* \xi^u))) \\ &= \text{Re}((\cos \alpha) \cdot \text{Re}(\sigma^* \xi^u) + (\sin \alpha) \cdot \text{Im}(\sigma^* \xi^u)) \\ &\quad + i((\cos \alpha) \cdot \text{Im}(\sigma^* \xi^u) - (\sin \alpha) \cdot \text{Re}(\sigma^* \xi^u)) \\ &= (\cos \alpha) \cdot \text{Re}(\sigma^* \xi^u) + (\sin \alpha) \cdot \text{Im}(\sigma^* \xi^u) \end{aligned}$$

From eq. (8.1.6) and eq. (8.1.7), we verify the formula for $\xi^{\text{ro},r}$ given in eq. (8.1.4). The other three formulas of eq. (8.1.4) follow from very similar computations.

Corollary 8.1.8. *At a point $q \in D_{i,j}^{\text{ro}}$ with $\varpi_i = \varpi_j = 0$, the vector field ξ_U^{ro} has a Hessian*

$$\text{Hess}_q \xi_U^{\text{ro}} = \begin{pmatrix} dc_{0,j} & 0 & 0 & 0 \\ 0 & -dc_{0,i} & 0 & 0 \\ 0 & 0 & 0 & 0 \\ 0 & 0 & 0 & 0 \end{pmatrix}.$$

Moreover, there exists a local change of coordinates such that

$$\xi_{i,j,\theta}^{\text{ro}} = (dc_{0,j} r', -dc_{0,i} s', 0, 0)^\top.$$

in coordinates r', s', α', β' .

PROOF. Using eq. (8.1.4) and eq. (8.0.7) we get

$$\xi^{\text{ro},r} = \text{Re}(e^{-i\alpha} dr e^{i\alpha} (c_{0,j} + \text{h.o.t.})) = r d c_{0,j} + \text{Re}(\text{h.o.t.})$$

where $\text{Re}(\text{h.o.t.})$ denotes the real part of the higher (than linear) order terms. This yields the first row of the Hessian in the statement. Similarly, we find

$$\xi^{\text{ro},\alpha} = \text{Im}(r^{-1} e^{-i\alpha} dr e^{i\alpha} (c_{0,j} + \text{h.o.t.})) = \text{Im}(d c_{0,j} + \text{h.o.t.}) = 0 + \text{Im}(\text{h.o.t.}),$$

which gives the third row of the Hessian. The second and fourth rows are completely analogous.

For the last statement we use that the vector field ξ_U satisfies the hypothesis of the Grobman-Hartman theorem by Lemma 8.1.2. This implies that there exists coordinates u', v' for U such that $\{u' = 0\} = D_i \cap U$ and $\{v' = 0\} = D_j \cap U$ and such that ξ_U in the coordinates u', v' is

$$(8.1.9) \quad \begin{pmatrix} \xi^{u'} \\ \xi^{v'} \end{pmatrix} = \begin{pmatrix} d c_{0,j} u' \\ -d c_{0,i} v' \end{pmatrix}.$$

So, after taking its pullback by the real oriented blow up $\sigma(r', \alpha', s', \beta') = (r' e^{i\alpha'}, s' e^{i\beta'})$, we get the vector field

$$(8.1.10) \quad \xi_U^{\text{ro}} = (dc_{0,j}r', -dc_{0,i}s', 0, 0)^\top$$

which proves the last statement. \square

In [fig. 8.1.11](#) we can see a drawing of the vector field ξ_U^{ro} restricted to $(D_{i,\theta}^{\text{ro}} \cup D_{j,\theta}^{\text{ro}}) \cap U$

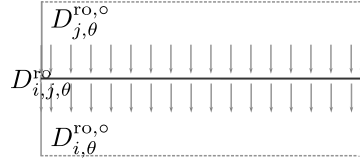


FIGURE 8.1.11. The vector field ξ_U^{ro} restricted to $(D_{i,\theta}^{\text{ro}} \cup D_{j,\theta}^{\text{ro}}) \cap U$ near a component of $D_{i,j,\theta}^{\text{ro}}$ for an edge $j \rightarrow i$ and with $\varpi_i = \varpi_j = 0$.

8.2. Non-invariant intersection points

Next we assume that ϖ_i, ϖ_j are not both 0. In this subsection we also use the formulas [eq. \(8.1.4\)](#).

Lemma 8.2.1. *In polar coordinates given by the real oriented blow up, the following expression holds*

$$\arg(f)(0, 0, \alpha, \beta) = m_i\alpha + m_j\beta + \Delta$$

with $\Delta \in \mathbb{R}/2\pi\mathbb{Z}$ a constant.

PROOF. This follows from [Lemma 4.1.2](#) and the observation that $\arg(f)(0, 0, \alpha, \beta)$ is equivariant with respect to \cdot_i of weight m_i and equivariant with respect to \cdot_j of weight m_j . \square

Definition 8.2.2. With $d \in \mathbb{C}^*$ as in [8.0.3](#), set $\delta = \arg(d) \in \mathbb{R}/2\pi\mathbb{Z}$, and

$$(8.2.3) \quad \begin{aligned} \Sigma_{i,j}^+ &= \{(0, 0, \alpha, \beta) \in U^{\text{ro}} \mid \delta + \varpi_i\alpha + \varpi_j\beta \equiv 0 \pmod{2\pi\mathbb{Z}}\} \subset D_{i,j}^{\text{ro}}, \\ \Sigma_{i,j}^- &= \{(0, 0, \alpha, \beta) \in U^{\text{ro}} \mid \delta + \varpi_i\alpha + \varpi_j\beta \equiv \pi \pmod{2\pi\mathbb{Z}}\} \subset D_{i,j}^{\text{ro}}, \end{aligned}$$

and $\Sigma_{i,j} = \Sigma_{i,j}^+ \cup \Sigma_{i,j}^-$.

Lemma 8.2.4. Fix $\theta \in \mathbb{R}/2\pi\mathbb{Z}$.

- (i) The set $\Sigma_{i,j}$ is a real 1-dimensional affine subspace homeomorphic to a disjoint union of $2 \gcd(\varpi_i, \varpi_j)$ circles.
- (ii) The set $D_{i,j}^{\text{ro}} \cap Y_\theta^{\text{ro}}$ is a real 1-dimensional affine subspace homeomorphic to a disjoint union of $\gcd(m_i, m_j)$ circles.
- (iii) The intersection $\Sigma_{i,j} \cap Y_\theta^{\text{ro}}$ is transverse and

$$|\Sigma_{i,j}^+ \cap Y_\theta^{\text{ro}}| = |\Sigma_{i,j}^- \cap Y_\theta^{\text{ro}}| = -\begin{vmatrix} m_i & \varpi_i \\ m_j & \varpi_j \end{vmatrix}.$$

Where $|\cdot|$ denotes cardinality in the first two terms and determinant in the last one.

PROOF. The map $\chi : D_{i,j}^{\text{ro}} \rightarrow \mathbb{R}/2\pi\mathbb{Z}$, $(\alpha, \beta) \mapsto \delta + \varpi_i \alpha + \varpi_j \beta$ with $\delta = \arg(d)$, is a surjective affine morphism, and therefore its preimages $\chi^{-1}(0)$ and $\chi^{-1}(\pi)$ are submanifolds of dimension $\dim_{\mathbb{R}} D_{i,j}^{\text{ro}} - \dim_{\mathbb{R}} (\mathbb{R}/2\pi\mathbb{Z}) = 1$. From eq. (8.2.3) we see that $\Sigma_{i,j}^{\pm}$ consists of $\gcd(\varpi_i, \varpi_j)$ connected components. In fact, each component can be parametrized as follows. Set $(\varpi'_i, \varpi'_j) = (\varpi_i, \varpi_j)/\gcd(\varpi_i, \varpi_j)$. We see that $\Sigma_{i,j}$ consists of components parametrized by $\gamma \in \mathbb{R}/2\pi\mathbb{Z}$ by

$$r = s = 0, \quad \alpha = -\varpi'_j \gamma + \delta', \quad \beta = \varpi'_i \gamma + \delta''$$

where δ' and δ'' are some constants in $\mathbb{R}/2\pi\mathbb{Z}$.

A similar argument works for the set $D_{i,j}^{\text{ro}} \cap Y_{\theta}^{\text{ro}}$ since

$$(8.2.5) \quad D_{i,j}^{\text{ro}} \cap Y_{\theta}^{\text{ro}} = \{(0, 0, \alpha, \beta) \in U^{\text{ro}} \mid m_i \alpha + m_j \beta + \Delta = \theta\}.$$

The composition

$$\arg(f)(0, 0, -\varpi'_j \gamma, \varpi'_i \gamma) = \frac{m_j \varpi_i - m_i \varpi_j}{\gcd(\varpi_i, \varpi_j)} \cdot \gamma + \Delta$$

is a submersion, since $m_i \varpi_j - m_j \varpi_i < 0$ by Corollary 6.3.7 and Corollary 6.3.6 5. which proves transversality. \square

Lemma 8.2.6. *Let $\theta \in \mathbb{R}/2\pi\mathbb{Z}$.*

- (i) *The vanishing set of ξ_U^{ro} is $\Sigma_{i,j}$.*
- (ii) *The Hessian of ξ_U^{ro} along the normal bundle of $\Sigma_{i,j}$ is elementary.*
- (iii) *If $q \in \Sigma_{i,j}^+$ and $\arg(f)(q) = \theta$, then the unstable manifold of ξ_U^{ro} at q is the germ $(D_{i,\theta}^{\text{ro}}, q)$, and its stable manifold is a single trajectory in $(D_{j,\theta}^{\text{ro}}, q)$.*
- (iv) *Similarly, if $q \in \Sigma_{i,j}^-$ and $\arg(f)(q) = \theta$, then the stable manifold of ξ_U^{ro} at q is $(D_{i,\theta}^{\text{ro}}, q)$, and its unstable manifold is a single trajectory in $(D_{j,\theta}^{\text{ro}}, q)$.*

Lemma 8.2.7. *Let $q \in \Sigma_{i,j}$. Set $\chi(\alpha, \beta) = \delta + \varpi_i \alpha + \varpi_j \beta$ with $\delta = \arg(d)$. Then*

$$(8.2.8) \quad \begin{aligned} r^{\tau_i} s^{\tau_j} \xi^{\text{ro},r} &\in r|d|c_{0,j} \cos(\chi(\alpha, \beta)) + \mathfrak{m}_{Y^{\text{ro}},q}^2, \\ r^{\tau_i} s^{\tau_j} \xi^{\text{ro},s} &\in -s|d|c_{0,i} \cos(\chi(\alpha, \beta)) + \mathfrak{m}_{Y^{\text{ro}},q}^2, \\ r^{\tau_i} s^{\tau_j} \xi^{\text{ro},\alpha} &\in |d|c_{0,j} \sin(\chi(\alpha, \beta)) + (r, s)\mathcal{C}_{Y^{\text{ro}},q}^{\omega}, \\ r^{\tau_i} s^{\tau_j} \xi^{\text{ro},\beta} &\in -|d|c_{0,i} \sin(\chi(\alpha, \beta)) + (r, s)\mathcal{C}_{Y^{\text{ro}},q}^{\omega}, \end{aligned}$$

where $\mathfrak{m}_{Y^{\text{ro}},q}$ is the maximal ideal of the local ring of real analytic functions $\mathcal{C}_{Y^{\text{ro}},q}^{\omega}$ and $(r, s)\mathcal{C}_{Y^{\text{ro}},q}^{\omega}$ is the ideal generated by r and s in the same local ring.

PROOF. We recall from eq. (8.1.4)

$$\xi^{\text{ro},r} = \text{Re}(e^{-i\alpha} \sigma^* \xi^u), \quad \xi^{\text{ro},\alpha} = \text{Im}(r^{-1} e^{-i\alpha} \sigma^* \xi^u).$$

Now, we look at eq. (8.0.7) and observe

$$\left(\frac{u}{|u|} \right)^{\varpi_i} \left(\frac{v}{|v|} \right)^{\varpi_j} d = |d|(\cos(\chi) + i \sin(\chi))$$

We compute

$$\begin{aligned} r^{\tau_i} s^{\tau_j} \text{Re}(e^{-i\alpha} \sigma^* \xi^u) &= \text{Re}(e^{-i\alpha} e^{i\chi} |d| r e^{i\alpha} (c_{0,j} + \text{h.o.t.})) \\ &= \text{Re}(|d| r e^{i\chi} (c_{0,j} + \text{h.o.t.})) \\ &= |d| r c_{0,j} \cos(\chi) + \text{Re}(r e^{i\chi} \text{h.o.t.}) \end{aligned}$$

The function r and all the higher order terms vanish at q . This settles the first line of [eq. \(8.2.8\)](#). On another hand, we have

$$\begin{aligned} r^{\tau_i} s^{\tau_j} \operatorname{Im}(r^{-1} e^{-i\alpha} \sigma^* \xi^u) &= \operatorname{Im}(r^{-1} e^{-i\alpha} |d| e^{i\chi} r e^{i\alpha} (c_{0,j} + \text{h.o.t.})) \\ &= \operatorname{Im}(|d| e^{i\chi} (c_{0,j} + \text{h.o.t.}))) \\ &= |d| c_{0,j} \sin(\chi) + \operatorname{Im}(e^{i\chi} \text{h.o.t.}) \end{aligned}$$

Each higher order term is divisible by r or s , this is because the higher order terms in [eq. \(8.0.7\)](#) are monomials in u, \bar{u}, v and \bar{v} . This settles the third line of [eq. \(8.2.8\)](#). The other two lines are completely analogous. \square

PROOF OF LEMMA 8.2.6. Given that U has been chosen small, these functions all vanish precisely when $r = s = 0$ and $\chi \in \mathbb{Z}\pi$, proving (i).

If $q \in \Sigma_{i,j}$, then [Lemma 8.2.7](#) shows that the linear terms of $\xi^{\text{ro},r}$ and $\xi^{\text{ro},s}$ are $|d|r c_{0,j}$ and $-|d|s c_{0,i}$, respectively. Furthermore, we have

$$\partial_\alpha \sin(\chi) = \varpi_i \cos(\chi), \quad \partial_\beta \sin(\chi) = \varpi_j \cos(\chi).$$

As a result, the Hessian of ξ_U^{ro} at $q \in \Sigma_{i,j}^\pm$ is

$$(8.2.9) \quad \pm |d| \cdot \begin{pmatrix} c_{0,j} & 0 & 0 \\ 0 & -c_{0,i} & * \\ * & c_{0,j} \varpi_i & c_{0,j} \varpi_j \\ & -c_{0,i} \varpi_i & -c_{0,i} \varpi_j \end{pmatrix}.$$

The lower right block of the above matrix has rank 1. Therefore its only non-zero eigenvalue equals its trace $c_{0,j} \varpi_i - c_{0,i} \varpi_j$. This number is positive by [Corollary 6.3.7](#). In particular, the Hessian has three nonzero real eigenvalues, which proves (ii), since $\dim_{\mathbb{R}} \Sigma_{i,j} = 1$.

For (iii), let $q \in \Sigma_{i,j}^+$. Then from the previous discussion we have that [eq. \(8.2.9\)](#) has two positive eigenvalues and one negative eigenvalue. As a result, following Kelley [[Kel67b](#), Theorem 1], ξ_U^{ro} has a unique 2-dimensional unstable manifold and a unique 1-dimensional stable manifold. The submanifold $D_{i,\theta}^{\text{ro}}$, given by $r = 0$ and $\chi = 0$, is an invariant submanifold and, again, it is unstable since the restriction of the Hessian [eq. \(8.2.9\)](#) to $T_q D_{i,\theta}^{\text{ro}}$ is positive definite. A similar observation gives that the restriction of the Hessian to $T_q D_{j,\theta}^{\text{ro}}$ has one positive and one negative eigenvalue. The statement (iv) is analogous to the previous one. \square

Notation 8.2.11. Take a connected component of some $D_{i,j,\theta}^{\text{ro}}$ with ϖ_i or ϖ_j not zero and such that $j \rightarrow i$. A point of $\Sigma_{i,j}^+$ will be called a *red point*, that is, a red point looks like half a fountain on $D_{i,\theta}^{\text{ro}}$ and half a saddle point on $D_{j,\theta}^{\text{ro}}$. Analogously, a point of $\Sigma_{i,j}^-$ will be called a *green point*, that is, a green point looks like half a sink on $D_{i,\theta}^{\text{ro}}$ and half a saddle point on $D_{j,\theta}^{\text{ro}}$. See [fig. 8.2.10](#) for a drawing of the vector field $\xi_{i,j,\theta}^{\text{ro}}$.

8.3. The strict transform

In this subsection we rescale the pull-back $\pi_{\text{pol}}^* \xi$ in a neighborhood of a component D_a of the strict transform C_{pol} , for some $a \in \mathcal{A}$. With the right rescaling, this vector field looks like a Morse-Bott attractor along D_a . As a result, the flow of the vector field retracts a neighborhood onto D_a , and, as we shall see, the strict

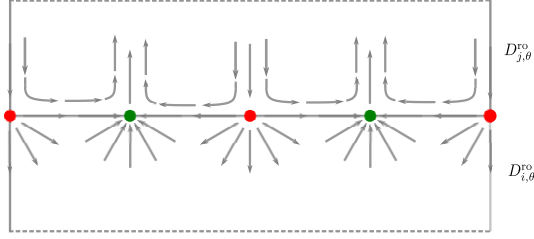


FIGURE 8.2.10. Trajectories of the scaled vector field along the boundary, near the corner locus. The winding number on $D_{j,\theta}^{ro}$ around the boundary component seen here, is computed by a path going from left to right in the upper half of the figure, and so coincides with the number of red (or green) points. On $D_{i,\theta}^{ro}$ we find the same number with the opposite sign.

transform $\overline{\pi_{\text{pol}}^{-1}(S \setminus \{0\})} \subset Y_{\text{pol}}$ of the total spine does not intersect a neighborhood of C_{pol} .

8.3.1. Let $a \in \mathcal{A}$ be an arrowhead in the graph Γ_{pol} , and let $i \in \mathcal{V}$ be the unique neighbor of a in Γ_{pol} . Then D_i is an exceptional component, and D_a is a component of the strict transform $C_{\text{pol}} \subset Y_{\text{pol}}$. These divisors intersect in a unique point, choose a small coordinate chart U around this point. We can assume that the coordinates u, v in U satisfy

$$\pi^* x|_U = u^{c_{0,i}}, \quad \pi^* f|_U = u^{m_i} v^{m_a}.$$

Since π_{pol} restricts to an isomorphism outside the exceptional divisor, and ξ is a well defined vector field outside the curve C , we have a well defined vector field $\pi_{\text{pol}}^* \xi$ on the set $U \setminus D = U \setminus (D_i \cup D_a)$.

After choosing a small neighborhood U , we can choose ε and η small enough that we can assume that $D_a \cap \pi_{\text{pol}}^{-1}(\text{Tub}(\varepsilon, \eta)) \subset U$.

Lemma 8.3.2. *The vector field*

$$(8.3.3) \quad |u|^{\tau_i} |v|^2 \cdot \pi_{\text{pol}}^* \xi|_{U \setminus D}$$

extends to an analytic vector field on U . Furthermore,

- (1) *the singular set of this extension is the submanifold $U \cap D_a$,*
- (2) *the Hessian of this extension has strictly negative real eigenvalues along the normal bundle of the singular set.*

PROOF. By the definition of a pull-back of a vector field, we find

$$\pi_{\text{pol}}^* \xi|_{U \setminus D} = \begin{pmatrix} \xi^u \\ \xi^v \end{pmatrix} = -(\text{Jac } \pi_{\text{pol}})^{-1} \cdot \begin{pmatrix} \bar{f}_x/\bar{f} \\ \bar{f}_y/\bar{f} \end{pmatrix} = -\text{Jac } \pi_{\text{pol}}^{-1} \cdot (\text{Jac } \pi_{\text{pol}}^{-1})^* \cdot \begin{pmatrix} m_i \bar{u}^{-1} \\ m_a \bar{v}^{-1} \end{pmatrix}$$

We recall that in this context $(\text{Jac } \pi_{\text{pol}}^{-1})^*$ stands for the hermitian adjoint of $\text{Jac } \pi_{\text{pol}}^{-1}$. Here we use the assumption that $f = u^{m_i} v^{m_a}$ is a monomial, and so its log derivatives are easily computed:

$$f_u/f = m_i u^{-1}, \quad f_v/f = m_a v^{-1}.$$

A computation gives (note that $x_v = 0$ and so $\det \text{Jac } \pi_{\text{pol}} = x_u y_v$)

$$\text{Jac } \pi_{\text{pol}}^{-1} (\text{Jac } \pi_{\text{pol}}^{-1})^* = \frac{1}{|x_u y_v|^2} \begin{pmatrix} |y_v|^2 & -y_v \bar{y}_u \\ -y_u \bar{y}_v & |x_u|^2 + |y_u|^2 \end{pmatrix} = \frac{1}{|y_v|^2} \begin{pmatrix} \left| \frac{y_v}{x_u} \right|^2 & -\frac{y_v}{x_u} \bar{y}_u \\ -\frac{y_u}{x_u} \bar{y}_v & 1 + \left| \frac{y_u}{x_u} \right|^2 \end{pmatrix}.$$

As a result, since $\tau_i = 2c_{1,i}$ because i is invariant (recall Remark 8.0.2 and Definition 6.1.1), we find

$$(8.3.4) \quad |u|^{\tau_i} |v|^2 \pi_{\text{pol}}^* \xi = v \cdot \left| \frac{u^{c_{1,i}}}{y_v} \right|^2 \cdot \begin{pmatrix} -m_i \bar{u} \left| \frac{y_v}{x_u} \right|^2 + m_a \frac{y_v}{x_u} \bar{y}_u \\ m_i \bar{u} \frac{y_u}{x_u} \bar{y}_v - m_a - m_a \left| \frac{y_u}{x_u} \right|^2 \end{pmatrix}.$$

Here, the factor $\left| \frac{u^{c_{1,i}}}{y_v} \right|^2$ is a positive unit, since y_v vanishes with order $c_{1,i}$ along D_i (see 3.3.4). In fact, since y_v and y_u both vanish with order strictly higher than x_u , all the summands in each coordinates of the vector to the right in eq. (8.3.4) are real analytic functions. As a result, eq. (8.3.3) has a real analytic extension. The factor v in eq. (8.3.4) guarantees that the extension vanishes along D_i . In fact, the extension of both functions

$$|u|^{\tau_i} |v|^2 \xi^u, \quad |u|^{\tau_i} |v|^2 \xi^v$$

vanish along D_a , and the latter has the linear term v with coefficient given by

$$-m_a - m_a \left| \frac{y_u}{x_u} \right|^2 < 0$$

at each point in D_a . It follows that the extension of eq. (8.3.3) vanishes precisely along D_a , and that the Hessian has negative eigenvalues along the normal bundle. \square

Lemma 8.3.5. *Let $U^{\text{ro}} = \sigma^{-1}(U) \subset Y_{\text{pol}}^{\text{ro}}$ with polar coordinates (r, s, α, β) so that $u = r e^{i\alpha}$ and $v = s e^{i\beta}$. The vector field*

$$(8.3.6) \quad r^{\tau_i} s (\pi_{\text{pol}}^{\text{ro}})^* \xi,$$

which is well defined on $U^{\text{ro}} \setminus \partial U^{\text{ro}}$, extends to a real analytic vector field on U^{ro} which does not vanish on U^{ro} and is tangent to D_i^{ro} and is transverse to D_a^{ro} , pointing outwards there.

PROOF. The vector field

$$(\pi_{\text{pol}}^{\text{ro}})^* \xi|_{U^{\text{ro}} \setminus \partial U^{\text{ro}}} = \begin{pmatrix} \xi^{\text{ro},r} \\ \xi^{\text{ro},\alpha} \\ \xi^{\text{ro},s} \\ \xi^{\text{ro},\beta} \end{pmatrix}$$

is the pull-back of $\pi_{\text{pol}}^* \xi|_{U \setminus D}$ to $U^{\text{ro}} \setminus \partial U^{\text{ro}}$, where the coordinates are given by eq. (8.1.4). Since ξ_U is tangent to D_i , the analytic function $|u|^{\tau_i} |v|^2 \xi^u$ is divisible by u . Furthermore, by eq. (8.3.4), $|u|^{\tau_i} |v|^2 \xi^u$ is also divisible by v . As a result,

$\sigma^*(|u|^{\tau_i}|v|^2\xi^u)$ is divisible by both r and s , and so the functions

$$\begin{aligned} r^{\tau_i}s\xi^{\text{ro},r} &= s^{-1}\operatorname{Re}(e^{-i\alpha}\sigma^*(|u|^{\tau_i}|v|^2\xi^u)) \\ r^{\tau_i}s\xi^{\text{ro},\alpha} &= s^{-1}r^{-1}\operatorname{Im}(e^{-i\alpha}\sigma^*(|u|^{\tau_i}|v|^2\xi^u)) \end{aligned}$$

extend to real analytic functions on U^{ro} . Similarly, we have

$$\begin{aligned} r^{\tau_i}s\xi^{\text{ro},s} &= s^{-1}\operatorname{Re}(e^{-i\alpha}\sigma^*(|u|^{\tau_i}|v|^2\xi^v)) \\ r^{\tau_i}s\xi^{\text{ro},\beta} &= s^{-2}\operatorname{Im}(e^{-i\alpha}\sigma^*(|u|^{\tau_i}|v|^2\xi^v)) \end{aligned}$$

The analytic function $|u|^{\tau_i}|v|^2\xi^v$ is divisible by v , and so $\operatorname{Re}(e^{-i\alpha}\sigma^*(|u|^{\tau_i}|v|^2)\xi^v)$ is divisible by s . As a result, $r^{\tau_i}s\xi^{\text{ro},s}$ extends as an analytic function.

In a similar way, the function $\operatorname{Im}(e^{-i\alpha}\sigma^*(|u|^{\tau_i}|v|^2\xi^v))$ is divisible by s . But the only term in the expansion of $|u|^{\tau_i}|v|^2\xi^v$ which has order 1 in v is a real multiple of the variable v , it follows that $\operatorname{Im}(e^{-i\alpha}\sigma^*(|u|^{\tau_i}|v|^2\xi^v))$ is divisible by s^2 . As a result, $r^{\tau_i}s\xi^{\text{ro},\beta}$ has an analytic extension to U^{ro} which is never 0.

We have seen that the function $r^{\tau_i}s\xi^{\text{ro},r}$ is divisible by r , and so vanishes along the boundary piece $D_i^{\text{ro}} \cap U^{\text{ro}}$. As a result, the vector field $r^{\tau_i}s(\pi_{\text{pol}}^{\text{ro}})^*\xi$ is tangent to $D_i^{\text{ro}} \cap U^{\text{ro}}$.

Similarly, since ξ^v has linear part which is a negative multiple of v , the function

$$r^{\tau_i}s\xi^{\text{ro},s} = s^{-1}\operatorname{Re}(e^{-i\alpha}\sigma^*(|u|^{\tau_i}|v|^2\xi^v))$$

takes negative values along the set defined by $s = 0$. This means that the extension of $r^{\tau_i}s(\pi_{\text{pol}}^{\text{ro}})^*\xi$ is transverse to the boundary piece D_a^{ro} and points outwards. \square

Definition 8.3.7. With U as in 8.3.1, and $U^{\text{ro}} = \sigma^{-1}(U)$, denote by

$$\xi_U, \quad \xi_U^{\text{ro}}$$

the unique extensions of the vector fields eq. (8.3.3) and eq. (8.3.6) to U and U^{ro} , respectively.

8.3.8. For $p \in U$, denote by γ_p the trajectory of ξ_U starting at p . If $p \in U \setminus D$, then γ_p is, up to reparametrization, the trajectory of ξ pulled back to U via π_{pol} .

Corollary 8.3.9. Let U be as in 8.3.1. Then, there exists a smaller neighborhood $V \subset U$ satisfying

- (1) if $p \in V$, then γ_p does not escape U ,
- (2) if $p \in V \cap D_i$, then γ_p converges to the unique intersection point in $D_i \cap D_a$,
- (3) if $p \in V \setminus D_i$, then γ_p converges to a point in $D_a \setminus D_i$.

Corollary 8.3.10. There exists an open set $V \subset Y_{\text{pol}}$ containing C_{pol} such that

$$\overline{\pi_{\text{pol}}^{-1}(S) \setminus \{0\}} \cap V = \emptyset.$$

8.4. Poincaré-Hopf indices

If ij is an invariant vertex, then the vector field ξ_U is tangent to the disks $D_i \cap U$ and $D_j \cap U$, and does not vanish outside the intersection point. As a result, restricting the vector field to either disk produces an index, see Definition 2.4.6.

Lemma 8.4.1. (1) Assume that ij is an invariant edge. Then the restriction $\xi_U|_{D_i \cap U}$ has an isolated singularity at $D_i \cap D_j$ of index one.

- (2) The set $D_{i,\theta}^{\text{ro},\circ} \cap U^{\text{ro}}$ consists of $\gcd(m_i, m_j)$ punctured disks. At each puncture, the restriction of ξ_U^{ro} has index

$$\frac{1}{\gcd(m_i, m_j)} \begin{vmatrix} \varpi_i & m_i \\ \varpi_j & m_j \end{vmatrix} + 1.$$

- (3) The set $D_{j,\theta}^{\text{ro},\circ} \cap U^{\text{ro}}$ consists of $\gcd(m_i, m_j)$ punctured disks. On each disk, the restriction of ξ_U^{ro} has index

$$\frac{-1}{\gcd(m_i, m_j)} \begin{vmatrix} \varpi_i & m_i \\ \varpi_j & m_j \end{vmatrix} + 1.$$

PROOF. First we prove 1. From [Lemmas 8.1.1](#) and [8.1.2](#), it follows that the Hessian of the restriction has two real nonzero eigenvalues with the same sign. As a result, it has index 1.

For 2 and 3, it suffices to have a look at [fig. 8.2.10](#), and use [eq. \(2.4.7\)](#). Indeed, observe that, by [Lemma 8.2.4](#), (ii) and (iii), the number of red points is

$$(8.4.2) \quad \frac{1}{\gcd(m_i, m_j)} \begin{vmatrix} \varpi_i & m_i \\ \varpi_j & m_j \end{vmatrix}.$$

Which is the same as the number of green points. After contracting each connected component of $D_{i,j,\theta}^{\text{ro}}$ to a point, we get a [eq. \(8.4.2\)](#)-pronged singularity on $D_{j,\theta}^{\text{ro}}$ and a [eq. \(8.4.2\)](#)-petal singularity on $D_{i,\theta}^{\text{ro}}$. So the result follows after [Example 2.4.8](#). \square

Lemma 8.4.3. *Assume that ik is an edge from i to k , and that i is invariant and k not invariant. Then the Poincaré-Hopf index of the vector field ξ_i at the intersection point $D_i \cap D_k$ equals $1 - \varpi_k$.*

PROOF. Consider the the vector field $\xi_{i,k,\theta}^{\text{ro}}|_{D_{i,\theta}^{\text{ro}}}$. Let L be one of the boundary components which is contained in $D_{i,k,\theta}^{\text{ro}}$. Then, by [Lemma 8.2.6](#) and [Lemma 8.2.4](#) (iii), the boundary component L has $\varpi_k m_i / \gcd(m_i, m_k)$ red vertices. So, after contracting L to a point, the vector field $\xi_{i,k,\theta}^{\text{ro}}|_{D_{i,\theta}^{\text{ro}}}$ has a $\varpi_k m_i / \gcd(m_i, m_k)$ -pronged singularity. Now recall that for an invariant vertex i , the vector field $\xi_{i,\theta}^{\text{ro}}$ is just the pullback by σ of ξ_i restricted to $D_{i,\theta}^{\text{ro}}$. Furthermore, the map $\sigma|_{D_{i,\theta}^{\text{ro}}} : D_{i,\theta}^{\text{ro}} \rightarrow D_i$ is an m_i regular cover, and, restricted to each connected component of $D_{i,\theta}^{\text{ro}}$ is an $m_i / \gcd(m_i, m_k)$ regular cover. We find that ξ_i has at $D_i \cap D_k$ a ϖ_k -pronged singularity. So, after [Example 2.4.8](#), [eq. \(2.4.9\)](#), it has Poincaré-Hopf index $1 - \varpi_k$. \square

CHAPTER 9

Other Exceptional Divisors

In this section, we consider an embedded resolution $\pi_{\text{pol}} : Y_{\text{pol}} \rightarrow \mathbb{C}^2$ (Definition 5.1.3) of the curve $(C, 0)$ that resolves the generic polar curves, and fix a vertex $i \in \mathcal{V}$, which does not correspond to the first blow-up, $i \neq 0$. It may be impossible to scale and extend the vector field ξ over the exceptional divisor D_i , to get a vector field on D_i° , similar to ξ_0 . In terms of numerical invariants on the graph, we characterize those divisors having such an extension. More concretely we show that it is precisely the vanishing of the polar weight ϖ_i that controls when it is possible to do such an extension prior without doing the real oriented blow-up. We describe a similar construction on the real oriented blow-up Y^{ro} , which can be done for any exceptional divisor, invariant or non-invariant. This is further exemplified in Example 9.2.6.

Notation 9.0.1. We fix a metric induced by a coordinate change in G_{pol} (Definition 5.1.10). Fix also isometric coordinates (recall Definition 2.3.1) x, y in \mathbb{C}^2 with respect to this metric chosen also so that the line $\{y = 0\}$ is the tangent to i . This can always be achieved by a further unitary change of coordinates.

As we have been doing so far, we usually simplify the notation by identifying functions defined in a neighborhood of the origin in \mathbb{C}^2 with their pullback to U via π_{pol} or U^{ro} via $\pi_{\text{pol}}^{\text{ro}}$. That is, we sometimes write simply f and f_x instead of $\pi_{\text{pol}}^* f$ and f_x , etc. Furthermore, the partials of $x = \pi_{\text{pol}}^* x$ with respect to u, v are denoted x_u, x_v , and so on.

As in Chapter 4, we have the real oriented blow-up $\sigma : Y_{\text{pol}}^{\text{ro}} \rightarrow Y_{\text{pol}}$, and the chart U induces the chart $U^{\text{ro}} = \sigma^{-1}(U)$ with coordinates $r = |u|$, $\alpha = \arg(u)$ and v . The boundary of U^{ro} is $\partial U^{\text{ro}} = (\pi_{\text{pol}}^{\text{ro}})^{-1}(D_i)$, given by $r = 0$.

We choose a point $p \in D_i^\circ$, and a coordinate neighborhood U containing p so that $u(p) = v(p) = 0$. Since x vanishes with order $c_{0,i}$ along D_i , and does not vanish on $U \setminus D_i$, we can choose the coordinates u, v so that

$$x = u^{c_{0,i}}.$$

Since the restriction $\pi_{\text{pol}}|_{U \setminus D} : U \setminus D \rightarrow \mathbb{C}^2 \setminus \{0\}$ is a local diffeomorphism, we can pull back ξ to get $\pi_{\text{pol}}|_{U \setminus D}^* \xi$.

In coordinates, we have complex functions ξ^u, ξ^v on $U \setminus D$ so that this vector field is given by the vector

$$(9.0.2) \quad \pi_{\text{pol}}|_{U \setminus D}^* \xi = \begin{pmatrix} \xi^u \\ \xi^v \end{pmatrix} = \frac{-1}{\det \text{Jac } \pi^{\bar{f}}} \begin{pmatrix} y_v \bar{f}_x - x_v \bar{f}_y \\ -y_u \bar{f}_x + x_u \bar{f}_y \end{pmatrix}.$$

Similarly, on $U^{\text{ro}} \setminus \partial U^{\text{ro}}$, we have a vector field

$$\pi_{\text{pol}}^{\text{ro}}|_{U^{\text{ro}} \setminus \partial U^{\text{ro}}}^* \xi = \begin{pmatrix} \xi^{\text{ro},r} \\ \xi^{\text{ro},\alpha} \\ \xi^{\text{ro},v} \end{pmatrix}$$

Here, $\xi^{\text{ro},r}$ and $\xi^{\text{ro},\alpha}$ are real analytic functions, while $\xi^{\text{ro},v}$ is, as before, a real analytic complex-valued function. We write $v = s + it$ and correspondingly $\xi^{\text{ro},v} = \xi^{\text{ro},s} + i\xi^{\text{ro},t}$. Recall, 8.1.3, that a computation in polar coordinates gives

$$(9.0.3) \quad \xi^{\text{ro},v} = \sigma^* \xi^v, \quad \xi^{\text{ro},r} = \operatorname{Re} (e^{-i\alpha} \sigma^* \xi^u), \quad \xi^{\text{ro},\alpha} = \operatorname{Im} ((re^{i\alpha})^{-1} \sigma^* \xi^u).$$

Definition 9.0.4. Let P_i be the relative polar curve defined by the partial f_y , and denote by \tilde{P}_i its strict transform by π_{pol} .

Definition 9.0.5. Let $i \in \mathcal{V}$ with $i \neq 0$. Set

$$\Sigma_i = \tilde{P}_i \cap D_i^\circ, \quad \Sigma_i^{\text{ro}} = \sigma^{-1}(\Sigma_i), \quad \Sigma_{i,\theta}^{\text{ro}} = \Sigma^{\text{ro}} \cap D_{i,\theta}^\circ.$$

and

$$\Sigma_U = \Sigma_i \cap U, \quad \Sigma_U^{\text{ro}} = \Sigma^{\text{ro}} \cap U^{\text{ro}}.$$

Note that we have a precise choice for the polar curve P_i , which depends on the metric and the vertex i . More precisely, P_i is the vanishing set of the partial derivative of f with respect to the direction orthogonal to the tangent associated with i . Therefore, even if we fix the underlying metric, the definition of Σ_i for different vertices i involves a different choice of the polar curve.

In contrast, Σ_0 cannot be seen as the intersection of D_0° with the strict transform of a particular polar curve. A signed count of singularities of the vector field ξ_0 , however, allows for estimating the number of points in Σ_0 as the following lemma shows:

Lemma 9.0.6. *Let F_0 and S_0 be the number of fountains and saddle points, respectively, of ξ_0 . If t is the number of tangents of C , then*

$$F_0 - S_0 = 2 - t$$

PROOF. By Lemma 7.4.12, ξ_0 has no sinks. By Lemma 7.4.13, the index of ξ_0 near $D_0 \cap \tilde{C}$ is 1. The Euler characteristic of D_0 is 2. A direct application of Poincaré-Hopf index theorem yields the result. \square

Remark 9.0.7. The intersection Σ_i consists of finitely many points. The preimage Σ_i^{ro} is therefore the union of finitely many fibers of the S^1 -bundle $D_i^{\text{ro},\circ} \rightarrow D_i^\circ$. These fibers are transverse to the foliation on $D_i^{\text{ro},\circ}$ given by $\arg(f)$, whose leaves are $D_{i,\theta}^{\text{ro},\circ}$ for $\theta \in \mathbb{R}/2\pi\mathbb{Z}$. In fact, $|\Sigma_{i,\theta}^{\text{ro}}| = m_i \cdot |\Sigma_i| < \infty$.

9.1. Extension over the boundary

Lemma 9.1.1. *We use Notation 9.0.1.*

(i) *The vector field*

$$(9.1.2) \quad r^{\tau_i} \pi_{\text{pol}}|_{U^{\text{ro}} \setminus \partial U^{\text{ro}}}^* \xi$$

on $U^{\text{ro}} \setminus \partial U^{\text{ro}}$ extends to an analytic vector field on U^{ro} which is tangent to ∂U^{ro} and whose vanishing set is Σ_U^{ro} .

(ii) *If i is an invariant vertex, that is, if $m_i - p_i = c_{1,i}$, then the vector field*

$$(9.1.3) \quad |u|^{2c_{1,i}} \pi_{\text{pol}}|_{U \setminus D}^* \xi = |u|^{\tau_i} \pi_{\text{pol}}|_{U \setminus D}^* \xi$$

on $U \setminus D$ extends to an analytic vector field on U , which is tangent to $D \cap U$ and whose vanishing set is Σ_U .

PROOF. Since $x = u^{c_{0,i}}$, we have $x_v = 0$. As a result

$$r^{\tau_i} \xi^u = r^{c_{1,i}+m_i-p_i} \frac{-y_v \bar{f}_x}{\det \text{Jac } \pi_{\text{pol}} \bar{f}} = r^{c_{1,i}-(c_{0,i}-1)} r^{c_{0,i}-1} \frac{-y_v}{\det \text{Jac } \pi_{\text{pol}}} r^{m_i-p_i} \frac{\bar{f}_x}{\bar{f}}$$

The second factor $r^{c_{0,i}-1} \frac{-y_v}{\det \text{Jac } \pi_{\text{pol}}}$ extends over the boundary by [Lemma 4.1.2](#). This is because by [3.3.4](#) we have $\text{ord}_u y_v = c_{1,i}$ and $\text{ord}_u \det \text{Jac } \pi_{\text{pol}} = \nu_i - 1 = c_{0,i} + c_{1,i} - 1$. The third factor $r^{m_i-p_i} \frac{\bar{f}_x}{\bar{f}}$ also extends over the boundary since $\text{ord}_u \bar{f}_x \geq p_i$ ([eq. \(5.1.7\)](#)) and $\text{ord}_u \bar{f} = m_i$. Finally, since $c_{1,i} - c_{0,i} + 1 \geq 2$ (because $i \neq 0$), the first factor $r^{c_{1,i}-c_{0,i}+1}$ vanishes identically along the boundary ∂U^{ro} . We conclude, by the last two formulas of [eq. \(9.0.3\)](#) that both $r^{\tau_i} \xi^{\text{ro},r}$ and $r^{\tau_i} \xi^{\text{ro},\alpha}$ extend over and vanish along ∂U^{ro} .

Similarly as above, again using [Lemma 4.1.2](#), the function

$$(9.1.4) \quad r^{c_{1,i}+m_i-p_i} \frac{x_u \bar{f}_y}{\det \text{Jac } \pi \bar{f}} = r^{c_{1,i}} \frac{c_{0,i} u^{c_{0,i}-1}}{\det \text{Jac } \pi} \cdot r^{m_i-p_i} \frac{\bar{f}_y}{\bar{f}}$$

extends to a real analytic \cdot_i -equivariant function of weight $c_{1,i} - m_i + p_i$ on U^{ro} . We are using that $\text{ord}_u \bar{f}_y = p_i$. Note that this function vanishes precisely along $\{r^{-p_i} f_y = 0\}$ because

$$r^{c_{1,i}} \frac{c_{0,i} u^{c_{0,i}-1}}{\det \text{Jac } \pi} \cdot r^{m_i} \frac{1}{\bar{f}}$$

is an unit. Also note that $\{r^{-p_i} f_y = 0\} \cap \partial U^{\text{ro}} = \tilde{P}_i \cap \partial U^{\text{ro}} = \Sigma_U^{\text{ro}}$.

By [Lemma 3.5.2](#), and our choice of coordinates x, y , we have

$$\text{ord}_u(y_u) = \text{ord}_u(y) - 1 > \text{ord}_u(x) - 1 = \text{ord}_u(x_u).$$

Furthermore, $\text{ord}_u(f_x) \geq \text{ord}_u(f_y)$ by [eq. \(5.1.7\)](#). Thus, as in the previous argument, the function

$$(9.1.5) \quad r^{c_{1,i}+m_i-p_i} \frac{-y_u \bar{f}_x}{\det \text{Jac } \pi \bar{f}} = r^{c_{1,i}} \frac{-y_u}{\det \text{Jac } \pi} \cdot r^{m_i-p_i} \frac{\bar{f}_x}{\bar{f}}$$

on $U^{\text{ro}} \setminus \partial U^{\text{ro}}$ extends over the boundary and vanishes there.

By [eq. \(9.0.2\)](#) and [eq. \(9.0.3\)](#), the function $r^{\tau_i} \xi^{\text{ro},v}$ is the sum of [eq. \(9.1.4\)](#) and [eq. \(9.1.5\)](#), and so extends to a function on U^{ro} . Outside the boundary, the vector field $r^{\tau_i} \pi_{\text{pol}}^{\text{ro}}|_{U^{\text{ro}} \setminus \partial U^{\text{ro}}}^* \xi$ does not vanish since $\pi_{\text{pol}}^{\text{ro}}$ is a local diffeomorphism on $U^{\text{ro}} \setminus \partial U^{\text{ro}}$ and ξ does not vanish outside the curve $C \subset \mathbb{C}^2$. Since the function in [eq. \(9.1.5\)](#) vanishes along ∂U^{ro} , the vanishing set of $\xi^{\text{ro},v}|_{\partial U^{\text{ro}}}$ is that of the function in [eq. \(9.1.4\)](#) which we have already seen to be Σ_U^{ro} . This finishes the proof of (i).

(ii) follows from a completely analogous argument by replacing $r^{c_{1,i}+m_i-p_i}$ by $|u|^{2c_{1,i}}$. \square

Lemma 9.1.6. *We use [Notation 9.0.1](#).*

(i) *The vector field*

$$(9.1.7) \quad \pi_{\text{pol}}^{\text{ro}}|_{Y^{\text{ro}} \setminus D^{\text{ro}}}^* (|x|^{\tau_i/c_{0,i}} \xi)$$

on $Y^{\text{ro}} \setminus D^{\text{ro}}$ extends to an analytic vector field on $(Y^{\text{ro}} \setminus D^{\text{ro}}) \cup D_i^{\text{ro},\circ}$ which is tangent to $D_i^{\text{ro},\circ}$ and whose vanishing set is Σ_i^{ro} . Moreover, for each $\theta \in \mathbb{R}/2\pi\mathbb{Z}$, the extension is tangent to $D_{i,\theta}^{\text{ro},\circ}$.

(ii) If i is an invariant vertex, that is, if $m_i - p_i = c_{1,i}$, then the vector field

$$(9.1.8) \quad \pi_{\text{pol}}|_{Y \setminus D}^*(|x|^{2c_{1,i}/c_{0,i}} \xi) = \pi_{\text{pol}}|_{Y \setminus D}^*(|x|^{\tau_i/c_{0,i}} \xi)$$

on $Y \setminus D$ extends to an analytic vector field on $(Y \setminus D) \cup D_i^\circ$, which is tangent to D_i° and whose vanishing set is Σ_i .

PROOF. It is always possible to cover $D_i^{\text{ro},\circ}$ by charts U^{ro} with coordinates r, α, v as in [Notation 9.0.1](#). In those coordinates, we have that

$$\pi_{\text{pol}}^{\text{ro}*}|x|^{\tau_i/c_{0,i}} = r^{\tau_i}.$$

Similarly, it is possible to cover D_i° by charts U with coordinates u, v such that

$$\pi_{\text{pol}}^*|x|^{\tau_i/c_{0,i}} = |u|^{\tau_i}.$$

Then, the proof follows from [Lemma 9.1.1](#). \square

Definition 9.1.9. Denote by ξ_U^{ro} the analytic vector field on U^{ro} whose restriction to $U^{\text{ro}} \setminus \partial U^{\text{ro}}$ coincides with [eq. \(9.1.2\)](#). If i is an invariant vertex then denote by ξ_U the analytic vector field on U whose restriction to $U \setminus D$ coincides with [eq. \(9.1.3\)](#).

Similarly, denote by $\hat{\xi}_i^{\text{ro}}$ the analytic vector field on $(Y \setminus D^{\text{ro}}) \cup D_i^{\text{ro},\circ}$ whose restriction to $Y^{\text{ro}} \setminus D^{\text{ro}}$ coincides with [eq. \(9.1.7\)](#). If i is an invariant vertex then denote by $\hat{\xi}_i$ the analytic vector field on $(Y \setminus D) \cup D_i^\circ$ whose restriction to $Y \setminus D$ coincides with [eq. \(9.1.8\)](#). Denote the restriction by $\xi_i = \hat{\xi}_i|_{D_i^\circ}$.

Finally, denote the other corresponding restrictions by $\xi_i^{\text{ro}} = \hat{\xi}_i^{\text{ro}}|_{D_i^{\text{ro},\circ}}$ and $\xi_{i,\theta}^{\text{ro}} = \hat{\xi}_i^{\text{ro}}|_{D_{i,\theta}^{\text{ro},\circ}}$.

Remark 9.1.10. Let $i \in \mathcal{V}_Y \setminus \{0\}$. In local coordinates on D_i , the vector field ξ_i is determined by the initial part of the pullback of the function f_y . If we start with a different metric, then the same construction gives a vector field which is a linear combination of the pullbacks of f_x and f_y . Since f_x vanishes with a higher order than f_y , by [Corollary 6.4.17](#), this construction gives the same result up to a real scalar. Therefore, the vector fields ξ_i and ξ_i^{ro} do not depend on the chosen generic metric, up to a positive scalar.

9.2. A potential for ξ_i on invariant vertices

In this subsection, we consider an invariant vertex $i \in \mathcal{V}_{\text{pol}} \setminus \{0\}$. We show that the vector field ξ_i , defined in the previous subsection, has a scalar potential with respect to the metric g_i , defined in [Definition 4.3.1](#). An analogous statement for $\xi_{i,\theta}^{\text{ro}}$, and its proof, can be found in the next subsection. We choose a coordinate chart around a point $p \in D_i^\circ$ as in [3.3.4](#), and set $U^{\text{ro}} = \sigma^{-1}(U)$.

Let $i \in \mathcal{V} \setminus \{0\}$ be an invariant vertex. The function

$$(9.2.1) \quad \pi^* \left(-\log \frac{|f|}{|x|^{m_i/c_{0,i}}} \right)$$

extends as an analytic function over D_i° . In fact, in coordinates u, v in U , satisfying $x = u^{c_{0,i}}$, the function f is divisible by u^{m_i} , and $|x|^{m_i/c_{0,i}} = |u^{m_i}|$.

Definition 9.2.2. Denote by $\phi_i : D_i^\circ \rightarrow \mathbb{R}$ the restriction of the extension of [eq. \(9.2.1\)](#) to D_i° .

In coordinates u, v , we can write $\pi^* f = u^{m_i} g(v) + \text{h.o.t.}$, where the higher order terms are divisible by u^{m_i+1} . Therefore, eq. (9.2.1) equals

$$\begin{aligned} -\log |f| + \log |u|^{m_i/c_{0,i}} &= -(\log |g(v)| + \text{h.o.t.}) + m_i \log |u| + \log |u|^{m_i} \\ &= -\log |g(v)| \end{aligned}$$

along D_i , where u vanishes. As a result,

$$(9.2.3) \quad \phi_i(v) = -\log |g(v)|.$$

Lemma 9.2.4. *Let $i \neq 0$ be an invariant vertex. The vector field ξ_i is the gradient of ϕ_i with respect to the Riemannian metric g_i from Definition 4.3.1.*

PROOF. From eq. (9.0.2) and observing that $x_v = 0$, we have the formula

$$(9.2.5) \quad |u|^{\tau_i} \xi^v = |u|^{\tau_i} \frac{y_u \bar{f}_x - x_u \bar{f}_y}{x_u y_v \bar{f}}.$$

We recall from Definition 8.0.1 that $\tau_i = c_{1,i} + m_i - p_i$. Since $\varpi_i = 0$ (recall Definition 6.1.1), we have that $\tau_i = 2c_{1,i}$ and so

$$|u|^{\tau_i} = |u|^{2c_{1,i}} = u^{c_{1,i}} \bar{u}^{c_{1,i}}.$$

Similarly as in eq. (9.1.5), the term $|u|^{\tau_i} \frac{y_u \bar{f}_x}{x_u y_v \bar{f}}$ vanishes along D_i° . The other term is

$$|u|^{2c_{1,i}} \frac{-x_u \bar{f}_y}{x_u y_v \bar{f}} = -\frac{|u|^{2c_{1,i}} \bar{f}_y}{y_v \bar{f}} = -\frac{|u|^{2c_{1,i}} \bar{f}_v}{|y_v|^2 \bar{f}}.$$

In the last inequality we have used that $\bar{f}_v = \bar{y}_v \bar{f}_y$. Since $\varpi_i = 0$, Lemma 6.1.3 implies that $\text{ord}_u \bar{f}_v = \text{ord}_u \bar{f} = m_i$. Therefore, we have $\text{in}_u f = u^{m_i} g(v)$ and $\text{in}_u f_v = u^{m_i} g'(v)$. Along $D_i \cap U$, we find

$$|u|^{\tau_i} \xi^v|_{D_i \cap U} = h_U^{-1}(v) \frac{g'(\bar{v})}{g(\bar{v})}.$$

where h_U is the real function defining the metric g_i , defined in Definition 4.3.1. The result now follows from Lemma 2.1.3, and Remark 4.3.2. \square

Before dealing with non-invariant vertices, we motivate the announced necessity to consider the real oriented blow-up with an example. In the next example we carefully analyze the cusp singularity and attempt an extension of the vector field in the style of the present subsection and observe the failure and its reason.

Example 9.2.6 (The cusp $f(x, y) = y^2 + x^3$). We derive the minimal embedded resolution and associated invariants step-by-step.

Step 1: First Blow-up and Divisor D_0 . We begin by blowing up the origin in \mathbb{C}^2 . In the chart $(x, y) = (u_0, u_0 v_0)$, the total transform of f is:

$$\pi_0^* f = (u_0 v_0)^2 + u_0^3 = u_0^2 (v_0^2 + u_0)$$

This creates the first exceptional divisor D_0 , given locally by $u_0 = 0$. The strict transform of the curve, C_1 , has the equation $g_1(u_0, v_0) = v_0^2 + u_0 = 0$. At the new origin $(u_0, v_0) = (0, 0)$, the curve C_1 is tangent to the divisor D_0 . This tangency must be resolved.

Invariants for D_0 :

- By definition, $c_{0,0} = 1, c_{1,0} = 1$.
- $m_0 = \text{ord}_{D_0}(f) = \text{mult}_0(f) = 2$.
- $p_0 = \text{ord}_{D_0}(f_y) = \text{ord}_{D_0}(y) = \text{ord}_{u_0}(u_0 v_0) = 1$.

- $\varpi_0 = c_{1,0} - m_0 + p_0 = 1 - 2 + 1 = 0$. D_0 is invariant.

Step 2: Second Blow-up and Divisor D_1 . We blow up the point of tangency $P_1 = (u_0, v_0) = (0, 0)$. This creates the divisor D_1 . Let's use the chart, $(u_0, v_0) = (u_1 v_1, v_1)$. The total transform of g_1 is $v_1^2 + u_1 v_1 = v_1(v_1 + u_1)$. Here, D_1 is given by $v_1 = 0$, the strict transform \tilde{D}_0 is $u_1 = 0$, and the strict transform of the curve is $\tilde{C}_1 : v_1 + u_1 = 0$. These three smooth curves intersect at the new origin $(u_1, v_1) = (0, 0)$, which is a triple point and not a normal crossing.

Invariants for D_1 :

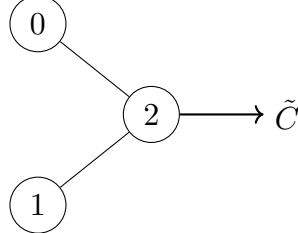
- The center P_1 is a smooth point on D_0 , so by Lemma 3.3.7, $c_{0,1} = c_{0,0} = 1$ and $c_{1,1} = c_{1,0} + 1 = 2$.
- We need the map from a chart seeing D_1 to \mathbb{C}^2 . Using the chart $(u_0, v_0) = (u_1, u_1 v_1)$ centered on P_1 , the map is $\pi(u_1, v_1) = (x, y) = (u_1, u_1^2 v_1)$, and D_1 is $\{u_1 = 0\}$.

$$m_1 = \text{ord}_{D_1}(f) = \text{ord}_{u_1}((u_1^2 v_1)^2 + u_1^3) = \text{ord}_{u_1}(u_1^3(u_1 v_1^2 + 1)) = 3$$

$$p_1 = \text{ord}_{D_1}(y) = \text{ord}_{u_1}(u_1^2 v_1) = 2$$

- $\varpi_1 = c_{1,1} - m_1 + p_1 = 2 - 3 + 2 = 1$. So D_1 is the **non-invariant divisor**.

Step 3: Third Blow-up and Divisor D_2 . We blow up the triple point $P_2 = (u_1, v_1) = (0, 0)$. This creates the divisor D_2 and separates the three intersecting curves. The final configuration is a normal crossings divisor. The resulting dual graph is:



Invariants for D_2 :

- The center P_2 is the intersection $\tilde{D}_0 \cap D_1$, so by Lemma 3.3.7, $c_{0,2} = c_{0,0} + c_{0,1} = 2$ and $c_{1,2} = c_{1,0} + c_{1,1} = 3$.
- A chart seeing $D_2 = \{u_2 = 0\}$ is given by $\pi(u_2, v_2) = (u_2^2 v_2, u_2^3 v_2^2)$.

$$m_2 = \text{ord}_{D_2}(f) = \text{ord}_{u_2}((u_2^3 v_2^2)^2 + (u_2^2 v_2)^3) = 6$$

$$p_2 = \text{ord}_{D_2}(y) = \text{ord}_{u_2}(u_2^3 v_2^2) = 3$$

- $\varpi_2 = c_{1,2} - m_2 + p_2 = 3 - 6 + 3 = 0$. D_2 is invariant.

The complete table of invariants confirms that D_1 is the unique non-invariant divisor:

i	0	1	2
$c_{0,i}$	1	1	2
$c_{1,i}$	1	2	3
m_i	2	3	6
p_i	1	2	3
ϖ_i	0	1	0
τ_i	2	3	6

Angle dependence

Now we show the angular dependence when approaching the non-invariant divisor, D_1 . To do this, we first find a local coordinate system (u, v) where D_1 is given by $\{u = 0\}$.

As derived above, the second blow-up π_1 (centered at $p_1 = (0, 0)$ in the (u_0, v_0) chart) can be described by the map $(u_0, v_0) = (u, uv)$. The new exceptional divisor D_1 is $\{u = 0\}$. Composing this with the first blow-up map $\pi_0(u_0, v_0) = (u_0, u_0 v_0)$ gives the map from our local chart to \mathbb{C}^2 :

$$(x, y) = \pi_0(\pi_1(u, v)) = \pi_0(u, uv) = (u, u(uv)) = (u, u^2v)$$

This map $\pi(u, v) = (u, u^2v)$ is therefore the correct local model for analyzing the vector field near D_1 . It correctly yields the invariants calculated for D_1 in the table above: $\varpi_1 = 1$ and $\tau_1 = 3$. We recall the formula for the pullback of $\xi = -\nabla \log |f|$ from [eq. \(9.0.2\)](#):

$$\pi^* \xi = \begin{pmatrix} \xi^u \\ \xi^v \end{pmatrix} = \frac{-1}{\det \text{Jac } \pi \cdot \bar{f}} \begin{pmatrix} y_v \bar{f}_x - x_v \bar{f}_y \\ -y_u \bar{f}_x + x_u \bar{f}_y \end{pmatrix}$$

The appropriate scaling factor, as per [Lemma 9.1.6](#), involves the radial weight $\tau_1 = 3$. We must analyze the vector field $|u|^{\tau_1} \pi^* \xi = |u|^3 \pi^* \xi$. Let's compute the components.

- **Jacobian:**

$$\text{Jac } \pi = \begin{pmatrix} x_u & x_v \\ y_u & y_v \end{pmatrix} = \begin{pmatrix} 1 & 0 \\ 2uv & u^2 \end{pmatrix} \implies \det \text{Jac } \pi = u^2.$$

- **Partials and pullbacks:**

$$f_x = 3x^2, \quad f_y = 2y$$

$$\pi^* f = u^3(uv^2 + 1), \quad \pi^* f_x = 3u^2, \quad \pi^* f_y = 2u^2v$$

- **Components of $\pi^* \xi$:**

$$\xi^u = \frac{-1}{u^2 \bar{f}} (y_v \bar{f}_x - x_v \bar{f}_y) = \frac{-1}{u^2 \bar{f}} (u^2 \cdot 3\bar{u}^2 - 0) = \frac{-3\bar{u}^2}{\bar{f}} = \frac{-3\bar{u}^2}{\bar{u}^3(1 + \bar{u}\bar{v}^2)} = \frac{-3}{\bar{u}(1 + \bar{u}\bar{v}^2)}$$

$$\xi^v = \frac{-1}{u^2 \bar{f}} (-y_u \bar{f}_x + x_u \bar{f}_y) = \frac{-1}{u^2 \bar{f}} (-2uv \cdot 3\bar{u}^2 + 1 \cdot 2\bar{u}^2\bar{v}) = \frac{-2\bar{u}^2(-3uv + \bar{v})}{u^2 \bar{f}} = \frac{-2(-3uv + \bar{v})}{u^2 \bar{u}(1 + \bar{u}\bar{v}^2)}$$

Now we apply the scaling factor $|u|^3$:

- **u-component:**

$$|u|^3 \xi^u = |u|^3 \frac{-3}{\bar{u}(1 + \bar{u}\bar{v}^2)} = \frac{-3u\bar{u}|u|}{\bar{u}(1 + \bar{u}\bar{v}^2)} = \frac{-3u|u|}{1 + \bar{u}\bar{v}^2}$$

As $u \rightarrow 0$, this component tends to 0. This is expected, as the extended vector field must be tangent to the divisor $D_1 = \{u = 0\}$.

- **v-component:** This is the crucial part.

$$|u|^3 \xi^v = |u|^3 \frac{-2(-3uv + \bar{v})}{u^2 \bar{u}(1 + \bar{u}\bar{v}^2)} = \frac{u\bar{u}|u| \cdot (-2(-3uv + \bar{v}))}{u^2 \bar{u}(1 + \bar{u}\bar{v}^2)} = \frac{|u|}{u} \frac{-2(-3uv + \bar{v})}{1 + \bar{u}\bar{v}^2}$$

Let's analyze the limit of the scaled v -component as we approach the divisor D_1 , i.e., as $u \rightarrow 0$. We introduce polar coordinates for u , setting

$u = re^{i\alpha}$ where $r = |u|$. The term $\frac{|u|}{u}$ becomes:

$$\frac{|u|}{u} = \frac{r}{re^{i\alpha}} = e^{-i\alpha}$$

Now we can compute the limit:

$$\lim_{u \rightarrow 0} (|u|^3 \xi^v) = \lim_{r \rightarrow 0} \left(e^{-i\alpha} \frac{-2(-3re^{i\alpha}v + \bar{v})}{1 + re^{-i\alpha}\bar{v}^2} \right) = e^{-i\alpha} \frac{-2(0 + \bar{v})}{1 + 0} = -2\bar{v}e^{-i\alpha}$$

The limit of the scaled vector field on the divisor D_1 is not a single well-defined vector field. Instead, it depends on the angle $\alpha = \arg(u)$ of approach to the divisor. For each direction of approach, we get a different resulting vector field on D_1 .

This explicit angular dependence, captured by the term $e^{-i\alpha}$, is precisely the reason a standard extension fails. As shown in the proof of [Lemma 9.1.1](#), the limit of the rescaled vector field is an equivariant function of weight ϖ_i . Here, for $i = 1$, we have $\varpi_1 = 1$, and indeed our resulting limit $-2\bar{v}e^{-i\alpha}$ is equivariant of weight 1 with respect to the \cdot_1 -action (which corresponds to rotating u).

The **real oriented blow-up** $\sigma : Y^{\text{ro}} \rightarrow Y$ resolves this indeterminacy. It replaces the divisor D_1 (a complex manifold) with its pre-image $D_1^{\text{ro}} = \sigma^{-1}(D_1)$, which is the space of oriented real normal directions to D_1 . In our local chart, D_1^{ro} is parametrized by (α, v) . The limit vector field now becomes a well-defined vector field on this new, larger space D_1^{ro} , with its value at a point (α, v) being precisely the limit we calculated for that specific angle of approach.

9.3. A potential for $\xi_{i,\theta}^{\text{ro}}$

In this subsection, we fix a non-invariant vertex $i \in \mathcal{V}_{\text{pol}}$, $\varpi_i \neq 0$, and a value $\theta \in \mathbb{R}/2\pi\mathbb{Z}$ of $\arg(f)$. We prove an analogous result to [Lemmas 7.4.4](#) and [9.2.4](#) but for non-invariant vertices, that is, we show the existence of a potential function for the vector field $\xi_{i,\theta}^{\text{ro}}$.

9.3.1. Consider the Riemann surface $D_{i,\theta}^{\text{ro},\circ}$, defined in [Definition 4.2.1](#), with the metric $g_{i,\theta}^{\text{ro}}$ defined in [Definition 4.3.1](#). If we contract each boundary component of $D_{i,\theta}^{\text{ro}}$ to a point, we get a branched covering over D_i . Thus, $D_{i,\theta}^{\text{ro},\circ}$ is a Riemann surface with punctures. If $j \in \mathcal{V}_{\text{pol}}$ is a neighbor of i , let $U \subset Y_{\text{pol}}$ be a small coordinate chart containing the intersection $D_i \cap D_j$, and let $U^{\text{ro}} = \sigma^{-1}(U)$. We can assume that $D_i \cap U$ is a disc. Thus, $D_{i,\theta}^{\text{ro},\circ} \cap U^{\text{ro}}$ covers a punctured disc, and so is a disjoint union of some number of punctured discs.

Lemma 9.3.2. Let $D \subset D_{i,\theta}^{\text{ro},\circ}$ be a connected component, and take $j \in \mathcal{V}_{\text{pol}}$ so that ji is the unique edge pointing to i . Let U and U^{ro} be as in the previous paragraph. Then D has genus zero, and $D \cap U^{\text{ro}}$ is connected.

PROOF. It follows from [Lemma 6.2.122](#) that the function $\arg(x)$ takes a constant value, say θ' , along D . Thus, D is a connected component of the set $\arg(x)^{-1}(\theta') \cap D_i^{\text{ro},\circ}$. Thus, D embeds into the Milnor fiber at radius zero of the function x . This Milnor fiber is a disk, and so D has genus zero. The modification $Y_{\text{pol}} \rightarrow \mathbb{C}^2$, and its real oriented blow-up, induce a decomposition of the Milnor fiber of the function x at radius zero (recall [Definition 4.2.4](#)) consisting of nested discs. Thus, each connected component has a unique outer boundary component. For the vertex 0, this outer component is the boundary of the Milnor fiber, whereas for other vertices i , the outer component corresponding to the unique edge pointing to i . Since the

closure of D has a unique outer boundary component, the set $D \cap U^{\text{ro}}$ is a single punctured disc, in particular, it is connected. \square

Lemma 9.3.3. *Let i be any vertex in $\mathcal{V}_{\text{pol}} \setminus \{0\}$. Then, there exists a function $\phi_{i,\theta}^{\text{ro}} : D_{i,\theta}^{\text{ro},\circ} \rightarrow \mathbb{R}$ so that*

$$\xi_{i,\theta}^{\text{ro}} = \nabla \phi_{i,\theta}^{\text{ro}}$$

where the gradient is taken with respect to the metric $g_{i,\theta}^{\text{ro}}$ defined in [Definition 4.3.1](#).

Furthermore, if k is a neighbor of i so that the edge ik is oriented from i to k , and $\varpi_k \neq 0$, then $\phi_{i,\theta}^{\text{ro}}$ extends over the corresponding boundary components with constant value there.

PROOF. If i is invariant, then we can take $\phi_{i,\theta}^{\text{ro}} = \sigma^* \phi_i$, where $\phi_i : D_i \rightarrow \mathbb{R}$ is defined in the previous subsection. We leave the second statement for invariant vertices to the end of this proof.

So assume that $\varpi_i \neq 0$. By the previous lemma, $D_{i,\theta}^{\text{ro},\circ}$ is a punctured sphere. To each neighbor of i , there corresponds a set of punctures. If j is the unique neighbor of i so that there is an edge from j to i , then there is only one puncture corresponding to j on each connected component. Let $D_{i,\theta}^{\text{ro},\cup}$ be the Riemann surface obtained by filling in all the other punctures, thus, $D_{i,\theta}^{\text{ro},\cup}$ is a disjoint union of copies of \mathbb{C} . Denote by $\kappa_{i,\theta}^{\text{ro}}$ the differential form dual to $\xi_{i,\theta}^{\text{ro}}$ with respect to the metric $g_{i,\theta}^{\text{ro}}$. Let u, v be a holomorphic coordinate system on a chart in Y_{pol} , near a point $p \in D_i$ as before, and expand

$$f(u, v) = u^{m_i} f_{m_i}(v) + \dots + u^{m_i + \varpi_i} f_{m_i + \varpi_i} + \text{h.o.t.}$$

Then, by [Lemma 6.1.3](#), we have

$$f'_{m_i} = \dots = f'_{m_i + \varpi_i - 1} = 0,$$

and

$$f'_{m_i + \varpi_i} \not\equiv 0.$$

As a result, we can write

$$\text{in}_u f = u^{m_i} f_{m_i}(v), \quad \text{in}_u f_v = u^{m_i + \varpi_i} f'_{m_i + \varpi_i}(v).$$

Similarly as in the proof of [Lemma 9.1.1](#), the restriction of $|u|^{\tau_i} \xi^v$ to ∂U^{ro} is given by

$$|u|^{\tau_i} \frac{x_u \text{in}_u \bar{f}_y}{x_u y_v \text{in}_u \bar{f}} = |u|^{\tau_i} \frac{\text{in}_u \bar{f}_v}{|y_v|^2 \text{in}_u \bar{f}} = \frac{|u|^{\tau_i} \bar{u}^{\varpi_i}}{|y_v|^2} \frac{\bar{f}'_{m_i + \varpi_i}}{\bar{f}_{m_i}} = \left(\frac{u}{|u|} \right)^{-\varpi_i} \frac{|u|^{2c_{1,i}}}{|y_v|^2} \frac{\bar{f}'_{m_i + \varpi_i}}{\bar{f}_{m_i}}.$$

Recall that the metric on $D_{i,\theta}^{\text{ro},\circ}$ is given by the function

$$h_U(v) = \lim_{u \rightarrow 0} \frac{|y_v|}{|u|^{c_{1,i}}}.$$

Furthermore, the function $u/|u|$ is locally constant on $D_{i,\theta}^{\text{ro},\circ}$ because of [Lemma 6.1.3](#).

By [Remark 4.3.2](#), the differential form $\kappa_{i,\theta}^{\text{ro}}$ is given, in the coordinate v , by the complex function

$$\left(\frac{u}{|u|} \right)^{-\varpi_i} \frac{\bar{f}'_{m_i + \varpi_i}}{\bar{f}_{m_i}},$$

which is antiholomorphic on $D_{i,\theta}^{\text{ro},\circ}$ for θ fixed. By the Cauchy-Riemann equations, the form $\kappa_{i,\theta}^{\text{ro}}$ is closed.

Now, assume that v is a holomorphic coordinate in a chart around a puncture, corresponding to a vertex k , so that the edge ik is oriented from i to k . Assume that the puncture is given by $v = 0$. As a result, we can represent $\kappa_{i,\theta}^{\text{ro}}$ by an antiholomorphic complex function $\alpha + i\beta$ on a punctured disk. Since

$$\lim_{v \rightarrow 0} |u|^{\tau_i} |v|^{\tau_k} \xi^v = 0,$$

the function $|v|^{\tau_k} (\alpha + i\beta)$ is bounded on the punctured disk. It follows from the Riemann extension theorem that the holomorphic function $\alpha - i\beta$ has a meromorphic singularity at $v = 0$.

As a result, the vanishing order of $\alpha - i\beta$ at $v = 0$ is minus the Poincaré-Hopf index of $\xi_{i,\theta}^{\text{ro}}$ at the puncture. By Lemma 8.4.1, this index is

$$\frac{-1}{\gcd(m_i, m_k)} \begin{vmatrix} \varpi_k & m_k \\ \varpi_i & m_i \end{vmatrix} + 1.$$

By Corollary 6.3.7 and Corollary 6.3.6 5, the index is nonpositive, and so $\kappa_{i,\theta}^{\text{ro}}$ does not have a pole at $v = 0$. Therefore, $\kappa_{i,\theta}^{\text{ro}}$ extends as a closed form on $D_{i,\theta}^{\text{ro},\circ}$, which is a disjoint union of copies of \mathbb{C} . It follows that $\kappa_{i,\theta}^{\text{ro}}$ is exact, i.e. there exists $\phi_{i,\theta}^{\text{ro}} : D_{i,\theta}^{\text{ro},\circ} \rightarrow \mathbb{R}$ with $\kappa_{i,\theta}^{\text{ro}} = d\phi_{i,\theta}^{\text{ro}}$, or equivalently, $\xi_{i,\theta}^{\text{ro}} = \nabla \phi_{i,\theta}^{\text{ro}}$. Furthermore, $\phi_{i,\theta}^{\text{ro}}$ extends continuously over the punctures corresponding to the edge ik , and so, has a constant limit at each corresponding boundary component.

If i is invariant, then the same argument as above applies to show that ϕ_i has a limit at a puncture corresponding to ik , if i is such that $i \rightarrow k$, using, again, Lemma 8.4.1. This finishes the proof. \square

CHAPTER 10

Singularities on the Boundary of $Y_{\text{pol}}^{\text{ro}}$

In this section we study the singularities of ξ_U^{ro} ([Definition 9.1.9](#)) on ∂U^{ro} . Fix a point $p \in \Sigma_i$ with $i \neq 0$ and assume that the strict transform of $\{f_y = 0\}$ defines the polar curve P_i . Since π_{pol} resolves the polar curve P_i ([Definition 9.0.4](#)), the function $\pi_{\text{pol}}^* f_y$ vanishes along a smooth curve \tilde{P}_i passing through p meeting D_i^o transversely. As a consequence, on top of choosing u so that $x = u^{c_{0,i}}$ as in [Notation 9.0.1](#), we can choose v so that

$$\pi_{\text{pol}}^* f_y = u^{p_i} v.$$

10.1. Spinal cells

In this subsection we give name to the sets of trajectories of the vector field $\pi_{\text{pol}}^* \xi$ that converge to points in the sets Σ_i .

Definition 10.1.1. Let $i \in \mathcal{V}_{\text{pol}} \setminus \{0\}$, let $p \in \Sigma_i$. We define the set

$$S(p) = \{b \in \text{Tub}^* \mid \text{the trajectory } (\pi_{\text{pol}})^* \gamma_b \text{ converges to } p \text{ in } Y_{\text{pol}}\}$$

Now fix $q \in \sigma^{-1}(p)$ and $\theta = \arg(q)$. We define the sets

$$S_\theta(p) = \{b \in \text{Tub}_\theta^* \mid \text{the trajectory } (\pi_{\text{pol}})^* \gamma_b \text{ converges to } p \text{ in } Y_{\text{pol},\theta}\}$$

and

$$S(q) = \{b \in \text{Tub}^* \mid \text{the trajectory } (\pi_{\text{pol}}^{\text{ro}})^* \gamma_b \text{ converges to } q \text{ in } Y_{\text{pol},\theta}^{\text{ro}}\}$$

Remark 10.1.2. We describe a few easy properties of the sets defined above. Recall the definition of the total spine S in [Definition 2.2.8](#).

Let $p \in \Sigma_i$. We have the containments,

$$S(q) \subset S_\theta(p) \subset S(p) \subset S.$$

with $\arg(q) = \theta$. Also, by definition

$$S(p) = \bigcup_{q \in \sigma^{-1}(p)} S(q)$$

and

$$S_\theta(p) = \bigcup_{\substack{q \in \sigma^{-1}(p) \\ \arg(q) = \theta}} S(q).$$

Finally observe that $\sigma^{-1}(p)$ is a circle and that there are exactly m_i points $q \in \sigma^{-1}(p)$ with $\arg(q) = \theta$ for each $\theta \in \mathbb{R}/2\pi\mathbb{Z}$.

All the sets in [Definition 10.1.1](#) are contained, by definition, in Tub^* . In the next definition we describe the counterpart of $S(q)$ in $Y_{\text{pol}}^{\text{ro}}$.

Definition 10.1.3. For $q \in \Sigma_{i,\theta}^{\text{ro}}$ we define the set

$$S^{\text{ro}}(q) = \{a \in Y_{\text{pol},\theta}^{\text{ro}} \setminus \partial Y_{\text{pol},\theta}^{\text{ro}} \mid \text{the trajectory } \gamma_a \text{ of } (\pi_{\text{pol}}^{\text{ro}})^* \xi \text{ converges to } q \text{ in } Y_{\text{pol},\theta}^{\text{ro}}\}.$$

Equivalently, $S^{\text{ro}}(q) = (\pi_{\text{pol}}^{\text{ro}})^{-1}(S(q))$. Analogously, we define

$$S^{\text{ro}}(p) = \{a \in Y_{\text{pol}}^{\text{ro}} \setminus \partial Y_{\text{pol}}^{\text{ro}} \mid \text{the trajectory } (\pi_{\text{pol}})^* \gamma_b \text{ converges to } p \text{ in } Y_{\text{pol}}\},$$

or, equivalently, $S^{\text{ro}}(p) = (\pi_{\text{pol}}^{\text{ro}})^{-1}(S(p))$.

Definition 10.1.4. Let U be a given coordinate chart around p as in the previous sections. Recall [Definition 9.1.9](#) of ξ_U^{ro} . We define

$$S_U^{\text{ro}} = \{a \in U^{\text{ro}} \mid \text{the trajectory } \gamma_a \text{ of } \xi_U^{\text{ro}} \text{ converges to a point in } \sigma^{-1}(p)\}.$$

Note that the set S_U^{ro} depends on p . We drop p from the notation to avoid cumbersome formulas but it should be remembered since U is a chart around p . Also note that it follows from the definition that the trajectory γ_a should be completely contained in U^{ro} since it is a trajectory of ξ_U^{ro} .

The main goal of this section is to prove the following proposition. Its proof is relegated to [Section 10.3](#) after enough theory is developed.

Proposition 10.1.5. *The set S_U^{ro} satisfies*

- (1) *It is a submanifold of U^{ro} of real dimension 3 transverse to ∂U^{ro} ,*
- (2) *it contains $\sigma^{-1}(p)$, and*
- (3) *if $q \in \sigma^{-1}(p)$ then the tangent space $T_q S_U^{\text{ro}}$ is the sum of the kernel and the negative eigenspace of $\text{Hess}_q \xi_U^{\text{ro}}$ (eq. (10.2.7)), which is generated by the three vectors*

$$\partial_r + P\partial_s + Q\partial_t, \quad \partial_\alpha, \quad P'\partial_s + Q'\partial_t,$$

where $P + iQ = -\bar{\lambda}_p^{-1} e^{-i\varpi_i \alpha} \overline{\partial_r r^{\tau_i} \xi^{\text{ro},v}(q)}$ and $P' + iQ' = \sqrt{-e^{-i\varpi_i \alpha} \lambda_p}$.

10.2. The Hessian in U^{ro}

In this subsection we compute the Hessian of ξ_U^{ro} along its singular set $\sigma^{-1}(p)$, for some $p \in \Sigma_i$. This Hessian is block-triangular.

Definition 10.2.1. For $\lambda \in \mathbb{C}$, define 2×2 real matrices

$$A(\lambda) = \begin{pmatrix} \text{Re}(\lambda) & -\text{Im}(\lambda) \\ \text{Im}(\lambda) & \text{Re}(\lambda) \end{pmatrix}, \quad \bar{A}(\lambda) = \begin{pmatrix} \text{Re}(\lambda) & \text{Im}(\lambda) \\ \text{Im}(\lambda) & -\text{Re}(\lambda) \end{pmatrix}.$$

Remark 10.2.2. A direct computation yields

$$\bar{A}(\lambda)^{-1} = \frac{1}{|\lambda|^2} \bar{A}(\lambda).$$

Remark 10.2.3. The matrices $A(\lambda)$, $\bar{A}(\lambda)$ describe real linear maps $\mathbb{C} \rightarrow \mathbb{C}$ which are either complex linear or antilinear. If $V \subset \mathbb{C}$ is an open set, and $h : V \rightarrow \mathbb{C}$ is differentiable, then the Jacobian of h is given by the formula

$$(10.2.4) \quad \text{Jac } h(v) = A(\partial_v h(v)) + \bar{A}(\partial_{\bar{v}} h(v)).$$

If $\lambda \neq 0$. Denote by $\sqrt{\lambda}$ a root of λ and by $\sqrt{-\lambda}$ a root of $-\lambda$. Then the matrix $\bar{A}(\lambda)$ has eigenvectors $\sqrt{\lambda}$, with eigenvalue $|\lambda| > 0$, and $\sqrt{-\lambda}$, with eigenvalue $-|\lambda| < 0$. Furthermore, these two eigenspaces are orthogonal with respect to any inner product that is compatible with the complex structure of \mathbb{C} .

The matrix in [eq. \(10.2.4\)](#) is the Jacobian matrix of the function $h : V \rightarrow \mathbb{C}$, where we identify \mathbb{C} with \mathbb{R}^2 as usual. This way, we can consider h as a vector field (recall [Remark 4.3.2](#)). If h vanishes at some point $v \in V$, then this Jacobian matrix is the Hessian matrix of h at v .

Lemma 10.2.5. *Let $V \subset \mathbb{C}$ be an open set, and $h, k : V \rightarrow \mathbb{C}$ differentiable functions. Assume that h is antiholomorphic and has a simple zero at $p \in V$, and that $k(p) \neq 0$. Then the function $k \cdot h$, seen as a vector field on V , has an elementary singularity at p whose Hessian is $\bar{A}(k(p)) \cdot \partial_{\bar{v}}h(p)$.*

PROOF. The lemma follows from [Remark 10.2.3](#), since

$$\begin{aligned}\partial_v(h \cdot k)(p) &= \partial_v h(p) \cdot k(p) + h(p) \cdot \partial_v k(p) = 0, \\ \partial_{\bar{v}}(h \cdot k)(p) &= \partial_{\bar{v}} h(p) \cdot k(p) + h(p) \cdot \partial_{\bar{v}} k(p) = k(p) \cdot \partial_{\bar{v}} h(p).\end{aligned}$$

□

In this subsection we use real coordinates r, α, s, t for U^{ro} with r, α (the pullback of) polar coordinates for u and $s + it = v$, and u, v coordinates in U .

Lemma 10.2.6. *There exists a $\lambda_p \in \mathbb{C}^*$ so that if $q \in \sigma^{-1}(p)$, and we set $\alpha = \arg(u)(q)$. Then, the matrix $\text{Hess}_q \xi_U^{\text{ro}}$ expressed in 2×2 blocks with respect to the coordinates r, α, s, t , is*

$$(10.2.7) \quad \text{Hess}_q \xi_U^{\text{ro}} = \begin{pmatrix} 0 & 0 \\ (\partial_r \text{Re}(r^{\tau_i} \xi_U^{\text{ro},v}))|_q & 0 \\ (\partial_r \text{Im}(r^{\tau_i} \xi_U^{\text{ro},v}))|_q & 0 \end{pmatrix} \bar{A}(e^{-i\varpi_i \alpha} \lambda_p).$$

PROOF. We split the proof into three parts.

Part 1. In this first part we take care of the first 2 rows of the matrix. In order to show that this 2×4 matrix is null, it is enough to show that both $r^{\tau_i} \xi_U^{\text{ro},r}$ and $r^{\tau_i} \xi_U^{\text{ro},\alpha}$ are divisible by r^2 , that is, in particular they are in the square of the maximal ideal of the local ring at q .

First we take care of $r^{\tau_i} \xi_U^{\text{ro},r}$ which, by [eq. \(9.0.3\)](#), equals $r^{\tau_i} \text{Re}(e^{-i\alpha} \sigma^* \xi^u)$. Now, using [eq. \(9.0.2\)](#) and our choice of coordinates we find that

$$\text{ord}_u(y_v \bar{f}_x) > c_{0,i} + p_i.$$

Because $\text{ord}_u(\bar{f}_x) \geq \text{ord}_u(\bar{f}_y)$ by [5.1.7](#) and $\text{ord}_u(y_v) = c_{1,i} > c_{0,i}$ by [Lemma 3.5.2](#). On another hand, the order of vanishing of the denominator is

$$\text{ord}_u(\det \text{Jac } \pi_{\text{pol}} \bar{f}) = c_{0,i} + c_{1,i} - 1 + m_i.$$

Finally, taking into account the factor r^{τ_i} , we estimate

$$\begin{aligned}\text{ord}_r(r^{\tau_i} \xi_U^{\text{ro},r}) &= \tau_i + \text{ord}_r(y_v \bar{f}_x) - c_{0,i} - c_{1,i} + 1 - m_i \\ &> c_{1,i} + m_i - p_i + c_{0,i} + p_i - c_{0,i} - c_{1,i} + 1 - m_i \\ &= 1.\end{aligned}$$

This implies that $r^{\tau_i} \xi_U^{\text{ro},r}$ vanishes with order at least 2 along the boundary.

Now we take care of $r^{\tau_i} \xi_U^{\text{ro},\alpha}$. The argument for this part is more delicate. Notice that in the expression for $\xi_U^{\text{ro},\alpha}$ in [eq. \(9.0.3\)](#) there is a factor r^{-1} that was not present in the step before. In this case, a similar computation yields only the weaker inequality $\text{ord}_r(r^{\tau_i} \xi_U^{\text{ro},\alpha}) \geq 1$. Next, we are going to argue that this function

actually vanishes with order 2 at q . If the above inequality is strict, there is nothing to prove. Assume otherwise that

$$(10.2.8) \quad \text{ord}_r(r^{\tau_i} \xi^{\text{ro}, \alpha}) = 1.$$

That is equivalent to saying that $\text{ord}_r(r^{\tau_i} \xi^u) = 2$, which in turn, is equivalent to saying that

$$(10.2.9) \quad \text{ord}_r(y_v \bar{f}_x) = c_{0,i} + 1 + p_i.$$

In general we know that $\text{ord}_r(y_v) \geq c_{0,i} + 1$ and $\text{ord}_r(\bar{f}_x) \geq p_i$ so, in order to have eq. (10.2.9), we need these two inequalities to be equalities, that is:

$$c_{1,i} = \text{ord}_r(y_v) = c_{0,i} + 1$$

and

$$\text{ord}_r(\bar{f}_x) = p_i$$

A computation gives (since $u_v = 0$):

$$\begin{pmatrix} f_u \\ f_v \end{pmatrix} = \begin{pmatrix} x_u & y_u \\ 0 & y_v \end{pmatrix} \begin{pmatrix} f_x \\ f_y \end{pmatrix}, \quad \begin{pmatrix} f_x \\ f_y \end{pmatrix} = \frac{1}{x_u y_v} \begin{pmatrix} y_v & -y_u \\ 0 & x_u \end{pmatrix} \begin{pmatrix} f_u \\ f_v \end{pmatrix} = \left(\frac{1}{x_u} f_u - \frac{y_u}{x_u y_v} f_v \right).$$

In particular, we use that $\det \text{Jac } \pi_{\text{pol}} = x_u y_v$, and so

$$(10.2.10) \quad \xi^u = \frac{-y_v \bar{f}_x}{\det \text{Jac } \pi_{\text{pol}} \cdot \bar{f}} = -\frac{1}{|x_u|^2} \cdot \frac{\bar{f}_u}{\bar{f}} + \frac{\bar{y}_u}{|x_u|^2 \bar{y}_v} \cdot \frac{\bar{f}_v}{\bar{f}}.$$

To compute the order of ξ^u , we find first

$$(10.2.11) \quad \text{ord}_r \left(-\frac{1}{|x_u|^2} \cdot \frac{\bar{f}_u}{\bar{f}} \right) = -2c_{0,i} + 1,$$

since $\text{ord}_r x_u = c_{0,i} - 1$, and the logarithmic derivative of f has a simple pole along the zero set of f . Next, we estimate the order of the second term on the right hand side of eq. (10.2.10). Since we assume that $c_{1,i} = c_{0,i} + 1$, we have $i \neq 0$. Indeed, $c_{0,0} = c_{1,0} = 1$, by Lemma 3.3.7. Furthermore, since we assumed $\text{ord}_r f_x = p_i$, we find that $i \notin \mathcal{V}_T$ by Corollary 6.4.17. By Lemma 6.2.3, the vertex i is not invariant, i.e. $\varpi_i > 0$. By Lemma 6.1.3, we have

$$\text{ord}_r f_v > m_i.$$

Since $c_{0,i} < \text{ord}_r y \leq c_{1,i} = c_{0,i} + 1$, we have $\text{ord}_r y = c_{0,i} + 1$, and so $\text{ord}_r y_u = c_{0,i}$. Also, $\text{ord}_r x_u = c_{0,i} - 1$ and $\text{ord}_r y_v = c_{1,i} = c_{0,i} + 1$, and so

$$(10.2.12) \quad \text{ord}_r \left(\frac{\bar{y}_u}{|x_u|^2 \bar{y}_v} \cdot \frac{\bar{f}_v}{\bar{f}} \right) > -2c_{0,i} + 1.$$

By eqs. (10.2.11) and (10.2.12), we find $\text{ord}_r \xi^u = -2c_{0,i} + 1$. This also gives

$$1 = \text{ord}_r(r^{\tau_i} r^{-1} e^{-i\alpha} \xi^u) = c_{0,i} + 1 + m_i - p_i - 1 - 2c_{0,i} + 1 = -\varpi_i + 2,$$

by eq. (10.2.8), and so $\varpi_i = 1$. Similarly,

$$\text{ord}_r \left(r^{\tau_i} r^{-1} e^{-i\alpha} \frac{\bar{y}_u}{|x_u|^2 \bar{y}_v} \cdot \frac{\bar{f}_v}{\bar{f}} \right) > -\varpi_i + 2 = 1,$$

and so the order on the left hand side of the equation right above is ≥ 2 . Similarly,

$$\text{ord}_r \left(-\frac{1}{|x_u|^2} \cdot \frac{\bar{f}_u}{\bar{f}} r^{\tau_i} r^{-1} e^{-i\alpha} \right) = -\varpi_i + 2 = 1,$$

However, we can write

$$\frac{f_u}{f} = \frac{m_i}{u} + g,$$

where g is holomorphic. As a result,

$$r^{\tau_i} r^{-1} e^{-i\alpha} \frac{-1}{|x_u|^2} \cdot \frac{\bar{f}_u}{\bar{f}} = -\frac{r^{\tau_i-2} m_i}{|x_u|^2} - \frac{r^{\tau_i-1} e^{-i\alpha} \bar{g}}{|x_u|^2}.$$

The first term on the right hand side above is real. Therefore,

$$r^{\tau_i} \operatorname{Im} \left(r^{-1} e^{-i\alpha} \frac{-1}{|x_u|^2} \cdot \frac{\bar{f}_u}{\bar{f}} \right) = \operatorname{Im} \left(\frac{r^{\tau_i-1} e^{-i\alpha} \bar{g}}{|x_u|^2} \right).$$

We find

$$\begin{aligned} \operatorname{ord}_r \left(\frac{r^{\tau_i-1} e^{-i\alpha} \bar{g}}{|x_u|^2} \right) &\geq \tau_i - 1 - 2c_{0,i} + 2 \\ &= c_{1,i} + m_i - p_i - 2c_{1,i} + 3 \\ &= -\varpi_i + 3 \\ &= 2. \end{aligned}$$

Part 2. Next, we take care of the lower right block of the Hessian in the statement.

As in [eqs. \(9.0.2\)](#) and [\(9.0.3\)](#), the v -component, i.e. the (s, t) -component of the vector field ξ_U^{ro} is given by the complex function

$$r^{\tau_i} \xi^{\text{ro},v} = r^{\tau_i} (\xi^{\text{ro},s} + i\xi^{\text{ro},t}) = r^{\tau_i} \sigma^* \xi^v = r^{\tau_i} \frac{-y_u \bar{f}_x + x_u \bar{f}_y}{\det \operatorname{Jac} \pi_{\text{pol}} \bar{f}}.$$

We consider the first term of the above expression

$$(10.2.13) \quad r^{\tau_i} \frac{-y_u \bar{f}_x}{\det \operatorname{Jac} \pi_{\text{pol}} \bar{f}},$$

and observe that because $\operatorname{ord}(y_u \bar{f}_x) \geq c_{0,i} + p_i$ and $\operatorname{ord}(\det \operatorname{Jac} \pi_{\text{pol}} \bar{f}) = c_{0,i} + c_{1,i} - 1 + m_i$,

$$\tau_i + \operatorname{ord}(y_u \bar{f}_x) - \operatorname{ord}(\det \operatorname{Jac} \pi_{\text{pol}} \bar{f}) \geq c_{1,i} + m_i - p_i + c_{0,i} + p_i - c_{0,i} - c_{1,i} + 1 - m_i = 1.$$

This means that [eq. \(10.2.13\)](#) is divisible by r and in particular, its partial derivatives with respect to s, t (and even α) vanish at q . Now we consider the second term

$$(10.2.14) \quad r^{\tau_i} \frac{x_u \bar{f}_y}{\det \operatorname{Jac} \pi \bar{f}} = r^{\tau_i} \frac{c_{0,i} u^{c_{0,i}-1} \bar{u}^{p_i} \bar{v}}{\det \operatorname{Jac} \pi \bar{f}}.$$

By taking,

$$\lambda_p = \frac{c_{0,i}}{u^{-\nu_i+1} \det \operatorname{Jac} \pi} \cdot \partial_{\bar{v}} \left(\frac{\bar{u}^{-p_i+m_i} \bar{u}^{p_i} \bar{v}}{\bar{f}} \right) \Big|_{\substack{u=0 \\ v=0}}.$$

and applying [Lemma 10.2.5](#) we get the expression for the lower right block.

Part 3. In this part we compute the 2×2 block under the diagonal.

Observe that the first column is just by the definition of Hessian of a vector field.

Now we take care of the partial derivatives with respect to α . Indeed, to prove that the 2×2 block matrix under the diagonal is as in the statement, we need to show that

$$\partial_\alpha (r^{\tau_i} \xi^{\text{ro},v})|_q = 0.$$

We already showed in Part 2, that ∂_α of eq. (10.2.13) vanishes at q . So we just need justify that

$$\partial_\alpha \left(r^{\tau_i} \frac{x_u \bar{f}_y}{\det \text{Jac } \pi \bar{f}} \right) \Big|_q = 0.$$

but again this is clear since eq. (10.2.14) shows that there is a factor of \bar{v} that vanishes at q . \square

10.3. Center-stable manifolds

In this subsection we prove the central technical result Proposition 10.1.5, using the theory developed in previous subsections. As before, $p \in \Sigma_i$, where $i \neq 0$.

10.3.1. In Lemma 10.2.6, we find that the Hessian of ξ_U^{ro} is a block triangular matrix. Using the following coordinates in U^{ro}

$$r' = r, \quad \alpha' = \alpha, \quad v' = v - r\partial_r(r^{\tau_i}\xi^{\text{ro},v}),$$

the Hessian of ξ_U^{ro} is the block diagonal matrix

$$\begin{pmatrix} 0 & 0 \\ 0 & \bar{A}(e^{-i\varpi_i \alpha'} \lambda_p) \end{pmatrix}.$$

In order to get a diagonal Hessian, we must take a double cover of U^{ro} . Define \tilde{U}^{ro} by a Cartesian diagram

$$\begin{array}{ccc} \tilde{U}^{\text{ro}} & \xrightarrow{\tilde{\alpha}} & \mathbb{R}/4\pi\mathbb{Z} \\ c \downarrow & & \downarrow 2:1 \\ U^{\text{ro}} & \xrightarrow{\alpha'} & \mathbb{R}/2\pi\mathbb{Z} \end{array}$$

where the vertical arrow on the right is the natural double cover of $\mathbb{R}/2\pi\mathbb{Z}$, inducing a double cover $c : \tilde{U}^{\text{ro}} \rightarrow U^{\text{ro}}$. Define

$$\tilde{\Sigma}_p^{\text{ro}} = c^{-1}(\sigma^{-1}(p)) \simeq \mathbb{R}/4\pi\mathbb{Z}.$$

Along with $\tilde{\alpha}$, we define coordinates

$$\tilde{r} = c^*(r'), \quad \tilde{v} = e^{-i\varpi_i \tilde{\alpha}'/2} \nu_p c^*(v'),$$

where ν_p is a fixed square root of λ_p , i.e. $\nu_p^2 = \lambda_p$. Let $\tilde{\xi}_U^{\text{ro}}$ be the pullback of ξ_U^{ro} to \tilde{U}^{ro} . At a point $\tilde{q} \in \tilde{\Sigma}_p^{\text{ro}}$, in the coordinates \tilde{r} , $\tilde{\alpha}$ and $\tilde{v} = \tilde{s} + i\tilde{t}$, this vector field has Hessian

$$(10.3.2) \quad \text{Hess}_{\tilde{q}} \tilde{\xi}_U^{\text{ro}} = \begin{pmatrix} 0 & 0 \\ 0 & |\lambda_p| & 0 \\ 0 & 0 & -|\lambda_p| \end{pmatrix}.$$

Thus, the system of ordinary differential equations corresponding to the vector field $\tilde{\xi}_U^{\text{ro}}$ is

$$(10.3.3) \quad \begin{aligned} \dot{\tilde{r}} &= R(\tilde{r}, \tilde{\alpha}, \tilde{s}, \tilde{t}), \\ \dot{\tilde{\alpha}} &= A(\tilde{r}, \tilde{\alpha}, \tilde{s}, \tilde{t}), \\ \dot{\tilde{s}} &= |\lambda_p| \tilde{s} + S(\tilde{r}, \tilde{\alpha}, \tilde{s}, \tilde{t}), \\ \dot{\tilde{t}} &= -|\lambda_p| \tilde{t} + T(\tilde{r}, \tilde{\alpha}, \tilde{s}, \tilde{t}), \end{aligned}$$

where the functions R, A, S, T are real analytic, vanish along $\tilde{\Sigma}_p^{\text{ro}}$, and their partials with respect to $\tilde{r}, \tilde{s}, \tilde{t}$ also vanish along $\tilde{\Sigma}_p^{\text{ro}}$.

We can assume that \hat{U}^{ro} is of the form

$$\hat{U}^{\text{ro}} = [0, \eta_r] \times \mathbb{R}/4\pi\mathbb{Z} \times [-\eta_v, \eta_v]^2.$$

where η_r and η_v are small. Set

$$(10.3.4) \quad \hat{U}^{\text{ro}} = [-\eta_r, \eta_r] \times \mathbb{R}/4\pi\mathbb{Z} \times [-\eta_v, \eta_v]^2.$$

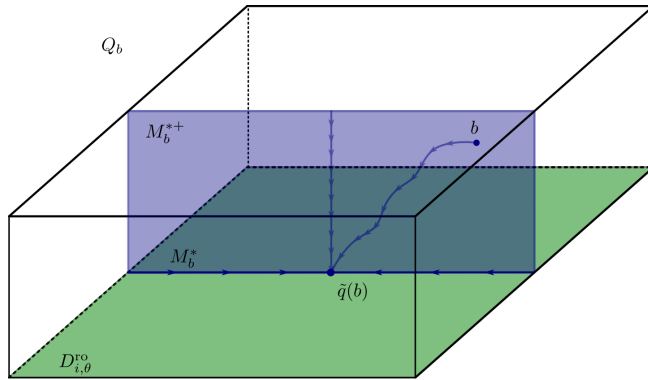


FIGURE 10.3.5. The space Q_b . In light blue we see M_b^{*+} containing the point b and intersecting transversely $D_{i,\theta}^{\text{ro}}$. The manifold M_b^* consists of two trajectories on $D_{i,\theta}^{\text{ro}}$ converging to the point $\tilde{q}(b)$.

We consider the system eq. (10.3.3) in \hat{U}^{ro} . Therefore, this is a system in one *periodic variable* $\tilde{\alpha}$ (by *periodic* here we mean that $\tilde{\alpha} \in \mathbb{R}/4\pi\mathbb{Z}$), and three real variables, where \tilde{r} takes negative values as well. By [Kel67b, Theorem 1], this system has a *center-stable manifold* $M^{*+} \subset \hat{U}^{\text{ro}}$. This means that, assuming that η_r and η_v are chosen small enough, M^{*+} is a manifold which is invariant by the vector field $\tilde{\xi}_U^{\text{ro}}$, and there exists a \mathcal{C}^∞ function \hat{w}^{*+} in the variables $\tilde{\alpha}, \tilde{t}, \tilde{r}$, so that

$$M^{*+} = \left\{ (\tilde{r}, \tilde{\alpha}, \tilde{s}, \tilde{t}) \in \hat{U}^{\text{ro}} \mid \tilde{s} = \hat{w}^{*+}(\tilde{\alpha}, \tilde{t}, \tilde{r}) \right\}.$$

and \hat{w}^{*+} and its derivatives with respect to \tilde{t}, \tilde{r} vanish when \tilde{r}, \tilde{t} are zero. Similarly, the system eq. (10.3.3) has a *center manifold*

$$M^* = \left\{ (\tilde{r}, \tilde{\alpha}, \tilde{s}, \tilde{t}) \in \hat{U}^{\text{ro}} \mid \tilde{s} = \hat{w}^*(\tilde{\alpha}, \tilde{r}), \tilde{t} = \hat{u}^*(\tilde{\alpha}, \tilde{r}) \right\}.$$

where \hat{w}^*, \hat{u}^* and their first partials with respect to \tilde{r} vanish along $\tilde{\Sigma}_p^{\text{ro}}$.

10.3.6. Let $b \in \tilde{U}^{\text{ro}}$, and let $\theta = \arg(f)(c(b))$. Then, the set $c^{-1}(\arg(f)^{-1}(\theta))$ has $2m_i$ connected components. Denote by Q_b the connected component which contains b . Then Q_b has coordinates $\tilde{r}, \tilde{s}, \tilde{t}$, and

$$Q_b \simeq [0, \eta_r] \times [-\eta_v, \eta_v]^2.$$

We define

$$(10.3.7) \quad \tilde{q}(b) \in Q_b$$

as the origin in this coordinate system, i.e., the unique point of Q_b that maps to p by $\sigma \circ c$. The restriction of $\tilde{\alpha}$ to Q_b is a function in the variables $\tilde{r}, \tilde{s}, \tilde{t}$. Since ξ_U^{ro} is tangent to Y_θ^{ro} , the system eq. (10.3.3) reduces to a system in three variables

$$(10.3.8) \quad \begin{aligned} \dot{\tilde{r}} &= R(\tilde{r}, \tilde{\alpha}(\tilde{r}, \tilde{s}, \tilde{t}), \tilde{s}, \tilde{t}), \\ \dot{\tilde{s}} &= |\lambda_p| \tilde{s} + S(\tilde{r}, \tilde{\alpha}(\tilde{r}, \tilde{s}, \tilde{t}), \tilde{s}, \tilde{t}), \\ \dot{\tilde{t}} &= -|\lambda_p| \tilde{t} + T(\tilde{r}, \tilde{\alpha}(\tilde{r}, \tilde{s}, \tilde{t}), \tilde{s}, \tilde{t}), \end{aligned}$$

This system has center-stable and center manifolds

$$M_b^{*+} = M^{*+} \cap Q_b, \quad M_b^* = M^* \cap Q_b.$$

Note that $\dim M_b^{*+} = 2$ and $\dim M_b^* = 1$. In particular, M_b^* consists of two trajectories, and one point.

Define $\tilde{S}_U^{\text{ro}} = M^{*+} \cap \tilde{U}^{\text{ro}}$. Then

$$(10.3.9) \quad \tilde{S}_U^{\text{ro}} = \left\{ (\tilde{r}, \tilde{\alpha}, \tilde{s}, \tilde{t}) \in \tilde{U}^{\text{ro}} \mid \tilde{s} = \tilde{w}^{*+}(\tilde{\alpha}, \tilde{r}, \tilde{t}) \right\},$$

where \tilde{w}^{*+} is the restriction of \hat{w}^{*+} . Moreover, the properties satisfied by M^{*+} imply the following lemma.

Lemma 10.3.10. *The following properties for \tilde{S}_U^{ro} hold:*

- (1) ξ_U^{ro} is tangent to \tilde{S}_U^{ro} ,
- (2) $\tilde{\Sigma}_p^{\text{ro}} \subset \tilde{S}_U^{\text{ro}}$,
- (3) for $\tilde{q} \in \tilde{\Sigma}_p^{\text{ro}}$, we have $T_{\tilde{q}} \tilde{S}_U^{\text{ro}} = \mathbb{R} \langle \partial_{\tilde{r}}, \partial_{\tilde{\alpha}}, \partial_{\tilde{t}} \rangle$. In other words, the $T_{\tilde{q}} \tilde{S}_U^{\text{ro}}$ is the sum of the kernel and the negative eigenspace of $\text{Hess}_{\tilde{q}} \xi_U^{\text{ro}}$ (see eq. (10.3.2)).

In particular, \tilde{S}_U^{ro} is transverse to $\partial \tilde{U}^{\text{ro}}$. For $b \in \tilde{U}^{\text{ro}}$, define also

$$\tilde{S}_{U,b}^{\text{ro}} = \tilde{S}_U^{\text{ro}} \cap Q_b.$$

The functions \tilde{r} and \tilde{t} are coordinates on $\tilde{S}_{U,b}^{\text{ro}}$ so that $\tilde{S}_{U,b}^{\text{ro}} \simeq [0, \eta_r] \times [-\eta_v, \eta_v]$.

PROOF. Property 1 follows from the fact that M^{*+} is an invariant manifold. Property 2 follows since \tilde{w}^{*+} vanishes along the α axis, i.e. when \tilde{r} and \tilde{t} vanish. Finally, 3 follows in the same way from the definition of a center-stable manifold, i.e. the vanishing of partials of \tilde{w}^{*+} . These properties of \tilde{w}^{*+} and the vanishing of its partials are also part of the statement of [Kel67b, Theorem 1]. \square

Lemma 10.3.11. *Assuming U is chosen small enough, then we have the following properties*

- (1) If $b \in \tilde{S}_U^{\text{ro}}$, then γ_b converges to $\tilde{q}(b)$.
- (2) If $b \in \tilde{U}^{\text{ro}} \setminus \tilde{S}_U^{\text{ro}}$, then γ_b exits \tilde{U}^{ro} .

PROOF. In this proof, we make a coordinate change, replacing \tilde{s} by $\tilde{s} - \hat{w}^{*+}(\tilde{r}, \tilde{\alpha}, \tilde{t})$ and \tilde{t} by $\tilde{t} - \hat{u}^*(\tilde{r}, \tilde{\alpha})$. Thus, the center-stable and center manifolds M^{*+} and M^* are coordinate subspaces. Similarly, if we fix a point $b \in \tilde{U}^{\text{ro}}$, then M_b^{*+} and M_b^* are coordinate subspaces in Q_b . We assume that \hat{U}^{ro} has the form eq. (10.3.4) in these new coordinates.

Assume first that $b \in \tilde{S}_U^{\text{ro}}$. Name the boundary pieces of $\tilde{S}_{U,b}^{\text{ro}}$ as follows:

$$\begin{aligned}\partial_0 \tilde{S}_{U,b}^{\text{ro}} &= \{0\} \times [-\eta_v, \eta_v], \\ \partial_r \tilde{S}_{U,b}^{\text{ro}} &= \{\eta_r\} \times [-\eta_v, \eta_v], \\ \partial_t \tilde{S}_{U,b}^{\text{ro}} &= [0, \eta_r] \times \{-\eta_v, \eta_v\}.\end{aligned}$$

The set $M_q^* \cap \tilde{U}^{\text{ro}}$ consists of a single trajectory and the point $\tilde{q}(b)$. The trajectory must be oriented towards $\tilde{q}(b)$, since no trajectory of ξ in \mathbb{C}^2 emanates from the origin. Therefore, there exists a neighborhood of the point $(\eta_r, 0)$ in $\partial_r \tilde{S}_{U,b}^{\text{ro}}$, where $\tilde{\xi}_U^{\text{ro}}$ points inwards. Fixing η_r and taking η_v small enough, we can assume that $\tilde{\xi}_U^{\text{ro}}$ points inwards along all of $\partial_r \tilde{S}_{U,b}^{\text{ro}}$.

We have

$$\frac{\partial}{\partial \tilde{t}} \dot{\tilde{t}}(\tilde{q}(b)) = -|\lambda_p| < 0.$$

Therefore, we can assume that

$$(10.3.12) \quad \frac{\partial}{\partial \tilde{t}} \dot{\tilde{t}} < 0$$

on $\tilde{S}_{U,b}^{\text{ro}}$. Furthermore, $\dot{\tilde{t}}|_{\tilde{S}_{U,b}^{\text{ro}}}$ vanishes precisely along $M_b^* \cap \tilde{U}^{\text{ro}}$. This implies that \tilde{t} and $\dot{\tilde{t}}$ have opposite signs on $\tilde{S}_{U,b}^{\text{ro}}$. As a result, $|\tilde{t}|$ decreases along the trajectory γ_b . Therefore, $|\tilde{t}|$ has a limit along γ_b , call it \tilde{t}_0 .

It also follows from eq. (10.3.12) that the vector field $\tilde{\xi}_U^{\text{ro}}$ restricted to $\tilde{S}_{U,b}^{\text{ro}}$ points inwards along $\partial_t \tilde{S}_{U,b}^{\text{ro}}$. As a result, a trajectory of $\tilde{\xi}_U^{\text{ro}}$ which starts at $b \in \tilde{S}_U^{\text{ro}}$ does not escape from $\tilde{S}_{U,b}^{\text{ro}}$. Since $\tilde{S}_{U,b}^{\text{ro}}$ is compact, γ_b is well defined on the whole nonnegative real axis.

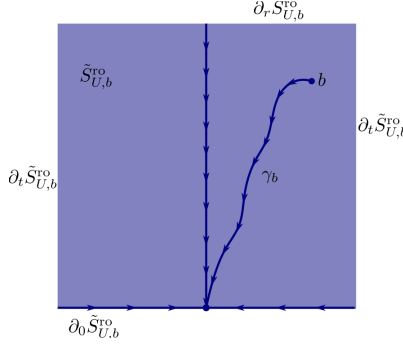
The function $c^*(\pi^{\text{ro}})^*|f|$ has the same vanishing set as \tilde{r} on $\tilde{S}_{U,b}^{\text{ro}}$, that is, $\partial_0 \tilde{S}_{U,b}^{\text{ro}}$. Furthermore, the limit of $c^*(\pi^{\text{ro}})^*|f|$ along γ_b is zero. Therefore, \tilde{r} has limit zero along γ_b , and so, in coordinates \tilde{r}, \tilde{t} in $\tilde{S}_{U,b}^{\text{ro}}$, γ_b converges to $(0, \tilde{t}_0)$. Since $\tilde{\xi}_U^{\text{ro}}$ does not vanish at $(0, \tilde{t}_0)$ unless $\tilde{t}_0 = 0$, we have $\tilde{t}_0 = 0$, and so γ_b converges to $\tilde{q}(b) = (0, 0)$, which concludes the proof of 1.

Next, we prove 2. Assume that $b \in \tilde{U}^{\text{ro}} \setminus \tilde{S}_U^{\text{ro}}$. Similarly as above, we can assume that

$$(10.3.13) \quad \frac{\partial}{\partial \tilde{s}} \dot{\tilde{s}} > 0$$

in Q_b . Therefore, the absolute value of the \tilde{s} coordinate of the trajectory γ_b increases. Therefore, γ_b escapes \tilde{U}^{ro} . \square

Corollary 10.3.15. *The function \tilde{w}^{*+} is the only function in variables $\tilde{\alpha}, \tilde{t}$ and $\tilde{r} \geq 0$, which vanishes together with its partials along $\tilde{t} = \tilde{r} = 0$, whose graph as in eq. (10.3.9) is an invariant submanifold.*

FIGURE 10.3.14. We see $S_{U,b}^{\text{ro}}$ containing a trajectory γ_b .

PROOF. If w is another such function, and $b = (\tilde{r}, \tilde{\alpha}, \tilde{t}, w(\tilde{r}, \tilde{\alpha}, \tilde{t}))$, then, by the proof of 1, the trajectory γ_b converges to $\tilde{q}(b)$. But by 2, it diverges. \square

Corollary 10.3.16. *The set $\tilde{S}_U^{\text{ro}} \subset \tilde{U}^{\text{ro}}$ is invariant under the Galois transformation of the covering map c .*

PROOF. Let ι be the Galois transformation. Then, $\tilde{w}^{*+} \circ \iota$ satisfies the conditions in the previous corollary, and so $\tilde{w}^{*+} = \tilde{w}^{*+} \circ \iota$. \square

Remark 10.3.17. The unicity statement [Corollary 10.3.15](#) may only apply to \tilde{S}_U^{ro} , the graph of \tilde{w}^{*+} , and not the whole center-stable submanifold M^{*+} , the graph of \hat{w}^{*+} .

Corollary 10.3.18. *We have the following equality of sets*

$$S_U^{\text{ro}} = c(\tilde{S}_U^{\text{ro}}).$$

Furthermore, the following properties are satisfied

- (1) ξ_U^{ro} is tangent to S_U^{ro} ,
- (2) $\sigma^{-1}(p) \subset S_U^{\text{ro}}$,
- (3) for $q \in \sigma^{-1}(p)$, and $\tilde{q} \in c^{-1}(q)$, we have $T_q S_U^{\text{ro}} = D_{\tilde{q}} c(T_{\tilde{q}} \tilde{S}_U)$.

PROOF. The first statement follows from [Lemma 10.3.11](#) and [Corollary 10.3.16](#). The three properties follow from [Lemma 10.3.10](#). \square

PROOF OF [PROPOSITION 10.1.5](#). The three properties follow from the results [Corollary 10.3.18](#) and [Lemma 10.3.10, 3](#). That the three vectors are like [Proposition 10.1.5, 3](#) is a direct computation using the previously cited results. Below you can find this direct (but tedious) computation. \square

DIRECT COMPUTATION FOR [PROPOSITION 10.1.5, 3](#). As established by the application of center-stable manifold theory in [Lemma 10.3.10, \(3\)](#) and [Corollary 10.3.18](#), the tangent space $T_q S_U^{\text{ro}}$ is the center-stable eigenspace of the linearized vector field ξ_U^{ro} at the singular point q . This space is spanned by the generalized eigenvectors of the Hessian matrix, $L = \text{Hess}_q \xi_U^{\text{ro}}$, corresponding to eigenvalues with non-positive real part. We compute this basis explicitly.

From eq. (10.2.7), the Hessian at q in coordinates (r, α, s, t) is the block lower-triangular matrix:

$$L = \text{Hess}_q \xi_U^{\text{ro}} = \begin{pmatrix} \mathbf{0}_{2 \times 2} & \mathbf{0}_{2 \times 2} \\ M_{bl} & M_{br} \end{pmatrix}$$

where the blocks are defined as follows:

- $M_{br} = \bar{A}(k)$, where $k = e^{-i\varpi_i \alpha} \lambda_p$. This is the Hessian of the $\xi^{\text{ro},v}$ component with respect to $v = s + it$.
- M_{bl} is a 2×2 matrix describing the partials of $\xi^{\text{ro},v}$ with respect to (r, α) . Its second column is zero, and its first column is the vector representation of $D = \partial_r(r^{\tau_i} \xi^{\text{ro},v})|_q$.

The eigenvalues of L are the eigenvalues of its diagonal blocks, which are 0 (with multiplicity 2) from the top-left block, and $\pm|k| = \pm|\lambda_p|$ from the bottom-right block. The center-stable eigenspace corresponds to the eigenvalues 0, 0, and $-|\lambda_p|$. We now compute the basis for this space.

Stable Eigenvector ($\lambda = -|\lambda_p|$). We seek an eigenvector $V = (V_r, V_\alpha, V_s, V_t)^\top$ such that $LV = -|\lambda_p|V$. The equation for the first two components is $\mathbf{0}_{2 \times 2} \begin{pmatrix} V_r \\ V_\alpha \end{pmatrix} = -|\lambda_p| \begin{pmatrix} V_r \\ V_\alpha \end{pmatrix}$, which implies $V_r = V_\alpha = 0$. The equation for the last two components is $M_{br} \begin{pmatrix} V_s \\ V_t \end{pmatrix} = -|\lambda_p| \begin{pmatrix} V_s \\ V_t \end{pmatrix}$. This identifies (V_s, V_t) as the eigenvector of $M_{br} = \bar{A}(k)$ for the eigenvalue $-|\lambda_p| = -|k|$. In complex notation, this eigenvector is a multiple of $\sqrt{-k}$.

$$\sqrt{-k} = \sqrt{-e^{-i\varpi_i \alpha} \lambda_p} = i\sqrt{e^{-i\varpi_i \alpha} \lambda_p} = ie^{-i\varpi_i \alpha/2} \nu_p, \quad \text{where } \nu_p^2 = \lambda_p.$$

This matches the definition of $P' + iQ'$ in the proposition. The corresponding basis vector is $(0, 0, P', Q')^\top$, which is:

$$\mathbf{V}_3 = P' \partial_s + Q' \partial_t.$$

Center Eigenvectors ($\lambda = 0$). We seek generalized eigenvectors for the eigenvalue 0, i.e., vectors V in the kernel of L . The equation is $LV = \mathbf{0}$. The component-wise equations are:

- (1) $\mathbf{0}_{2 \times 2} \begin{pmatrix} V_r \\ V_\alpha \end{pmatrix} = \mathbf{0}$, which is trivially satisfied.
- (2) $M_{bl} \begin{pmatrix} V_r \\ V_\alpha \end{pmatrix} + M_{br} \begin{pmatrix} V_s \\ V_t \end{pmatrix} = \mathbf{0}$.

We find a basis for the two-dimensional solution space.

- **First center vector:** Choose $(V_r, V_\alpha) = (0, 1)$. The second equation becomes $M_{br} \begin{pmatrix} V_s \\ V_t \end{pmatrix} = \mathbf{0}$. Since M_{br} is invertible ($|\lambda_p| \neq 0$), this implies $V_s = V_t = 0$. The resulting eigenvector is $(0, 1, 0, 0)^\top$:

$$\mathbf{V}_2 = \partial_\alpha.$$

- **Second center vector:** Choose $(V_r, V_\alpha) = (1, 0)$. The second equation becomes $M_{br} \begin{pmatrix} V_s \\ V_t \end{pmatrix} = -M_{bl} \begin{pmatrix} 1 \\ 0 \end{pmatrix}$. In complex notation, this is $k \cdot \overline{(V_s + iV_t)} = -D$. We solve for $V_s + iV_t$:

$$\overline{V_s + iV_t} = -k^{-1}D \implies V_s + iV_t = -\overline{k^{-1}D}.$$

We compute the coefficient $\overline{k^{-1}}$:

$$\overline{k^{-1}} = \frac{1}{\bar{k}} = \frac{k}{|k|^2} = \frac{e^{-i\varpi_i \alpha} \lambda_p}{|\lambda_p|^2} = e^{-i\varpi_i \alpha} \frac{\lambda_p}{|\lambda_p|^2} = e^{-i\varpi_i \alpha} (\bar{\lambda}_p)^{-1}.$$

Thus, the complex number representing the (s, t) components of the eigenvector is

$$P + iQ = V_s + iV_t = -e^{-i\varpi_i \alpha} (\bar{\lambda}_p)^{-1} \bar{D},$$

which is precisely the formula given in the proposition. The eigenvector is $(1, 0, P, Q)^\top$:

$$\mathbf{V}_1 = \partial_r + P\partial_s + Q\partial_t.$$

The three vectors $\mathbf{V}_1, \mathbf{V}_2, \mathbf{V}_3$ form a basis for the center-stable eigenspace, which is tangent to S_U^{ro} at q . \square

Remark 10.3.19. It follows from construction that the restriction of the Galois transformation ι to \tilde{S}_U^{ro} either respects or reverses orientation, depending on whether ϖ_i is even or odd. Since \tilde{S}_U^{ro} is a solid torus, the quotient by ι is a solid torus if ϖ_i is even, and a solid Klein bottle if ϖ_i is odd.

CHAPTER 11

The Total Spine of the Milnor Fibration

11.1. Broken trajectories

11.1.1. Construct a C^∞ real function $\psi : Y_{\text{pol}} \rightarrow \mathbb{R}_{\geq 0}$ as follows. If $p \in D = \pi_{\text{pol}}^{-1}(0)$, take a chart U containing p with coordinates u, v . Let $i, j \in \mathcal{W}$, in particular i or j might be an arrowhead. If $p \in D_i^\circ$ assume that $D \cap U = D_i \cap U = \{u = 0\}$. Otherwise, if $p \in D_i \cap D_j$ is an intersection point, assume that $U \cap D = U \cap (D_i \cup D_j)$ and that $D_i \cap U = \{u = 0\}$ and $D_j \cap U = \{v = 0\}$. If $i \in \mathcal{A}$, that is, if i is an arrowhead, set $\tau_i = 2$ (as in [Lemma 8.3.2](#)). In the former case set $\psi_U = |u|^{\tau_i}$ and in the latter $\psi_U = |u|^{\tau_i} |v|^{\tau_j}$. Set

$$\psi = \sum_U \chi_U \psi_U$$

where $\{\chi_U\}$ is a partition of unity subordinate to some finite open cover by charts U .

Definition 11.1.2. The vector field $\xi_{\text{pol}}^{\text{ro}}$ is the unique continuous extension over all $Y_{\text{pol}}^{\text{ro}}$ of the vector field

$$\sigma^* \psi \cdot (\pi_{\text{pol}}^{\text{ro}})^* \xi.$$

Remark 11.1.3. By construction,

- (1) the vector field $\xi_{\text{pol}}^{\text{ro}}|_{U^{\text{ro}}}$ coincides with the vector field ξ_U^{ro} (see [Definitions 8.0.11](#) and [9.1.9](#)) on U^{ro} up to multiplication by a positive real function $U^{\text{ro}} \rightarrow \mathbb{R}_{>0}$, and
- (2) the vector field $\xi_{\text{pol}}^{\text{ro}}|_{D_{i,\theta}^{\text{ro},\circ}}$ coincides, up to a positive real factor, with the vector field $\xi_{i,\theta}^{\text{ro}}$.

Definition 11.1.4. For $\theta \in \mathbb{R}/2\pi\mathbb{Z}$, set

$$\Sigma = \bigcup_{i \in \mathcal{V}} \Sigma_i, \quad \Sigma_\theta^{\text{ro}} = \bigcup_{i \in \mathcal{V}} \Sigma_{i,\theta}^{\text{ro}}.$$

Definition 11.1.5. A *broken trajectory* γ in $D_{\text{pol}} = (\pi_{\text{pol}}^{\text{ro}})^{-1}(0)$ a family of trajectories $\{\gamma_k\}_{k \in I}$ of the vector field $\xi_{\text{pol}}^{\text{ro}}$ in D_{pol} , satisfying

$$\lim_{t \rightarrow +\infty} \gamma_k(t) = \lim_{t \rightarrow -\infty} \gamma_{k+1}(t), \quad k \in I.$$

If $|I| = n < \infty$ we say that the broken trajectory has length n .

Remark 11.1.6.

- (1) The fact that $\xi_{\text{pol}}^{\text{ro}}$ is tangent to $Y_{\text{pol},\theta}^{\text{ro}}$ ([Remark 2.1.6 \(iii\)](#)) implies that there exists a $\theta \in \mathbb{R}/2\pi\mathbb{Z}$ such that all parts γ_i of a broken trajectory are contained in $Y_{\text{pol},\theta}^{\text{ro}}$.
- (2) The definition allows for parts γ_k of a broken trajectory γ to be included in the connecting parts $D_{i,j,\theta}^{\text{ro}}$. Observe that this might only happen when

the edge ij is non-invariant, that is, when at least one of ϖ_i or ϖ_j is non-zero. Indeed, if ij is invariant, then the restriction of $\xi_{\text{pol}}^{\text{ro}}$ to $D_{ij}^{\text{ro},\circ}$ is identically zero, see 8.1.3.

A broken trajectory γ defines a path in the graph Γ_{pol} . Here we understand a path in the following sense: a sequence of vertices (it is not necessary to specify the edges since Γ_{pol} is a tree). The path is defined by a sequence of vertices i_k and edges e_k , with $k = 1, \dots, n$ where $i_k \in \mathcal{V}$ appears in the sequence if $\gamma_k \subset D_{i_k,\theta}^{\text{ro},\circ}$ and $e_k = ij$ appears in the sequence if γ_k is contained in $D_{i,j,\theta}^{\text{ro},\circ}$.

Lemma 11.1.7. *If $\gamma_k \subset D_{i,j,\theta}^{\text{ro},\circ}$, that is, if $e_k = ij$ and $j \rightarrow i$, then $i_{k+1} = j$.*

PROOF. By Remark 11.1.6,2 we know that ij is a non-invariant edge. By fig. 8.2.10 the path γ_k must go from a red vertex to a green vertex on $D_{i,j,\theta}^{\text{ro},\circ}$. But there is a unique trajectory emanating from a green vertex and it is contained in $D_{j,\theta}^{\text{ro},\circ}$. \square

We introduce some notation that is useful for this section and later on.

Notation 11.1.8. Let Γ be the dual graph of some resolution of a plane curve singularity and let Γ' be a subgraph. We denote by $F_\theta^{\text{ro}}[\Gamma']$ the part of the Milnor fiber at radius 0 and angle θ that corresponds to Γ' , that is, if $\mathcal{V}_{\Gamma'} \subset \mathcal{V}$ is the set of vertices of Γ' , then (recall Definition 4.2.1):

$$F_\theta^{\text{ro}}[\Gamma'] = \bigcup_{i \in \mathcal{V}_{\Gamma'}} D_{i,\theta}^{\text{ro}}.$$

Lemma 11.1.9. *A broken trajectory γ can pass through a non-invariant edge ij at most $2\gcd(m_i, m_j)$ times.*

PROOF. Assume that $j \rightarrow i$. We know that $D_{i,j,\theta}^{\text{ro},\circ}$ has $\gcd(m_i, m_j)$ connected components. If γ passes through $D_{i,j,\theta}^{\text{ro},\circ}$ more than $2\gcd(m_i, m_j)$ times, then by the pigeonhole principle, it must pass at least 3 times through the same connected component, let's say $\tilde{D}_{i,j,\theta}^{\text{ro},\circ}$ of $D_{i,j,\theta}^{\text{ro},\circ}$. Let Ξ_j be the branch of Γ_{pol} at the vertex j . Then, since γ' passes at least 3 times through $\tilde{D}_{i,j,\theta}^{\text{ro},\circ}$, there exists a sub-broken trajectory $\gamma' \subset \gamma$ of length n' such that

- (1) γ'_1 starts at $\tilde{D}_{i,j,\theta}^{\text{ro},\circ}$,
- (2) $\gamma'_{n'}$ ends at $\tilde{D}_{i,j,\theta}^{\text{ro},\circ}$
- (3) $\gamma' \subset F_\theta^{\text{ro}}[\Gamma_{\text{pol}} \setminus \Xi_j]$

The last condition means that γ' is contained in parts of the Milnor fiber at radius 0 corresponding to vertices that are closer 0 than j . The fig. 11.1.10 makes it easier to follow this proof.

Let $\Gamma' \subset \Gamma_{\text{pol}}$ be the smallest subgraph such that $F_\theta^{\text{ro}}[\Gamma']$ contains γ' . Observe that Γ' is connected since γ' is connected. The graph Γ is a directed tree naturally rooted at 0, so Γ' is also a directed tree rooted at some vertex k which minimizes the distance to 0 among all vertices in $\mathcal{V}_{\Gamma'}$. By definition of Γ' , we have that $D_{k,\theta}^{\text{ro}}$ contains a part of γ' and moreover, there is at least a boundary component of $D_{k,\theta}^{\text{ro}}$ that γ' intersects twice since γ' must return to $\tilde{D}_{i,j,\theta}^{\text{ro},\circ}$.

Now, for each $\ell \in \mathcal{V}_{\Gamma'}$ such that $k\ell$ is an edge of Γ' with $k \rightarrow \ell$, we contract each of the boundary components of $D_{k,\theta}^{\text{ro}}$ contained in $D_{k,\ell,\theta}^{\text{ro}}$ to a point. We obtain a compact surface $\widehat{D_{k,\theta}^{\text{ro}}}$. The image of γ' in this quotient surface must consist of

some loops. But, by Lemma 9.3.3 (if $k \neq 0$) or by Lemma 7.4.4 (if $v_i = 0$), the vector field $\xi_{k,\theta}^{\text{ro}}$ admits a potential that takes constant values on all the contracted boundary components (so the potential is equivariant under the quotient and yields a potential in $\widehat{D}_{k,\theta}^{\text{ro}}$) and it is impossible to have loops formed by integral lines of potentials. \square

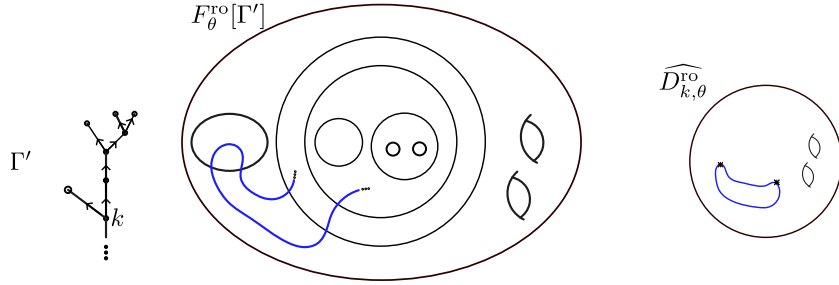


FIGURE 11.1.10. On the left hand side we see the surface $F_\theta^{\text{ro}}[\Gamma']$. On the right hand side, we see the surface $\widehat{D}_{k,\theta}^{\text{ro}}$ after contracting two boundary components of $D_{k,\theta}^{\text{ro}}$.

Lemma 11.1.11. *There exists a number $M = M(\Gamma_{\text{pol}}, (\pi^* f)) \in \mathbb{Z}_{>0}$ which only depends on the graph Γ_{pol} and the multiplicities of the total transform of f , so that all continuous broken trajectories in Y_{pol} have length $\leq M$.*

PROOF. The dynamics of $\xi_{\text{pol}}^{\text{ro}}$ near $D_{i,j,\theta}^{\text{ro}}$ for ij an invariant edge (fig. 8.1.11) and the fact that Γ is a tree, imply that a broken trajectory can pass at most once through a invariant edge. By Lemma 11.1.9, a broken trajectory can pass at most $2 \gcd(m_i, m_j)$ times through a non-invariant edge. Also, by the dynamics of $\xi_{\text{pol}}^{\text{ro}}$ near the corner parts (Fig. 8.1.11 and 8.2.10) and by Lemma 11.1.7, two consecutive vertices v_k, v_{k+1} of the path defined by a broken trajectory cannot be on the same connected component $D_{i,\theta}^{\text{ro},\circ}$. The result follows by the finiteness of Γ . \square

11.2. The total spine

So far, we have described certain families of trajectories of ξ which converge to the origin in \mathbb{C}^2 , i.e. that are contained in the total spine S , Definition 2.2.8. These are the stable (for $i = 0$) and center stable (for $i \neq 0$) manifolds $S(p)$, for $p \in \Sigma_i$, constructed in Chapter 7 and Section 10.3. In this section, we show that this is the whole total spine.

Theorem 11.2.1. *The total spine admits a finite partition*

$$(11.2.2) \quad S = \{0\} \sqcup \bigsqcup_{p \in \Sigma} S(p),$$

- If $p \in \Sigma_0$ is a repeller then $S(p) \setminus f^{-1}(S_\eta^1)$ is an open punctured disk.
- If $p \in \Sigma_0$ is a saddle point, then $S(p) \setminus f^{-1}(S_\eta^1)$ is an open solid torus.
- If $p \in \Sigma_i$ with $i \neq 0$, then $S(p) \setminus f^{-1}(S_\eta^1)$ is an open solid torus if ϖ_i is even, and an open solid Klein bottle if ϖ_i is odd.

PROOF. Let $\gamma \subset \text{Tub}^*$ be a trajectory of the vector field ξ which converges to the origin, and assume that γ is not contained in a (center) stable manifold $S(p)$, $p \in \Sigma$. Then γ lifts to a trajectory γ_{pol} of ξ_{pol} in Y_{pol} , and to a trajectory $\gamma_{\text{pol}}^{\text{ro}}$ of $\xi_{\text{pol}}^{\text{ro}}$ in $Y_{\text{pol}}^{\text{ro}}$. Denote by A_{pol} and $A_{\text{pol}}^{\text{ro}}$ the accumulation sets of γ_{pol} and $\gamma_{\text{pol}}^{\text{ro}}$. Since σ is a proper map, we have $A_{\text{pol}} = \sigma(A_{\text{pol}}^{\text{ro}})$. Furthermore, the set $A_{\text{pol}}^{\text{ro}}$ is invariant under the flow of $\xi_{\text{pol}}^{\text{ro}}$.

Claim: If $p \in A_{\text{pol}}^{\text{ro}}$ and $\xi_{\text{pol}}(p) = 0$, then there exists a trajectory $\gamma_p \subset A_{\text{pol}}^{\text{ro}}$ satisfying

$$\lim_{t \rightarrow -\infty} \gamma_p(t) = p.$$

To prove the claim, we consider two cases; either $p \in D_i^{\text{ro}, \circ}$ for some vertex $i \in \mathcal{V}_{\text{pol}}$, or $p \in D_{ij}^{\text{ro}}$ for some edge ij .

In the first case, we have $p \in \Sigma_i^{\text{ro}}$, and $\gamma \cap S(p) = \emptyset$, by assumption. Fix some small half-ball B_p around p in $Y_{\text{pol}}^{\text{ro}}$. Let $p_i = \gamma_{\text{pol}}^{\text{ro}}(t_i) \in \gamma_{\text{pol}}^{\text{ro}} \cap B_p$ be a sequence that converges to p . Since the trajectory of $\xi_{\text{pol}}^{\text{ro}}$ starting at p_i diverges from p , there exists some $t'_i > t_i$ so that $p'_i = \gamma_{\text{pol}}^{\text{ro}}(t'_i) \in \partial B_p$, and γ is exiting B_p at p'_i . By compactness, we can restrict this sequence to a subsequence, and assume that $p'_i \rightarrow p' \in \partial B_p$. By the assumption that γ converges to the origin, we must have $p' \in (\pi_{\text{pol}}^{\text{ro}})^{-1}(0)$, and so $p' \in D_i^{\text{ro}, \circ}$. The trajectory of $\xi_{\text{pol}}^{\text{ro}}$ in D_i^{ro} which passes through p' satisfies the conditions of the claim.

Consider next the case when $p \in D_{ij}^{\text{ro}}$ for some edge ij . By [Corollary 8.3.10](#), both vertices i and j are nonarrowheads, i.e. $i, j \in \mathcal{V}_{\text{pol}}$. As a result, this case follows by [Lemma 8.1.2](#) if the edge ij is invariant, and [Lemma 8.2.6](#) if it is not, which finishes the proof of the claim.

We will now construct a broken trajectory in $A_{\text{pol}}^{\text{ro}}$, as follows. The set $A_{\text{pol}}^{\text{ro}}$ is nonempty, since the map $\pi_{\text{pol}}^{\text{ro}}$ is proper. Take some $p_1 \in A_{\text{pol}}^{\text{ro}}$. If $\xi_{\text{pol}}(p_1) \neq 0$, let γ_1 be the trajectory passing through p_1 . Otherwise, choose γ_1 as some trajectory in $A_{\text{pol}}^{\text{ro}}$ as in the claim. Assuming that we have constructed a broken trajectory $\gamma_1, \dots, \gamma_{n-1}$ in $A_{\text{pol}}^{\text{ro}}$, let p_n be the limit of γ_{n-1} at plus infinity, and choose γ_n using the point $p = p_n$ in the claim. This process never ends, in contradiction to [Lemma 11.1.11](#). This proves eq. (11.2.2).

If p is a repeller on D_0 , then $S(p)$ is the punctured stable manifold at p , in this case a disk. Similarly, if $p \in D_0$ is a saddle point, then the punctured (open) stable manifold at p is an open solid torus. The cases when $p \in D_i$ with $i \neq 0$ follow from [Remark 10.3.19](#). \square

CHAPTER 12

The Invariant Spine

In this section we construct a \mathcal{C}^∞ fibration equivalent to the Milnor fibration by contracting the parts of the Milnor fiber at radius 0 corresponding to non-invariant vertices. Furthermore, we construct a piecewise smooth spine for all the fibers of this fibration at the same time.

Lemma 12.0.1. *Let $i \in \mathcal{V}_{\text{pol}}$ and $\theta \in \mathbb{R}/2\pi\mathbb{Z}$. Any trajectory of the vector field $\xi_{i,\theta}^{\text{ro}}$ in $D_{i,\theta}^{\text{ro},\circ}$ has a limit at each end in $D_{i,\theta}^{\text{ro}}$, each of which is either:*

- (1) *a singularity of $\xi_{i,j,\theta}^{\text{ro}}$ in the corner circle $D_{i,j,\theta}^{\text{ro}}$,*
- (2) *a saddle point q of $\xi_{i,\theta}^{\text{ro}}$, or*
- (3) *a repeller on $D_{0,\theta}^{\text{ro}}$.*

The last case can only happen if $i = 0$.

PROOF. Let $\gamma \subset D_{i,\theta}^{\text{ro},\circ}$ be a maximal trajectory, defined on an interval (a, b) . It suffices to show that $\gamma(t)$ has a limit, when $t \rightarrow b^-$, the case $t \rightarrow a^+$ follows similarly.

Assume first that γ has an accumulation point q in $D_{i,\theta}^{\text{ro},\circ}$ when $t \rightarrow b^-$. Since the potential $\phi_{i,\theta}^{\text{ro}}$ increases along γ , it is bounded on γ by $\phi_{i,\theta}^{\text{ro}}(q)$, and it follows that necessarily $\xi_{i,\theta}^{\text{ro}}(q) = 0$. It now follows from [Loj84] that $b = +\infty$, and $\gamma(t) \rightarrow q$ when $t \rightarrow +\infty$.

Otherwise, γ has an accumulation point on the boundary of the compact space $D_{i,\theta}^{\text{ro}}$. In this case, it is clear from the description of $\xi_{i,\theta}^{\text{ro}}$ near the boundary in Chapter 8 that γ has a limit at some point, see Fig. 8.1.11 and 8.2.10. \square

12.1. Broken trajectories

In this subsection we construct two broken trajectories (recall Definition 11.1.5) associated to each saddle point of $\xi_{\text{pol}}^{\text{ro}}$ and define a topological path, the *total broken trajectory* as the union of their closures.

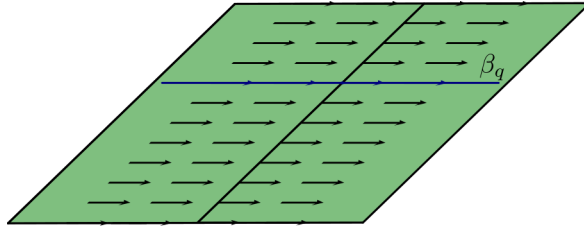


FIGURE 12.0.2. The vector field near a corner where both adjacent vertices are invariant.

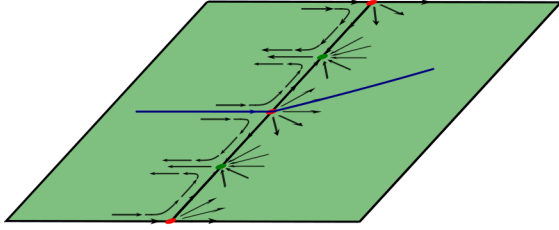


FIGURE 12.0.3. The vector field near a non-invariant corner where the broken trajectory (followed backwards) arrives at a red point. In this case, the continuation of the broken trajectory is determined by the dynamics of the vector field.

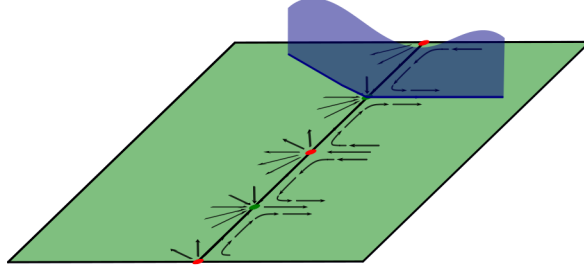


FIGURE 12.0.4. The vector field near a non-invariant corner where the broken trajectory (followed backwards) arrives at a green point. In this case, the continuation of the broken trajectory is determined by the center-stable manifold of the saddle point where the broken trajectory started.

Let $\beta_q^+[0]$ be one of the two trajectories contained in the stable manifold of $\xi_{i,\theta}^{\text{ro}}$ at a saddle point $q[0] = q \in D_{i,\theta}^{\text{ro},\circ}$. We observe that since $\beta_q^+[0]$ is a trajectory of $\xi_{i,\theta}^{\text{ro}}$, Lemma 12.0.1 says that its closure consists of $q[0]$ and another point $q[1] \neq q[0]$. Furthermore, since the center-stable manifold $S^{\text{ro}}(q)$ meets transversely $D_{i,\theta}^{\text{ro},\circ}$ at q and it is an invariant (by $\hat{\xi}_i^{\text{ro}}$) manifold we also have

$$\beta_q^+[0] \subset \overline{S^{\text{ro}}(q)} \cap Y_\theta^{\text{ro}}.$$

Assume that we have constructed a topological path $\beta_q^+[\ell]$ endowed with a filtration

$$\beta_q^+[0] \subseteq \beta_q^+[1] \subseteq \cdots \subseteq \beta_q^+[\ell]$$

such that for each $k = 0, \dots, \ell$

- (a) the set $\text{int}(\beta_q^+[k] \setminus \beta_q^+[k-1])$ is an integral line of $\xi_{j,\theta}^{\text{ro}}$ for some $j \in \mathcal{V}_{\text{pol}}$.
- (b) the boundary of the closure $\overline{\beta_q^+[k] \setminus \beta_q^+[k-1]}$ consists of two points $q[k]$ and $q[k+1]$ which, by Lemma 12.0.1 satisfy that $q[k] \neq q[k+1]$.
- (c) $\beta_q^+[k] \subset \overline{S^{\text{ro}}(q)} \cap \partial Y_\theta^{\text{ro}}$.

The next is an exhaustive list, depending on where the point $q[\ell+1]$ lies, that indicates if the construction of the broken trajectory finishes or one has to construct $\beta_q^+[\ell+1]$ and iterate. At each step in which the algorithm is not finished, we verify that items (a) to (c) above are satisfied.

- (1) The point $q[\ell + 1] \in D_{j,\theta}^{\text{ro},\circ}$ is a saddle point of $\xi_{j,\theta}^{\text{ro}}$ for some $j \in \mathcal{V}$. Define

$$\beta_q^+ = \beta_q^+[\ell] \cup \{q[\ell + 1]\}$$

and finish the construction here.

- (2) The point $q[\ell + 1] \in D_{0,\theta}^{\text{ro},\circ}$ and it is a fountain of $\xi_{0,\theta}^{\text{ro}}$. Define

$$\beta_q^+ = \beta_q^+[\ell] \cup \{q[\ell + 1]\}$$

and finish the construction here.

- (3) The point $q[\ell + 1] \in D_{j,k}^{\text{ro}}$ and both j and k are invariant vertices with $k \rightarrow j$ (as in figure [Figure 12.0.2](#)). In this case there is a unique trajectory $\gamma[\ell + 1]$ of $\xi_{k,\theta}^{\text{ro}}$ that has $q[\ell + 1]$ in its closure. We define

$$\beta_q^+[\ell + 1] = \beta_q^+[\ell] \cup q[\ell + 1] \cup \gamma.$$

Now we check that in this case the induction hypothesis [items \(a\)](#) to [\(c\)](#) above are still satisfied. Indeed:

- (a) $\text{int}(\beta_q^+[\ell + 1] \setminus \beta_q^+[\ell]) = \gamma[\ell + 1]$ which is, by definition, an integral line.
- (b) By [Lemma 12.0.1](#), we have that the boundary of $\overline{\gamma[\ell + 1]}$ consists exactly of two different points.
- (c) By the last statement of [Corollary 8.1.8](#), the closure of the center stable manifold $\overline{S^{\text{ro}}(q)}$ meets ∂U^{ro} precisely at $(\{q[\ell + 1]\} \cup \gamma[\ell] \cup \gamma[\ell + 1]) \cap \partial U^{\text{ro}}$. Here we are using that $S^{\text{ro}}(q)$ is an invariant manifold contained in Y_θ^{ro} that has $\gamma[\ell]$ in its closure. A complete proof of this point is below.

PROOF OF (C). Our goal is to demonstrate that the property $\beta_q^+[k] \subset \overline{S^{\text{ro}}(q)} \cap \partial Y_\theta^{\text{ro}}$ is preserved at each step of the construction. We assume, by induction, that the constructed path so far, $\beta_q^+[\ell]$, lies within the closure of the center-stable manifold $\overline{S^{\text{ro}}(q)}$. The terminal segment, $\gamma[\ell]$, is a trajectory of a vector field $\xi_{j,\theta}^{\text{ro}}$ which converges to the point $q[\ell + 1] \in D_{j,k}^{\text{ro}}$.

The current step of the construction addresses Case (iii), where the edge jk is invariant. This implies that the corner point $q[\ell + 1]$ is an elementary singularity of the extended vector field, as established in [Lemma 8.1.2](#).

By [Corollary 8.1.8](#), there exists a local coordinate system $(r', s', \alpha', \beta')$ in a neighborhood U^{ro} of $q[\ell + 1]$ such that the vector field ξ_U^{ro} is linearized to the form:

$$\xi_U^{\text{ro}} = (C_k r', -C_j s', 0, 0)$$

where $C_k = dc_{0,k}$ and $C_j = dc_{0,j}$ are positive constants. The flow is described by the equations $\dot{r}' = C_k r'$ and $\dot{s}' = -C_j s'$. In this chart, the point $q[\ell + 1]$ corresponds to the origin. The local manifold $D_{j,\theta}^{\text{ro},\circ}$ is represented by the half-space $\{s' = 0, r' > 0\}$, and $D_{k,\theta}^{\text{ro},\circ}$ is represented by $\{r' = 0, s' > 0\}$. The trajectory $\gamma[\ell]$ approaches the origin along the positive r' -axis. The next segment of the broken trajectory, $\gamma[\ell + 1]$, must be the unique trajectory emanating from the origin within $D_{k,\theta}^{\text{ro},\circ}$, which is the positive s' -axis.

The center-stable manifold $S^{\text{ro}}(q)$ is, by definition, invariant under the flow of $\xi_{\text{pol}}^{\text{ro}}$. The induction hypothesis, $\gamma[\ell] \subset \overline{S^{\text{ro}}(q)}$, implies that $\overline{S^{\text{ro}}(q)}$ contains the positive r' -axis in the chart U^{ro} . Consequently, there exists a sequence of points $\{p_n\}_{n \in \mathbb{N}}$ in $S^{\text{ro}}(q) \cap U^{\text{ro}}$ that converges to the positive r' -axis. Let the coordinates of these points be $p_n = (r'_n, s'_n, \alpha'_n, \beta'_n)$, where $r'_n > 0$ and $s'_n \rightarrow 0$ as $n \rightarrow \infty$.

By the invariance of $S^{\text{ro}}(q)$, the full trajectory γ_{p_n} through each point p_n is contained in $S^{\text{ro}}(q)$. The coordinates of this trajectory at time t are given by $\gamma_{p_n}(t) = (r'_n e^{C_k t}, s'_n e^{-C_j t}, \alpha'_n, \beta'_n)$.

Consider the backward flow ($t < 0$) of these trajectories. As $t \rightarrow -\infty$, the r' -coordinate, $r'_n e^{C_k t}$, converges to 0, while the s' -coordinate, $s'_n e^{-C_j t}$, grows without bound. This shows that trajectories originating in $S^{\text{ro}}(q)$ near the $\{s' = 0\}$ plane are swept towards the $\{r' = 0\}$ plane under the backward flow.

Since $\overline{S^{\text{ro}}(q)}$ is a closed set, it must contain the accumulation points of all trajectories contained within it. Let $p_s = (0, s'_0, \alpha', \beta')$ be an arbitrary point on the positive s' -axis, which represents the trajectory $\gamma[\ell + 1]$. For any such p_s , we can construct a sequence of points in $S^{\text{ro}}(q)$ that converges to it. Specifically, for each n , we can choose a time $t_n < 0$ such that $s'_n e^{-C_j t_n} = s'_0$. Then the sequence of points $q_n = \gamma_{p_n}(t_n)$ lies in $S^{\text{ro}}(q)$, and as $n \rightarrow \infty$, we have $s'_n \rightarrow 0$, which forces $t_n \rightarrow -\infty$. Consequently, the r' -coordinate $r'_n e^{C_k t_n}$ converges to 0. Thus, the sequence $\{q_n\}$ converges to p_s .

This demonstrates that any point on the positive s' -axis is a limit point of $\overline{S^{\text{ro}}(q)}$. Therefore, the entire trajectory $\gamma[\ell + 1]$ is contained within $\overline{S^{\text{ro}}(q)}$. This completes the induction. \square

- (4) The point $q[\ell + 1] \in D_{j,k}^{\text{ro}}$ and, at least one of the two vertices j or k is a non-invariant vertex. Assume $k \rightarrow j$. In this case, one of the following happens,
 - (1) See [Figure 12.0.3](#). This case is similar to the previous one: there is a unique trajectory $\gamma[\ell + 1]$ of $\xi_{k,\theta}^{\text{ro}}$ that has $q[\ell + 1]$ in its closure. We define

$$\beta_q^+[\ell + 1] = \beta_q^+[\ell] \cup q[\ell + 1] \cup \gamma[\ell + 1].$$

Again, the items (a) and (b) are verified directly. And (c) follows because by [Lemma 8.2.6](#), (ii) the Hessian of ξ_U^{ro} is elementary along the normal bundle and, since $S^{\text{ro}}(q)$ is an invariant manifold contained in Y_θ^{ro} that has $\gamma[\ell] \cup \{q[\ell]\}$ in its closure, then $S^{\text{ro}}(q)$ must also have the only trajectory of $\xi_{k,\theta}^{\text{ro}}$ that has $q[\ell]$ in its closure.

- (2) Assume now that $\gamma[\ell]$ is the single unstable trajectory going out of a green point in its half-saddle part as in [Figure 12.0.4](#). In this case there is not a unique trajectory of $\xi_{j,\theta}^{\text{ro}}$ that has $q[\ell + 1]$ in its closure. Note that in this case, the right-hand part of [Figure 12.0.4](#) corresponds with $D_{k,\theta}^{\text{ro}}$.

Using the same methods as above, it is possible to choose a trajectory in $D_{j,\theta}^{\text{ro},\circ}$, which continues the broken trajectory, and is contained in $\overline{S^{\text{ro}}(q)}$. We choose any such trajectory for the sake of this algorithm. However, uniqueness is not guaranteed by this argument. Observe

that the chosen trajectory may necessarily be the corner locus, in which case, we follow the corner locus until we hit an adjacent red point, and continue as before. In subsequent work, we plan on describing in more details the structure of the cell near the boundary. As a result of this work, we expect the choice made in this step to be unique. Furthermore, in this subsequent work we show that this (iv)(2) case can be avoided by a small equisingular perturbation *a la Kodaira* of the analytic type of the defining function f .

Definition 12.1.1. For each $q \in \Sigma_{i,\theta}^{\text{ro}}$ that is a saddle point of $\xi_{i,\theta}^{\text{ro}}$ define the set

$$\beta_q = \beta_q^+ \cup \beta_q^- \cup \{q\}$$

and call it *the total broken trajectory of $\xi_{i,\theta}^{\text{ro}}$ at q* .

Lemma 12.1.2. *We have*

$$\beta_q \subset \overline{S^{\text{ro}}(q)} \cap \partial Y_\theta^{\text{ro}}.$$

PROOF. It follows from the construction of the broken trajectory above and that the property (c), which is satisfied at each step of the construction, says that $\beta_q^+[k] \subset S^{\text{ro}}(q) \cap \partial Y_\theta^{\text{ro}}$. \square

Definition 12.1.3. We define the spine at radius 0 and angle θ , and denote it by S_θ^{ro} , as the union of all the total broken trajectories associated with all the saddle points of the vector fields $\xi_{i,\theta}^{\text{ro}}$ for all $i \in \mathcal{V}$. That is,

$$S_\theta^{\text{ro}} = \bigcup_{\substack{i \in \mathcal{V} \\ q \text{ is a saddle point of } \xi_{i,\theta}^{\text{ro}}}} \beta_q$$

As we will see later in [Example 12.2.21](#), the spine at radius 0 and angle θ is not in general a spine as in [Definition 2.2.4](#). In a sequel to this work we will work out some further genericity conditions under which for a generic analytical type representing a particular topological type and for a generic angle, the spine at radius 0 and angle θ is a spine. In [Section 12.3](#) we construct a quotient of the spine at radius 0 which is always a spine for a quotient of the Milnor fiber at radius 0 which is homeomorphic to the Milnor fiber.

12.2. The Petri dishes

In this section we analyze the vector field and the broken trajectories inside the connected components of the part of the Milnor fiber that corresponds to the non-invariant graph. We use [Notation 11.1.8](#).

Lemma 12.2.1. *Let Ξ be a branch (recall [Definition 3.4.4](#)) of Γ_{pol} at a vertex i of $\Gamma_{\text{pol}} \setminus \Upsilon$. Then $F_\theta^{\text{ro}}[\Xi]$ is a disjoint union of disks. Moreover, if ij is the edge that joins Ξ with $\Gamma_{\text{pol}} \setminus \Xi$, then $F_\theta^{\text{ro}}[\Xi]$ is a disjoint union of $\gcd(m_i, m_j)$ disks.*

PROOF. That $F_\theta^{\text{ro}}[\Xi]$ is a disjoint union of disks follows from [Lemma 6.4.2](#) that implies, that in Γ_{min} , the graph Ξ is a bamboo. The process of blowing up more to get to Γ_{pol} may introduce new vertices, but does not change the topology of the Milnor fiber. The statement on the number of connected components follows because near the intersection point of Ξ with the rest of Γ_{pol} , the Milnor fiber at radius 0 looks like the Milnor fiber of $u^{m_i} v^{m_j}$ which is a disjoint union of $\gcd(m_i, m_j)$ cylinders. \square

Definition 12.2.2. Let Ξ be a branch of Γ_{pol} at a vertex i of $\Gamma_{\text{pol}} \setminus \Upsilon$. We call each of the disks in $F_\theta^{\text{ro}}[\Xi]$, a *Petri dish*. We denote Petri dishes by \mathbb{D}_θ .

We say that a Petri dish is *maximal* if it is not strictly contained in any other Petri dish.

Next we introduce some useful notation for this subsection.

Notation 12.2.3. Let \mathbb{D}_θ be a Petri dish coming from some branch Ξ as in Definition 12.2.2.

We denote by $\beta[\mathbb{D}_\theta]$ the union of all the broken trajectories that start at some $D_{i,\theta}^{\text{ro}}$ with $i \in \mathcal{V}_\Xi$, intersected with \mathbb{D}_θ . That is,

$$\beta[\mathbb{D}_\theta] = \left(\bigcup_{\substack{q \in \Sigma_{i,\theta} \\ i \in \mathcal{V}_\Xi}} \beta_q \right) \cap \mathbb{D}_\theta.$$

We denote by $S[\mathbb{D}_\theta]$ the part of the spine at radius 0 that lies in \mathbb{D}_θ . That is

$$S[\mathbb{D}_\theta] = S_\theta^{\text{ro}} \cap \mathbb{D}_\theta.$$

A Petri dish \mathbb{D}_θ inherits a the structure of a stratified topological manifold with smooth strata. But it does not have, a priori, a smooth structure. In the the rest of this section we make use of Poincaré-Hopf index theorem to prove results about the set $\beta[\mathbb{D}_\theta]$ and, in order to formalize such arguments we need to put a smooth structure on \mathbb{D}_θ .

Lemma 12.2.4. *Let \mathbb{D}_θ be a Petri dish associated with a branch Ξ with vertex set \mathcal{V}_Ξ . Then, \mathbb{D}_θ admits a smooth structure, which is compatible with that of $D_{i,\theta}^{\text{ro},\circ} \subset \mathbb{D}_\theta$, for each i on Ξ , and the restricted vector field $\xi_{\mathbb{D}_\theta}^{\text{ro}} = \xi_{\text{pol}}^{\text{ro}}|_{D_\theta}$ is a continuous vector field on \mathbb{D}_θ .*

PROOF. Each connected component $\mathbb{D}_{i,\theta}$ of $D_{i,\theta}^{\text{ro}}$ can be thought of as a cobordism between the connected components $\partial_j \mathbb{D}_{i,\theta}$ of $\partial \mathbb{D}_{i,\theta}$ corresponding to edges $j \rightarrow i$ and the connected components $\partial_k \mathbb{D}_{i,\theta}$ of $\partial \mathbb{D}_{i,\theta}$ corresponding to edges $i \rightarrow k$.

Furthermore, let ij be an edge $j \rightarrow i$. Then, there is a diffeomorphism

$$\iota_{ij} : \partial_j \mathbb{D}_{i,\theta} \rightarrow \partial_i \mathbb{D}_{j,\theta}$$

induced by the structure of fiber product that identifies both sets of boundary components. Then, by [Mil65, Theorem 1.4], there exists a smooth structure on $\mathbb{D}_{i,\theta} \sqcup_{\iota_{ij}} \mathbb{D}_{j,\theta}$ which is compatible with each of the smooth structures on $\mathbb{D}_{i,\theta}$ and $\mathbb{D}_{j,\theta}$.

By definition, the vector field $\xi_{\mathbb{D}_\theta}^{\text{ro}}$ is well defined on (and tangent to) $D_{i,j,\theta}^{\text{ro}}$.

By iteratively applying this reasoning, we get a smooth structure on all \mathbb{D}_θ and a continuous vector field on it. Furthermore, this vector field coincides with $\xi_{i,\theta}^{\text{ro}}$, up to multiplication by a real positive function, on each of the pieces of \mathbb{D}_θ . □

Remark 12.2.5. Note that the vector field $\xi_{\mathbb{D}_\theta}^{\text{ro}}$ is a continuous (by construction) vector field but, in general, it is not C^1 .

Remark 12.2.6. (1) By definition, $\beta[\mathbb{D}_\theta] \subseteq S[\mathbb{D}_\theta]$. And, in general, the above is not an equality as we will see later in an example.

- (2) The vector field $\xi_{\mathbb{D}_\theta}^{\text{ro}}$ does not have any nonzero index singularities in the interior of $\mathbb{D}_\theta \setminus \beta[\mathbb{D}_\theta]$. This is because $\beta[\mathbb{D}_\theta]$ contains all the saddle points by construction and the other singularities are by [Lemma 8.2.6](#) half-fountain-half-saddle or half-sink-half saddle points, (i.e. they are green and red points like those of [fig. 8.2.10](#)) which all have index 0.
- (3) By definition of broken trajectory, the set $\beta[\mathbb{D}_\theta]$ seen as graph, if it has vertices of valency 1, then they have to lie on $\partial\mathbb{D}_\theta$.

12.2.7. Here we deduce an easy relative version of the Poincaré-Hopf index theorem for vector fields on surfaces with boundary. Let F be an oriented compact surface of genus g with $b > 0$ boundary components, and let ξ_F be a vector field on F which is also tangent to ∂F . Assume furthermore that ξ has isolated singularities (some of them might be on the boundary). Now take the double-surface $2F$ of F : that is, consider $-F$ (which is the surface with opposite orientation) and glue $-F$ to F along their boundaries by the identity map (note that the identity map inverts the orientation from ∂F to $\partial(-F)$). The surface $-F$ comes naturally equipped with a vector field ξ_{-F} which is identified with ξ_F on $\partial(-F)$ by the identity map. Thus, we have a well defined vector field ξ_{2F} defined on $2F$ with isolated singularities. Observe that the surface $2F$ is a closed oriented surface of genus $2g + b - 1$. This construction allows us to do two things:

- (1) Assign an index to isolated singularities on the boundary: for an isolated singularity $p \in \partial F$ of ξ_F , we define the index of ξ_f at p by the formula

$$(12.2.8) \quad \text{Ind}_{\xi_F}(p) = \frac{1}{2} \text{Ind}_{\xi_{2F}}(p)$$

where, on the right-hand side, p is seen as a point in $2F$.

- (2) We compute a relative version of the Poincaré-Hopf index theorem. By applying the classical theorem to the surface $2F$, we get:

$$2 \sum_{p \in F} \text{Ind}_{\xi_F}(p) + \sum_{p \in \partial F \subset F} \text{Ind}_{\xi_{2F}}(p) = 2 - 2(2g + b - 1).$$

which, after dividing by 2 and applying the previous definition [eq. \(12.2.8\)](#) yields,

$$(12.2.9) \quad \sum_{p \in F} \text{Ind}_{\xi_F}(p) = 2 - 2g - b = \chi(F).$$

Where the term on the left-hand side allows for ξ_F to have isolated singularities on the boundary of F .

Next we classify all the singularities that might appear on the boundary of connected components of $\mathbb{D}_\theta \setminus \beta[\mathbb{D}_\theta]$.

Lemma 12.2.10. *Let Δ be the closure of a connected component of $\mathbb{D}_\theta \setminus \beta[\mathbb{D}_\theta]$ and assume that $\partial\Delta$ is an embedded circle. Then the vector field $\xi_{\mathbb{D}_\theta}^{\text{ro}}|_\Delta$ has no nonzero index singularities on the interior of Δ and, on $\partial\Delta$ it may have*

- (1) Quarter-fountain-quarter-saddle, quarter-sink-quarter-saddle, quarter saddle points as the only singularities of index 0 (see [fig. 12.2.11](#)),
- (2) half-sink, half-fountain points as the only singularities of index 1/2 (see [fig. 12.2.12](#)),

- (3) half-saddle points as the only singularities of index $-1/2$ (see the right-hand side of [fig. 12.2.13](#)).

PROOF. The first part of the statement on the singularities in the interior of Δ is exactly [Remark 12.2.6 2](#). Now we notice that the only singularities that $\partial\Delta$ might have, happen when $\partial\Delta$ crosses a singularity of $\xi_{\mathbb{D}_\theta}^{\text{ro}}|_\Delta$. So let $p \in \partial\Delta$ be a singularity of $\xi_{\mathbb{D}_\theta}^{\text{ro}}|_\Delta$, next we go through all the possible cases depending on where p lies.

Case 1. If $p \in \partial\mathbb{D}_\theta$, then p is either a half-fountain or a half-sink point when seen as a singularity of $\xi_{\mathbb{D}_\theta}^{\text{ro}}$ (because of [Lemma 8.2.6](#)). In this case, p seen as a singularity of $\xi_{\mathbb{D}_\theta}^{\text{ro}}|_\Delta$ can only be a half-fountain (red vertex) or a half-sink (green vertex) singularity. This covers 2.

Case 2. If p is in the interior of \mathbb{D}_θ , then there are two possibilities:

Case (2.a) p is a saddle point of $\xi_{\mathbb{D}_\theta}^{\text{ro}}$. In this case the segment of $\partial\Delta$ that passes through p might be formed either by a stable trajectory and an unstable trajectory (the blue singularity of [fig. 12.2.11](#)) giving a singularity of index 0, or by two stable trajectories (the right-hand side of [fig. 12.2.13](#)) giving a singularity of index $-1/2$. Note that it can't happen that this segment is formed by two unstable trajectories (left-hand side of [fig. 12.2.13](#)) since $\beta[\mathbb{D}_\theta]$ contains by definition the stable trajectories of all saddle points.

Case (2.b) p is a red or green point of a smaller Petri dish $\mathbb{D}'_\theta \subset \mathbb{D}_\theta$. In this case the segment of $\partial\Delta$ that passes through p must correspond to a broken trajectory that either enters the smaller Petri dish \mathbb{D}'_θ or exits \mathbb{D}_θ (this corresponds to the two left figures of [fig. 12.2.11](#)). Note that by the construction of broken trajectories, no broken trajectory can contain a segment of the boundary of a Petri dish since boundaries of Petri dishes do not have saddle points of $\xi_{\mathbb{D}_\theta}^{\text{ro}}$.

These two subcases cover all the possibilities in 1 and 3 finishing the proof. \square

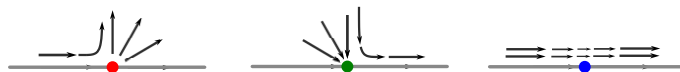


FIGURE 12.2.11. Singularities (red, green and blue points) of index 0 of a vector field tangent to the boundary (gray thick line) of a surface.



FIGURE 12.2.12. Singularities (green and red points) of index $1/2$ of a vector field tangent to the boundary (gray thick line) of a surface.



FIGURE 12.2.13. Singularities (blue points) of index $-1/2$ of a vector field tangent to the boundary (gray thick line) of a surface. The situation on the left hand side does not occur in the above algorithm.

Lemma 12.2.14. *Let \mathbb{D}_θ be a Petri dish coming from some branch Ξ . Let i be the root of Ξ and let j be the vertex in $\Gamma_{\text{pol}} \setminus \Xi$ to which it is connected. Then the number of saddle points I of $\xi_{\mathbb{D}_\theta}^{\text{ro}}$ is equal to:*

$$(12.2.15) \quad I = -\frac{\begin{vmatrix} \varpi_i & m_i \\ \varpi_j & m_j \end{vmatrix}}{\gcd(m_i, m_j)} - 1.$$

In particular, $\beta[\mathbb{D}_\theta]$ is non-empty if and only if $I \geq 1$, equivalently, if there are at least 2 red points on $\partial\mathbb{D}_\theta$.

PROOF. The term with the fraction on eq. (12.2.15) equals the number of red points (which equals the number of green points, too) on $\partial\mathbb{D}_\theta$ (Lemma 8.4.1). These singularities look on \mathbb{D}_θ like half sinks (green points) and half fountains (red points). See fig. 12.2.12. These have relative Poincaré-Hopf index equal to $1/2$. By Remark 12.2.6 2 the only singularities of nonzero index on the interior of \mathbb{D}_θ are saddle points. A direct application of eq. (12.2.9) yields the result since:

$$-\frac{\begin{vmatrix} \varpi_i & m_i \\ \varpi_j & m_j \end{vmatrix}}{\gcd(m_i, m_j)} - I = 1.$$

That $\beta[\mathbb{D}_\theta]$ is non-empty if and only if there is at least 1 saddle point in \mathbb{D}_θ follows from the definition of the broken trajectories which start at all saddle points. \square

Lemma 12.2.16. *Let \mathbb{D}_θ be a maximal Petri dish and let γ be a broken trajectory. If a segment of γ is contained in \mathbb{D}_θ and exits through a point $p \in \partial\mathbb{D}_\theta$, then no subsequent segment of γ can re-enter \mathbb{D}_θ .*

PROOF. The Petri dish corresponds to a connected component of $\Gamma \setminus \Upsilon$, adjacent to an invariant vertex, say $i \in \mathcal{V}$. Let k be the neighbor of i in this component, i.e. the unique non-invariant neighbor of i . After exiting \mathbb{D}_θ , we have a segment of γ , which we follow (backwards) until we end in a limit point, which exists by Lemma 12.0.1. If this limit point is a saddle point of ξ_i^{ro} , then this is the end of the broken trajectory, and the proof is finished, in this case.

Otherwise, this limit point is on the corner locus $D_{i,j,\theta}^{\text{ro}}$ for some neighbor j . Since the potential $\phi_{i,\theta}^{\text{ro}}$ decreases along this trajectory, and is constant along $D_{i,k,\theta}^{\text{ro}}$ it cannot happen that $j = k$. Therefore, j is invariant. It cannot happen that we have a directed edge $i \rightarrow j$, since any trajectory of $\xi_{i,\theta}^{\text{ro}}$ projects to a trajectory of ξ_i on D_i , and ξ_i has an attractor at $D_i \cap D_j$, if $i \rightarrow j$. Therefore, we have $j \rightarrow i$. Now, continuing the trajectory beyond this step, we can never return through $D_{i,j,\theta}^{\text{ro}}$ again, since $D_j \cap D_i$ is a repeller of ξ_i . \square

Corollary 12.2.17. *Let \mathbb{D}_θ be a maximal Petri dish. The set $\beta[\mathbb{D}_\theta]$ does not contain any green points in $\partial\mathbb{D}_\theta$.*

PROOF. A green point is, by definition, half a sink. In order for $\beta[\mathbb{D}_\theta]$ to contain a green point it must have happened that a broken trajectory starting at $q \in \mathbb{D}_\theta$ must have exited \mathbb{D}_θ and re-entered it through that green point. But Lemma 12.2.16 prevents this. \square

Lemma 12.2.18. *Let \mathbb{D}_θ be a maximal Petri dish. Each connected component of $\beta[\mathbb{D}_\theta]$:*

- (1) *is connected to some red vertex on $\partial\mathbb{D}_\theta$ and*
- (2) *is contractible.*

PROOF. Let $q \in \beta[\mathbb{D}_\theta]$ be a saddle point of some $\xi_{i,\theta}^{\text{ro}}$ with $i \in \mathcal{V}_\Xi$.

Claim 1. The broken trajectory β_q^+ can't end at q .

PROOF OF CLAIM 1. If β_q^+ ends at q , because of Lemma 12.2.16, it must be contained entirely in \mathbb{D}_θ . Now we apply a similar reasoning as in the proof of Lemma 12.2.16: contract each of the smaller Petri dishes contained in \mathbb{D}_θ to a point. We obtain a loop, formed by integral lines of a vector field that, by Lemma 9.3.3, admits a potential which is contradictory. \square

By the previous claim, either the broken trajectory ends at another saddle point $q' \in \mathbb{D}_\theta$ or it has to exit $\partial\mathbb{D}_\theta$ by some red point on $\partial\mathbb{D}_\theta$ (note that it can only exit \mathbb{D}_θ through a red point since broken trajectories are constructed following the flow backwards). If it exits \mathbb{D}_θ through a red point, we are done proving 1.

Assume otherwise it arrives at another saddle point q' . Now consider one of the broken trajectories $\beta_{q'}^{'+}$ associated with q' .

Claim 2. The broken trajectory $\beta_{q'}^{'+}$ can't end at q .

PROOF OF CLAIM 2. The proof is very similar to the previous claim: contract each of the smaller Petri dishes contained in \mathbb{D}_θ to a point. We obtain a loop, formed by integral lines of a vector field that, by Lemma 9.3.3, admits a potential which is contradictory. \square

After claim 2, we get that the broken trajectory $\beta_{q'}^{'+}$ either ends at a red point in $\partial\mathbb{D}_\theta$ or it gets to another saddle point q'' that, following a similar reasoning to that of Claim 1 and 2, must be different from q and q' . Now we can iterate this process and get that, after each step, we either arrive at a red point in $\partial\mathbb{D}_\theta$ or to a saddle point that we have not visited before. But there are only finitely many saddle points contained in \mathbb{D}_θ . This proves 1.

Now we prove 2. The proof of 1 already shows that there can be no loops in the interior of \mathbb{D}_θ . Assume that we have a loop L that contains at least a point p in $\partial\mathbb{D}_\theta$. This point is necessarily red by Corollary 12.2.17. Furthermore, assume that this loop does not contain any other loops of $\beta[\mathbb{D}_\theta]$ in the disk that it encloses, for if it does, we can always choose one of the smaller loops. Then L is a concatenation of paths L_1, \dots, L_n and red points p_1, \dots, p_n . The loop L encloses a disk, which by Remark 12.2.6 2 and by our hypothesis on the minimality of L , does not contain any nonzero index singularities. Since each L_k joins two red points, it must contain at least one singularity of index $-1/2$: indeed, if for example L_1 joins p_1 with p_2 ,

then there are two trajectories of $\xi_{\mathbb{D}_\theta}^{\text{ro}}$ inside L_1 with opposite sign, so necessarily there is a saddle point on L_1 . Thus, using eq. (12.2.9) we get

$$\sum_{i=1}^n \left(\text{Ind}_{\xi_{\mathbb{D}_\theta}^{\text{ro}}}(p_i) + \sum_{q \in L_i} \text{Ind}_{\xi_{\mathbb{D}_\theta}^{\text{ro}}}(q) \right) \leq \frac{n}{2} - \frac{n}{2} = 0.$$

which contradicts the fact that the Euler characteristic of the disk enclosed by L is equal to 1. \square

Corollary 12.2.19. *The closure of each connected component of $\mathbb{D}_\theta \setminus \beta[\mathbb{D}_\theta]$ is a closed disk.*

PROOF. By Lemma 12.2.18, each connected component $\beta[\mathbb{D}_\theta]$ is connected to some red vertex and it is a tree. The interior of the complement of a tree contained in a disk is a disjoint union of open disks provided that the tree is connected to at least a point of the boundary of the disk. Now, by Remark 12.2.6 3, each connected component of $\beta[\mathbb{D}_\theta]$ does not have vertices of valency 1 in the interior of \mathbb{D}_θ , so the boundary of the closure of each connected component must be an embedded circle. \square

Proposition 12.2.20. *If the set $\beta[\mathbb{D}_\theta]$ is non-empty, then*

- (1) *it is connected,*
- (2) *it is contractible,*
- (3) *it contains all the red points in $\partial\mathbb{D}_\theta$.*

PROOF. We construct a (possibly disconnected) abstract graph $\tilde{\beta}$:

- (1) The set of vertices is the union of the saddle points of $\xi_{\mathbb{D}_\theta}^{\text{ro}}$ and the red vertices on $\partial\mathbb{D}_\theta$.
- (2) there is an edge between a saddle point and another saddle point or between a saddle point and a red point if there is a broken trajectory in $\beta[\mathbb{D}_\theta]$ that joins them.

The underlying 1-dimensional CW-complex of $\tilde{\beta}$ is homeomorphic to $\beta[\mathbb{D}_\theta]$ union all the red vertices. And we have a natural injective map $\beta[\mathbb{D}_\theta] \hookrightarrow \tilde{\beta}$ that realizes $\beta[\mathbb{D}_\theta]$ in $\tilde{\beta}$. Since each red vertex can be thought of as a tree and the connected components of $\beta[\mathbb{D}_\theta]$ are trees by Lemma 12.2.18 2, the Euler characteristic of $\tilde{\beta}$ counts the number of connected components. If we let R be the number of red points, I the number of saddle points and e the number edges, then we have $e = 2I$, since every edge is a trajectory coming out of exactly one saddle point, and every saddle point has two such trajectories. Therefore,

$$\chi(\tilde{\beta}) = R + I - e = R - I.$$

But $R - I = 1$ by Lemma 12.2.14. So $\tilde{\beta}$ is connected and contains all the red points, we conclude items 1 and 3.

That $\beta[\mathbb{D}_\theta]$ is contractible 2 follows directly from Lemma 12.2.18 2. \square

Example 12.2.21. In this example we show that the union of broken trajectories starting at all saddle points does not, in general, form a spine for the Milnor fiber at radius 0.

Consider the plane curve singularity C defined by $f(x, y) = y^6 - 2y^3x^4 - 3x^8 + yx^7$. The plane curve C consists of two branches which are Brieskorn-Pham singularities of type $(3, 4)$ with the same tangent. The polar curve P is defined by

the equation $f_y = 6y^5 - 6y^2x^4 + x^7$ and has two branches. The strict transform of one of the branches passes through the exceptional divisor D_2 and the other one through the divisor D_3 . The divisor D_3 is an invariant divisor and so the point $\tilde{P} \cap D_3$ is a base point of the Jacobian ideal by [Lemma 6.4.11 3](#). After blowing up this base point once, we get the dual graph on the bottom of [fig. 12.2.22](#).

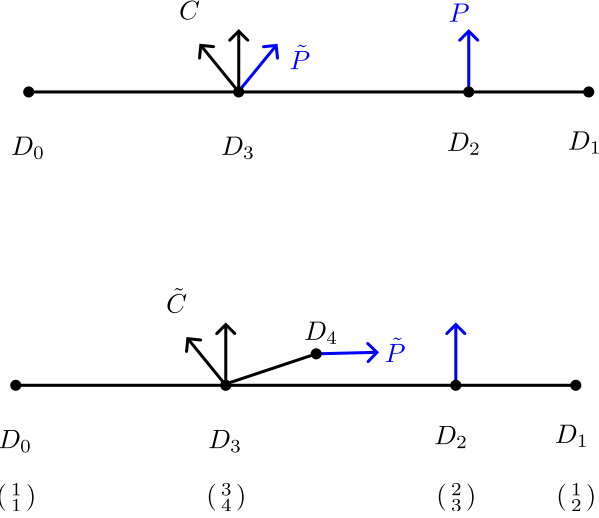


FIGURE 12.2.22. On top the dual graph of the minimal resolution of C . On bottom, the resolution resulting from blowing up the base point of the divisor D_3 once. In blue we have the strict transform of the polar curve P which has two branches.

Let's look at the divisor D_3 in the minimal resolution of the plane curve. For that, we consider the monomial transformation

$$\pi(u, v) = (u^3v^2, u^4v^3)$$

which sees a neighborhood around $D_3 \cap D_2$. Using $\tau_3 = 8$ and $\tau_2 = 5$ we can compute the restriction of the extension of the vector field over D_3° in this chart (see [fig. 12.2.23](#) for its representation) and we get the expression:

$$\xi_3 = -\frac{18(\bar{v} - 1)}{|v|^4 (\bar{v}^2 - 2\bar{v} - 3)}.$$

The intersection with the two components of the strict transform of C are on the real points $-1, 3 \in \mathbb{C}$. We see ([fig. 12.2.23](#)) that there is a trajectory of ξ_3 on D_3° that goes from the saddle point corresponding to the intersection point $D_3 \cap D_4$. On D_2 there is another intersection point $\tilde{P} \cap D_2$.

Now we analyze what happens at the level of the Milnor fiber at radius 0. The multiplicity m_2 of $\pi^* f$ at D_2 is 16. The multiplicity m_1 is 8. This says that $D_{1,\theta}^{\text{ro}}$ consists of 8 disks and $D_{2,\theta}^{\text{ro}}$ consists of 8 cylinders for each $\theta \in \mathbb{R}/2\pi\mathbb{Z}$. Thus, on each of these 8 cylinders, the vector field $\xi_{2,\theta}^{\text{ro}}$ has 2 saddle points. Furthermore, a computation yields that $\varpi_2 = 1$ and we know that $\varpi_3 = 0$. Therefore, using [Lemma 8.2.4 \(iii\)](#) we get that each connected component of $D_{2,3,\theta}^{\text{ro}}$ has 3 red points (and 3 green points). We conclude that for a generic angle θ , one of the three red

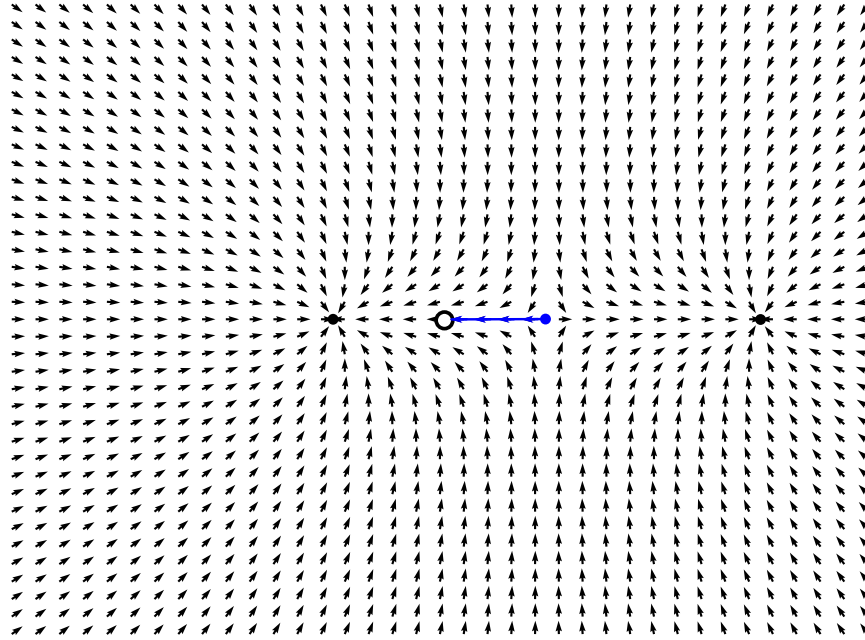


FIGURE 12.2.23. The divisor D_3 . The two black dots correspond with the intersection points of the strict transforms of the curve C . The blue dot corresponds with the intersection point of D_3 and D_4 . The circled dot corresponds with the intersection point of D_2 and D_3 . The blue segment is a trajectory.

points on each cylinder is chosen by two half broken trajectories starting at the two saddle points on each connected component of $D_{2,\theta}^{\text{ro}}$. We have, in total 24 red points and 8 of these are chosen by two half broken trajectories on their corresponding cylinders.

We analyze now what happens in D_4 . The multiplicity $m_4 = m_3 = 24$, so $D_{4,\theta}^{\text{ro}}$ consists of 24 disks. Since $\varpi_4 = 2$, each of these disks has 2 red points and 2 green points (48 of each in total). Moreover, D_4 intersects \tilde{P} and so each of the 24 disks of $D_{4,\theta}^{\text{ro}}$ has a saddle point of $\xi_{4,\theta}^{\text{ro}}$ on its interior. Each of the two red points on each component of $\partial D_{4,\theta}^{\text{ro}}$ gets chosen by one of the broken trajectories associated with the saddle point.

The fact that there is a trajectory going from $D_4 \cap D_3$ to $D_3 \cap D_2$ yields that there are 24 trajectories in $D_{3,\theta}^{\text{ro}}$ joining the 24 red points of $D_{2,3,\theta}^{\text{ro}}$ with 24 of the 48 green points lying on $D_{3,4,\theta}^{\text{ro}}$.

Let $p_1, p_2 \in D_{2,\theta}^{\text{ro}}$ be two saddle points of $\xi_{2,\theta}^{\text{ro}}$ lying on the same connected component of $D_{2,\theta}^{\text{ro}}$. We know that the Hessian of $\xi_{2,3,\theta}^{\text{ro}}$ at the red points is non degenerate, so the two broken trajectories that start at p_1 and p_2 and end at the same red point, arrive (flowing backwards) at this red point, with different tangents. After passing through the red points, both broken trajectories choose the same trajectory on $D_{3,\theta}^{\text{ro}}$ and this is one of the 24 trajectories that lie above the trajectory on D_3^{ro} connecting $D_2 \cap D_3$ with $D_3 \cap D_4$. Here, the closures of $S^{\text{ro}}(p_1)$ and $S^{\text{ro}}(p_2)$ intersect transversely along the trajectory in $D_{3,\theta}^{\text{ro},\circ}$.

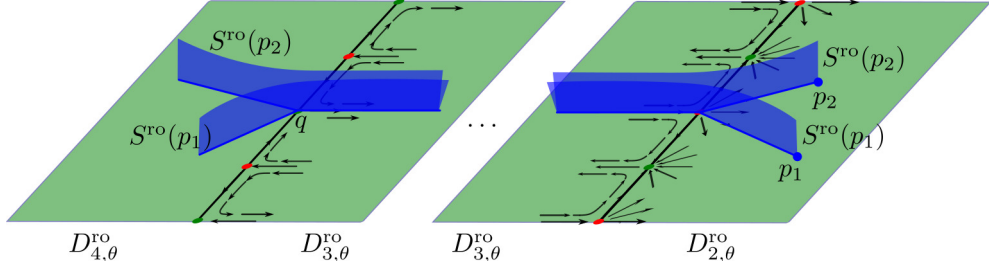


FIGURE 12.2.24. On the right part of the picture we see a neighborhood of the $D_{2,3,\theta}^{\text{ro}}$. On the right we also see, in blue, the center-stable manifolds $S^{\text{ro}}(p_1)$ and $S^{\text{ro}}(p_2)$. On the left part of the picture we see a neighborhood of $D_{3,4,\theta}^{\text{ro}}$. We see how the two center-stable manifolds define different trajectories in $D_{4,\theta}^{\text{ro}}$ even though they define the same in $D_{3,\theta}^{\text{ro}}$.

If q is the green point in $D_{3,4,\theta}^{\text{ro}}$ chosen by the common segment of the two broken trajectories, then the germs of $\overline{S^{\text{ro}}(p_1)}$ and $\overline{S^{\text{ro}}(p_2)}$ at q define different manifolds, which by the non-degeneracy of the vector field $\xi_{\text{pol}}^{\text{ro}}$ at q , define different trajectories in $D_{4,\theta}^{\text{ro}}$, that is $\overline{S^{\text{ro}}(p_1)} \cap D_{4,\theta}^{\text{ro},\circ}$ and $\overline{S^{\text{ro}}(p_2)} \cap D_{4,\theta}^{\text{ro},\circ}$ are two distinct trajectories of $\xi_{4,\theta}^{\text{ro}}$. In fig. 12.2.25 we see the three qualitatively different possibilities and we see how all of them form CW complexes that enclose a disk and so we conclude that in general the spine at radius 0 and angle θ (Definition 12.1.3) is not a spine.

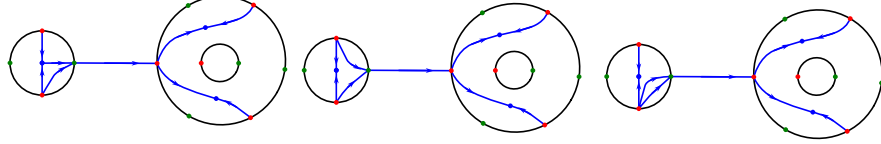


FIGURE 12.2.25. The three possibilities for the broken trajectories coming from one Petri dish and entering the Petri dish (flowing backwards) corresponding to the component of the polar curve that intersects D_4 .

Remark 12.2.26. In the previous example, a special situation occurs, which can be seen in fig. 12.2.23. The blue point has two trajectories emerging from it, and one of the trajectories converges to the white point. In a generic situation, each trajectory emerging from the blue point would converge to one of the sinks. This picture cannot be made generic by perturbing the metric by Remark 9.1.10. It can, however be made generic by an equisingular deformation of the analytic structure of $(C, 0)$. Such deformations will be further studied in a subsequent manuscript.

12.3. The invariant Milnor fibration

In this subsection we introduce a \mathcal{C}^∞ -fibration which is equivalent to the Milnor fibration and whose total space is a quotient of the exceptional part of the boundary of $Y_{\text{pol}}^{\text{ro}}$.

12.3.1. Let

$$\partial_{\mathcal{V}} Y_{\text{pol}}^{\text{ro}} = \bigcup_{i \in \mathcal{V}_{\text{pol}}} D_i^{\text{ro}}.$$

We consider the equivalence relation \sim_{Υ} that collapses each Petri dish \mathbb{D}_{θ} to a point. Thus, \sim_{Υ} is the finest equivalence relation of $\partial_{\mathcal{V}} Y_{\text{pol}}^{\text{ro}}$ for which $p \sim_{\Upsilon} p'$ for all $p, p' \in D_{i,\theta}^{\text{ro}}$, for any θ and $i \in \mathcal{V}_{\text{pol}} \setminus \mathcal{V}_{\Upsilon}$. Denote the quotient space by

$$D_{\Upsilon}^{\text{ro}} = \partial_{\mathcal{V}} Y_{\text{pol}}^{\text{ro}} / \sim_{\Upsilon}$$

Thus, the image of the Milnor fiber at radius 0 in this quotient space is homeomorphic to the Milnor fiber at radius 0. Since \arg^{ro} takes constant value along Petri dishes, we have a well defined map

$$\arg_{\Upsilon}^{\text{ro}} : D_{\Upsilon}^{\text{ro}} \rightarrow \mathbb{R}/2\pi\mathbb{Z}$$

on the quotient space.

12.3.2. We construct a \mathcal{C}^{∞} structure on the space D_{Υ}^{ro} as follows. First, we construct a \mathcal{C}^{∞} structure on $D_i^{\text{ro}} / \sim_{\Upsilon}$, for $i \in \mathcal{V}_{\Upsilon}$. This space contains some number of copies of embedded S^1 , which are the collapsed Petri dishes. More precisely, if ik is an edge corresponding to an invariant vertex i and a non-invariant vertex k , take a coordinate v in a neighborhood $V \subset D_i$ of $D_i \cap D_k$. Then σ^*v takes constant value along $D_{i,k}^{\text{ro}}$. This induces a function $v^{\text{ro}} : \sigma^{-1}(V) \rightarrow \mathbb{C}$, which, along with $\arg^{\text{ro}}(f)$ endows $\sigma^{-1}(V)$ with a smooth structure. This way, $D_i^{\text{ro}} / \sim_{\Upsilon}$ is a compact 3 dimensional manifold with boundary components which are tori, corresponding to invariant edges.

The space D_{Υ}^{ro} is obtained by gluing together the pieces $D_i^{\text{ro}} / \sim_{\Upsilon}$ along the boundary tori (via the identity map). Let ij be an invariant edge with $j \rightarrow i$. We obtain coordinates near the embedded torus D_{ij}^{ro} as follows. Take Grobman-Hartman coordinates u, v in a chart U around the intersection point $D_i \cap D_j$ as given by [Lemma 8.1.2](#) such that $\{u = 0\} = D_i \cap U$ and $\{v = 0\} = D_j \cap U$. In particular, as in [eq. \(8.1.9\)](#), the vector field ξ_U is given as

$$\xi_U = d \begin{pmatrix} c_{0,j} u \\ -c_{0,i} v \end{pmatrix}$$

where $d > 0$ by [Lemma 8.1.1](#). This way, we get polar coordinates $u = re^{i\alpha}$ and $v = se^{i\beta}$ in $U^{\text{ro}} = \sigma^{-1}(U)$. The functions $\alpha, \beta : U^{\text{ro}} \rightarrow S^1$ restrict to functions in a neighborhood of $D_{ij}^{\text{ro}} = D_i^{\text{ro}} \cap D_j^{\text{ro}}$, giving two coordinates in $D_{\Upsilon}^{\text{ro}} \cap U^{\text{ro}}$. A third coordinate t is constructed by setting

$$t : D_{\Upsilon}^{\text{ro}} \rightarrow \mathbb{R}, \quad t(q) = \begin{cases} s(q) & q \in D_i^{\text{ro}}, \\ -r(q) & q \in D_j^{\text{ro}}. \end{cases}$$

Lemma 12.3.3. *The map $\arg_{\Upsilon}^{\text{ro}}(f) : D_{\Upsilon}^{\text{ro}} \rightarrow \mathbb{R}/2\pi\mathbb{Z}$, induced by $\arg^{\text{ro}}(f)$ is a \mathcal{C}^{∞} locally trivial fibration with fiber $F_{\Upsilon, \theta}^{\text{ro}}$, which is equivalent to the Milnor fibration.*

PROOF. The space D_{Υ}^{ro} is compact, and the function $\arg_{\Upsilon}^{\text{ro}}(f)$, and its restriction to the boundary of D_{Υ}^{ro} , is a submersion. Therefore, the lemma follows from Ehresmann's fibration theorem.

Indeed, take any $q \in D_{\Upsilon}^{\text{ro}}$. If $q \in D_i^{\text{ro}, \circ}$ for some $i \in \mathcal{V}_{\Upsilon}$, then it is clear that $\arg_{\Upsilon}^{\text{ro}}(f)$ is a submersion at q . If q is the image of some Petri dish, then $\arg_{\Upsilon}^{\text{ro}}(f)$ is a coordinate near q , in particular, it is a submersion at q . If $q \in D_{ij}^{\text{ro}}$, where ij is an

invariant edge, then $\arg_{\Upsilon}^{\text{ro}}(f)|_{D_{ij}^{\text{ro}}}$ is already a submersion, as seen in [Lemma 4.2.3](#), and the same argument applies to the boundary components of D_{Υ}^{ro} . \square

Definition 12.3.4. We call

$$\arg_{\Upsilon}^{\text{ro}}(f) : D_{\Upsilon}^{\text{ro}} \hookrightarrow \mathbb{R}/2\pi\mathbb{Z}$$

the *invariant Milnor fibration*. For each $\theta \in \mathbb{R}/2\pi\mathbb{Z}$ we denote by

$$F_{\Upsilon,\theta}^{\text{ro}} = (\arg_{\Upsilon}^{\text{ro}})(f)^{-1}(\theta)$$

the corresponding fiber and call it *the invariant Milnor fiber*.

12.3.5. Next, we construct a vector field defined on D_{Υ}^{ro} . In $D_i^{\text{ro},\circ}$, outside a small neighborhood of the boundary tori D_{ij}^{ro} , the vector field coincides with ξ_i^{ro} . Let ij be an invariant edge, directed as $j \rightarrow i$. Then, with a coordinate neighborhood U with coordinates u, v as in the above construction, define a vector field

$$\xi_{U,\Upsilon}^{\text{ro}} = (1, 0, 0)$$

in the coordinates (t, α, β) . Note that this vector field is parallel to ξ_i^{ro} and ξ_j^{ro} outside D_{ij}^{ro} . Using partition of unity, these vector fields add up to a global vector field on all of D_{Υ}^{ro} . This vector field is tangent to the Milnor fibers $F_{\Upsilon,\theta}^{\text{ro}}$ for $\theta \in \mathbb{R}/2\pi\mathbb{Z}$.

Definition 12.3.6. Denote by $\xi_{\Upsilon}^{\text{ro}}$ the vector field on D_{Υ}^{ro} constructed in the previous paragraph, and by $\xi_{\Upsilon,\theta}^{\text{ro}}$ its restriction to the invariant Milnor fiber $F_{\Upsilon,\theta}^{\text{ro}}$, for $\theta \in \mathbb{R}/2\pi\mathbb{Z}$.

Remark 12.3.7. By construction, the trajectories of $\xi_{\Upsilon}^{\text{ro}}$ pass transversely through the tori D_{ij}^{ro} . In fact, as a set, a trajectory of $\xi_{\Upsilon}^{\text{ro}}$ is a broken trajectory of ξ^{ro} in the invariant part of $\partial Y_{\text{pol}}^{\text{ro}}$.

Lemma 12.3.8. *There exists a real function $\phi_{\Upsilon}^{\text{ro}} : D_{\Upsilon}^{\text{ro}} \rightarrow \mathbb{R}$ such that $\xi_{\Upsilon}^{\text{ro}}$ is gradient-like for it. That is,*

$$d\phi_{\Upsilon}^{\text{ro}}(\xi_{\Upsilon}^{\text{ro}}) > 0$$

outside the singular points of $\xi_{\Upsilon}^{\text{ro}}$. Setting $\phi_{\Upsilon,\theta}^{\text{ro}} = \phi_{\Upsilon}^{\text{ro}}|_{F_{\Upsilon,\theta}^{\text{ro}}}$, we also have

$$d\phi_{\Upsilon,\theta}^{\text{ro}}(\xi_{\Upsilon,\theta}^{\text{ro}}) > 0$$

outside the singular points of $\xi_{\Upsilon,\theta}^{\text{ro}}$.

PROOF. For any $i \in \mathcal{V}_{\Upsilon}$, the vector field ξ_i has a potential ϕ_i , given in [Definitions 7.4.3](#) and [9.2.2](#). We set $\phi_i^{\text{ro}} = \sigma^* \phi_i$. If i has distance k to 0 in Υ , rescale ϕ_i^{ro} to take values in $[k, k+1]$. These functions glue together to the desired global function $\phi_{\Upsilon,\theta}^{\text{ro}}$. \square

Remark 12.3.9. Let ij be an edge of Γ_{pol} with j invariant and i non-invariant (necessarily $j \rightarrow i$). Then, by [Lemma 8.2.6](#) (see also [fig. 8.2.10](#)), the vector field $\xi_{\Upsilon,\theta}^{\text{ro}}$ (by [Lemma 8.4.1 3](#)) has $\varpi_i m_j / \gcd(m_j, m_i)$ -pronged singularities near the intersection points of $D_{j,\theta}^{\text{ro}}$ with $\sigma_{\Upsilon}^{-1}(D_i)$. See [fig. 12.3.13](#).

12.3.10. We extend the equivalence relation \sim_{Υ} trivially over $Y_{\text{pol}}^{\text{ro}}$, so that equivalence classes outside $\partial_{\mathcal{V}} Y_{\text{pol}}^{\text{ro}} \subset Y_{\text{pol}}^{\text{ro}}$ contain only one point. This way, the invariant Milnor fibration sits inside the space $Y_{\text{pol}}^{\text{ro}} / \sim_{\Upsilon}$, which projects by $\pi_{\text{pol}}^{\text{ro}}$ to \mathbb{C}^2 isomorphically outside C .

Definition 12.3.11. Denote by

$$p_Y : Y_{\text{pol}}^{\text{ro}} \rightarrow Y_{\text{pol}}^{\text{ro}} / \sim_Y$$

the natural projection. Let $S_{Y,\theta}^{\text{ro}}$ be the intersection of $F_{Y,\theta}^{\text{ro}}$ with the closure of the strict transform of the total spine, that is,

$$S_{Y,\theta}^{\text{ro}} = F_{Y,\theta}^{\text{ro}} \cap \overline{p_Y \left((\pi_{\text{pol}}^{\text{ro}})^{-1}(S \setminus \{0\}) \right)}.$$

We call $S_{Y,\theta}^{\text{ro}}$ the *invariant spine*. Define also the *total invariant spine* as

$$S_Y^{\text{ro}} = \bigcup_{\theta \in \mathbb{R}/2\pi\mathbb{Z}} S_{Y,\theta}^{\text{ro}}.$$

Theorem 12.3.12. *The invariant spine $S_{Y,\theta}^{\text{ro}}$ satisfies the following:*

- (1) *It coincides with the union of all trajectories of $\xi_{Y,\theta}^{\text{ro}}$ that do not escape to the boundary of the invariant Milnor fiber $\partial F_{Y,\theta}^{\text{ro}}$.*
- (2) *It is a spine of the invariant Milnor fiber $F_{Y,\theta}^{\text{ro}}$.*
- (3) *It is a piecewise smooth CW-complex of dimension 1 and all 1-cells meet transversely at 0-cells.*

PROOF. By [Proposition 12.2.203](#) and [Remark 12.3.7](#), $S_{Y,\theta}^{\text{ro}}$ contains all trajectories converging to singularities of the vector field $\xi_{Y,\theta}^{\text{ro}}$. It follows from [Theorem 11.2.1](#) that no other point in $F_{Y,\theta}^{\text{ro}}$ is contained in the invariant spine. This proves 1.

For 2, the flow of $\xi_{Y,\theta}^{\text{ro}}$ trivializes the complement of the spine as a collar neighborhood of the boundary. 3 follows from construction. \square

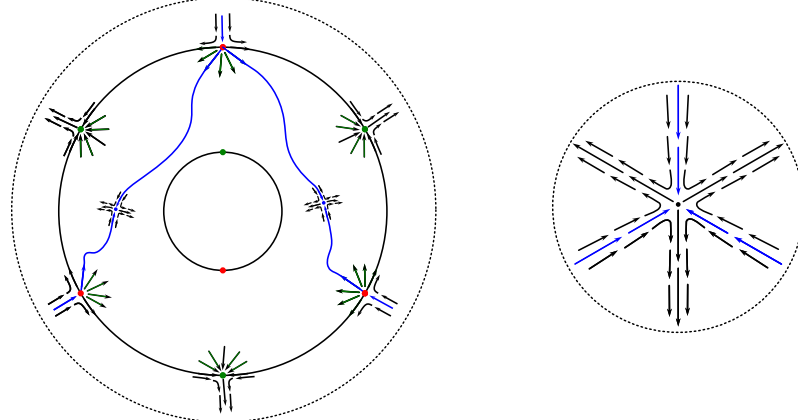


FIGURE 12.3.13. On the left we see a small neighborhood (dotted disk) of a Petri dish, in blue the broken trajectories that appear in this neighborhood. On the right we see the same neighborhood after collapsing the Petri dish to a point. The contracted Petri dish behaves as a trivalent vertex

CHAPTER 13

Example

Example 13.0.1. Consider the plane curve defined by the function

$$f(x, y) = y^3 + x^4 + x^3y.$$

Since the curve is irreducible, it has only one tangent $\{y = 0\}$. Also note that we are already using the coordinates of [Notation 9.0.1](#) and, in particular, the polar curve P_i associated with $i = 1, 2, 3$ is the same, and it is the curve defined by

$$P = \{f_y = 0\} = \{3y^2 + x^3 = 0\}.$$

Next we compute the minimal resolution $\pi : Y \rightarrow \text{Tub}$ of the curve f and observe that the curve P gets resolved by this resolution. See [Figure 13.0.2](#).

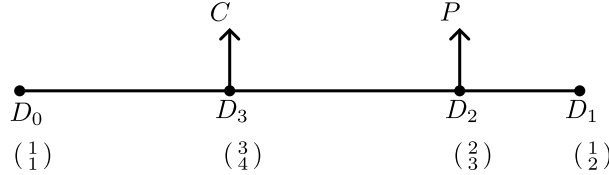


FIGURE 13.0.2. The dual resolution graph of the curve defined by f . The blue arrow represents the strict transform \tilde{P} of the polar curve $\{f_y = 0\}$.

Now we compute all the numerical invariants introduced in this work: $c_{0,i}, c_{1,i}, m_i, p_i, \tau_i$ and ϖ_i for $i = 0, 1, 2, 3$. See [13.0.3](#).

i	0	3	2	1
$c_{0,i}$	1	3	2	1
$c_{1,i}$	1	4	3	2
m_i	3	12	8	4
p_i	2	8	6	3
τ_i	2	8	5	3
ϖ_i	0	0	1	1

(13.0.3)

The topology of the Milnor fiber. Next, we compute the topology of the Milnor fiber. We do this by looking at the multiplicities m_i of $\pi^* f$: near D_i° the Milnor fiber is an m_i -fold cover of D_i° . Moreover, the part of the Milnor fiber that covers D_i° can be identified with $D_{i,\theta}^{\text{ro},\circ}$ for each $\theta \in \mathbb{R}/2\pi\mathbb{Z}$. Also, we know that $D_{i,\theta}^{\text{ro},\circ}$ has

$$\sum_j \gcd(m_i, m_j)$$

boundary components, where j runs over vertices adjacent to i . Using this information we can conclude that $D_{0,\theta}^{\text{ro},\circ}$ is a disjoint union of 3 disks, $D_{3,\theta}^{\text{ro},\circ}$ is the surface of genus 3 and 8 boundary components, $D_{2,\theta}^{\text{ro},\circ}$ is a disjoint union of 4 annuli and $D_{1,\theta}^{\text{ro},\circ}$ is a disjoint union of 4 disks, see fig. 13.0.4. With these invariants, we are ready to start computing the vector fields ξ_i for $i \in \mathcal{V}$.

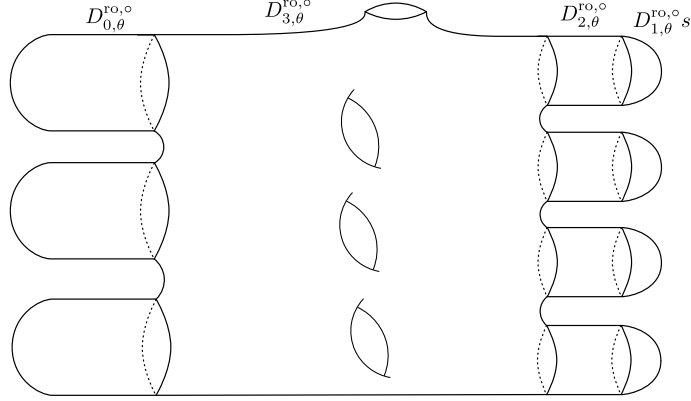


FIGURE 13.0.4. The Milnor fiber at radius 0 at an angle θ separated in the parts corresponding to each exceptional divisor. The marked simple closed curves correspond with parts of the Milnor fiber that lie in the corners of Y^{ro} .

The 1st blow up. We follow Chapter 7 for this part of the example. We are going to check that the standard metric is already generic in the sense of (Definition 7.4.10). Let $\pi_0 : Y_0 \rightarrow \text{Tub}$ be the first blow up and take a coordinate chart $U \subset Y_0$ with coordinates u, v so that $\pi_0(u, v) = (u, uv)$ in these coordinates. In order to check that the standard metric is generic, we need to verify that

$$-\log \left| \frac{\pi_0^* f}{(\pi_0^* d_{\text{id}})^{3/2}} \right|_{D_0^\circ}$$

is a Morse function. Equivalently, by Lemma 7.4.4, we need to verify that the vector field

$$\xi_0 = \pi_0^*(d \cdot \xi)|_{D_0^\circ}$$

is elementary. A direct computation in the coordinates u, v gives, (following eq. (7.1.2)):

$$\pi_0^* \xi = \begin{pmatrix} \xi^u \\ \xi^v \end{pmatrix} = \begin{pmatrix} -\frac{3\bar{v} + 4}{\bar{v}^3 + \bar{u}\bar{v} + \bar{u}} \\ \frac{3v\bar{u}\bar{v} + 4v\bar{u} - 3\bar{v}^2 - \bar{u}}{u\bar{u}\bar{v}^3 + u\bar{u}^2\bar{v} + u\bar{u}^2} \end{pmatrix}.$$

So, on $U \cap D_0^\circ$,

$$\xi_0 = (|u|^2 + |uv|^2) \xi^v|_{\{u=0\}} = -\frac{3(1 + |v|^2)}{\bar{v}}.$$

Since $4(1 + |v|^2)$ is a unit on $U \cap D_0^\circ$ and $-1/\bar{v} = -v/|v|^2$ is an elementary vector field on $U \cap D_0^\circ$ so we are done in this chart. Actually, on $U \cap D_0^\circ$ the vector field

ξ_0 never vanishes. Now, we verify the other chart where $\pi_0(u, v) = (uv, u)$. An analogous computations gives,

$$\xi_0 = 3(1 + |v|^2)v,$$

which has the same dynamics as the vector field v which is elementary. This vector field has a single singularity which is a fountain at the origin of this chart. The vector field ξ_0 is defined on D_0° , to compute the vector field $\xi_{0,\theta}^{\text{ro}}$ for some $\theta \in \mathbb{R}/2\pi\mathbb{Z}$, we need to compute the real oriented blow up. In this case, since $\varpi_0 = 0$, the vector field does not depend on $\arg(u) = \alpha$.

The invariant part. Now we observe that the invariant graph Υ is the bamboo induced by the vertices 0 and 3, equivalently, it is the smallest connected subgraph containing 0 and all vertices that intersect with the strict transform of C (recall Lemma 6.3.4). So the only other vertex of Γ with $\varpi_i = 0$ is the vertex $i = 3$. In this case, by Lemma 9.1.6, the zero set of ξ_3 should be the intersection points of D_3 with \tilde{P} , but this intersection is empty. So the vector fields ξ_3 and ξ_3^{ro} are nowhere vanishing on D_3° and $D_3^{\text{ro},\circ}$ respectively.

The non-invariant part. The non-invariant part of the graph is the graph induced by the vertices 1 and 2. Let us take a chart $U \subset Y$ with coordinates u, v that contains most of these two divisors. For that, following the weight vectors of Figure 13.0.2 we take the chart U in which the resolution map π looks like:

$$\pi(u, v) = (u^2v, u^3v^2).$$

In this chart, D_2° is given by $\{u = 0\}$, and D_1° by $\{v = 0\}$. We have

$$\begin{aligned} f &= u^8v^4 + u^9v^6 + u^9v^5 = u^8v^4(1 + uv^2 + uv), \\ f_x &= u^6v^3(4 + 3uv), \\ f_y &= u^6v^3(3v + 1). \end{aligned}$$

Recall here we are identifying its function with its pullback by π to ease the notation. Notice that the two partials have the same weight w.r.t. u and v , i.e. the weight vectors $(2, 3)$ and $(1, 2)$.

We compute the Jacobian of the transformation and its inverse:

$$\text{Jac } \pi = \begin{pmatrix} 2uv & u^2 \\ 3u^2v & 2u^3v \end{pmatrix}, \quad (\text{Jac } \pi)^{-1} = \frac{1}{u^4v^2} \begin{pmatrix} 2u^3v & -u^2 \\ -3u^2v & 2uv \end{pmatrix}.$$

We find that

$$\pi^*\xi = \begin{pmatrix} \frac{8uv + 3(2uv\bar{u} - 1)\bar{v} - 1}{u^2v^2\bar{u}^3\bar{v}^3 + u^2v^2\bar{u}^3\bar{v}^2 + u^2v^2\bar{u}^2\bar{v}} \\ \frac{12uv + 3(3uv\bar{u} - 2)\bar{v} - 2}{u^3v\bar{u}^3\bar{v}^3 + u^3v\bar{u}^3\bar{v}^2 + u^3v\bar{u}^2\bar{v}} \end{pmatrix}$$

Note that this formula holds only outside the exceptional set, that is, for $(u, v) \in (\mathbb{C}^*)^2$. Following Lemma 8.0.8 and the table 13.0.3, we use the function $|u|^5|v|^3$ to rescale and extend the vector field over the boundary of the real oriented blow-up. In particular, to see the extension over $D_2^{\text{ro},\circ}$, we take coordinates $(r, \alpha, s, \beta) \in (\mathbb{R}_{\geq 0} \times \mathbb{R}/2\pi\mathbb{Z})^2$ and compute the vector field over $D_2^{\text{ro},\circ}$ which, in this coordinates is defined by $\{r = 0\}$. First we compute the pullback of ξ^v rescaled using the corresponding τ exponents:

$$(13.0.5) \quad (r^5s^3\sigma^*\xi^v)|_{D_2^{\text{ro},\circ}} = -2s(3\bar{v} + 1)e^{-i\alpha}$$

Recall that on $D_2^{\text{ro},\circ}$, the coordinate s does not vanish. Now, following [eq. \(8.1.4\)](#), we compute the rescaled $\xi^{\text{ro},s}$ and $\xi^{\text{ro},\beta}$. We start by $\xi^{\text{ro},s}$,

$$\begin{aligned} r^5 s^3 \xi^{\text{ro},s} &= \operatorname{Re}(e^{-i\beta} \sigma^* \xi^v) \\ (13.0.6) \quad &= \operatorname{Re}(e^{-i\beta} (-2s(3se^{-i\beta} + 1)e^{-i\alpha})) \\ &= \operatorname{Re}(-6s^2 e^{-i(2\beta+\alpha)} - 2se^{-i(\alpha+\beta)}) \\ &= -6s^2 \cos(2\beta + \alpha) - 2s \cos(\alpha + \beta). \end{aligned}$$

Similarly, we compute $\xi^{\text{ro},\beta}$:

$$\begin{aligned} r^5 s^3 \xi^{\text{ro},\beta} &= \operatorname{Im}(s^{-1} e^{-i\beta} \sigma^* \xi^v) \\ (13.0.7) \quad &= \operatorname{Im}(s^{-1} e^{-i\beta} (-2s(3se^{-i\beta} + 1)e^{-i\alpha})) \\ &= \operatorname{Im}(-6se^{-i(2\beta+\alpha)} - 2e^{-i(\alpha+\beta)}) \\ &= 6s \sin(2\beta + \alpha) + 2 \sin(\alpha + \beta) \end{aligned}$$

Now we fix θ in order to compute $\xi_\theta^{\text{ro},s}$ and $\xi_\theta^{\text{ro},\beta}$. That is, we fix $f^{\text{ro}} = \frac{f}{|f|} = e^{i\theta}$ so we get:

$$\left. \left(\frac{f}{|f|} \right) \right|_{r=0} = e^{i8\alpha} e^{i4\beta} = e^{i\theta},$$

that is

$$8\alpha + 4\beta = \theta \bmod 2\pi.$$

For each $\theta \in \mathbb{R}/2\pi\mathbb{Z}$, this equation has four circles of solutions in the torus $(\mathbb{R}/2\pi\mathbb{Z})^2$. These four circles are defined by the equations $\{2\alpha + \beta = \theta/4 + k\pi/2\}$ with $k = 0, 1, 2, 3$. These four circles are exactly $D_{3,2,\theta}^{\text{ro}}$. Note that each of these circles admits a parametrization

$$\tilde{\beta} \mapsto \left(\frac{\theta}{8} + \frac{k\pi}{4} - \frac{\tilde{\beta}}{2}, \tilde{\beta} \right), \quad \tilde{\beta} \in [0, 4\pi)$$

Moreover, we know that $D_{2,\theta}^{\text{ro},\circ}$ consists of four cylinders. Each of these cylinders has one of the previous four circles in its closure in Y_θ^{ro} and is defined by

$$\{r = 0\} \cap \{2\alpha + \beta = \theta/4 + k\pi/2\} \subset Y_\theta^{\text{ro}}.$$

Therefore, we can consider coordinates, s and β , with $s \in \mathbb{R}_{\geq 0}$ and $\beta \in [0, 4\pi)$.

Substituting the above expression for α in [eqs. \(13.0.6\)](#) and [\(13.0.7\)](#) we get the formula for $\xi_{2,\theta}^{\text{ro}}$ in the coordinate patch $U^{\text{ro}} \cap D_{2,\theta}^{\text{ro},\circ}$ in the connected component where $\delta = 0$:

$$\xi_{2,\theta}^{\text{ro}} = \begin{pmatrix} -6s^2 \cos\left(\frac{3\beta}{2} + \frac{\theta}{8} + \frac{k\pi}{4}\right) - 2s \cos\left(\frac{\beta}{2} + \frac{\theta}{8} + \frac{k\pi}{4}\right) \\ 6s \sin\left(\frac{3\beta}{2} + \frac{\theta}{8} + \frac{k\pi}{4}\right) + 2 \sin\left(\frac{\beta}{2} + \frac{\theta}{8} + \frac{k\pi}{4}\right) \end{pmatrix}$$

In [fig. 13.0.12](#) we can see the cylinder corresponding to $k = 0$ and $\theta = 0$ and in [fig. 13.0.9](#) we can see the cylinder corresponding to $\theta = 0$ and $k = 2$. This last cylinder represents a non-generic picture: the broken trajectory corresponding to the stable manifold of one of the saddle points, goes through one of the discs of

$D_{1,\theta}^{\text{ro},\circ}$, comes back again to $D_{2,\theta}^{\text{ro},\circ}$ and has the other saddle point in its closure. Also, following Lemma 8.2.4 (iii) we get

$$|\Sigma_{1,2}^+ \cap Y_\theta^{\text{ro}}| = |\Sigma_{1,2}^- \cap Y_\theta^{\text{ro}}| = -\begin{vmatrix} 4 & 1 \\ 8 & 1 \end{vmatrix} = 4.$$

Where $|\cdot|$ denotes cardinality in the first two terms and determinant in the third one. Since $D_{1,2,\theta}^{\text{ro}}$ has 4 connected components, we conclude that there is $4/4 = 1$ point of $\Sigma_{i,j}^+$ and one point of $\Sigma_{i,j}^-$ on each connected component. These are the green and red points in fig. 13.0.8.

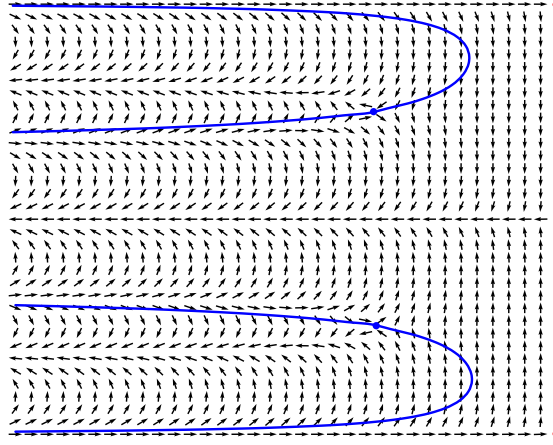


FIGURE 13.0.8. The vector field $\xi_{2,\theta}^{\text{ro}}$ on one of the four connected components of $D_{2,\theta}^{\text{ro},\circ}$ for $\theta = 0$. The right vertical line is one of the connected components of $D_{2,1,\theta}^{\text{ro}}$. In blue the stable manifolds of the two saddle points.

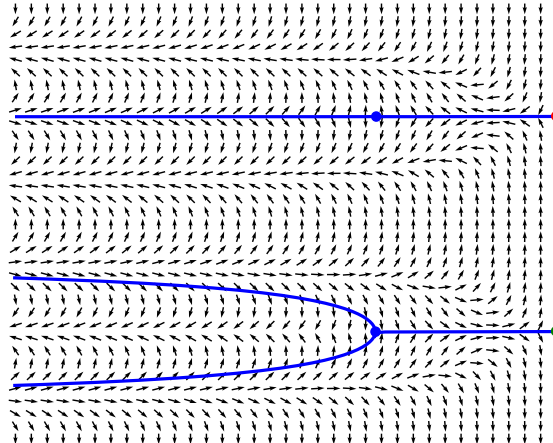


FIGURE 13.0.9. The vector field $\xi_{2,\theta}^{\text{ro}}$ on one of the four connected components of $D_{2,\theta}^{\text{ro},\circ}$ for $\theta = 4\pi$. The left side of the box is one of the connected components of $D_{3,2,\theta}^{\text{ro}}$.

We take now a chart near $D_2 \cap D_3$. In this chart the resolution takes the form

$$\pi(u, v) = (u^3v^2, u^4v^3)$$

and D_2 is defined by $\{v = 0\}$. In this case, we get

$$(r^8 s^5 \sigma^* \xi^u)|_{D_2^{\text{ro}, \circ}} = r^2 \frac{2(\bar{u} + 3)e^{-i\beta}}{\bar{u}} = 2r(\bar{u} + 3)e^{-i\beta}e^{i\alpha}.$$

As in [eqs. \(13.0.6\)](#) and [\(13.0.7\)](#), we compute

$$\begin{aligned} r^8 s^5 \xi^{\text{ro}, r} &= 2r^2 \cos(\beta + \alpha) + 6r \cos(\beta) \\ r^8 s^5 \xi^{\text{ro}, \alpha} &= -2r \sin(\beta + \alpha) - 6 \sin(\beta). \end{aligned}$$

Now we use the relation $12\alpha + 8\beta = \theta + k\pi/2$, and we get

$$\xi_{2,\theta}^{\text{ro}} = \begin{pmatrix} 2r^2 \cos\left(-\frac{\alpha}{2} + \frac{\theta}{8} + \frac{k\pi}{16}\right) + 6r \cos\left(\frac{\theta}{8} - \frac{3\alpha}{2} + \frac{k\pi}{16}\right) \\ -2r \sin\left(-\frac{\alpha}{2} + \frac{\theta}{8} + \frac{k\pi}{16}\right) - 6 \sin\left(\frac{\theta}{8} - \frac{3\alpha}{2} + \frac{k\pi}{16}\right) \end{pmatrix}$$

in these coordinates. In [fig. 13.0.10](#) we can see the cylinder corresponding to $k = 0$ and $\theta = 0$ and in [fig. 13.0.11](#) we can see the cylinder corresponding to the non-generic cylinder $\theta = 0$ and $k = 2$. In this case, the computation from [Lemma 8.2.4 \(iii\)](#) yields

$$|\Sigma_{2,3}^+ \cap Y_\theta^{\text{ro}}| = |\Sigma_{2,3}^- \cap Y_\theta^{\text{ro}}| = - \begin{vmatrix} 8 & 1 \\ 12 & 0 \end{vmatrix} = 12.$$

Which gives $12/4 = 3$ green points and three red points.

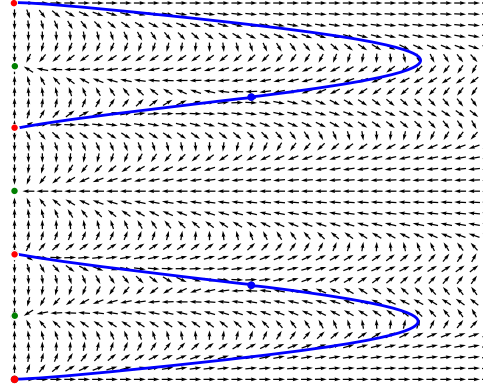


FIGURE 13.0.10. The vector field $\xi_{2,\theta}^{\text{ro}}$ on one of the four connected components of $D_{2,\theta}^{\text{ro}, \circ}$ for $\theta = 0$. The left vertical line is one of the connected components of $D_{3,2,\theta}^{\text{ro}}$.

Similarly, in order to finish the computations for the non-invariant part of the graph, we can compute $\xi_{1,\theta}^{\text{ro}}$ which is defined on the adjacent divisor $D_{1,\theta}^{\text{ro}, \circ}$. We obtain:

$$(r^5 s^3 \sigma^* \xi^u)|_{D_1^{\text{ro}, \circ}} = r e^{-i\beta}$$

which, after a computation similar to that of [eqs. \(13.0.6\)](#) and [\(13.0.7\)](#), yields:

$$r^5 s^3 \xi^{\text{ro}, r} = r \cos(\beta + \alpha) \quad r^5 s^3 \xi^{\text{ro}, \alpha} = -\sin(\beta + \alpha).$$

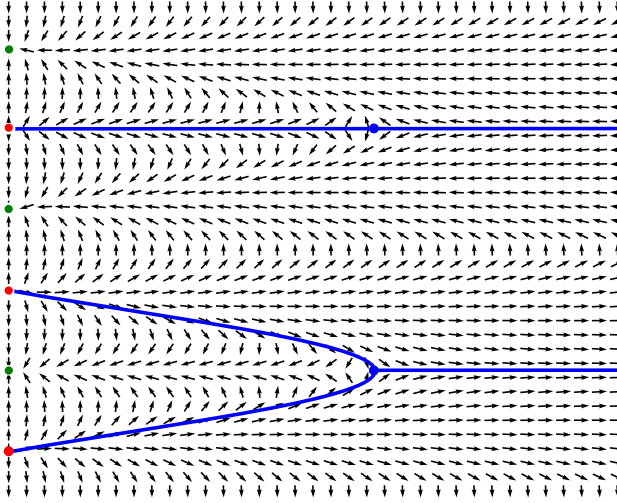


FIGURE 13.0.11. The vector field $\xi_{2,\theta}^{\text{ro}}$ on one of the four connected components of $D_{2,\theta}^{\text{ro},\circ}$ for $\theta = 0$. The left vertical line is one of the connected components of $D_{3,2,\theta}^{\text{ro}}$.

Using the relation $\beta = \theta/4 - 2\alpha$ we get:

$$(\xi_{1,\theta}^{\text{ro}})^\top = (r \cos(\theta/4 - \alpha), -\sin(\theta/4 - \alpha)).$$

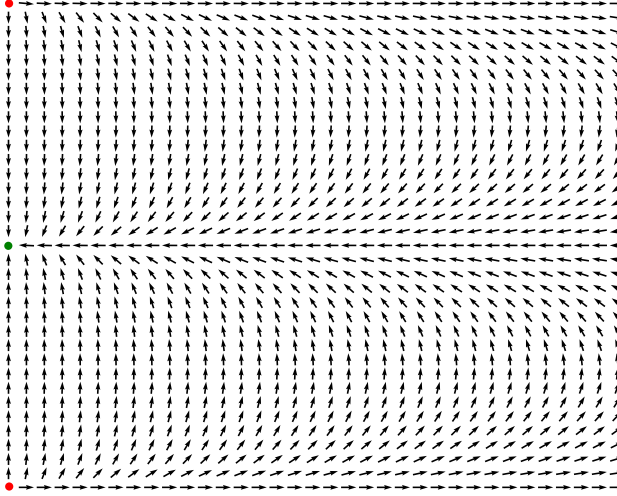


FIGURE 13.0.12. The vector field $\xi_{1,\theta}^{\text{ro}}$ on one of the four connected components (disks) of $D_{1,\theta}^{\text{ro},\circ}$ for $\theta = 0$. The left vertical line is one of the connected components (circles) of $D_{1,2,\theta}^{\text{ro}}$. The two red points and the top and bottom of the picture are identified. The horizontal line converging to the green point actually forms part of the same segment as the horizontal line emerging from the red point.

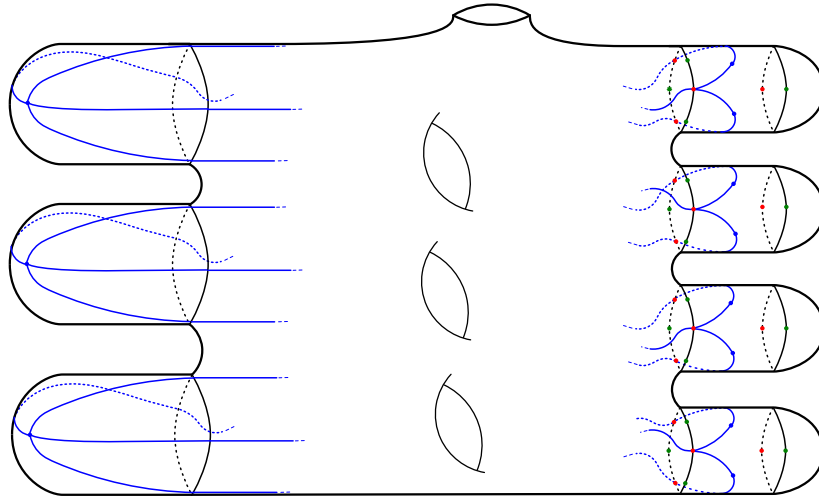


FIGURE 13.0.13. The Milnor fiber with the relevant parts of the spine (in blue) drawn. This is the case for an angle $\theta \neq 0$.

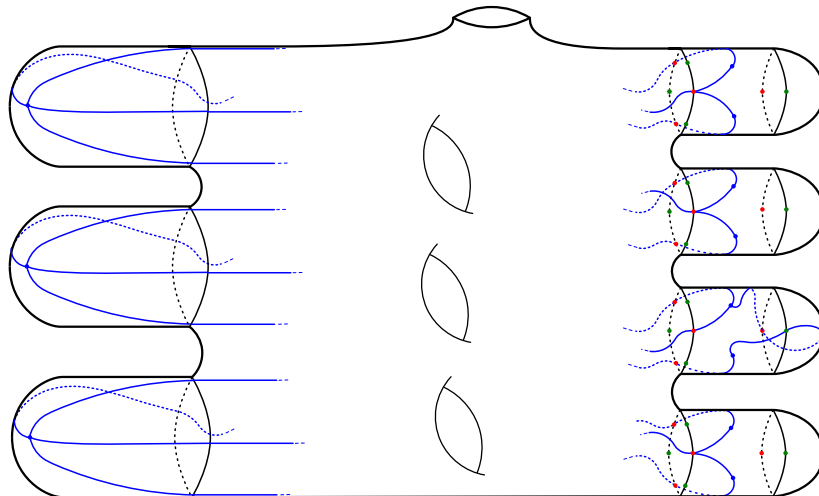


FIGURE 13.0.14. The Milnor fiber with the relevant parts of the spine (in blue) drawn. This is the special angle $\theta = 0$.

The invariant spine and invariant Milnor fiber. Following [Chapter 12](#), we contract each Petri dish to a point. In this case there are four Petri dishes, each one corresponding to a connected component of the branch Ξ at the vertex 2. Each of these Petri dishes consists of a cylinder and a disk. After contracting them, we get four 3-pronged singularities (see [fig. 13.0.15](#)). The invariant spine in this case is the $(3, 4)$ bipartite graph.

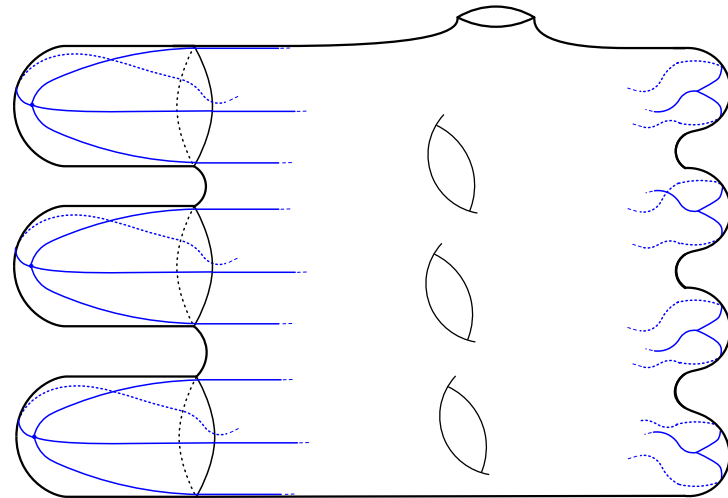


FIGURE 13.0.15. The invariant Milnor fiber with the invariant spine in blue.

Bibliography

- [A'C75] Norbert A'Campo, *La fonction zêta d'une monodromie*, Comment. Math. Helv. **50** (1975), 233–248. MR 0371889 (51 \#8106)
- [A'C18] ———, *Lagrangian spine and symplectic monodromy*, 2018.
- [AR67] Ralph Abraham and Joel Robbin, *Transversal mappings and flows*, W. A. Benjamin, Inc., New York-Amsterdam, 1967, An appendix by Al Kelley. MR 0240836
- [BdSFP22] André Belotto da Silva, Lorenzo Fantini, and Anne Pichon, *Inner geometry of complex surfaces: a valuative approach*, Geom. Topol. **26** (2022), no. 1, 163–219 (English).
- [Chi72] D. R. J. Chillingworth, *Winding numbers on surfaces. I*, Math. Ann. **196** (1972), 218–249. MR 300304
- [Ful93] William Fulton, *Introduction to toric varieties*, Annals of Mathematics Studies, vol. 131, Princeton University Press, Princeton, NJ, 1993, The William H. Roever Lectures in Geometry. MR 1234037 (94g:14028)
- [HJ89] Stephen P. Humphries and Dennis Johnson, *A generalization of winding number functions on surfaces*, Proc. London Math. Soc. (3) **58** (1989), no. 2, 366–386. MR 977482
- [Kel67a] Al Kelley, *Stability of the center-stable manifold*, J. Math. Anal. Appl. **18** (1967), 336–344. MR 210998
- [Kel67b] ———, *The stable, center-stable, center, center-unstable, unstable manifolds*, J. Differ. Equations **3** (1967), 546–570 (English).
- [KN99] Kazuya Kato and Chikara Nakayama, *Log Betti cohomology, log étale cohomology, and log de Rham cohomology of log schemes over \mathbf{C}* , Kodai Math. J. **22** (1999), no. 2, 161–186. MR 1700591
- [Lê88] Dũng Tráng Lê, *Polyèdres évanescents et effondrements.*, A fête of topology, Pap. Dedic. Itiro Tamura, 293–329 (1988)., 1988.
- [LM17] Dũng Tráng Lê and Aurélio Menegon Neto, *Vanishing polyhedron and collapsing map.*, Math. Z. **286** (2017), no. 3–4, 1003–1040 (English).
- [LMW89] Dũng Tráng Lê, Françoise Michel, and Claude Weber, *Sur le comportement des polaires associées aux germes de courbes planes. (On the behaviour of polar curves associated to plane germs of curves.)*, Compos. Math. **72** (1989), no. 1, 87–113 (French).
- [Loj84] Stanisław Łojasiewicz, *Sur les trajectoires du gradient d'une fonction analytique. (Trajectories of the gradient of an analytic function)*, Semin. Geom., Univ. Studi Bologna **1982/1983** (1984), 115–117 (French).
- [Mic08] Françoise Michel, *Jacobian curves for normal complex surfaces*, Singularities II. Geometric and topological aspects. Proceedings of the international conference “School and workshop on the geometry and topology of singularities” in honor of the 60th birthday of Lê Dũng Tráng, Cuernavaca, Mexico, January 8–26, 2007, Providence, RI: American Mathematical Society (AMS), 2008, pp. 135–150 (English).
- [Mil65] John Milnor, *Lectures on the h-cobordism theorem*, Princeton University Press, Princeton, N.J., 1965, Notes by L. Siebenmann and J. Sondow. MR 0190942
- [Mil68] ———, *Singular points of complex hypersurfaces*, Ann. of Math. Stud., vol. 61, Princeton University Press, Princeton, N.J.; University of Tokyo Press, Tokyo, 1968. MR 0239612 (39 \#969)
- [Ném99] András Némethi, *Five lectures on normal surface singularities.*, Low dimensional topology, Bolyai Soc. Math. Stud., vol. 8, Budapest: János Bolyai Math. Soc., Budapest, 1999, pp. 269–351 (English).
- [Nic11] Liviu I. Nicolaescu, *An invitation to Morse theory*, 2nd ed. ed., Universitext, Berlin: Springer, 2011 (English).

- [NW05] Walter D. Neumann and Jonathan Wahl, *Complete intersection singularities of splice type as universal Abelian covers*, Geom. Topol. **9** (2005), 699–755 (English).
- [Tei77] B. Teissier, *Variétés polaires. I. Invariants polaires des singularités d'hypersurfaces*, Invent. Math. **40** (1977), no. 3, 267–292. MR 470246
- [Wal04] C. T. C. Wall, *Singular points of plane curves*, London Mathematical Society Student Texts, vol. 63, Cambridge University Press, Cambridge, 2004. MR 2107253

Index

- K , 20
- $S(p)$, 87
- S_0 , 58
- \mathbb{D}_θ , 108
- D_i^{ro} , 28
- F_θ^{ro} , 30
- Γ , 18
- Σ_0 , 57
- Σ_i , 78
- $\Sigma_{i,j}^\pm$, 69
- $\Sigma_\theta^{\text{ro}}$, 99
- Υ , 38
- $\arg(f^{\text{ro}})$, 27
- \cdot_i , 28
- f^{ro} , 27
- \mathcal{H} , 54
- ν_i , 20
- ord_{D_i} , 19
- ϕ_0 , 55
- ϕ_i , 80
- $\phi_{i,\theta}^{\text{ro}}$, 85
- $\phi_\Upsilon^{\text{ro}}$, 118
- π , 17
- π_0 , 51
- π_{\min} , 17
- π_{pol} , 17, 33
- π^{ro} , 27
- τ_i , 65
- ϖ_i , 37
- ξ , 9
- ξ_0 , 52
- ξ_i^{ro} , 80
- $\xi_{\text{pol}}^{\text{ro}}$, 99
- $c_{0,i}$, 19
- $c_{1,i}$, 21
- d , 66
- p_i , 34
- antidual basis, 18
- attractor, 13
- branch, 23
- broken trajectory, 99
 - total, 107
- canonical cycle, 20
- collapsing map, 10
- degree, 38
- dual graph, 18
- elementary singularity, 13
- embedded resolution, 17
 - minimal, 17
 - resolving polar locus, 17
- end, 44
- fountain, 13
 - half, 71, 109
 - of ξ_0 , 57
 - quarter, 109
- green point, 71, 104
- group of cycles, 18
- Hessian matrix, 12
- Hironaka number, 48
- initial part, 18
- invariant, 38
- isometric coordinates, 12, 51, 65, 77
- manifold
 - center, 93
 - center-stable, 93, 104
 - stable, 67, 70
 - unstable, 67, 70
- maximal cycle, 19
- metric
 - P -generic, 35
 - Fubini-Study, 55, 56
 - on $D_{i,\theta}^{\text{ro},\circ}$, 31, 85
 - on D_i° , 31, 81
- Milnor fibration, 7
 - at radius zero, 30, 100
 - invariant, 118
- Milnor tube, 7
- Morse singularity, 59
- node, 44

Petri dish, 108
 Poincaré-Hopf index, 13, 57, 75, 109
 polar curve, 33
 polar weight, 37
 radial weight, 65
 real oriented blow-up, 27
 red point, 71, 104
 repeller, 13, 101, 103
 of ξ_0 , 58
 saddle, 13, 101, 103
 half, 71
 of ξ_0 , 57
 quarter, 109
 sink, 13
 half, 109
 of ξ_0 , 57
 quarter, 109
 solid Klein bottle, 98, 101
 solid torus, 98, 101
 spine, 10
 at radius zero, 107, 113
 for D_0° , 58
 invariant, 119
 total, 12
 symplectic connection, 7
 tangent associated with D_i , 24
 toric modification, 24
 total spine, 101
 vanishing order
 along D_i , 19
 winding number, 13